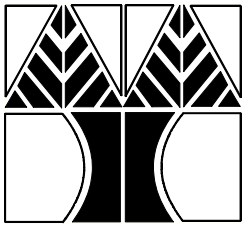

UNIVERSITY OF CYPRUS

DEPARTMENT OF CHEMISTRY

PhD DISSERTATION

SYNTHESIS AND CHARACTERIZATION OF LINEAR AND STAR ABC TRIBLOCK TERPOLYMERS AND ABCBA PENTABLOCK TERPOLYMER NETWORKS

Aggeliki I. Triftaridou

Nicosia

SEPTEMBER 2005

UNIVERSITY OF CYPRUS

DEPARTMENT OF CHEMISTRY

PhD DISSERTATION

SYNTHESIS AND CHARACTERIZATION OF LINEAR AND STAR ABC TRIBLOCK TERPOLYMERS AND ABCBA PENTABLOCK TERPOLYMER NETWORKS

Aggeliki I. Triftaridou

Thesis Supervisor:

Assoc. Prof. **Costas S. Patrickios**

Examining Committee:

Assoc. Prof. **Epameinondas Leontidis** (Internal Member, Committee Chairman)

Assoc. Prof. **Costas S. Patrickios** (Internal Member, Thesis Supervisor)

Assist. Prof. **Ioannis Pashalidis** (Internal Member)

Prof. **Constantinos Tsitsilianis** University of Patras (External Member)

Prof. **Spiros H. Anastasiadis** University of Crete (External Member)

To my family for their support and understanding

Acknowledgments

Reaching the end is not always easy… At times like that, a lot of memories, usually the pleasant ones, come to mind. The time to thank all the people that have been supporting me all these years has come…as if it is going to be easy…

At first I would like to thank my supervisor Associate Professor Costas Patrickios for introducing me to Polymer Science and his constant guidance during all these five years. So many things to thank him for, the fruitful discussions on my work and for his valuable scientific advice when reaching a dead-end.

Assistant Professor Maria Vamvakaki, now at the University of Crete, for guiding me on how to work in the lab during my first year as a graduate student.

Professor Costantinos Tsitsilianis and Mrs. Nicoletta Stavrouli of the University of Patras, for some of the static light scattering measurements.

Professor G. Krausch and Dr. M. Lysetska of the University of Bayreuth in Germany for the AFM imaging of one of my samples.

A special “thank you” goes to my colleagues and most of all friends: Theodora, Stella, Theoni, Froso, Demetris and especially Natalie for all those unforgettable times we shared, our agonies (especially when we broke both vacuum lines!) or our successes. The “friend” group with which we used to share our old lab, A 061, Lefkia, Evgenios, Panayiota, Maria, Marios and especially the “group friend” Eleni. Those ice-cream afternoon breaks we used to have during the hot summers and especially the jokes we used to make are not things one can easily forget.

I would also like to thank my friends Despo for her support when I needed it, for providing me with coffee and food during my working late days, and Sophia for coming by my lab to greet me, especially during the weekends.

ACKNOWLEDGMENTS

Most of all I would like to say a big "**thank you for always being there**" to my parents Yannakis and Vera, my sister Constantia, my brother Michalis and my grandparents Costas and Aggeliki, to each one for a different reason. My father for always standing by my side and supporting my decisions both emotionally and financially, my mother for calling me when I was working late to remind me of how late it went and for the chocolate rescues especially during very stressful time periods, my brother and sister for dropping by the lab to say hello during the weekends and to provide me with food. My grandparents for their emotional support, for the piece of advice they gave me when I needed it, and for providing me with their home to study in times I needed to change my environment. I also thank them all for their love and understanding all these years.

Well, that's it!

THANK YOU ALL!!!

Abstract

Linear and star ABC triblock terpolymers and ABCBA pentablock terpolymer-based model networks of two hydrophilic and one hydrophobic monomers were synthesized by group transfer polymerization (GTP). All the statistical terpolymer analogues were also prepared. Methoxy hexa(ethylene glycol) methacrylate (HEGMA, nonionic) and 2-(dimethylamino)ethyl methacrylate (DMAEMA, temperature- and pH-sensitive) were employed as the two hydrophilic monomers, whereas either methyl methacrylate (MMA) or *n*-butyl methacrylate (BuMA) served as the hydrophobic monomer. Ethylene glycol dimethacrylate (EGDMA) was used as the cross-linker to effect the interconnection of the linear chains to stars or networks, respectively. The monofunctional 1-methoxy-1-(trimethylsiloxy)-2-methyl propene (MTS) GTP initiator was employed for the synthesis of the linear and the star terpolymers, whereas the bifunctional 1,4-bis(methoxytrimethylsiloxymethylene)cyclohexane (MTSMC) initiator served for the preparation of the networks. Six terpolymer families were prepared in total, three of which comprised linear or novel star terpolymers, while the other three consisted of novel networks of well-defined structures, the first-known prepared networks of that kind. Five out of the six families comprised equimolar block sequence isomeric terpolymers, whereas the sixth contained network terpolymers with varying BuMA hydrophobic content.

The molecular weights and molecular weight distributions of all the terpolymers and the linear terpolymer precursors to the networks were obtained using gel permeation chromatography (GPC) in tetrahydrofuran (THF) and were found to agree reasonably well with the theoretically expected. Static light scattering (SLS) in THF revealed that the star terpolymers bore a large number of arms, between 40 and 80. The terpolymer compositions were determined by proton nuclear magnetic resonance (^{1}H NMR) spectroscopy. The compositions of the BuMA-containing terpolymers were in accord with the theoretically expected values, whereas lack of peak resolution impaired the accurate composition determination of the MMA-containing terpolymers.

All the terpolymers were characterized in an aqueous environment. In particular, the hydrodynamic diameters, aggregation numbers and cloud points of the linear and star terpolymers were determined using dynamic light scattering (DLS), SLS and turbidimetry, whereas the degrees of swelling (DSs) of the terpolymer networks were measured gravimetrically. The linear terpolymers formed small micelles in water, with the terpolymer having the hydrophobic block in the middle forming even smaller micelles. Star-star aggregation was observed with one block sequence isomer, whereas the non-aggregating stars exhibited block sequence-dependent hydrodynamic diameters, indicating differences in their internal structures. The cloud points of the linear and star terpolymers depended on block sequence, with the cloud points of the stars being higher than those of the linear due to the larger number of arms in the stars than the aggregation numbers in the linears. The statistical linear and stars exhibited the lowest cloud points due to the full exposure of their hydrophobic units to water.

In contrast to the linear and star terpolymers, no differentiation was observed in the behavior of the isomeric networks in neutral water, reflecting the dense and constrained nature of the networks. However, differentiations in the DSs were measured for ionized networks, in which the statistical terpolymer-based isomers swelled more than the pentablock isomers which separated into microphases. This discrepancy was pronounced for the more hydrophobic BuMA-containing networks, which also displayed swelling differences among the isomeric pentablock networks. Finally, the network DSs in both neutral and acidic water decreased as the BuMA hydrophobic content increased.

Περίληψη

Γραμμικά και αστεροειδή ΑΒΓ τριαδρομερή τριπολυμερή και ΑΒΓΒΑ πενταδρομερή τριπολυμερή πρότυπα πλέγματα, αποτελούμενα από δύο υδρόφιλα μονομερή και ένα υδρόφοβο μονομερές, παρασκευάστηκαν με πολυμερισμό μεταφοράς ομάδας (group transfer polymerization, GTP). Παρασκευάστηκαν επίσης όλα τα αντίστοιχα τυχαία τριπολυμερή. Ο μεθακρυλικός εστέρας της μεθοξυ-εξα(αιθυλενογλυκόλης) [methoxy hexa(ethylene glycol) methacrylate, HEGMA, μη ιοντικός] και ο μεθακρυλικός 2-(διμεθυλαμινο)αιθυλεστέρας [2-(dimethylamino)ethyl methacrylate DMAEMA, θερμοευαίσθητος και ιοντιζόμενος] χρησιμοποιήθηκαν ως τα δύο υδρόφιλα μονομερή, ενώ είτε ο μεθακρυλικός μεθυλεστέρας (methyl methacrylate, MMA) είτε ο μεθακρυλικός *κ*-βουτυλεστέρας (*n*-butyl methacrylate, BuMA) χρησίμευσε ως το υδρόφοβο μονομερές. Ο διμεθακρυλικός διεστέρας της αιθυλενογλυκόλης (ethylene glycol dimethacrylate, EGDMA) ήταν ο διασταυρωτής που διασύνδεσε τις γραμμικές αλυσίδες σε αστεροειδή πολυμερή ή πλέγματα. Ο μονοδραστικός εκκινητής 1-μεθοξυ-1-(τριμεθυλοσιλοξυ)-2-μεθυλοπροπένιο (1-methoxy-1-(trimethylsiloxy)-2-methyl propene, MTS) χρησιμοποιήθηκε για τη σύνθεση των γραμμικών και των αστεροειδών τριπολυμερών, ενώ ο διδραστικός εκκινητής 1,4-δισ(μεθοξυ-τριμεθυλο-σιλοξυ-μεθυλενο)κυκλοεξάνιο (1,4-bis(methoxytrimethylsiloxymethylene)cyclohexane, MTSMC) χρησίμευσε για την παρασκευή των πλεγμάτων. Έξι ομάδες τριπολυμερών συντέθηκαν συνολικά, τρεις από τις οποίες αποτελούνταν από γραμμικά και καινοτόμα αστεροειδή τριπολυμερή, ενώ οι υπόλοιπες τρεις αποτελούνταν από καινοτόμα πλέγματα με καλά ορισμένες δομές που παρασκευάστηκαν για πρώτη φορά. Πέντε από τις έξι ομάδες αποτελούνταν από ισομοριακά αδρομερή τριπολυμερή που ήσαν ισομερή διαδοχής τμημάτων, ενώ η έκτη ομάδα αποτελείτο από πλέγματα τριπολυμερών με διαφορετικές περιεκτικότητες στο υδρόφοβο BuMA.

Τα μοριακά βάρη και οι κατανομές των μοριακών βαρών όλων των τριπολυμερών καθώς και των γραμμικών πρόδρομων των πλεγμάτων λήφθηκαν με χρωματογραφία αποκλεισμού μεγέθους (gel permeation chromatography, GPC) σε τετραϋδροφουράνιο (tetrahydrofuran, THF). Τα μοριακά αυτά βάρη είχαν τιμές κοντά στις θεωρητικά αναμενόμενες. Στατική σκέδαση φωτός (static light scattering, SLS) σε THF έδειξε ότι τα αστεροειδή τριπολυμερή έφεραν μεγάλους αριθμούς βραχιόνων, μεταξύ 40 και 80. Οι συστάσεις όλων των τριπολυμερών προσδιορίστηκαν με φασματοσκοπία πυρηνικού μαγνητικού συντονισμού πρωτονίων (proton nuclear magnetic resonance, ^{1}H NMR). Οι προσδιορισθείσες συστάσεις των τριπολυμερών που περιείχαν BuMA ήταν κοντά στις θεωρητικά αναμενόμενες, σε αντίθεση με αυτές των τριπολυμερών που περιείχαν MMA όπου μειωμένη ευκρίνεια στο διαχωρισμό των φασματικών κορυφών δεν επέτρεψε τον ακριβή προσδιορισμό των συστάσεων.

Όλα τα τριπολυμερή χαρακτηρίστηκαν σε υδατικό περιβάλλον. Συγκεκριμένα, οι υδροδυναμικές διάμετροι, οι αριθμοί συσσωμάτωσης, οι θερμοκρασίες νεφέλωσης των γραμμικών και των αστεροειδών τριπολυμερών προσδιορίστηκαν με δυναμική σκέδαση φωτός (dynamic light scattering, DLS), SLS και νεφελομετρία, αντίστοιχα, ενώ οι βαθμοί διόγκωσης (ΒΔ) των τριπολυμερών πλεγμάτων προσδιορίστηκαν σταθμομετρικά. Τα γραμμικά τριπολυμερή σχημάτισαν μικρά μικύλια στο νερό, με το τριπολυμερές που έφερε το υδρόφοβο τμήμα στο κέντρο να σχηματίζει ακόμη μικρότερα μικύλια. Συσσωμάτωση μεταξύ αστεροειδών τριπολυμερών παρατηρήθηκε μόνο σε μία περίπτωση. Τα υπόλοιπα, μη συσσωματωνόμενα, αστεροειδή τριπολυμερή παρουσίασαν υδροδυναμικές διαμέτρους που ήταν εξαρτώμενες από τη σειρά διαδοχής των τμημάτων, κάτι που αντανακλούσε διαφορετικές εσωτερικές δομές. Οι θερμοκρασίες νεφέλωσης των γραμμικών και των αστεροειδών τριπολυμερών εξαρτούνταν από τη σειρά διαδοχής

των τμημάτων, με τις θερμοκρασίες νεφέλωσης των αστεροειδών να είναι υψηλότερες από αυτές των γραμμικών λόγω του μεγαλύτερου αριθμού βραχιόνων των αστεροειδών σε σχέση με τους αριθμούς συσσωμάτωσης των μικυλίων των γραμμικών. Τα τυχαία γραμμικά και αστεροειδή τριπολυμερή είχαν τις χαμηλότερες θερμοκρασίες νεφέλωσης λόγω της πλήρους έκθεσης των υδρόφοβων μονάδων τους στο νερό.

Σε αντίθεση με τα γραμμικά και τα αστεροειδή τριπλυμερή, καμία διαφοροποίηση δεν παρατηρήθηκε στη συμπεριφορά των ισομερών πλεγμάτων σε ουδέτερο νερό, αντανακλώντας την πυκνή και με περιορισμένη ευελιξία φύση των πλεγμάτων. Παρόλα ταύτα, διαφοροποιήσεις στους ΒΔ εντοπίστηκαν στα ιοντισμένα πλέγματα, όπου τα πλέγματα βασισμένα σε τυχαία τριπολυμερή διογκώθηκαν περισσότερο από τα πλέγματα πενταδρομερών που ήταν μικροφασικά διαχωρισμένα. Αυτή η διαφορά ήταν μεγαλύτερη στα πιο υδρόφοβα πλέγματα με BuMA, τα οποία επέδειξαν διαφοροποιήσεις και ανάμεσα στους ΒΔ των διαφόρων ισομερών πενταδρομερών πλεγμάτων. Τέλος, οι ΒΔ των πλεγμάτων τόσο σε ουδέτερο όσο και σε όξινο (που επιφέρει ιοντισμό των πλεγμάτων) νερό ελαττώνονταν με αύξηση της σύστασης σε υδρόφοβο BuMA.

CONTENTS

TABLE LEGENDS

FIGURE LEGENDS

Figure 2.4. Annual number of papers on solution studies of ABC triblock terpolymers.

Figure 2.5. Linear terpolymer polyampholytes and their corresponding micelles formed in slightly alkaline aqueous solutions. D, A and M denote the DMAEMA, MAA and MMA units, which are depicted in grey, white and black, respectively.

Figure 2.6. Time transformation of aggregates from vesicles to Janus micelles and to shell cross-linked micelles at pH 1 for $2VP_{260}$-*b*-MMA_{50}-*b*-*t*BuA_{320} triblock terpolymer.

Figure 2.7. The three different micellar structures obtained for the MAA_{102}-*b*-$DMAEMA_{67}$-*b*-C_{60} terpolymer under different conditions.

Figure 2.8. TEM images of aggregates from solutions of the triblock terpolymer S_{180}-*b*-MMA_{67}-*b*-*t*BuA_{37} obtained at different water contents: (a) from a dioxane solution with 18 % w/w added water, (b) from a dioxane solution with 25 % w/w added water, (c) from a THF solution with 40 % w/w added water and (d) from a DMF solution with 55 % w/w water.

Figure 2.9. TEM image of the S_{200}-*b*-$2VP_{140}$-*b*-EO_{590} micelles prepared from a 75/25 w/w DMF-benzene mixture. Rods co-existing with spheres are observed.

Figure 2.10. Schematic representation of the ABC miktoarm stars reported by Li *et al.* The three different monomers constituting the arms of the star terpolymer, namely PEO, PFPO and PEE are depicted in three different colors.

Figure 2.11. Cryo-TEM images of 1 % w/w aqueous solutions of (a) the most hydrophilic μ-ABC terpolymers and (b) the least hydrophilic ones comprise PEO, PFPO and PEE arms.

Figure 2.12. Schematic illustration of the transition between the two micellar structures obtained at neutral and acidic pH for the PI-*b*-P2VP-*b*-PEO triblock terpolymers.

Figure 2.13. Schematic representation of the synthetic strategy followed for the preparation of Janus micelles. The figure displays the Janus micelles formed by the S_{930}-*b*-BD_{211}-*b*-MMA_{816} triblock terpolymer.

Figure 2.14. Schematic illustration of the conformation adopted by a Janus micelle monolayer at the air/water interface. The Janus micelle was formed by the S_{930}-*b*-BD_{211}-*b*-MMA_{816} triblock terpolymer.

Figure 2.15. Synthetic steps followed for the preparation of the nanotubes with PAA-lined cores formed by the hydrolyzed *t*-BuA units of the $BuMA_{1270}$-*b*-$CEMA_{190}$-*b*-*t*-BuA_{270} triblock terpolymer.

Figure 3.1. The separation of molecules with respect to their hydrodynamic volume by GPC. The smaller molecules (illustrated with the black circles) penetrate in the pores of the column, whereas the larger molecules pass through and are eluted faster.

Figure 3.2. The frequency distribution of the scattered light.

Figure 5.1. Chemical structures and names of the monomers and the cross-linker employed for the preparation of the terpolymers.

Figure 5.2. Chemical structures and names of the monofunctional and bifunctional initiators as well as the catalyst used for the GTP syntheses of all the terpolymers in this study.

Figure 5.3. Schematic representation of the synthetic procedure followed for the preparation of the $HEGMA_{10}$-*b*-MMA_{10}-*b*-$DMAEMA_{10}$ triblock terpolymer. The HEGMA units are shown in white, the MMA units in black and the DMAEMA units in gray. The "*" symbols indicate the "living" sites of the polymerization.

Figure 5.4. Schematic representation of the three diblock copolymers, the three triblock terpolymers and the statistical terpolymer, constituting the first polymer family, whose synthesis and characterization are presented in this Section. The color coding is the same as that employed in Figure 5.3 above.

Figure 5.5. ^{1}H NMR spectrum of the HEGMA$_{10}$-*b*-DMAEMA$_{10}$-*b*-MMA$_{10}$ ABC triblock terpolymer in $CDCl_3$.

Figure 5.6. Schematic representation of the structures of the spherical micelles formed by the three ABC triblock terpolymers in aqueous solution.

Figure 5.7. Schematic representation of the synthetic procedure followed for the preparation of the DMAEMA$_{10}$-*b*-HEGMA$_{10}$-*b*-MMA$_{10}$-*star* triblock terpolymer. The DMAEMA units are shown in gray, the HEGMA units in white, and the MMA units in black. The "∗" symbols indicate the "living" sites of the polymerization. The number of arms at the cross-links is not six, as indicated in the Figure, but 40 or higher.

Figure 5.8. Schematic representation of the eight terpolymers prepared and studied in the present Section. The color coding is the same as that used in Figure 5.7. The cross-linker is represented by the black circles.

Figure 5.9. GPC chromatograms of the DMAEMA$_{10}$-*b*-HEGMA$_{10}$-*b*-MMA$_{10}$-*star* and its three linear precursors. D, H, and M are further abbreviations for the DMAEMA, HEGMA and MMA units, respectively.

Figure 5.10. Schematic representations of the structures formed by the three linear ABC triblock terpolymers in water. H, D and M stand for HEGMA, DMAEMA and MMA, respectively. The color coding is the same as that employed in Figure 5.3.

Figure 5.11. AFM images of HEGMA$_{10}$-*b*-DMAEMA$_{10}$-*b*-MMA$_{10}$-*star* nanoparticles deposited on mica from aqueous solution.

Figure 5.12. Dependence of the cloud points of the linear and star terpolymers on their monomer distribution. The H, D and M abbreviations employed in the Figure stand for the HEGMA, DMAEMA and MMA monomer repeating units, respectively.

Figure 5.13. Dependence of the surface tension at the air-water interface on the

concentration of the linear and star terpolymers studied in the present Section.

Figure 5.14. Schematic representations of the seven star terpolymers prepared. HEGMA monomer repeating units are shown in white, DMAEMA units in gray and MMA units in black. The cross-linker is represented by the black circles.

Figure 5.15. Cloud points of the seven equimolar, isomeric star terpolymers.

Figure 5.16. Synthetic routes followed for the preparation of the eight isomeric networks.

Figure 5.17. Schematic representation of the synthetic procedure followed for the preparation of the model network based on the symmetrical pentablock terpolymer $DMAEMA_5$-*b*-$HEGMA_5$-*b*-MMA_{10}-*b*-$HEGMA_5$-*b*-$DMAEMA_5$. The DMAEMA units are shown in gray, the HEGMA units in white, and the MMA units in black. The "∗" symbols indicate the "living" sites of the polymerization. The number of arms at the cross-links is not three, as indicated in the Figure, but between 15 and 50.

Figure 5.18. Schematic representations of the structures of the eight networks of this study. The color-coding is the same as that in Figure 5.17. For the first six networks, the two networks in the same row have the same middle-block.

Figure 5.19. Degrees of swelling and degrees of ionization as a function of pH for all the networks discussed in this Section.

Figure 5.20. Degrees of swelling of the networks in THF, in neutral water, and in acidic water.

Figure 5.21. Temperature dependence of the degrees of swelling of the networks in neutral water.

Figure 5.22. ^{1}H NMR spectrum of the $DMAEMA_5$-*b*-$BuMA_5$-*b*-$HEGMA_{10}$-*b*-$BuMA_5$-*b*-$DMAEMA_5$ network precursor. The peaks corresponding to the *d*, *k* and *f*

CHAPTER 1: Introduction

1.1. General Introduction – Aim

A careful survey of the rapidly growing literature on the solution properties of ABC triblock terpolymers (see Chapter 2) revealed that most of the focus is on the preparation and study of linear systems. Only a small number of studies deals with cross-linked terpolymer systems such as mikto-arm stars, shell cross-linked micelles and Janus micelles (micelles with a corona having two different faces). None of the reported studies involved the preparation and solution characterization of stars with ABC triblock terpolymer arms. Furthermore, none of the reported studies was concerned with the preparation of terpolymer network structures. The scope of this Thesis was to contribute toward filling this gap. In particular, the aim of this Thesis was the synthesis and aqueous solution characterization of linear, star and network terpolymers and the elucidation of the effect of architecture, block sequence and terpolymer composition on their aqueous solution properties.

To this end, six families of amphiphilic terpolymers were prepared. Three out of the six families comprised the block sequence isomers of equimolar linear and star ABC triblock terpolymers (Sections 5.1-5.3). Two other families consisted of equimolar, symmetrical, block sequence isomeric networks based on linear ABCBA pentablock terpolymers (Sections 5.4 and 5.5). The sixth family was also based on ABCBA pentablock terpolymer networks in which, however, the length of the hydrophobic blocks was varied systematically (Section 5.6). For better comparison between the properties of the terpolymers within a family, some of the terpolymers were prepared twice, in two different families (Sections 5.1-5.2, 5.2-5.3 and 5.5-5.6), with the terpolymers presented in each Section being prepared the same day to ensure the same initiator reactivity and, therefore, comparable molecular weights between the different polymers within a certain family.

Group transfer polymerization (GTP) was the synthetic method employed for the preparation of all the terpolymer families studied in the present Thesis. GTP is a "living" polymerization method, providing control over the molecular weight and composition of the polymers. Furthermore, it enables the preparation of block copolymers and block sequence isomers simply by altering the order of monomer

addition. Moreover, GTP is rather less demanding than other "living" polymerization methods since it can also be carried out at room temperature. However, due to its main applicability to methacrylate monomers which present similar reactivities, GTP is the most appropriate synthetic method for the preparation of ABC triblock terpolymers of all the possible block sequences as well as statistical (random) terpolymers. Thus, GTP was the polymerization method of choice for the present syntheses.

In order to ensure water compatibility, all the terpolymers prepared in this study were composed of two hydrophilic and one hydrophobic component. All the three monomers used for the synthesis of each of the terpolymer families were commercially available. In particular, the two hydrophilic monomers employed were the bulky, non-ionizable methoxy hexa(ethylene glycol) methacrylate (HEGMA) and the marginally hydrophilic, temperature- and pH-sensitive 2-(dimethylamino)ethyl methacrylate (DMAEMA). In four out of the six terpolymer families, the hydrophobic blocks were composed of methyl methacrylate (MMA) units, whereas the more hydrophobic *n*-butyl methacrylate (BuMA) monomer was used in the remaining two families.

For the synthesis of the linear and the star terpolymers, 1-methoxy-1-(trimethylsiloxy)-2-methyl propene (MTS), a monofunctional initiator, was used, whereas the bifunctional initiator 1,4-bis(methoxytrimethylsiloxymethylene)cyclohexane (MTSMC) was employed for the preparation of the networks. Activation of the initiator was achieved by the tetrabutylammonium bibenzoate (TBABB) catalyst. Ethylene glycol dimethacrylate (EGDMA) was employed as the cross-linker to effect the interconnection of the linear chains at one or at both active ends, resulting in the formation of star polymers or polymer networks, respectively.

The presence of the hydrophobic blocks in the terpolymers would lead to microphase separation in water, resulting in various micellar structures depending on the topology of the hydrophobic block in the terpolymer chain. Indeed, the results of the present study confirmed this assumption, with the terpolymers bearing the hydrophobic block at the end of the linear terpolymer chains forming the largest micelles. Furthermore, a differentiation in the solution properties was expected for the various architectures

(linear, star and networks) being less pronounced for the terpolymer networks due to their denser nature, also confirmed by the experimental results obtained by the present study.

The novelty of the present Study lies in the fact that it combines the linear ABC triblock terpolymer architecture with the star architecture by the preparation of stars composed of many arms each one being an ABC triblock terpolymer and the investigation of their solution properties. The same applies for the preparation of the model networks based on linear pentablock terpolymer chains and the study of their swelling properties in various solvents.

1.2. Definitions

Polymers are molecules of high molecular weight composed of many repeating units called *monomers*. A *linear homopolymer* comprises only one type of repeating units, with each unit connected exactly with two others, with the exception of the two end units. Polymers composed of two different types of monomer repeating units are called *copolymers*, while those comprising three different types of monomer repeating units are called *terpolymers*. When the different types of repeating units are located in discrete blocks along the polymer chain the copolymer or terpolymer is called *block copolymer* or *terpolymer*, whereas when they are randomly distributed it is called *random or statistical*.[1] *ABC triblock* terpolymers preserve the properties of the three constituting homopolymers much better than the corresponding *statistical* terpolymers where the three components are randomly distributed along the polymer chain.

Figure 1.1 shows schematic representations of one linear diblock and one statistical copolymer. The two different monomer repeating units are shown in different colors.

(a) (b)

Figure 1.1. Schematic representation of (a) a block and (b) a statistical copolymer.

The various segments that constitute the block copolymers are usually mutually incompatible, resulting in their self-assembly in melts and in solutions. Such polymers have at least one lyophilic and one lyophobic segment and are called amphiphilic block copolymers.

The microstructures formed in solvents selective for one block resemble micelles formed by low molecular weight surfactants.[1] In particular, the lyophobic segment collapses forming the core of the micelle, whereas the lyophilic segment expands in the solution and forms the micellar corona surrounding the lyophobic core. A representation of such aggregates is given in Figure 1.2.

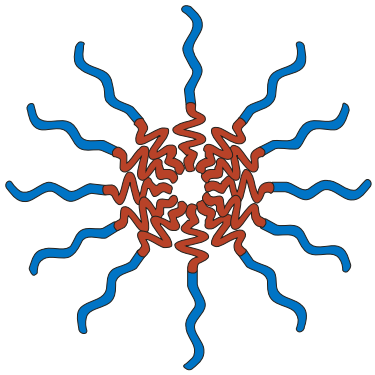

Figure 1.2. Schematic representation of a spherical micelle. Lyophobic segments forming the micellar core are shown in red color, while the lyophilic corona-forming segments are colored blue.

The cross-linking of the linear polymeric chains at one end results in the formation of *star* polymers. When the arms emanating from the star central core are the same (all the same homopolymers or all the same copolymers), these stars are called homoarm[2] stars, and when they are different, those star are called heteroarm[3] stars. Heteroarm star copolymers have been extensively studied.[3] These two categories are shown in Figure 1.3 below:

(a) (b)

Figure 1.3. The two types of star copolymers: (a) heteroarm star block copolymer (b) homo-arm star copolymer. Different colors are used for the different segments.

When the polymer chains are cross-linked at both ends, three dimensional structures called polymer *networks* are formed. Polymer networks can be divided in two large categories based on the distribution of the cross-links in the polymeric chains: randomly cross-linked networks and model networks. *Randomly cross-linked* networks are the networks in which the cross-links are randomly distributed, resulting in a broad distribution of the length of the chains between cross-links (called *elastic*

chains). In this type of networks the length of the elastic chains between cross-links varies. In contrast, *model networks* have their cross-links placed regularly, usually at equal distances, leading to elastic chains of narrow size distribution.[4] Figures 1.4(a) and (b) display parts of a randomly cross-linked network and a model network, respectively.

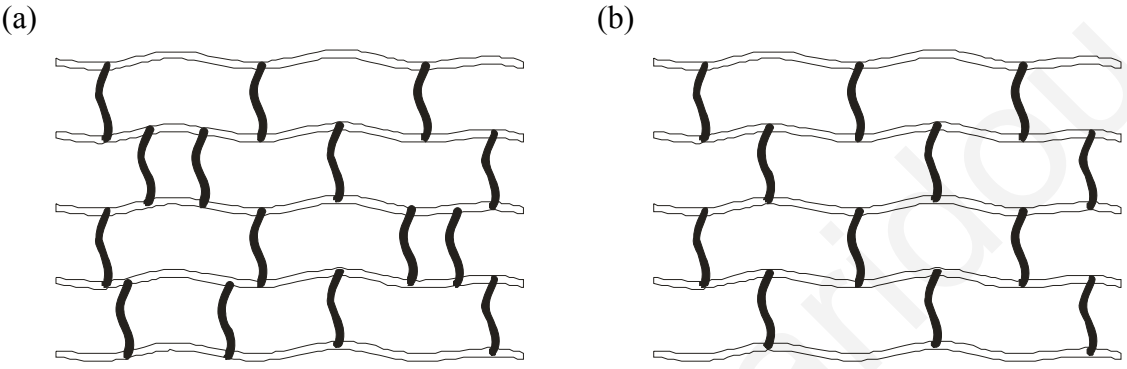

Figure 1.4. Schematic representations of (a) a randomly cross-linked network and (b) a model network. Cross-link nodules are represented as vertical black-colored segments.

Networks are elastic materials that usually absorb a large amount of the solvents they are in, resulting in their swelling without dissolving. When networks are placed in a *good solvent*, that is a solvent with which they experience favorable interactions, they swell, their elastic chains expand, and the adjacent cross-linking nodules move away from each other. On the other hand, when networks are placed in a *poor solvent*, that is a solvent with which they experience unfavorable interactions, their elastic chains contract and the neighboring cross-links approach each other. The swelling and shrinking processes are fully reversible. Networks comprising at least one hydrophilic structural unit are called *hydrogels*. Hydrogels have the ability, when in aqueous environment, to absorb water quantities that are many times their dry mass and swell.

An amphiphilic hydrogel is a polymer network with both hydrophilic and hydrophobic units.[4] One such network is shown in Figure 1.5. White color is used to symbolize the hydrophilic segments and black color the hydrophobic ones. In a *non-selective* solvent, such as tetrahydrofuran (THF), both the hydrophilic and the

hydrophobic segments expand. When placed in water, which is a *selective* solvent, the hydrophilic segments expand, whereas the hydrophobic segments collapse, that is the network undergoes *microphase separation*.[5]

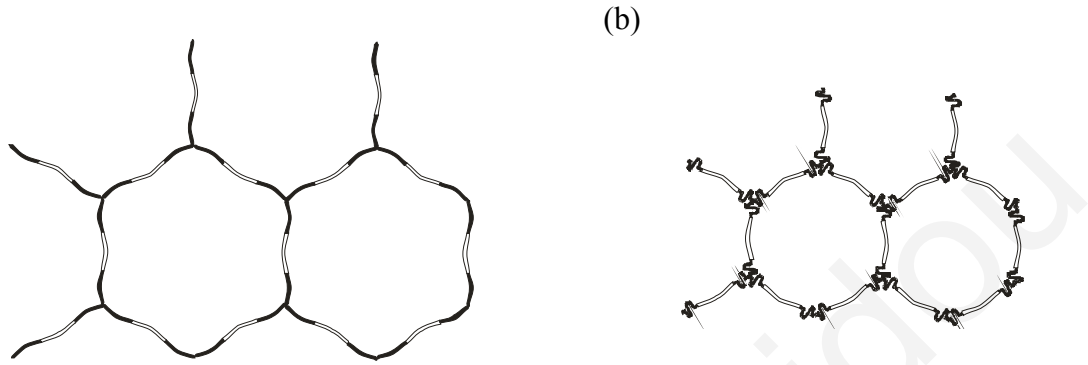

Figure 1.5. Schematic representation of the chain conformations of an amphiphilic network in (a) a non-selective solvent and (b) water. White color is used for the hydrophilic segments and black color for the hydrophobic.

The relative amount of solvent that a network can absorb is called the *degree of swelling* (DS). In this Thesis, the DS is defined as the ratio of the network wet mass divided by its dry mass. Some other authors define DS as the ratio of the mass of the adsorbed solvent divided by the network dry mass. DSs are usually determined gravimetrically, but they can also be determined from the geometric dimensions of the network in the wet and dry states.

1.3. Micellization

Polymers are usually mutually incompatible to one another. This incompatibility between the blocks of a block copolymer results in *microphase separation*, a situation where block copolymer molecules aggregate, forming various morphologies in the bulk (see Chapter 2). A similar situation is observed in solutions with the self-assembly of block copolymer molecules into micellar structures. The latter is commonly observed upon the dissolution of amphiphilic molecules in a selective solvent. As mentioned above, amphiphilic molecules are composed of a lyophilic and a lyophobic part. The word amphiphilic originates from the Greek word "αμφίφιλος" (αμφί + φίλος), denoting the double nature of these molecules due to the presence of

lyophilic and lyophobic parts. The lyophilic part likes being in the solvent, whereas the interactions of the lyophobic block with the solvent molecules are not favored.
The micellization process of block copolymers in solvents selectively poor for one of the blocks is generally considered to resemble that of low molecular weight amphiphilic molecules in aqueous or organic media. In very dilute solutions, block copolymers exist as single chains. When the concentration of the block copolymer reaches a critical value, the so-called *critical micelle concentration (cmc)*, block copolymer molecules begin to associate to form micelles[6] with the insoluble block in the core and the soluble block pointing outward. The *cmcs* of the block copolymers are normally much lower than those of low molecular weight surfactants and are, therefore, difficult to determine with some experimental techniques (light scattering).[7]
The tendency of amphiphilic molecules to form micelles in water is a consequence of the *hydrophobic effect*.[6,8,9] Water is a liquid with a highly ordered structure, forming four hydrogen bonds per molecule. Addition of hydrocarbon molecules in water disrupts of this order. Upon the self-assembly of the hydrocarbon molecules into micelles, the water molecules are reoriented so they can participate in hydrogen bond formation more or less as in bulk water.[10] This reorientation or restructuring of water molecules around the hydrocarbon solutes is *entropically* very unfavorable, since it disrupts the existing water structure and imposes a new and more ordered structure on the surrounding water molecules.

The self-assembly behavior of the block copolymers in organic and aqueous media depends on the degree of polymerization, the composition of each block and the Flory-Huggins polymer-solvent interaction parameters. Furthermore, the statistical segment length and the monomer volume are taken into account.

Assuming a diblock copolymer comprising lyophobic A and lyophilic B blocks is placed in a solvent selective for the B blocks, then the A blocks form the micellar core, while the B blocks form the corona. Depending on the lengths of the A and B blocks two types of micelles can be formed:[11]
(a) *crew cut micelles*, composed of a large core and very short corona chains. These micelles are formed when the length of the lyophobic block is larger than the length of the lyophilic block. And

(b) *hairy micelles*, constituted of a small core and a large corona. This type of micelles is observed in the case of block copolymers bearing long lyophilic and short lyophobic blocks.

Similar spherical micellar morphologies are formed by ABC triblock terpolymers depending on the number of lyophobic and lyophilic blocks in the terpolymer chain. In particular,

(a) *core-shell-corona* micelles are formed by ABC triblock terpolymers composed of one lyophobic and two lyophilic blocks

(b) and *core-shell micelles* are formed by ABC triblock terpolymers comprising two mutually compatible lyophobic and one lyophilic block.

Different morphologies were obtained for water-organic solvent mixtures (see Chapter 2).

1.4. Polymer Synthesis by Group Transfer Polymerization

Group transfer polymerization (GTP) was the method employed for the preparation of the linear, star and network polymers presented in this Thesis. GTP is a "living" polymerization technique for (meth)acrylates developed in 1983 by O. W. Webster and co-workers[12] and patented by DuPont for the preparation of dispersants for water-based printing ink for inkjet printers.[13,14] About 10 years ago the GTP patents were sold to ICI, but are co-owned by DuPont. As in all "living" polymerization processes, also in GTP no termination of the active sites occurs, and the active anionic chain-ends remain active after the depletion of all monomer.[15] Upon further monomer addition the polymerization resumes. In the absence of moisture or protic impurities the "living" sites remain active unless a terminating agent is added to the polymerization flask. As in anionic polymerizations, monomers bearing labile hydrogens would deactivate the sites, hence these proton-donating sites should be protected, for instance by silylation or by means of dihydropyran.[16] The initiator triggers chain growth and its residue is attached to the non-growing chain end. A catalyst is necessary for initiation and propagation. This catalyst is not consumed during GTP. In all systems the initiation step must be faster than or of the same rate as chain propagation to achieve homogenous chain growth. This can suitably be accomplished if the structure of the initiator is the same as that of the growing chain-end. In GTP this structure is of a silyl ketene acetal.[17] Since all initiator molecules

are activated and all monomer is polymerized, the degree of polymerization (DP) is determined by the relative amounts of monomer and initiator used:

$$\mathrm{DP} = \frac{[\mathrm{monomer}]}{[\mathrm{initiator}]} \tag{1.1}$$

The polymers obtained by "living" polymerization techniques exhibit narrow molecular weight distributions. The molecular weight polydispersity (PDI) obeys a Poisson distribution, expressed:

$$PDI \equiv \frac{M_w}{M_n} = 1 + \frac{1}{DP} \tag{1.2}$$

where M_w is the weight-average molecular weight, and M_n is the number-average molecular weight. During a "living" polymerization the M_n is directly proportional to monomer conversion. GTP is particularly applicable to unsaturated monomers carrying electron withdrawing substituents, such as methacrylate or acrylate esters, and it enables the synthesis of block copolymers by sequential monomer addition as well as the synthesis of end-functional polymers by selective termination of the "living" ends with the appropriate reagents.

GTP is a fast, convenient polymerization method taking place at ambient temperatures and providing quantitative polymer yields. On the other hand, polymers obtained by GTP can have maximum molecular weights only up to around 50 000 g mol^{-1}. Another disadvantage of the method is its limited applicability, since only monomers bearing carbonyl or cyanide groups in their side chains can be employed.[16] Methacrylate monomers are the most suitable for polymerization by GTP. The simplest initiator for GTP is 1-methoxy-1-(trimethylsiloxy)-2-methyl propene (MTS), which is commercially available but rather expensive.

In order for the initiator to be activated, the presence of a catalyst is required. The catalysts used are either Lewis acids (at 10 mol % with respect to monomer) or nucleophilic anions. The most active catalysts used are fluorides and bifluorides, whereas carboxylates and bicarboxylates are preferred for use at above ambient temperatures.[17] A large counterion is required for maximum efficiency to be achieved. Tetrabutylammonium salts (TBA) gained favor because they are more

readily available. The catalysts should be used at about 0.1-1 mol % with respect to the initiator concentration. If an excessive amount of catalyst is used, the polymerization ceases.

Two possible mechanistic routes were proposed for the nucleophilically catalyzed GTP,[17,18] the associative, and the dissociative path:

(a) the associative path proposed by Sogah and co-workers[19] where the silyl ketene acetal group is activated by complexation with the catalyst, forming a pentacoordinated siliconate for addition to monomer. The silyl group transfers to the carbonyl group of an incoming monomer and remains on the same polymer chain during the polymerization step. The associative mechanism is illustrated in Figure 1.6.

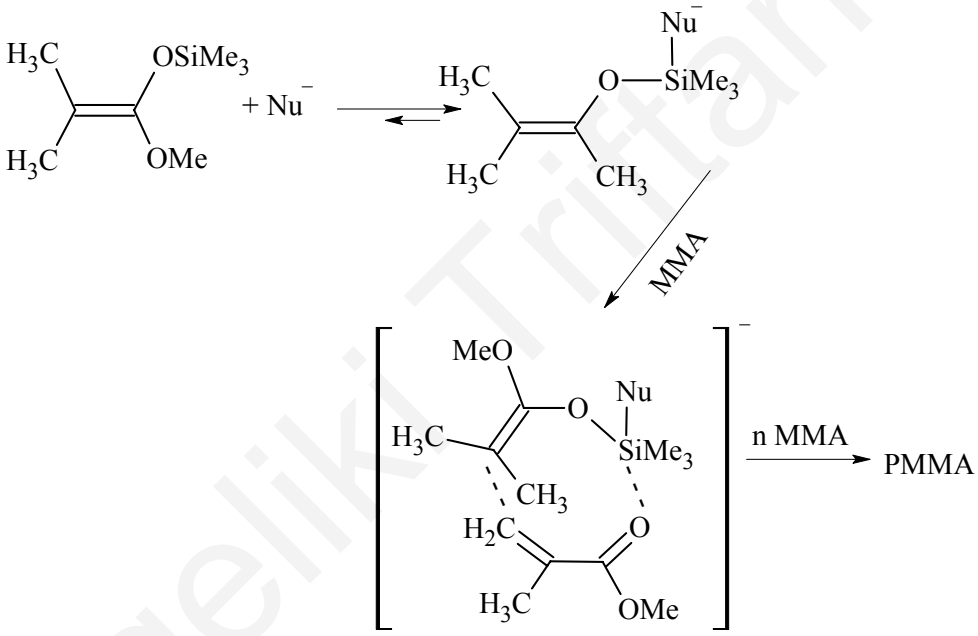

Figure 1.6. The associative mechanism for nucleophilically catalyzed GTP.

(b) the dissociative path[20,21] where the nucleophilic catalyst complexes with the silyl ketene acetal end groups of the initiator, forming the pentacoordinate siliconate, which generates a reactive enolate anion through a reversible cleavage step. The enolate anion then undergoes 1,4-addition[20,22] to the monomer forming a new C-C bond at the C-atom of the enolate forming an anion bearing a monomer unit. The end groups are then capped by R_3SiNu to regenerate the silyl ketene acetal ends and the nucleophilic catalyst. The dissociative mechanism is shown in Figure 1.7.

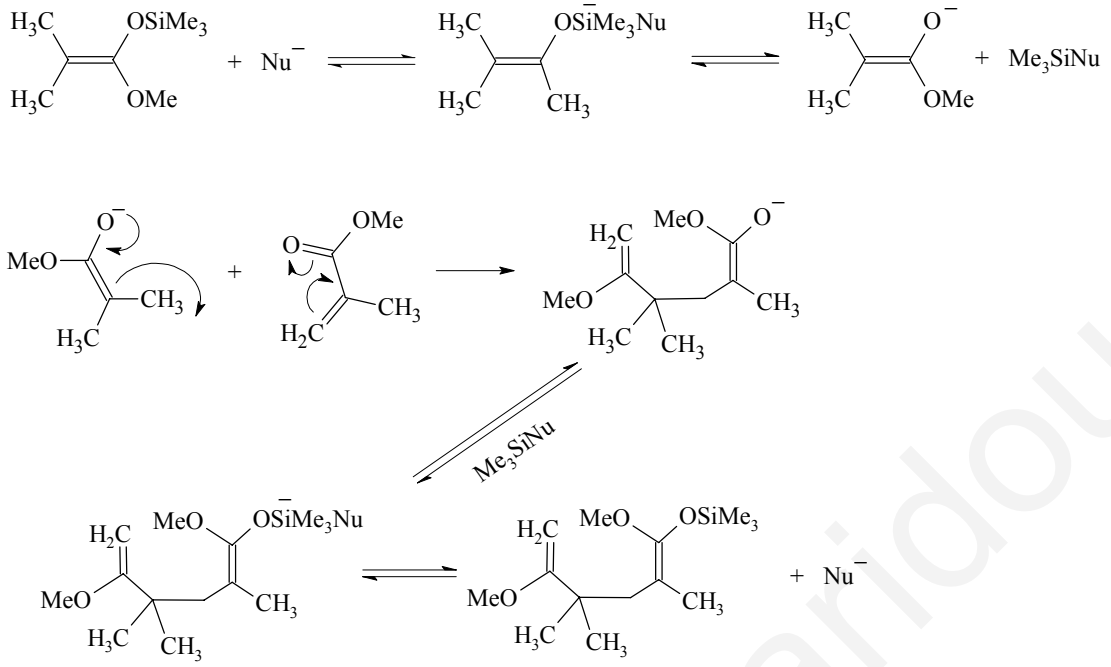

Figure 1.7. Dissociative mechanism for nucleophilically catalyzed GTP.

In order for the criteria for the production of controlled molecular weight polymers with low molecular weight polydispersities to be met, the equilibrium that generates the enolate ends must be faster than the rate of polymerization.

Some of the GTP phenomena that were taken into account for the resolution of the GTP mechanism are listed below:[17]

- a large amount of catalyst decreased the rate of the polymerization reaction due to the possible generation of more enolate than can be stabilized.
- the induction periods observed before the beginning of the polymerization indicated the production of a small amount of enolate by the catalyst. In the case of an assosiative mechanism the formation of the catalyst/silylketene acetal complex would not need an induction period.
- rapid end group exchange in the presence of anionic catalysts attributed to the formation and dissociation of an ester enolate end with neutral silyl ketene acetal ends.

The above observations suggested a dissociative mechanism, including a nucleophilic Mukiayama-Michael addition of the silyl ketene acetal group to the double bond of a monomer as explained above and shown in Figure 1.7.

CHAPTER 2: Literature Review on ABC Triblock Terpolymers

Even though the synthesis of ABC triblock terpolymers was first reported about two decades ago,[23] there is only a relatively small number of studies investigating their solution properties. In the following Section (2.1) we briefly review literature on ABC in bulk, and in the next Section (2.2) we review solution characterization.

2.1. Studies in the Bulk

The first studies of ABC triblock terpolymers involved the investigation of their morphology in the bulk. The syntheses were usually performed using anionic polymerization and the monomers most commonly used were styrene (S), butadiene (BD) (with or without post-polymerization hydrogenation), isoprene (I), methyl methacrylate (MMA) and vinyl pyridine (VP). The nature of the monomers and their degree of polymerization are the parameters determining the incompatibility between the blocks. Triblock terpolymer systems of sufficient interblock incompatibility microphase-separate in the bulk, providing morphologies consisting of three rather than two microphases. Figure 2.1 below depicts the morphologies exhibited in the bulk by triblock terpolymers of various compositions.

Many of the morphologies shown in the Figure are direct extensions of the morphologies presented by diblock copolymers in the bulk (bilamellae, cylinders and spheres) such as trilamellae,[23] and cylinders or spheres at dilamellar interfaces.[25] However, some unique morphologies also appear, such as cylinders surrounded by rings or helices, embedded in a continuous matrix. These morphologies were predicted by Zheng and Wang[25] who reported theoretical predictions of the morphological phase diagrams for ABC triblock terpolymers in the strong segregation limit. Their study focused on the morphology dependence on the block sequence and the relative strength of various interaction parameters. The free energy of the system can be separated into two parts: (a) an entropic chain-conformational free energy and (b) an interfacial free energy, the strength of which is characterized by the Flory-Huggins interaction parameters.

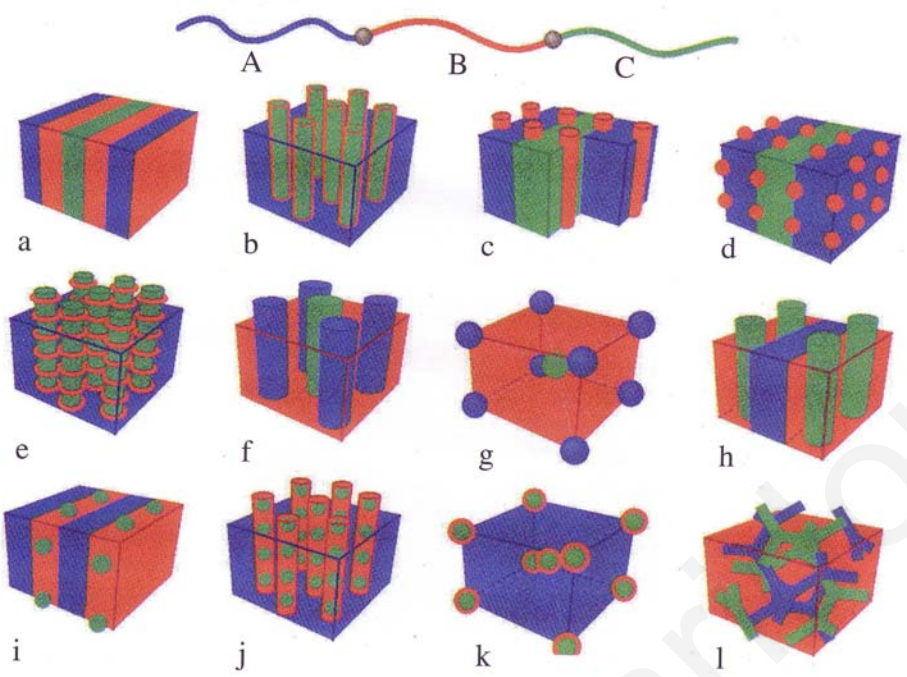

Figure 2.1. Morphologies formed by ABC triblock terpolymers in the bulk.[24] The three chemically different components are shown in three different colors: red, blue and green.

The ABC triblock terpolymers can be classified into six categories according to the relative ratios of the interfacial tensions γ_1 and γ_2, as illustrated in Table 2.1.

Table 2.1. The six categories of ABC triblock terpolymers based on their interfacial tensions.[25]

(1) $\gamma_1 = 1, \gamma_2 < 1$	(2) $\gamma_1 = 1, \gamma_2 = 1$	(3) $\gamma_1 = 1, \gamma_2 > 1$
(4) $\gamma_1 > 1, \gamma_2 < 1$	(5) $\gamma_1 > \gamma_2 > 1$	(6) $\gamma_2 > \gamma_1 > 1$

where $\gamma_1 = \frac{\sigma_{bc}}{\sigma_{ab}}$ and $\gamma_2 = \frac{\sigma_{ac}}{\sigma_{ab}}$, with σ denoting the interfacial tension between the two interfaces. Once the relative strength of the interaction parameters is specified, then the morphology is uniquely determined by the composition of the system. At each grid point of the phase diagram, the free energies of all the morphologies listed in Figure 2.2 were calculated and the equilibrium state was determined by the morphology with the lowest free energy.

The phase diagrams obtained for the block sequence isomers PS-*b*-P(E-*co*-B)-*b*-PMMA, PS-*b*-PMMA-*b*-P(E-*co*-B) and PMMA-*b*-PS-*b*-P(E-*co*-B), where P(E-*co*-B) denotes the ethylene-*co*-1-butene block, are given in Figure 2.2.

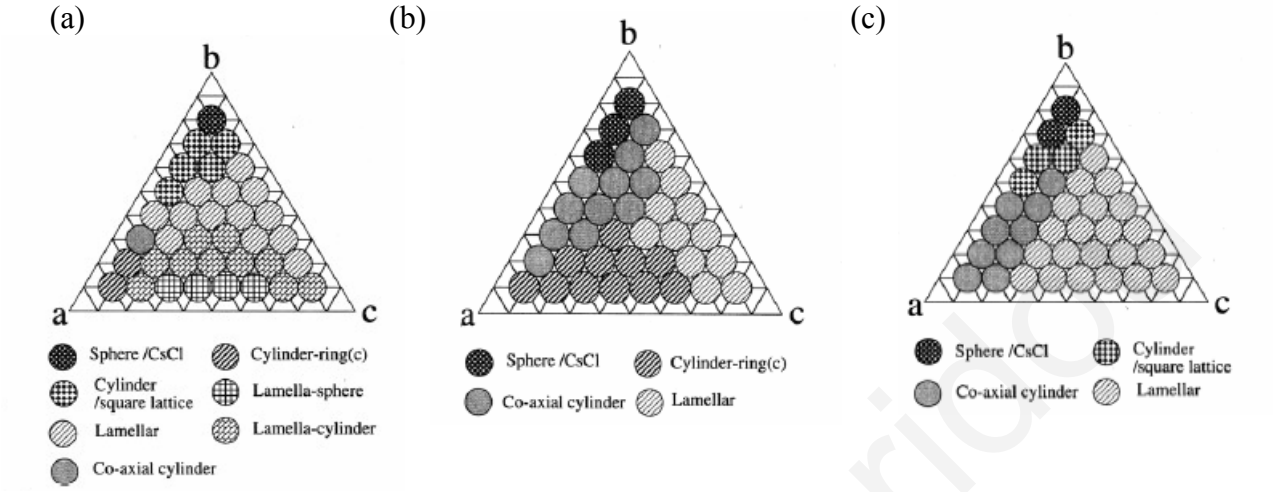

Figure 2.2. Phase diagrams obtained for (a) PS-*b*-P(E-*co*-B)-*b*-PMMA with γ_1=1.9 and γ_2=0.3 (b) PS-*b*-PMMA-*b*-P(E-*co*-B) with γ_1=6.33 and γ_2=3.33 and (c) PMMA-*b*-PS-*b*-P(E-*co*-B) of with γ_1=3.33 and γ_2=6.33.[25]

Comparing Figures 2.2(b) and (c), it is apparent that the morphologies obtained depend on the sequence of the blocks in the polymer chain. In addition to the already experimentally observed morphologies, these researchers predicted some new structures not yet identified by the experiment. These were the lamella-cylinder II phase (depicted in Figure 2.2(h)), the lamella-sphere II phase (Figure 2.2(i)) and the cylinder-sphere phase (Figure 2.2(j)).

Krappe and colleagues[26] reported on the microphase separation of the two triblock terpolymers S_{528}-*b*-BD_{480}-*b*-MMA_{1370} and S_{470}-*b*-BD_{277}-*b*-MMA_{1418} prepared by anionic polymerization. In both terpolymers the middle block was shorter than the two end-blocks. Transmission electron microscopy (TEM) was employed for their morphological characterization. A transition of the hexagonally packed cylindrical core-shell morphology to a morphology where the PBD block formed cylinders at the PS-PMMA interface was observed. TEM images obtained for the S_{528}-*b*-BD_{480}-*b*-MMA_{1370} triblock terpolymer revealed the formation of PS cylinders surrounded by PBD helices in a PMMA matrix. Both left- and right-handed helical structures were observed, located either on the same cylinder or on different cylinders. The helical

morphology was obtained by casting the terpolymers from various solvents with different solubilities for the three components, and annealing for different periods. The observed morphologies did not change with annealing time implying that these morphologies were the equilibrium morphologies.

The same monomer combination was prepared also by anionic polymerization and studied by Stadler and co-workers.[27] In particular, they prepared three PS-*b*-PBD-*b*-PMMA triblock terpolymers that were symmetrical with respect to the PMMA and PS end-blocks, while their middle block had a composition that varied from 6-38 % w/w. TEM was employed for the characterization of the morphologies obtained with the PS-*b*-PBD-*b*-PMMA triblock terpolymers and their hydrogenated analogues PS-*b*-P(E-*co*-B)-*b*-PMMA. They also reported on the morphologies expected based on theoretical calculations. Both PS-*b*-PBD-*b*-PMMA and PS-*b*-P(E-*co*-B)-*b*-PMMA with 38 % w/w in the middle block were found to form lamellae. Different morphologies were obtained for the different middle block compositions as well as in the case of the hydrogenated analogues. In particular, in the case of PS-*b*-P(E-*co*-B)-*b*-PMMA with 17 % w/w in the middle block, TEM revealed the formation of cylinders of the (E-*co*-B) block at the PMMA/PS interface. The same pattern was also observed for the non-hydrogenated analogue. Upon reducing the amount of PBD to 6 % w/w, a change in morphology was observed to PS/PMMA lamellae with PBD spheres at their interface. In its hydrogenated analogue, PS was found to form cylinders surrounded by P(E-*co*-B) rings embedded in a PMMA matrix.

Hückstädt and colleagues[28] employed anionic polymerization to prepare four ABC triblock terpolymers with block sequence PS-*b*-PBD-*b*-P2VP and three ABC triblock terpolymers with the sequence PBD-*b*-PS-*b*-P2VP. The seven terpolymers prepared had constant weight fraction ratios of the PS to the PBD blocks (1.5 for the PS-*b*-PBD-*b*-P2VP terpolymers and 1.9 for the PBD-*b*-PS-*b*-P2VP), while the P2VP weight fraction varied. TEM revealed that all three PBD-*b*-PS-*b*-P2VP triblock terpolymers formed morphologies where the three different components were separated into different lamellae. The authors attributed this to the strong incompatibility among the three components. In some regions of the same TEM image, cylinders were observed and were attributed to the molecular weight polydispersity. For the triblock terpolymers with block sequence PS-*b*-PBD-*b*-P2VP, they observed the formation of hexagonally packed P2VP cylinders surrounded by a PBD shell in a PS matrix.

Upon increasing the P2VP content, the morphology changed to core-shell double gyroid, while further increase of the P2VP content led to a distorted core-shell gyroid morphology.

Ludwigs *et al.*[29] also employed PS and P2VP to prepare by anionic preparation fifteen PS-*b*-P2VP-*b*-Poly(*tert*-butyl methacrylate) (PS-*b*-P2VP-*b*-P*t*BuMA) triblock terpolymers and two PS-*b*-P2VP diblock copolymers. In the triblock terpolymers the block length ratios of the PS and P2VP blocks were kept constant at 1:1.2 and 1:1.4, while the length of P*t*BuMA was systematically varied. The aim in this work was to explore certain regions of the ternary phase diagram. TEM and SAXS were employed for the determination of the morphologies of the bulk phases of the triblock terpolymers as well as the diblocks. A change in morphology from lamellae (obtained for the symmetric composition) via a core-shell double gyroid to core-shell cylinders was found upon decreasing the P*t*BuMA content. A slight decrease of the P*t*BuMA content from the symmetrical composition led to the formation of an inverse core-shell double gyroid, whereas further decrease led to a cylinder-in-lamella morphology which did not have an analogue in diblock copolymers. This was due to the asymmetry of the interactions between the adjacent blocks. Further decrease in the content of the P*t*BuMA block led to a morphology comparable to binary block copolymers, where only two different microphases can be distinguished. This was attributed to the vanishing repulsion between the two outer blocks in combination with an entropic gain of the middle block.

Mogi and co-workers[30] reported on the bulk characterization of five PI-*b*-PS-*b*-P2VP triblock terpolymers, prepared by anionic polymerization, bearing two symmetrical end-blocks, while the volume fraction of the middle block varied from 35-66 % w/w. TEM revealed the formation of a complex structure, named "ordered tricontinuous double-diamond, OTDD", where each of the end-blocks formed a diamond framework domain, mutually interwoven, where the middle block formed the matrix. The two diamond frameworks are illustrated in Figure 2.3.

Figure 2.3. Representation of the double-diamond frameworks. The diamond structures formed by each of the end-blocks mutually interpenetrate.[30]

The same structure was observed by Matsushita *et al.*[31] for two ABC triblock terpolymers, prepared using anionic polymerization, with structure PS-*b*-PI-*b*-P2VP.

2.2. Studies in Solution

As mentioned above, the study of the properties of ABC triblock terpolymers in the bulk received sufficient attention. Recently, the study of the solution properties of ABC triblock terpolymers has started to attract the interest of the scientific community,[32] as evidenced by the increasing number of publications reported in this research area (see Figure 2.4). The number of publications on ABC terpolymers characterized in solution per year reported until today is illustrated in Figure 2.4.

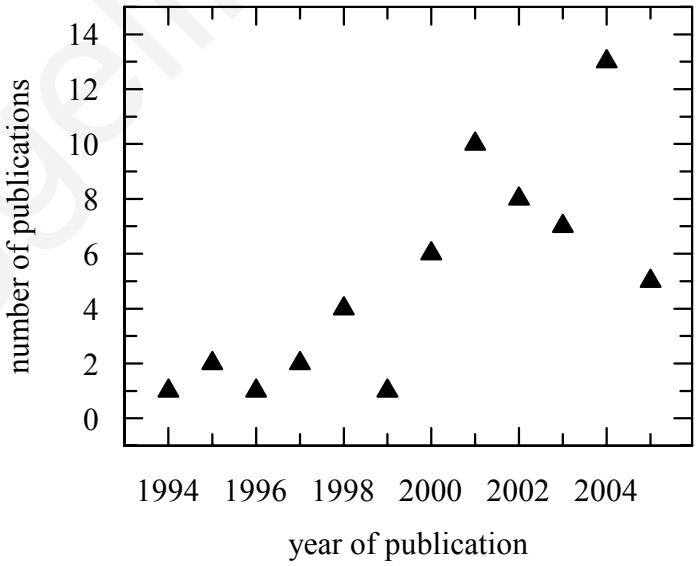

Figure 2.4. Annual number of papers on solution studies of ABC triblock terpolymers.

These publications can be divided into the following three main categories based on the combination of the functions of the three monomer repeating units. Each one of these categories consists of subcategories that are shown below:

(a) terpolymers with two lyophilic and one lyophobic blocks (27 publications)
- Two simple lyophilic and one lyophobic blocks (8)
- One neutral lyophilic, one temperature-sensitive lyophilic and one neutral lyophobic blocks (5)
- One positively charged, one negatively charged and one neutral lyophobic blocks (12)
- Two hydrogen bonding and one lyophobic/lyophilic blocks (2)

(b) terpolymers with one lyophilic and two lyophobic blocks (16 publications)
- One lyophilic and two compatible lyophobic blocks (8)
- One lyophilic and two mutually-incompatible lyophobic (8)

(c) terpolymers with one lyophilic, one lyophobic and one cross-linkable blocks (17 publications)
- Shell cross-linked micelles (10)
- Janus micelles (7)

The names of the monomers used for the synthesis of the triblock terpolymers and their abbreviations as will be used in the text below are listed in Table 2.2. The references wherein each monomer was reported for the preparation of the terpolymers are also shown in the Table. The names and abbreviations for the characterization methods employed for the terpolymer characterization and the various solvents used are given in Tables 2.3 and 2.4, respectively.

Table 2.2. Monomers constituting the various ABC triblock terpolymers of this review, placed alphabetically with respect to their abbreviated names, and some of their relevant physical and chemical properties.

Abbrevation	Name	solvent	lyophilic	lyophobic	T-sens	pH-sens	H-bonding	cross-linkable	ref.no.
2VP	2-vinylpyridine	water		yes		yes			56,61-63, 65,75
		THF	yes					yes	88
		THF/water				yes			51
		DMF					yes		59
		toluene		yes					33,88
4VP	4-vinylpyridine	DMF/water				yes		yes	54
		THF/water				yes			51,54
A	exo-7-oxabicyclo[2.2.1]hept-5-ene-2,3-dicarboximideAA: acrylic acid	$CHCl_3$					yes		58
AA	acrylic acid	dioxane	yes						60
		THF	yes						60
		DMF	yes				yes		59,60
		water	yes			yes		yes	56,66-68, 71,80
		DMF/water	yes			yes			54,60
		dioxane/water	yes						38,60
		THF/water	yes			yes			51,54,60
Ai	5-(N,N-dimethylamino) isoprene	THF/water				yes			53
AMA	allyl methacrylate	toluene/methanol	yes						81
		methanol		yes					81
		methanol/THF		yes					81

Table 2.2. Monomers constituting the various ABC triblock terpolymers of this review, placed alphabetically with respect to their abbreviated names, and some of their relevant physical and chemical properties.

Abbrevation	Name	solvent	lyophilic	lyophobic	T-sens	pH-sens	H-bonding	cross-linkable	ref.no.
B	2-acetylamino-6-[exo-hexan-7-oxabicyclo[2.2.1]hept-5-ene-2,3-dicarboximidoylamino]pyridine	$CHCl_3$					yes		58
BD	butadiene	water		yes				yes	72,91,92
		THF						yes	91
BuMA	butyl methacrylate	water		yes					66,71
		cyclohexane		yes					
		THF	yes						
		acetone	yes						
		toluene	yes						87,88
		dichloromethane	yes						
		chloroform	yes						87
BzMA	benzyl methacrylate	water		yes					44
C	exo-N-butyl-7-oxabicyclo[2.2.1]hept-5-ene-2,3-dicarboximide	$CHCl_3$		yes					58
C_{60}	fullerene	water		yes					57
CEMA	cinnamoyloxyethyl methacrylate	THF/hexane						yes	78-79,81
								yes	93-94

Table 2.2. Monomers constituting the various ABC triblock terpolymers of this review, placed alphabetically with respect to their abbreviated names, and some of their relevant physical and chemical properties.

Abbrevation	Name	solvent	lyophilic	lyophobic	T-sens	pH-sens	H-bonding	cross-linkable	ref.no.
DEAEMA	2-(diethylamino)ethyl methacrylate	water		yes		yes			39,55,84-86
		THF/methanol	yes						84
DMAEMA	2-(dimethylamino)ethyl methacrylate	water			yes	yes		yes	39,42-44, 52,46-50,57,82,83,85
DMS	dimethylsiloxane	hexane	yes						64
		water		yes					35
EE	ethyl ethylene	water		yes					73,74
EG	ethylene glycol	benzene	yes						89
		wate	yes						89
EHA	2-ethylhexyl acrylate	water		yes					68
EO	ethylene oxide	water	yes						35-37,39,61-63,65,72-75,82,85,86
		water/dioxane	yes						38
EOEOVE	2-(2-ethoxy)ethoxy ethyl vinyl ether	water			yes				45
EOVE	2-ethoxyethyl vinyl ether	water		yes					45

Table 2.2. Monomers constituting the various ABC triblock terpolymers of this review, placed alphabetically with respect to their abbreviated names, and some of their relevant physical and chemical properties.

Abbrevation	Name	solvent	lyophilic	lyophobic	T-sens	pH-sens	H-bonding	cross-linkable	ref.no.
EVE	ethyl vinyl ether	water		yes					41
F	C8H4F17	water		yes					69,70
FBEMA	2-(perfluorobutyl)ethyl methacrylate	methanol		yes					40
FP	ferrocenylphenylphosphine	hexane		yes					64
FPO	perfluoropropylene oxide	water		yes					73,74
FS	ferrocenyldimethylsilane	hexane		yes					64
Gly	glycidol	water	yes						36
GMA	glyceryl monomethacrylate	toluene/methanol		yes					81
		methanol	yes						81
		methanol/THF	yes					yes	81
		water						yes	86
HEGMA	methoxy hexa(ethylene glycol) methacrylate	water	yes						42-44
HEMA	2-hydroxyethyl methacrylate	benzene						yes	89
		water						yes	86,89
		methanol	yes						40

Table 2.2. Monomers constituting the various ABC triblock terpolymers of this review, placed alphabetically with respect to their abbreviated names, and some of their relevant physical and chemical properties.

Abbrevation	Name	solvent	lyophilic	lyophobic	T-sens	pH-sens	H-bonding	cross-linkable	ref.no.
I	isoprene	water		yes					75
		THF/hexane	yes						78,79
		water	yes						75,78,79
		DMF		yes					34
		DMA		yes					34
		THF	yes						34
L	n-alkyl (C_nH_{2n+1})	water		yes					69,70
LLA	L, L lactide	water		yes					36
MA	methyl acrylate	water		yes					67,80
MAA	methacrylic acid	water				yes			52,46-50,57
		THf/water				yes			53
MeOx	2-methyl-2-oxazoline	water	yes						35,69,70
MMA	methyl methacrylate	water		yes					52,46-50,56,60,68
		toluene	yes						33
		DMA	yes						34
		DMF	yes						34

Table 2.2. Monomers constituting the various ABC triblock terpolymers of this review, placed alphabetically with respect to their abbreviated names, and some of their relevant physical and chemical properties.

Abbrevation	Name	solvent	lyophilic	lyophobic	T-sens	pH-sens	H-bonding	cross-linkable	ref.no.
MOVE	2-methoxyethyl vinyl ether	water	yes						45
MPC	methacryloyloxy phosphatylcholine	water	yes						84
		THF/methanol		yes					84
MVE	methyl vinyl ether	water			yes				41
OEGMA	methoxy capped ethylene glycol	water	yes						83
PhEMA	2-phenylethyl methacrylate	water		yes					46-48
PO	propylene oxide	water		yes					83
S	styrene	water		yes					37,61-63, 65-67, 71,72, 80,91,92
		toluene	yes						33,88
		THF	yes						34,88,90, 93
		DMA	yes						34
		DMF	yes						34,59
		benzene	yes						88,89
		water/dioxane		yes					38,60
		acetone		yes					88
		cyclohexane	yes						88

Table 2.2. Monomers constituting the various ABC triblock terpolymers of this review, placed alphabetically with respect to their abbreviated names, and some of their relevant physical and chemical properties.

Abbrevation	Name	solvent	lyophilic	lyophobic	T-sens	pH-sens	H-bonding	cross-linkable	ref.no.
SEMA	2-succinyloxyethyl methacrylate	water				yes			55
*t*BAEMA	*tert*-(butylamino)ethyl methacrylate	water		yes					82
*t*BuA	*tert*-butyl acrylate	THF/water		yes					52-54,60
		THF	yes						78,79
		THF/2-propanol	yes						87
		water		yes					78,79
		THF/hexane		yes					78,79
*t*BuMA	*tert*-butyl methacrylate	DMF/water		yes					54,60
		methanol	yes						40

Table 2.3. Names and abbreviations employed in the text below for the various solvents used for the synthesis and characterization of the terpolymers.

Abbreviation	Solvent
B	Benzene
CH	cyclohexane
DMA	dimethylacetamide
DMF	dimethylformamide
CH_2Cl_2	dichloromethane
$CHCl_3$	chloroform
MeOH	methanol
PrOH	propanol
THF	tetrahydrofuran

Table 2.4. Names and abbreviations of the methods used for the characterization of the terpolymers.

Abbreviation	Characterization Method
AFM	Atomic force microscopy
DLS	Dynamic light scattering
FCS	Fluorescence correlation spectroscopy
GPC	Gel permeation chromatography
LALLS	Low angle laser light scattering
SANS	Small angle neutron scattering
SAXS	Small angle X-ray scattering
SEM	Scanning electron microscopy
SFM	Scanning force microscopy
SLS	Static light scattering
TEM	Transmission electron microscopy
WAXS	Wide angle X-ray scattering

2.2.1. Terpolymers with two lyophilic and one lyophobic blocks

2.2.1.1. Two simple lyophilic and one lyophobic blocks

Tsitsilianis and Sfika[33] reported on the preparation of the two triblock terpolymers S_{322}-*b*-$2VP_{62}$-*b*-MMA_{300} and S_{274}-*b*-$2VP_{252}$-*b*-MMA_{290} by anionic polymerization and the investigation of their solution properties in toluene, which is a poor solvent for the P2VP middle block and a good solvent for the PS and PMMA end-blocks. Static light scattering (SLS) performed on the terpolymer solutions in toluene provided their aggregation numbers and revealed the dependence of the aggregation number, N_{agg}, on the lyophobic content. In particular, the higher the lyophobic content the higher the aggregation number. TEM images revealed a spherical morphology for the aggregates with a P2VP core and a mixed PS-PMMA corona. TEM and viscometry were also employed to estimate the hydrodynamic size of the aggregates. The hydrodynamic diameters obtained for the two terpolymers differed due to their different content in the lyophobic P2VP block. The corona thicknesses of the aggregates were also determined for the two terpolymers, and they were found to differ significantly. This difference was attributed to the chain density on the surface of the micellar cores due to the different aggregation numbers, with the chains constituting micelles of a higher aggregation number exhibiting a more stretched conformation.

Triblock terpolymers bearing the same end-blocks as those reported above[33] were synthesized by Fernyhough and co-workers.[34] These researchers employed sequential anionic polymerization for the synthesis of four PS-*b*-PI-*b*-PMMA triblock terpolymers with various compositions in the three monomer repeating units and different molecular weights of the resulting triblock terpolymers. The solution properties of the terpolymers were investigated in THF, a good solvent for all the blocks, and in two selective solvents for the PS and PMMA blocks, namely DMA and DMF, using LALLS, DLS and viscometry. The polymer chains dissolved in THF unimolecularly, as expected. In contrast, formation of multimolecular micelles was observed in DMF and DMA, with the PI-middle block forming the micellar core, while the two soluble in these solvents PS and PMMA blocks constituted the mixed corona of the micelle. DLS revealed that the formed micelles had a spherical morphology. Moreover, the aggregation numbers of the micelles formed by the

triblock terpolymers were found to depend on the solvent chosen and the PI content of the triblock terpolymers. In particular, the aggregation numbers of the triblock terpolymers in DMA and DMF were found to increase with increasing length of the PI insoluble block, as expected. Hydrodynamic diameters were also found to depend on the micelle aggregation number and the length of the corona-forming PS and PMMA blocks. Viscosity studies suggested that the micelles formed in DMF and in DMA were of spherical shape, with those formed in DMF being compact, while those formed in DMA were less compact. The authors attributed this different behavior to the solubility parameters of the constituting blocks and the solvents. Based on these parameters, PI, the core forming block, must be completely insoluble in DMF and DMA, and therefore, the core should be free of solvent. On the other hand, the solvent-polymer interactions between DMA and the PS and PMMA blocks must be more favorable than those for either polymer block in DMF. Considering all of the above, it was proposed that the greater chain extension of the polystyrene block led to the increased protection of the core but also to chain-chain repulsions between the solvated blocks, which ultimately led to the decrease in the aggregation number observed for the triblock terpolymers in DMA.

Stoenescu and Meier[35] described for the first time the preparation of two amphiphilic PEO-*b*-DMS-*b*-PMeOx triblock terpolymers using anionic and cationic ring opening polymerization. Both EO_{45}-*b*-DMS_{40}-*b*-$MeOx_{97}$ and EO_{45}-*b*-DMS_{67}-*b*-$MeOx_{346}$ triblock terpolymers self-assembled into asymmetric, membrane-like superstructures in aqueous media. TEM and DLS were used to confirm the formation of vesicles in water. To this end, the terpolymers were dispersed in water and visualized by TEM, revealing the presence of vesicles. DLS showed that the size of these vesicles ranged between 60-300 nm. The authors wished to determine the orientation of the two hydrophilic blocks along the polymeric membrane. In order to do that, they labelled one of the hydrophilic end-blocks with 7-methoxycoumarinazide. DLS on the labelled and the control samples revealed no disturbance of the terpolymer self-assemblies by the presence of coumarin. In order to gather information for the orientation of the PMeOx blocks they added Co^{2+} to the external solution. Co^{2+} is known to quench the fluorescence of coumarin. It was concluded that the PMeOx blocks of the EO_{45}-*b*-DMS_{67}-*b*-$MeOx_{346}$ triblock terpolymer were located on the exterior of the vesicles and the PEO blocks in the interior. In contrast, for the EO_{45}-*b*-

DMS_{40}-*b*-$MeOx_{97}$ triblock terpolymer the inverse orientation was observed, that is the PMeOx blocks were inside the vesicles and the PEO block outside. According to the authors, this was due to the shorter PMeOx blocks in the EO_{45}-*b*-DMS_{40}-*b*-$MeOx_{97}$ inducing less steric hindrance than the PMeOx blocks in the EO_{45}-*b*-DMS_{67}-*b*-$MeOx_{346}$ triblock terpolymer, in agreement with geometrical demands: due to the curvature of the vesicle walls, it was favorable for the hydrophilic blocks with the smaller volume to segregate toward the interior.

Gadzinowski and Sosnowski[36] reported on the synthesis and characterization of the biodegradable/biocompatible triblock terpolymer PEO-*b*-PGly-*b*-PLLA. The synthesis of eight terpolymers, with the same block sequence and different molecular weights for each block, was achieved by successive anionic and ring opening copolymerization. Terpolymers with PLLA M_ns 5000 and higher did not dissolve in water. The molecular weights of the terpolymers were determined by gel permeation chromatography (GPC), proton nuclear magnetic resonance spectroscopy (^{1}H NMR) and GPC with a multi-angle light scattering detection. GPC and ^{1}H NMR estimations of the M_ns were close, whereas there was a significant overestimation of the molecular weights obtained from the GPC with the multi-angle light scattering detection. This was attributed to the presence of subpopulations differing with respect to their compositions, for macromolecules with the same hydrodynamic radii. DLS was employed for their aqueous solution characterization. From the diameters determined at various concentrations, the *cmc*s of the terpolymers were calculated. As far as the hydrodynamic diameters were concerned, it was found that those obtained for terpolymers bearing similar lengths of the hydrophobic PLLA block were smaller for longer hydrophilic PEO blocks. In the same sense, the diameters of the particles were larger for the terpolymers bearing the longer PLLA hydrophobic blocks. Furthermore, the authors compared these findings with those obtained for the aqueous solution characterization of the diblock PEO-*b*-PLLA and concluded that the presence of the reactive hydroxyl groups in the shells of the nanoparticles, through the presence of the PGly block, did not have any significant effect on the particle diameter.

Khanal and colleagues[37] investigated the interactions of the triblock terpolymer S_{135}-*b*-$2VP_{117}$-*b*-EO_{795}, arising from the protonation of the P2VP block, with the anionic surfactant sodium dodecyl sulphate (SDS). To that end, the terpolymer was positively

charged at pH < 5 through the protonation of P2VP blocks that changed from shrunk water-insoluble blocks to swollen water-soluble blocks. At pH >5 the P2VP blocks were deprotonated and shrunk. DLS was performed on the terpolymer-surfactant mixtures to determine the effect of the anionic surfactant on the hydrodynamic diameter of the terpolymer. At 100% ionization of the P2VP block (pH ~ 2-3), a decrease in the hydrodynamic diameter was observed when SDS was added. Further addition of SDS did not significantly affect the hydrodynamic diameters. The decrease of the hydrodynamic diameters upon the first addition of SDS was attributed to the conformational changes induced to the P2VP blocks. In particular, at solution pH 2 and 3, the P2VP blocks were protonated adopting a stretched conformation due to the electrostatic repulsions arising between the positively charged chains. Addition of the anionic surfactant SDS to the solution led to the binding of the sulfate group to the polymer, neutralizing the positive charges, hence reducing the solubility of the P2VP blocks, resulting in the change of their conformation from fully stretched to shrunk, resulting in the decreased hydrodynamic diameters. The effect of the SDS on the micellar dimensions was also supported by atomic force microscopy (AFM) images of the pure micelles and of micelles with SDS.

Niu *et al.*[38] reported on the preparation of the AA_{33}-*b*-S_{47}-*b*-EO_{113} triblock terpolymer by atom transfer radical polymerization (ATRP) and investigated the preparation of CdTe nanowires coated with this triblock teprolymer. Formation of spherical micelles with Cd^{2+} was observed upon the addition of $CdCl_2$ aqueous solution into the dioxane solution of the triblock terpolymer. A change in the micelle morphology from spherical to "pearl-necklace" was observed from the TEM images after the formation of CdTe through the reaction of the metal ions with NaHTe. The formation of this structure was attributed to dipole interactions between the neighbouring CdTe nanoparticles. TEM was used to monitor any changes in this morphology with time upon refluxing the solution. The "pearl-necklace" structure observed was not stable, but changed into single CdTe nanowires bearing PS dense shells. In this study, each one of the blocks constituting the triblock terpolymer was carefully chosen to confer to it a different function. In particular, the PAA blocks were used to form complexes with the Cd^{2+} ions. In addition to that, they induced cross-linking of the triblock terpolymers due to the coordination of the divalent cadmium ions with carboxylic groups from different polymers, resulting in micelle formation with Cd^{2+} rich cores.

The PS blocks were employed because of their aggregation in dioxane/water mixtures forming a densely packed shell on the CdTe nanowires. Finally, the PEO blocks secured the water-dispersibility of the formed CdTe nanowires.

Tang and coworkers[39] reported the ATRP synthesis of four triblock terpolymers comprising two hydrophilic monomers, the nonionic methoxy-capped PEO and the ionizable DMAEMA, and one hydrophobic monomer, the ionizable DEAEMA. All four terpolymers had the same block sequence, PEO-*b*-PDMAEMA-*b*-PDEAEMA, but their compositions varied. At pH > 7, micelle formation occurred with the water-insoluble DEAEMA blocks forming the micellar core, the DMAEMA blocks constituting the inner shells and the hydrophilic PEO blocks providing the corona. Dipyridamole (DIP), a drug which is water-soluble at pH < 5.8, was dissolved with the terpolymers at low pH, followed by an increase in the pH, leading to the formation of micelles by the terpolymer and their loading with the drug. DLS in water showed that the hydrodynamic diameters of the micelles ranged depending on terpolymer composition, terpolymer concentration and drug loading, with the triblock terpolymer bearing the highest hydrophobic content forming the largest micelles. This was attributed to the increased hydrophobic interactions between the micelles, leading to intermicellar aggregation. TEM images of the drug-loaded micelles revealed spherical morphologies and uniform particle size distributions. The PEO-*b*-PDMAEMA-*b*-PDEAEMA micelles acted as drug carriers releasing the drug slowly over a period of days to the surrounding solution. In contrast, upon abrupt decrease of the solution pH, dissociation of the drug-loaded micelles occurred, and the DIP was rapidly released in the solution.

Sugiyama et al.[40] synthesized six ABC triblock terpolymers based on the three strongly mutually incompatible monomers HEMA, *t*BuMA, and FBEMA and one diblock copolymer based on HEMA and FBEMA, using anionic polymerization. Three out of the six triblock terpolymers prepared were the equimolar block sequence isomers: HEMA-*b*-*t*BuMA-*b*-FBEMA, HEMA-*b*-FBEMA-*b*-*t*BuMA, and FBEMA-*b*-HEMA-*b*-*t*BuMA, whereas the remaining terpolymers had different compositions in the three monomer repeating units. Investigation of the solution properties exhibited by the three equimolar triblock terpolymers in methanol, a selective solvent for the HEMA and the *t*BuMA blocks, was performed using light scattering. Block sequence was found to have a strong effect on terpolymer aggregation in methanolic solutions.

According to the authors, aggregation was only observed for the HEMA-*b*-*t*BuMA-*b*-FBEMA triblock terpolymer and the HEMA-*b*-FBEMA diblock copolymer. This result is surprising, since micelle formation would have been expected to also occur for the other triblock terpolymers as well.

All the monomers, the polymerization methods and the methods employed for the solution characterization of the ABC triblock terpolymers reported in the above studies are listed in Table 2.5.

Table 2.5. Summary of the information about the reviewed ABC triblock terpolymers comprising two lyophilic and one lyophobic blocks.

Monomer Type			No. of synthesized and studied polymers	Polymerization Method	Solution Characterization Methods	Characterization Solvent	Ref. no.
Lyophilic 1	**Lyophilic 2**	**Lyophobic**					
S	MMA	2VP	2	anionic	SLS, TEM, viscometry	toluene	33
S	MMA	I	4	anionic	SLS, DLS, TEM, viscometry	THF, DMA, DMF	34
EO	MeOx	DMS	2	anionic/cationic ring opening	DLS, TEM	water	35
EO	Gly	LLA	8	Anionic, ring opening	DLS	water	36
EO	$2VPH^+$	S	1	*	DLS, AFM	water	37
EO	AA	S	1	ATRP	TEM	water/dioxane	38
PEO	DMAEMA	DEAEMA	4	ATRP	DLS, fluorescence, TEM	water	39
HEMA	*t*BuMA	FBEMA	7	anionic	LS	methanol	40

* not mentioned in the reference.

2.2.1.2. One neutral lyophilic, one temperature-sensitive lyophilic and one neutral lyophobic blocks

Patrickios and co-workers[41] reported the synthesis and aqueous solution characterization of water-soluble ABC triblock terpolymers composed of the hydrophobic ethyl vinyl ether (EVE), the temperature-sensitive, marginally-hydrophilic methyl vinyl ether (MVE) and the hydrophilic methyl tri(ethylene glycol) vinyl ether (MTEGVE). Living cationic polymerization was the method employed for the preparation of these terpolymers. Each block comprised 20 monomer repeating units and the block sequence in the polymer chain varied. The effect of block sequence on the aqueous solution properties was investigated using aqueous GPC, with and without salt in the mobile phase, at room temperature. In a salt-free aqueous environment, the terpolymers did not exhibit micellar behavior as they eluted as unimers, whereas in the presence of a sufficiently high salt concentration micelle formation was observed and attributed to the greater insolubility of the EVE units under the latter conditions. The triblock terpolymers bearing the hydrophobic block at the polymer chain end could not be effectively stabilized in solution by the hydrophilic blocks as evidenced by their lowest cloud points. Block sequence isomers presented different susceptibility to the salt-induced micellization, in agreement with their cloud points, suggesting that the intermicellar association might affect terpolymer precipitation.

Triftaridou and colleagues[42] synthesized by GTP three equimolar, isomeric ABC triblock terpolymers based on the neutral hydrophilic methoxy hexa(ethylene glycol) methacrylate (HEGMA), the temperature-sensitive, marginally-hydrophilic DMAEMA and the neutral hydrophobic MMA. The three block sequence isomers ABC, ACB and BAC as well as their statistical analogue were prepared. All four terpolymers had an overall theoretical degree of polymerization (DP) 30, containing 10 monomer repeating units from each of the different monomers. The three diblock copolymers derived from the pairwise combinations of the three different monomer repeating units were also synthesized (again with 10 units in each block). Their aqueous solution properties were investigated using DLS and turbidimetry. The micellar size of the triblock terpolymers having the hydrophobic block at the end of the polymer chain was larger than that of the diblock copolymers due to the greater overall DP of the terpolymers. As far as the triblock terpolymers are concerned, the

triblock terpolymers bearing the hydrophobic blocks at the end of the polymer chains presented the largest micellar sizes, while the triblock terpolymer having the hydrophobic block located in the middle of the polymer chain exhibited micelles with half the size of its isomers. The statistical terpolymer, where the three monomer units were randomly distributed in the polymer chain, exhibited the smallest hydrodynamic size due to its incapability of micelle formation. The cloud points of the diblock copolymers increased with their hydrophilicity. In the case of the terpolymers, cloud points were also found to depend on the monomer distribution along the polymer chain. In particular, triblock terpolymers forming micelles with the HEGMA in the corona, DMAEMA in the inner shell and MMA in the core had the highest cloud point, followed by the terpolymers having the temperature sensitive DMAEMA in the micellar corona and the statistical terpolymer that did not form micelles.

Recently, the same workers[43] combined the same three monomers to prepare amphiphilic star and linear ABC triblock terpolymers in an effort to explore the effect of star architecture, in addition to the block sequence effect, on the aqueous solution properties. To this end, they again employed GTP for the synthesis of multiarm star-shaped polymers with ABC triblock terpolymer arms and their linear counterparts. The three block sequence isomers ABC, ACB and BAC as well as their statistical analogue were prepared. Again, the overall theoretical DP of the arm was 30, containing 10 repeating units from each of the different monomers. Preliminary aqueous solution characterization of the terpolymers was performed to determine their cloud points which were found to depend on the terpolymer architecture and the distribution of the monomers in the polymer chain. In particular, star terpolymers exhibited higher cloud points than their linear counterparts. This was attributed to the relatively large number of arms in the case of the star terpolymers compared to the aggregation number of the micelles formed by the linear terpolymers in aqueous solutions, offering better steric stabilization and minimizing the unfavorable contact between the hydrophobic MMA units and water. The cloud points of the linear terpolymer block sequence isomers were found to differ, reflecting differences in their aggregation in aqueous solution and were consistent with those discussed in the previous publication.[42] The cloud points of the star terpolymer isomers followed the same order as that of the corresponding linear terpolymers. The results of this and the

previous reference will be fully presented and discussed in more detail in Chapter 5 of this Thesis.

The same two hydrophilic monomers and the neutral hydrophobic aromatic benzyl methacrylate (BzMA) were used by Kyriacou et al.[44] for the GTP synthesis of four isomeric $HEGMA_5$-*b*-$DMAEMA_{11}$-*b*-$BzMA_{10}$ terpolymers in which each of the three monomer repeating units contributed the same weight (rather than molar) percentage. Three of the terpolymers were the block sequence isomers, whereas the fourth was the statistical isomer. The aqueous solution properties of the terpolymers were investigated using DLS and turbidimetry and were found to depend on the monomer distribution in the polymer chain, in agreement with previous results.[42] In particular, terpolymers bearing the hydrophobic block at the end of the polymer chain formed micelles with higher hydrodynamic diameters and higher cloud points. The statistical terpolymer exhibited, as expected, the lowest hydrodynamic diameter and lowest cloud point due to its inability to form micelles. These ABC terpolymers were evaluated as emulsifiers. They were used to stabilize 1% w/w polymer concentration to prepare xylene-water and diazinon (pesticide)-water emulsions. All the emulsions prepared were found to be oil dispersions in an aqueous continuous phase (oil-in-water emulsions, o/w). The emulsification properties were found to depend on the monomer distribution in the polymer chain, with the emulsifier efficiency (considered higher when the emulsion droplets were smaller) following the order $HEGMA_5$-*b*-$BzMA_{10}$-*b*-$DMAEMA_{11}$ > $HEGMA_5$-*b*-$DMAEMA_{11}$-*b*-$BzMA_{10}$ > $DMAEMA_{11}$-*b*-$HEGMA_5$-*b*-$BzMA_{10}$ > $HEGMA_5$-*co*-$DMAEMA_{11}$-*co*-$BzMA_{10}$.

Sugihara and co-workers[45] reported the synthesis and aqueous solution characterization of two block sequence isomeric triblock terpolymers based on three temperature sensitive monomers: 2-ethoxyethyl vinyl ether (EOVE), 2-methoxethyl vinyl ether (MOVE) and 2-(2-ethoxy)ethoxyethyl vinyl ether (EOEOVE). The synthesis was carried out using sequential "living" cationic polymerization. The temperature dependence of the aqueous solution properties of these terpolymers reflected the three different phase-separation temperatures of the three segment: poly(EOVE) 20 °C, poly(EOEOVE) 41 °C, and poly(MOVE) 70 °C. The aqueous solution of the terpolymer $EOVE_{200}$-*b*-$MOVE_{200}$-*b*-$EOEOVE_{200}$ underwent multiple reversible associations, from sol (< 20 °C) to micellization (20-41 °C), to physical gelation (physical cross-linking, 41-64 °C) and finally to precipitation (> 64 °C). The

triblock teprolymer with block sequence $EOVE_{200}$-*b*-$EOEOVE_{200}$-*b*-$MOVE_{200}$ scarcely exhibited an increase in viscosity above 41 °C. The authors attributed this to the gradual dehydration of the EOEOVE middle-block with increasing temperature and the placement of this block in the cores of the existing micelles. Comparison of the terpolymer properties with those of an ABA triblock copolymer of the same molecular weight was also mentioned. Regardless of the copolymer type, physical gelation through the packing (or interaction) of micelles, similar to that of two diblock copolymers also studied, occurred rapidly. Above 41 °C, at which point the triblock terpolymers began a second-stage association, ABA and AB copolymers exhibited no increase in the apparent viscosity. This was due to the two different phase separation temperatures of the two blocks constituting the ABA triblock and the AB diblock copolymers precluding the second stage association observed in the triblock terpolymers.

All the monomers, the polymerization methods and the methods employed for the solution characterization of the ABC triblock terpolymers reported in the above studies are listed in Table 2.6.

Table 2.6. Summary of the information about the reviewed ABC triblock terpolymers comprising one neutral lyophilic, one temperature-sensitive lyophilic and one lyophobic block.

Monomer Type			No. of Polymers synthesized & studied	Polym. Method	Solution Character. Method	Character. Solvent	Applications	Ref. no.
lyophilic	T-sensitive	lyophobic						
MTEGVE	MVE	EVE	10	cationic	aqueous GPC, turbidimetry	water		41
HEGMA	DMAEMA	MMA	7	GTP	DLS, turbidimetry	water		42
HEGMA	DMAEMA	MMA	8	GTP	turbidimetry	water		43
HEGMA	DMAEMA	BzMA	4	GTP	DLS, turbidimetry	water	emulsifiers	44
MOVE	EOEOVE	EOVE	6	cationic	viscosity	water		45

2.2.1.3. One positively charged, one negatively charged and one neutral lyophobic blocks

Patrickios and colleagues[46] reported the GTP synthesis of ten, low molecular weight, water-soluble, amphiphilic ABC triblock polyampholytes composed of one hydrophobic monomer which was either MMA or PhEMA, and two hydrophilic ionizable monomers, namely DMAEMA and MAA. The MAA monomer repeating units were obtained via the thermolysis of tetrahydropyranyl methacrylate (THPMA) or by the acid hydrolysis of trimethylsilyl methacrylate (TMSMA) units. The terpolymers prepared covered various ratios of the two hydrophilic monomers. In addition to the ten ABC triblock terpolymers, two statistical terpolymers and one DMAEMA-MAA diblock copolymer were also synthesized. SLS and DLS studies on aqueous solutions of the equimolar DMAEMA-*b*-MMA-*b*-MAA terpolymer and its isomeric statistical counterpart revealed that the triblock terpolymer formed micelles but not the statistical. Moreover, fluorescence studies showed that the triblock terpolymer associated more strongly with pyrene than its statistical counterpart, which was also attributed to the micellization in the case of the triblock and the lack of it for the statistical. The statistical terpolymers were water-soluble over the entire pH range, whereas the triblock terpolymers precipitated around the isoelectric point. This was attributed to the smaller effective size of the statistical terpolymers which, unlike the triblocks, were incapable of forming micelles because of the random distribution of the hydrophobic units, and to the weaker electrostatic attractions between the opposite charges because of their random distribution. Additional studies showed that all the triblock terpolymers formed micelles, whereas the DMAEMA-MAA diblock copolymer did not due to the absence of a hydrophobic PMMA block in the diblock.

The terpolymers prepared in the afore-mentioned study were characterized by the same research group[47] in terms of the effect of solution pH, salt concentration and type on their phase separation behavior with poly(vinyl alcohol) (PVA). Three different phase regions were observed: (a) Complete miscibility of the polyampholytes with PVA at acidic and alkaline pH. The miscibility in the former case was attributed to the formation of hydrogen bonds between the alcohol oxygen of PVA and the carboxylic hydrogen of the undissociated methacrylic acid residue of the polyampholytes, whereas in the latter case this miscibility was attributed to the unscreened electrostatic interactions at low ionic strength, (b) Phase separation due to

polyampholyte precipitation near their isoelectric point at low salt concentrations, which is a typical polyampholyte property. (c) Phase separation into two fluid phases in the pH region near the isoelectric point at high salt concentrations with the polyampholyte-rich phase in the bottom and the PVA-rich phase on the top. The formation of the two phases was attributed to a large enthalpy of contact between the two types of polymers, arising from chemical differences between the methacrylic acid and vinyl alcohol monomer repeating units, rendering their existence in two separate phases energetically more favorable than their coexistence in a single phase. Phase separation also appeared to depend on block sequence, since the ABC triblock terpolymer bearing the acidic block in the middle exhibited phase separation also below the isoelectric point and at relatively low salt concentrations. This was probably due to the inability of the PMAA block to hydrogen bond with PVA because it was presumably located between the shell and the core of the terpolymer micelles and was, therefore, "invisible" to the PVA repeating units. Statistical terpolymers mostly exhibited one-phase solutions, also attributed to entropic factors, since the small unimer size of the statistical polyampholytes, compared to the larger effective micellar size of their triblock counterparts, resulted in a greater entropy of mixing at constant polymer concentration which lowered the free energy of the system leading to complete miscibility. The effect of salt type on the phase separation behavior of all the triblock polyampholytes with PVA was found to be consistent with the Hofmeister series which orders the salts according to their salting out power.

Aqueous GPC was employed by Patrickios *et al.*[48] in order to further investigate the aggregation behavior of these polyampholytes in aqueous solutions. The molecular weights obtained from aqueous GPC for the ABC triblock terpolymers were much higher than those of their unimers (obtained by GPC in THF) whereas those obtained for the statistical terpolymers and the AB diblock polyampholyte were close to those of the unimer, suggesting that triblock polyampholytes aggregated into micellar structures whereas the statistical terpolymers and the diblock copolymer did not. As explained in their first publication on the subject,[46] micellization was due to the presence of the hydrophobic PMMA block in the triblock terpolymers. Aggregation numbers ranging from 10 to 40 were calculated, with the larger value obtained for polyampholytes with the hydrophobic block at the end of polymer chain. The aggregation number also exhibited dependence on the type of the hydrophobic

monomer used since triblock terpolymers bearing the PPhEMA more hydrophobic block exhibited higher aggregation numbers than those with PMMA as the hydrophobic block.

Further studies on the same polyampholytes were conducted[49] employing fluorescence spectroscopy, SLS and DLS to monitor micelle formation from these terpolymers. The effects of terpolymer composition, block sequence and temperature on the *cmc* were investigated. Fluorescence studies at low solution pH showed that the *cmc* values decreased in the order $DMAEMA_{16}$-*b*-MMA_{12}-*b*-MAA_8 > $DMAEMA_{12}$-*b*-MMA_{12}-*b*-MAA_{12} > $DMAEMA_8$-*b*-MMA_{12}-*b*-MAA_{16}. This was attributed to the decreasing electrostatic repulsions between the fully positively charged DMAEMA blocks as their size decreased, coupled with the simultaneous increase in the size of the uncharged MAA block, facilitating the association of the polyampholyte macromolecules into micelles. Comparison of the *cmc*s at low pH of the two equimolar block sequence isomeric polyampholytes, $DMAEMA_{12}$-*b*-MMA_{12}-*b*-MAA_{12} and $DMAEMA_{12}$-*b*-MAA_{12}-*b*-MMA_{12} revealed that the cmc of the triblock terpolymer with the hydrophobic block at the end of the polymer chain was lower. DLS on low pH (~3) aqueous solutions of the equimolar triblock terpolymer with PMMA as the mid-block suggested the formation of small micelles, also supported by SLS data giving an aggregation number of 5. An increase of the pH to values toward and higher than the isoelectric point (p*I*) led to larger hydrodynamic diameters at pHs near the p*I* and lower values at pH > p*I*. DLS performed over the 2-12 pH range gave hydrodynamic diameters decreasing in the order $DMAEMA_{16}$-*b*-MMA_{12}-*b*-MAA_8 > $DMAEMA_8$-*b*-MMA_{12}-*b*-MAA_{16} > $DMAEMA_{12}$-*b*-MMA_{12}-*b*-MAA_{12}. The authors attributed this behavior to the presence of both DMAEMA and MAA units in the micellar corona, hence having blocks consisting of 16 units in the corona, larger than that of the equimolar terpolymer having 12 units in the micelle corona-forming block. The differentiation in the hydrodynamic diameters observed for the $DMAEMA_{16}$-*b*-MMA_{12}-*b*-MAA_8 and $DMAEMA_8$-*b*-MMA_{12}-*b*-MAA_{16} triblock terpolymers was attributed to the bulkier nature of the DMAEMA blocks compared to the MAA blocks, the larger Kuhn length in the case of DMAEMA enabling the accommodation of a higher number of waters of hydration than in the case of MAA, conferring a more extended structure to DMAEMA blocks than to the MAA blocks resulting in the higher hydrodynamic diameter of the $DMAEMA_{16}$-*b*-MMA_{12}-*b*-MAA_8 triblock

terpolymer. SLS studies on the triblock terpolymer solutions, at both low (~3.1) and high (~10.3) pH, showed that the aggregation numbers and micelle molecular weight had the same trend as the hydrodynamic diameters obtained from DLS.

In a more recent study, Patrickios and co-workers[50] investigated the effect of pH, polymer concentration and salt concentration on the precipitation of the triblock polyampholyte $DMAEMA_8$-*b*-MMA_{12}-*b*-MAA_{16} solutions prepared earlier[46] from its dilute aqueous solutions and compared the results with those obtained for ampholytic latex under the same conditions. The authors experimentally confirmed that the transition from complete solubility to polyampholyte precipitation occurred at the same critical pHs, independent of polymer concentration, because this parameter does not affect the charge of the polyampholyte. On the other hand, an increasing salt concentration reduced the terpolymer pH range of precipitation. Furthermore, the optical density 30 minutes after the adjustment of pH at 4.6, 5.4 and 6.2 was found to increase linearly with polyampholyte concentration, suggesting that at higher polymer concentrations more aggregates of the same average size were formed. The experiments with the ampholytic latex gave similar results, suggesting that no extra features were introduced by the micellar nature of the triblock polyampholyte.

Giebeler and Stadler[51] used sequential anionic polymerization for the preparation of seven S-*b*-2VP-*b*-*t*BuA and one S-*b*-4VP-*b*-*t*BuA triblock terpolymers. The *t*BuA blocks were hydrolyzed using hydrochloric acid, yielding the PS-*b*-PVP-*b*-PAA triblock ter-polyampholyte which exhibited solution properties sensitive to pH. The solution properties were investigated in THF/water 2/1 (v/v) mixtures. Potentiometric, conductometric and turbidimetric titrations were used to study the pH dependence of the interpolymer complexation of the PVP and PAA blocks in the micellar solution. FTIR was the method used for the same type of characterization in the bulk. The potentiometric titration curve obtained exhibited two equivalent points corresponding to the deprotonation of the pyridinium groups followed by the deprotonation of the carboxylic acid groups. Turbidimetric titration and FTIR spectroscopy demonstrated the formation of an interpolymer complex at the isoelectric point. Furthermore, the P2VP and PAA blocks were immiscible at low pH, whereas at the isoelectric point the formation of an interpolymer complex was observed.

In an extension of previous work[46] with emphasis on block sequence, Patrickios and colleagues[52] reported on the GTP synthesis and solution characterization of three equimolar, block sequence isomers, ABC triblock terpolymers based on the pH-sensitive DMAEMA, tetrahydropyranyl methacrylate (THPMA) and the neutral hydrophobic MMA. The isomers prepared were $DMAEMA_{12}$-*b*-$THPMA_{12}$-*b*-MMA_{12}, $DMAEMA_{12}$-*b*-MMA_{12}-*b*-$THPMA_{12}$ and $THPMA_{12}$-*b*-$DMAEMA_{12}$-*b*-MMA_{12}. The THPMA blocks were converted to MAA by acid hydrolysis at room temperature. The aqueous solution properties of the resulting polyampholytic terpolymers were investigated using hydrogen ion titration, determination of the isoelectric point, and GPC in aqueous salt solution. Block sequence did not seem to affect the titration characteristics or the isoelectric points of the three terpolymers. In contrast, block sequence was found to have a profound effect on their micellization properties as evidenced by GPC in aqueous salt solution. The polyampholytes bearing the hydrophobic block at the end of the terpolymer chain, $DMAEMA_{12}$-*b*-MAA_{12}-*b*-MMA_{12} and MAA_{12}-*b*-$DMAEMA_{12}$-*b*-MMA_{12}, exhibited higher micellar hydrodynamic volumes than the terpolymer having polyMMA as a middle block, $DMAEMA_{12}$-*b*-MMA_{12}-*b*-MAA_{12}. This was consistent with the fact that the former type of terpolymers formed AB-diblock copolymer type of micelles, whereas the latter formed ABA-triblock copolymer type micelles in aqueous solution. Figure 2.5 schematically represents the three terpolymers and the proposed structure of their corresponding micelles at pH 8.5.

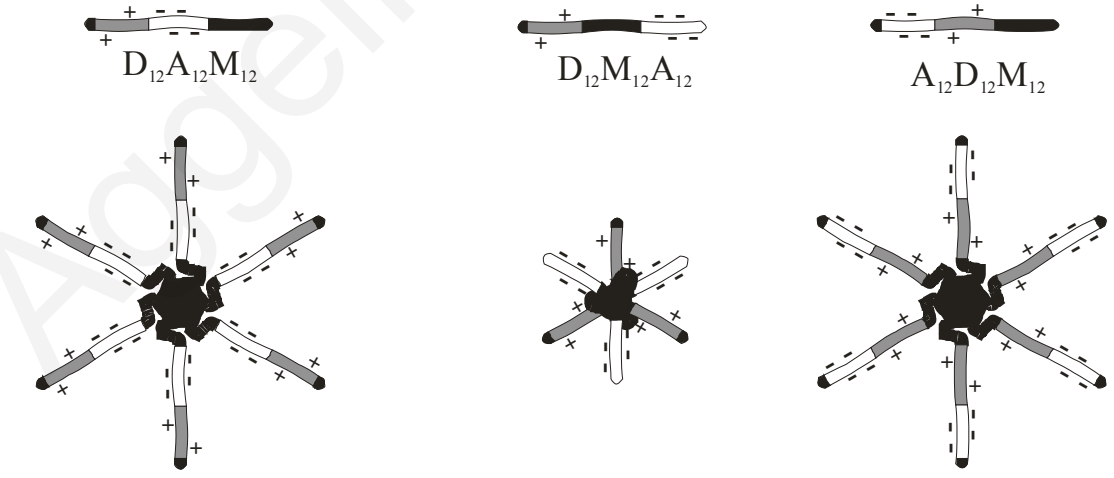

Figure 2.5. Linear terpolymer polyampholytes and their corresponding micelles formed in slightly alkaline aqueous solutions.[52] D, A and M denote the DMAEMA, MAA and MMA units, which are depicted in grey, white and black, respectively.

Bieringer and colleagues[53] prepared a series of triblock terpolymers with the structure poly[5-(N,N-dimethylamino)isoprene]-*b*-PS-*b*-P*t*BuMA (PAi-*b*-PS-*b*-P*t*BuMA) and hydrolyzed them to yield triblock amphiphilic polyampholytes with the structure Ai-*b*-PS-*b*-PMAA. The synthesis was carried out using anionic polymerization. The aggregation of the triblock terpolymers in THF/water mixtures was studied using DLS and cryo-TEM as a function of pH. Cryo-TEM showed the formation of vesicular micelles at pH = 4, with the soluble PAi and PMAA end-blocks stabilizing the vesicles in solution, while the insoluble PS formed the insoluble shell. At pH 10 the charged PMAA blocks stabilized the vesicular structure in solution, while both PS and PAi were insoluble. The micellar diameters obtained using DLS and cryo-TEM at pH 4 differed. The authors attributed this difference to the increased intensity of light scattered by the charged, highly stretched Ai blocks. Unlike the DLS measurements, the TEM measurements taken for the samples with the same pH values were not pH sensitive since the diameters obtained by the cryo-TEM measurements are, most likely, along the pH-insensitive PS shell. In contrast, at pH 10 the diameters obtained by both DLS and TEM were very close.

Liu and Eisenberg[54] reported the synthesis by anionic polymerization, and characterization of the ampholytic triblock terpolymer PAA_{26}-*b*-PS_{890}-*b*-$P4VP_{40}$ in DMF/THF/water mixtures. The aggregates formed underwent morphological changes with pH in organic solvent/water mixtures and were monitored by TEM. The segregation of the terpolymer was regulated by the difference in the repulsive interactions within the PAA or P4VP corona under different pH conditions. At low pH (~1) both the P4VP and PAA chains were protonated and strong repulsive interactions arose among the P4VP chains, while PAA chains were neutral, resulting in the formation of vesicles bearing the charged P4VP chains outside and the neutral PAA chains inside the vesicles. At high pH (~14) the PAA chains became negatively charged and strongly repelled each other, whereas the repulsive interactions between the now neutral P4VP chains were eliminated. This led to the formation of vesicles with the charged PAA chains outside and the neutral P4VP chains inside the vesicles. At intermediate pH, solid spherical or ellipsoidal micelles were observed, with the insoluble PS chains forming the core and the soluble PAA and P4VP chains forming the mixed corona.

Cai and Armes[55] prepared two triblock terpolymers with the structure EO_{45}-*b*-$DEAEMA_{26}$-*b*-$HEMA_{31}$ and EO_{45}-*b*-$DEAEMA_{42}$-*b*-$HEMA_{51}$ using ATRP in methanol. The hydroxyl groups of the HEMA segments were esterified with succinic anhydride, resulting in the formation of the zwiterionic EO-*b*-DEAEMA-*b*-SEMA triblock terpolymer. The aqueous solution properties of the terpolymers were studied using ^{1}H NMR and DLS as a function of pH. Three types of micelles were observed depending on the solution pH. At low pH, ^{1}H NMR revealed the formation of hydrogen-bonded, flower-like micelles with PSEMA/PEO complex cores and PDEAEMA coronas. These micelles were disrupted either with the addition of methanol, leading to the solvation of the PEO chains and the formation of more compact PSEMA-core micelles, or at higher temperatures due to the disruption of the hydrogen-bonded PSEMA-PEO complex, leading to aggregates with again a PSEMA core. At pH values around the isolectric point (=5.48), polyelectrolyte micelles with PSEMA/PDEAEMA cores and PEO coronas were formed that were very sensitive to the ionic strength of the aqueous solution. Dilution of the micellar solutions led to the swelling of the micelles and eventually to their dissociation. At high pH, the PDEAEMA blocks were neutral and hydrophobic and formed the core of the micelle through hydrophobic interactions, while the neutral PEO and the negatively charged PSEMA blocks formed a mixed corona. The hydrodynamic diameters of the three different micellar structures were found to be close but lower than that corresponding to fully stretched chains, indicating the formation of spherical micelles. Micelle formation through hydrogen bonding (PSEMA/PEO core), interpolyelectrolyte complexation (PSEMA, PDEAEMA) and hydrophobic interactions highlights the three different functions conferred by each one of the three different blocks to the terpolymers reported in this study.

Sfika and co-workers[56] reported the synthesis of the $2VP_{260}$-*b*-MMA_{50}-*b*-*t*BuA_{320} terpolymer using anionic polymerization. The *t*BuA blocks were hydrolyzed under acidic conditions and the aqueous solution behavior of the resulting $2VP_{260}$-*b*-MMA_{50}-*b*-AA_{320} triblock polyampholyte was investigated by turbidimetry, SLS, DLS, and AFM as a function of pH. The terpolymer exhibited self-assembly into different structures depending on the solution pH. Several pH regions were distinguished. At pH 1-2, vesicles comprising segregated arms of the heteroarm micelles were observed by AFM, with the P2VP and PAA chains forming the micellar corona. This structure

was found to be unstable with time. The effect of time on the micellar morphologies obtained from the terpolymer dissolution in water was also studied. To this end, terpolymer aqueous solutions were observed 1, 10 and 240 h after their preparation, using AFM. Aging phenomena due to intramicellar interactions led to morphological changes from Janus (segregated arms) to shell cross-linked micelles (mixed arms). A schematic explanation given by the authors is depicted in Figure 2.6.

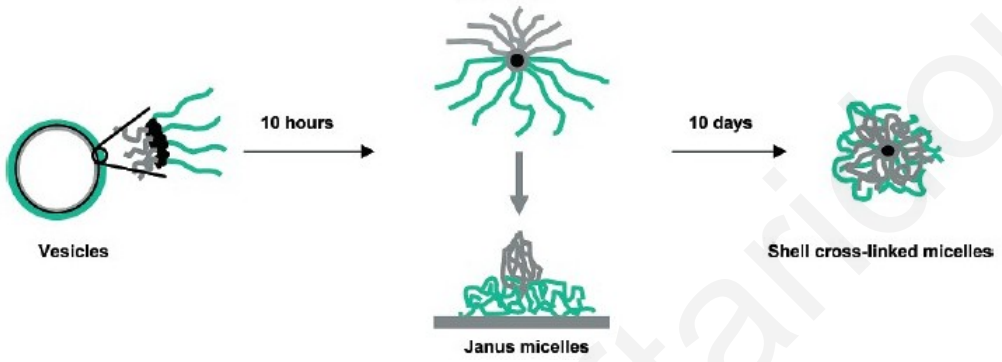

Figure 2.6. Time transformation of aggregates from vesicles to Janus micelles and to shell cross-linked micelles at pH 1 for $2VP_{260}$-*b*-MMA_{50}-*b*-*t*BuA_{320} triblock terpolymer.[56]

In particular, at pH 1, the vesicular structures observed were not stable with time and transformed to nanostructures with a spatially separated corona composed of PAA and charged P2VP blocks. The charged P2VP blocks of these micelles were adsorbed on the negatively charged mica surface (AFM substrate) as shown in Figure 2.6. The transformation of the Janus micelle structure to the core shell structure illustrated in this Figure was attributed by the authors to the development of hydrogen bonds between some of the 2VP units that remained uncharged with the un-dissociated PAA units. The corona of the resulting micellar structure was composed of a mixture of P2VP and PAA chains, hydrogen-bonded to each other. As the pH increased from 2 to 3, electrostatic intermicellar attractive interactions between the different corona chains arose, leading to the formation of irregular aggregates. An insoluble, two-phase region around the isoelectric point of the ampholytic chains was observed between pH 3.2 and 5.8. Finally, at higher pH, an unexpected, probably non-equilibrium morphology of aggregated amphiphilic heteroarm starlike micelles was observed after deposition on the mica substrate, probably due to the P2VP

hydrophobic nature at alkaline pH, leading to further aggregation of the Janus micelles.

Teoh *et al.*[57] prepared by ATRP the ampholytic terpolymer MAA_{102}-*b*-$DMAEMA_{67}$-*b*-C_{60} and investigated its aggregation behavior in aqueous solution using potentiometric and conductometric titration, DLS and TEM. C_{60} in the above structure is Buckminster fullerene (the spherical form of carbon). The aggregation behavior of the terpolymer was studied at pH 3 and 11 at two temperatures, 25 and 55 °C. Depending on the conditions, three microstructures were obtained and are illustrated in Figure 2.7.

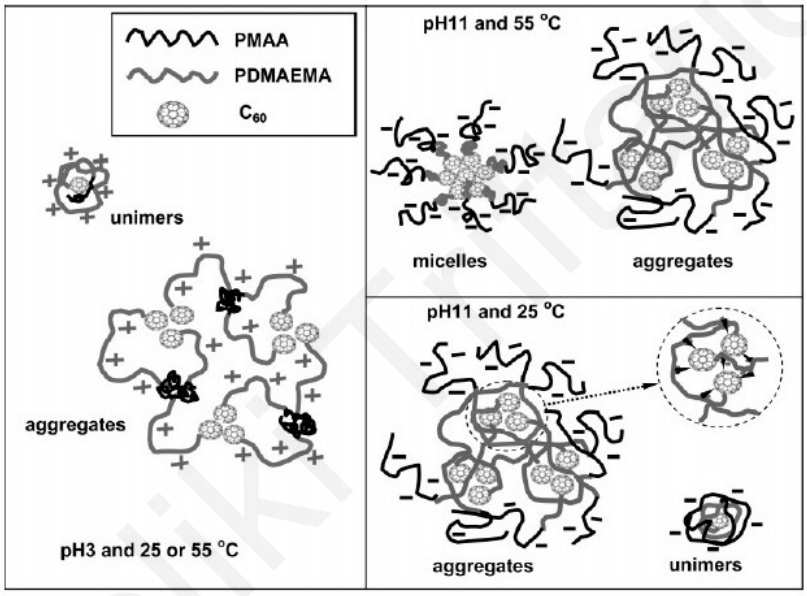

Figure 2.7. The three different micellar structures obtained for the MAA_{102}-*b*-$DMAEMA_{67}$-*b*-C_{60} terpolymer under different conditions. [57]

At pH 3 and temperatures 25 °C and 55 °C, hydrophobic interactions arising from the C_{60} domain and the PMAA segments led to chain association. The aggregates formed possessed a microgel-like structure, coexisting with unimers, as depicted in Figure 2.7. At 25 °C and alkaline pH (pH=11), unimers with negatively charged PMAA chains were found to coexist with aggregates consisting of hydrophobic domains of C_{60} "cross-linked" with DMAEMA blocks via the formation of charge transfer complexes (the lone electron pair of the nitrogen atoms is the electron donor and the C_{60} domain is the electron acceptor). In agreement with TEM results, the cores

obtained in the latter case were more compact than those visualized at pH 3. At pH 11 and temperature 55 °C, the charge transfer complexes continued to exist, the PMAA block became negatively charged and hydrophilic, whereas the PDMAEMA blocks became hydrophobic, resulting in the formation of micelles with a hydrophilic PMAA shell and a hydrophobic PDMAEMA / C_{60} mixed core.

All the monomers, the polymerization methods and the methods employed for the solution characterization of the ABC triblock terpolymers reported in the above studies are listed in Table 2.7.

Table 2.7. Summary of the information about the reviewed ABC triblock terpolymers comprising one positively charged, one negatively charged and one neutral hydrophobic block.

Monomer Type			No. of synthesized and studied polymers	Polymerization Method	Solution Characterization Methods	Characterization Solvent	Ref. no.
Positively charged	Negatively charged	lyophobic					
DMAEMA	MAA	MMA, PhEMA	13	GTP	SLS, DLS, fluorescence spectroscopy	water	46
DMAEMA	MAA	MMA, PhEMA	13	GTP	Aqueous phase behavior with PVA	water	47
DMAEMA	MAA	MMA, PhEMA	13	GTP	Aqueous GPC	water	48
DMAEMA	MAA	MMA	10	GTP	SLS, DLS, Fluorescence	water	49
DMAEMA	MAA	MMA	1	GTP	Turbidimetry	water	50
2VP, 4VP	AA	S	2	anionic	Potentiomerty, conductivity, turbidimetry	water	51
DMAEMA	MAA	MMA	3	GTP	H^+ titration, aqueous GPC	water	52
Ai	MAA	S	5	anionic	DLS, cryo-TEM	THF/water	53
4VP	AA	S	1	anionic	TEM	DMF/ water THF/water	54
DEAEMA**	SEMA	EO***	2	ATRP	^{1}H NMR, DLS		55
2VP	AA	MMA	1	anionic	DLS, AFM, turbidimimetry	water	56
DMAEMA	MAA	C_{60}	1	ATRP	Potentiomerty, conductivity, DLS, TEM	water	57

** DEAEMA: is hydrophobic when neutral (pH > 8), but hydrophilic when ionized (pH < 7).

*** EO: is hydrophilic rather than hydrophobic.

2.2.1.4. Two hydrogen bonding and one lyophobic / lyophilic blocks

Bazzi and co-workers[58] reported the synthesis by ring opening metathesis polymerization (ROMP) and characterization of three equimolar, ABC triblock terpolymers which were the block sequence isomers. Two out of the three blocks (A and C) were complementary to each other in terms of hydrogen bonding capability. These were the exo-7-oxabicyclo[2.2.1]hept-5-ene-2,3-dicarboximide (A) and the 2-acetylamino-6-[exo-hexan-7-oxabicyclo[2.2.1]hept-5-ene-2,3-dicarboximidoylamino]pyridine (B) capable of hydrogen-bonding with each other to three points in each monomer repeating unit. The third block (C) was the exo-N-butyl-7-oxabicyclo[2.2.1]hept-5-ene-2,3-dicarboximide and was hydrophobic. The ABC and BAC triblock terpolymer isomers were synthesized at a higher conversion than their ACB isomer (during the synthesis of the ACB triblock terpolymer, the conversion of the B monomer to the third block was only 70%), due to the insolubility of the AC diblock in THF, the polymerization solvent. Solution characterization of the terpolymers was performed in chloroform ($CHCl_3$). Two out of the three triblock terpolymers, the ABC and the BAC, were soluble in $CHCl_3$ whereas the ACB isomer was not. DLS at multiple angles in $CHCl_3$ solutions of the two soluble triblock terpolymers revealed the formation of small and large aggregates by the ABC isomer, in agreement with TEM images. On the other hand, the BAC isomer did not form aggregates in $CHCl_3$. The authors attributed the differences in the aggregation behavior of the ABC and BAC triblock terpolymers to their block sequence. It is noteworthy that the exact aggregation mechanism has not yet been elucidated.

Gohy and colleagues[59] studied in DMF the micelle formation originating from hydrogen-bonding interactions between the anionically prepared S_{750}-*b*-$2VP_{210}$-*b*-EO_{365} triblock terpolymer with the PAA homopolymer or the [oligo(ethylene oxide) methyl ether methacrylate]$_{63}$-*b*-AA_{657}-*b*-[oligo(ethylene oxide) methyl ether methacrylate]$_{63}$, $(EO_{11}MA)_{63}$-*b*-AA_{657}-*b*-$(EO_{11}MA)_{63}$, triblock copolymer prepared by reversible addition fragmentation chain transfer (RAFT) polymerization, and reported the formation of core-shell-corona micelles by the neutral polymers. The neutral copolymers were mixed in DMF which is a good solvent for both the PS and the PEO blocks resulting in the formation of micelles with a P2VP/PAA core surrounded by a mixed corona of PS and PEO blocks. This was attributed to the hydrogen-bonding between the P2VP and the carboxylic acid moieties of the PAA blocks, which is

stronger than the hydrogen bonding between the PAA and the PEO blocks. DLS on pure triblock solutions showed that no aggregates or micelles were present in the solution. In contrast, DLS performed after mixing the triblocks revealed the formation of almost monodisperse micelles in solution. These results were also supported by TEM and AFM observations. For the mixture of the PS-*b*-P2VP-*b*-PEO triblock terpolymer with the PAA homopolymer, formation of spherical micelles was also reported with a PAA/P2VP core and PS together with PEO chains intermingled in the corona. Transfer of these micelles to an aqueous environment had an impact on the micellar morphology. When the pH was around 7, the micelles remained unchanged, whereas at lower or higher pH the P2VP/PAA hydrogen bonding between the core forming blocks was perturbed due to the protonation/deprotonation of these two blocks.

All the monomers, the polymerization methods and the methods employed for the solution characterization of the ABC triblock terpolymers reported in the above studies are listed in Table 2.8.

Table 2.8. Information about the preparation and characterization of the H-bonding ABC triblock terpolymers.

Monomer Type			No. of Polymers synthesized & studied	Polym. Method	Solution Character. Method	Character. Solvent	Ref. no.
Complementary 1	**Complementary 2**	**Lyophobic* / lyophilic**					
A	B	C*	3	ROMP	DLS, TEM	$CHCl_3$	58
AA	2VP	S**	3	anionic**/ RAFT	DLS, AFM, TEM	DMF	59

*C is lyophobic, whereas S is lyophilic.

**a mixture of a triblock terpolymer and an ABA triblock copolymer. The triblock teprolymer was prepared by anionic polymerization, whereas the ABA triblock copolymer was prepared by RAFT.

2.2.2. Terpolymers with one lyophilic and two lyophobic blocks

2.2.2.1. One lyophilic and two compatible lyophobic blocks

Yu and Eisenberg[60] reported the anionic polymerization synthesis of the S_{180}-*b*-MMA_{67}-*b*-*t*BuA_{37} terpolymer. The P*t*BuA block was hydrolyzed in toluene using *p*-toluenesulfonic acid to yield a PAA block. The resulting terpolymer was insoluble in water due to the long hydrophobic PS and PMMA blocks. Hence, the terpolymer was molecularly dissolved in three different non-selective solvents, dioxane, THF and DMF, and water was subsequently added to those solutions. The addition of water led to the formation of micelles with the hydrophobic blocks constituting the cores. Depending on the percentage of water content, various morphologies were obtained. The morphological changes induced by varying the water content were monitored by SLS, DLS and TEM. The increase of the water content above certain values resulted in abrupt increases of the scattering intensity. At these water content values, TEM images were taken. In dioxane, at a water content of 18 % w/w, short rods and spherical aggregates were obtained, illustrated in Figure 2.8(a), whereas at a 20 % w/w water content, vesicles were formed co-existing with spherical aggregates as shown in Figure 2.8(b). In THF – water mixtures, as the water content increased above 16 % w/w, small spheres, primary micelles and larger particles were successively observed, in this sequence. In DMF, for water content 35 % w/w, spherical aggregates were observed by TEM, while for higher water contents a "necklace" structure, illustrated in Figure 2.8(d), was obtained. The formation of this structure was attributed to the one-dimensional aggregation of the spherical aggregates due to the decreasing solubility of the PMMA block. According to the authors, upon increasing the water content above 35 % w/w, the PMMA blocks formed a shell surrounding the PS core, whereas the PAA hydrophilic-corona forming blocks were too short to stabilize the micellar structure resulting in inter-micelle aggregation which reduced the hydrophobic area exposed to water, leading to the formation of the "necklace" structure. The hydrodynamic radii of the spherical micelles from one solution of each system at high water contents were measured by DLS. In all cases, three aggregate populations were detected: spherical, rodlike and vesicles.

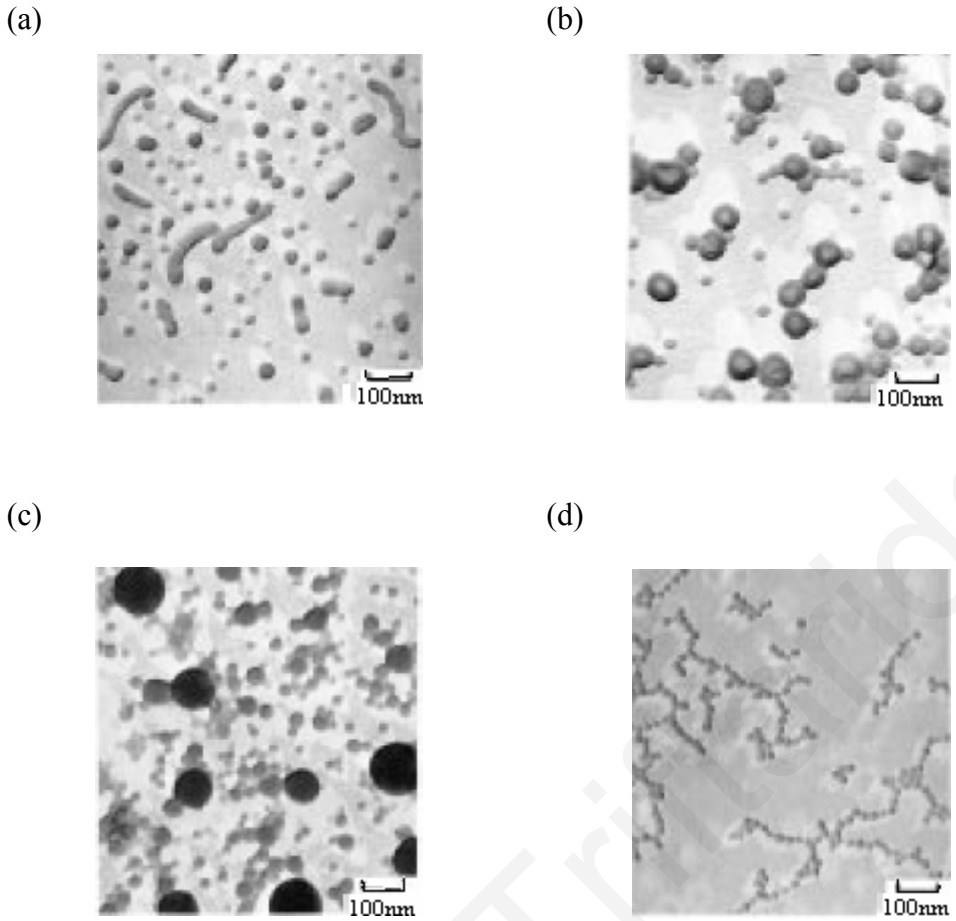

Figure 2.8. TEM images of aggregates from solutions of the triblock terpolymer S_{180}-*b*-MMA_{67}-*b*-*t*BuA_{37} obtained at different water contents: (a) from a dioxane solution with 18 % w/w added water, (b) from a dioxane solution with 25 % w/w added water, (c) from a THF solution with 40 % w/w added water and (d) from a DMF solution with 55 % w/w water.[60]

Gohy and co-workers[61] reported on the synthesis of the S_{200}-*b*-$2VP_{140}$-*b*-EO_{590} triblock terpolymer by anionic polymerization and the investigation of its properties in aqueous environment. TEM images revealed the formation of spherical core-shell-corona micelles in water. The hydrodynamic diameters of the micelles were determined by DLS and found to be pH-dependent as expected, due to the protonation of the P2VP blocks at pH < 5. In particular, the determined hydrodynamic diameters at pH > 5 (74 nm) were smaller than those at pH < 5 (135 nm) due to the protonation of P2VP and the subsequent creation of intra- and inter-segment electrostatic repulsions. The reversibility of the pH effect on the micellar size was also studied by cycling the pH a number of times. The hydrodynamic diameters at pH > 5 remained

constant upon pH cycling, while those at pH < 5 decreased with pH cycling probably due to the increasing ionic strength of the solution, resulting in reduced electrostatic repulsions between the charged P2VP blocks. In addition to DLS, TEM was also employed for the determination of the micellar hydrodynamic diameters. At pH > 5, the diameter determined using TEM (core plus shell: 35 nm) was half of that determined by DLS, attributed to the absence of solvent in the TEM studies. The core was found to be uniformly surrounded by a dense P2VP shell. At pH < 5, an increase in the diameter, from ~ 35 to ~50 nm, was observed by TEM, due to the protonation of the P2VP blocks. The core-shell-corona micelles were also observed using AFM at pH < 5 and found to be deformed. This was attributed to the electrostatic interactions between the positively charged P2VP blocks and the positively charged (at pH < 3.8) substrate used for the AFM measurements. Subsequently, the micelles formed were used as reactors for the synthesis of gold nanoparticles. In particular, the protonated P2VP shell of the micelles was selectively loaded with $AuCl_4^-$ driven by the attractive electrostatic interactions, followed by the reduction of $AuCl_4^-$ to form gold particles.

The same researchers[62] prepared the triblock terpolymers S_{200}-*b*-$2VP_{140}$-*b*-EO_{590} and S_{140}-*b*-$2VP_{120}$-*b*-EO_{795} by anionic polymerization and investigated their aqueous solution properties using DLS and TEM. The terpolymers were not readily water-soluble, which prompted the authors to employ the method reported by Yu and Eisenberg[60] for the preparation of the micelles. To this end, the terpolymers were first molecularly dissolved in DMF, which is a common solvent for all three monomer repeating units, followed by the addition of water. The effect of pH on the micellar characteristics was monitored by DLS and TEM. At pH > 5, monodisperse micelles were found by DLS in the aqueous solutions of both terpolymers. These findings were also supported by TEM using RuO_4 as staining agent, staining PS more intensely than the P2VP block. The TEM images, revealed that the observed spherical core-shell-corona micelles had the hydrophobic PS blocks in the core, the pH-responsive 2VP blocks in the shell, and the EO blocks in the corona. In particular, at pH > 5 the P2VP blocks were hydrophobic and adopted a collapsed conformation surrounding the PS core, whereas the hydrophilic PEO blocks were swollen. At pH < 5, the P2VP blocks were protonated and expanded due to the resulting repulsive interactions between the positively charged blocks, leading to larger hydrodynamic diameters. The pH effect and reversibility was studied with pH cycling. An initial reversibility

of the pH effect on the size of the P2VP shell was observed for the terpolymer S_{200}-*b*-$2VP_{140}$-*b*-EO_{590}. However, this reversibility was reduced with the number of cycles due to the electrostatic screening by the increasing amount of salt formed by the repeated neutralization of HCl by NaOH. This partial reversibility was not observed for the S_{140}-*b*-$2VP_{120}$-*b*-EO_{795} terpolymer. Athough the hydrodynamic diameter increased when the pH was decreased, it was not restored to the previous value when the charge was neutralized by the addition of excess NaOH. According to the authors, this difference was due to the longer PEO block in this case exhibiting a hysteresis in its structuring. In particular, at low pH, the P2VP units in both triblock terpolymers became positively charged inducing repulsive interactions between the P2VP blocks leading to stretching of the chains, with the hydrophilic PEO blocks being next to the charged P2VP blocks swelling further. Upon an increase in the pH, the P2VP blocks started collapsing, as they became hydrophobic due to their deprotonation causing a restructuring to the PEO segments. This restructuring of the PEO blocks occured in the S_{200}-*b*-$2VP_{140}$-*b*-EO_{590} triblock terpolymer, whereas in the case of the triblock terpolymer S_{140}-*b*-$2VP_{120}$-*b*-EO_{795}, a hysteresis was observed.

Following this work, the same research group[63] reported on the synthesis and aqueous solution characterization of the metallo-supramolecular S_{32}-*b*-$2VP_{13}$-*b*-[Ru]-EO_{70} triblock terpolymer. For the synthesis of the terpolymer, the S_{32}-*b*-$2VP_{13}$ hydroxy-terminated diblock copolymer prepared by anionic polymerization was converted to the terpyridine-terminated analogue and was left to react with the ruthenium complexed-terpyridine-terminated EO_{70}. The resulting S_{32}-*b*-$2VP_{13}$-*b*-[Ru]-EO_{70} triblock terpolymer was not readily soluble in water. This was attributed to the short PEO blocks, which probably were not long enough to offer effective steric stabilization to the S_{32}-*b*-$2VP_{13}$-*b*-[Ru]-EO_{70} micelles. Thus, the authors adopted the method introduced by Yu and Eisenberg[60] for the preparation of the micelles in water. In particular, the terpolymer was first dissolved in DMF, followed by dropwise addition of dilute HCl solution, resulting in kinetically frozen micelles with a PS core, a P2VP shell and a PEO corona. DLS on acidic terpolymer solutions revealed the existence of two populations, with the smaller one corresponding to micelles and the larger to intermicellar aggregates. TEM images of the terpolymer micelles confirmed their spherical shape with a core-shell-corona structure. AFM also illustrated the existence of micelles and micellar aggregates, in agreement with the DLS and the

TEM findings. In addition, after neutralization of the micellar terpolymer solution, DLS revealed that the deprotonated micelles remained stable under these conditions, although direct preparation of the micelles in neutral water was not possible. DLS, TEM and AFM showed a bimodal particle size distribution due to the coexistence of micelles and micellar aggregates. The micelles formed under neutral conditions were smaller than those prepared at low pH, due to the stretching of the P2VP blocks resulting from the protonation of the 2VP moieties at low pH. The size variation of the micelles with the solution pH was not reversible in contrast to the micelles formed by the corresponding S_{200}-*b*-$2VP_{140}$-*b*-EO_{590} triblock terpolymer. The authors attributed this non-reversibility to the decreased solubility of the PEO blocks in the presence of the NaCl salt. Furthermore, the effect of ionic strength and temperature on the micellar characteristics was also studied. Addition of a small amount of salt was found to favor the formation of micelles, suggesting that the equilibrium between micelle-micellar aggregate was dominated by electrostatic interactions. Further addition of salt favored the formation of intermicellar aggregates. An increase in the temperature of the micellar solution was found to favor the formation of micellar aggregates due to the progressive dehydration of the PEO blocks, reducing the steric stabilization of the micelles conferred by the PEO corona. The salt and temperature effects on the micellar sizes were found to be irreversible, leading the authors to the conclusion that the S_{32}-*b*-$2VP_{13}$-*b*-[Ru]-EO_{70} micelles were kinetically stable. Addition of a strong competitive ligand in the terpolymer solution resulted in the opening of the terpyridine bis-complex, evidenced by the reduction in the hydrodynamic diameter measured using DLS.

Wang and co-workers[64] employed anionic ring opening polymerization for the preparation of four triblock terpolymers with block sequence Poly(ferrocenylphenylphosphine)-*b*-Poly(ferrocenyldimethylsilane)-*b*-Poly(dimethylsiloxane), PFP-*b*-PFS-*b*-PDMS. The prepared terpolymers had short PFP blocks of various lengths and PFS:PDMS ratios of 1:5-1:12, and their micellization properties in hexane were investigated. The terpolymers were first dissolved in THF which is a common solvent. Subsequently, hexane, which is a selective solvent for the PDMS block, was slowly added to the THF solutions. TEM images revealed that the length of the PFP end-block determined the micellar morphology, since both FP_1-*b*-FS_{40}-*b*-DMS_{304} and FP_6-*b*-FS_{45}-*b*-DMS_{220} exhibited a

cylindrical morphology, whereas the FP_{11}-*b*-FS_{50}-*b*-DMS_{600} triblock terpolymer formed spherical micelles. The authors attributed this to the disruption of the crystallization of the PFS blocks in the micelle core by the presence of the longer PFP chains. Furthermore, in an effort to explore the effect of PFP blocks on the micelle structure at elevated temperatures, the hexane solution of the cylinder-forming FP_6-*b*-FS_{45}-*b*-DMS_{220} triblock terpolymer was heated to 70 °C for 30 min, resulting in the formation of aggregates with irregular shapes. According to the authors, this was also due to the disrupting influence of the PFP blocks on the crystallization of the PFS blocks. In an effort to shed more light on that hypothesis, wide angle X-ray scattering (WAXS) was performed on hexane solutions of the terpolymers, confirming the crystalline nature of the PFS blocks in the FP_1-*b*-FS_{40}-*b*-DMS_{304} and FP_6-*b*-FS_{45}-*b*-DMS_{220} cylinder-forming triblock terpolymers and the amorphous nature of the PFS blocks in the FP_{11}-*b*-FS_{50}-*b*-DMS_{600} sphere-forming triblock terpolymer.

Lei and colleagues[65] used anionic polymerization to prepare two triblock terpolymers with block sequence PS-*b*-P2VP-*b*-PEO. Both triblock terpolymers were dissolved in a DMF-benzene mixture, followed by the slow, dropwise addition of water, which is a selective solvent for the PEO blocks, resulting in the formation of spherical micelles with a PS core, a P2VP shell and a PEO corona. The micelle formation was monitored by DLS measurements. Addition of benzene, which is a selective solvent for the core-forming block, dramatically affected the micellar morphology as depicted in Figure 2.9.

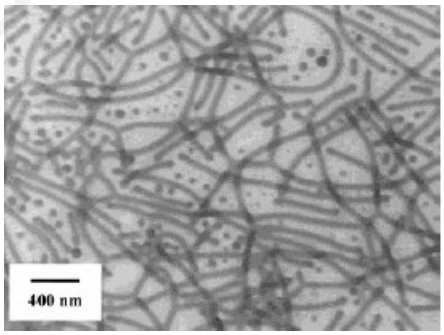

Figure 2.9. TEM image of the S_{200}-*b*-$2VP_{140}$-*b*-EO_{590} micelles prepared from a 75/25 w/w DMF-benzene mixture. Rods co-existing with spheres are observed.[65]

Depending on the benzene content, various morphologies were obtained. In particular, when the benzene content was < 5% w/w, only spherical micelles were formed, whereas when the benzene content was > 5% w/w, a mixture of cylindrical and spherical micelles was obtained. For a benzene content ranging between 20-30 % w/w, cylindrical micelles predominated. The cylindrical and spherical micelles obtained were protonated, and their TEM images showed no pH effect on the morphology. The authors claimed that this was due to the stretched conformation already adopted by the P2VP blocks under neutral conditions in the presence of benzene, therefore eliminating the pH effect.

Katsampas and Tsitsilianis[66] synthesized a triblock terpolymer with a long hydrophilic PAA block located in the middle of the polymer chain, end-capped with short hydrophobic blocks of PS and PBuMA. Anionic polymerization with sequential monomer addition and selective hydrolysis of the middle block were employed for the synthesis. SLS, DLS, rheology and scanning electron microscopy (SEM) were used to study the hierarchical self-assembly as a function of terpolymer concentration in water. The behavior of the PS-PAA diblock precursor was also studied. Both the PS-*b*-PAA diblock copolymer and the ABC triblock terpolymer underwent micellization in water, and their micelle aggregation numbers were determined by SLS to be 102 and 50, respectively. DLS showed a smaller hydrodynamic radius for the triblock terpolymer (81 nm) than the diblock precursor (162 nm). SEM images revealed that the ABC triblock terpolymer formed well-shaped small spherical particles, although smaller than the aggregates formed by the AB diblock precursor. These findings were in agreement with the light scattering results, and according to the authors they illustrate the effect of architecture on the micelle formation. In the range of the concentrations studied, the micelles formed by the ABC triblock terpolymer seem to have flower-like structures with a homogeneous PS, PBuMA micellar core. At higher concentrations, intermicelle association occurred to dendron like micelles and finally resulting in the formation of 3D transient networks. The ABC architecture was found to be capable of forming the physical networks at very low concentrations, in contrast to the AB diblock precursor. Hence, the importance of the third component was proved.

Chen *et al.*[67] reported on the preparation of a series of PAA-*b*-PMA-*b*-PS, triblock terpolymers and investigated their aqueous solution properties using TEM. Spherical

and worm-like micelles were observed by adjusting the pH of the terpolymer aqueous solutions. Cryo-TEM revealed the existence of a vesicular morphology. The vesicles formed remained stable in solution over a two-month period. Furthermore, control experiments performed on diblock copolymers of similar block lengths and compositions demonstrated that the vesicular morphology was unique for the triblock terpolymers relative to the diblock copolymers.

All the monomers, the polymerization methods and the methods employed for the solution characterization of the ABC triblock terpolymers reported in the above studies are listed in Table 2.9.

Table 2.9. Summary of the information about the reviewed ABC triblock terpolymers comprising one lyophilic and two lyophobic blocks.

Monomer Type			No. of synthesized and studied polymers	Polymerization Method	Solution Characterization Methods	Characterization Solvent	Ref. no.
Lyophilic	**Lyophobic 1**	**Lyophobic 2**					
AA	S	MMA	1	anionic	SLS, DLS, TEM	dioxane/water, DMF/water, THF/water	60
EO	S	2VP	2	anionic	DLS, TEM, AFM	water	61
EO	S	2VP	2	anionic	DLS, TEM	water	62
EO	S	2VP	1	anionic	DLS, TEM, AFM	water	63
DMS	FS	FP	4	anionic	TEM, WAXS	hexane	64
EO	S	2VP	2	anionic	DLS, TEM, AFM	water	65
AA	S	BuMA	1	anionic	SLS, DLS, SEM, rheology	water	66
AA, MA	S		*	*	TEM, cryo-TEM	water	67

* information not given in the manuscript.

2.2.2.2. One lyophilic and two mutually-incompatible lyophobic blocks

Kříž and colleagues[68] reported the synthesis by GTP of the triblock terpolymer PEHA-*b*-PMMA-*b*-PAA. Using SLS and DLS in water, they observed the formation of spherical micelles with a narrow size distribution. Small angle neutron scattering (SANS) was employed to investigate the core morphology and revealed that the core was composed of two concentric layers consisting of blocks of microphase separated PEHA and PMMA, with the PEHA blocks located in the inner region and the PMMA blocks located in the outer region. The microphase separation of the hydrophobic core was attributed to the incompatibility between PEHA and PMMA. The PAA blocks formed the water-swollen micellar corona. Hence, each one of the three blocks exhibited a different microphase behavior, indicating that full use of the three components was made in this investigation.

Nuyken and co-workers[69,70] employed cationic polymerization to synthesize ABC triblock terpolymers composed of PMeOx, end-capped with a fluorocarbon segment ($C_8F_{17}CH_2CH_2$) at one end and a hydrocarbon alkyl segment at the other. The hydrocarbon segment length varied from C_6 to C_{18}. Aqueous solution properties of these systems were investigated using fluorescence spectroscopy and DLS at various terpolymer concentrations, as well as using ^{19}F NMR. It was found that a subtle change in the length of the hydrocarbon end-group, with respect to the constant fluorocarbon group, allowed control of the first micellization point. In particular, when the alkyl segment was short (C_6 to C_{10}), the fluorocarbon end-group was more hydrophobic and aggregated first, whereas for longer alkyl chains (C_{14} to C_{18}) the hydrocarbon endgroup aggregated first. Above the *cmc* of the first hydrophobic block, formation of micellar aggregates was observed, whereas a further increase of the terpolymer concentration above the *cmc* of the second hydrophobic block led to separate aggregation of the hydrocarbon and the fluorocarbon segments. ^{19}F NMR revealed that the two different hydrophobic blocks aggregated into two separate cores due to their mutual incompatibility resulting in network formation, since the T_2 relaxation times obtained indicated pure fluorocarbon domains. In contrast, this was not observed in similar ABA and AB systems where their micellization behavior was ruled by one *cmc*, that of the hydrophobic block.

Tsitsilianis and colleagues[71] used sequential anionic polymerization to prepare the S_{35}-*b*-AA_{844}-*b*-$BuMA_9$ triblock terpolymer with very short hydrophobic end-blocks

compared to the hydrophilic PAA mid-block. The aqueous solution behavior of this terpolymer was studied and compared to that of the symmetrical S_{23}-*b*-AA_{1134}-*b*-S_{23} triblock copolymer. The PS-*b*-PAA-*b*-PBuMA triblock terpolymer exhibited a greater increase of its aqueous solution viscosity than the PS-*b*-PAA-*b*-PS triblock copolymer. This was attributed to the incompatibility between the PS and PBuMA blocks, resulting in the formation of a transient network comprising PS and PBuMA physical cross-links interconnected by stretched polyelectrolyte chains.

Zhou and co-workers[72] reported the synthesis by anionic polymerization of a EO_{299}-*b*-S_{45}-*b*-BD_{24} triblock terpolymer and a triblock terpolymer with the same block sequence having the PBD block selectively fluorinated. Both terpolymers were directly dissolved in water and their solution properties were determined using DLS, small angle X-ray scattering (SAXS), SANS and TEM. Formation of spherical micelles with a PEO corona and a homogeneous core from PS and PBD was observed for the non-fluorinated terpolymer. On the other hand, a different morphology was obtained for the aggregates formed by the fluorinated terpolymer. In particular, SANS and SAXS showed oblate elliptical core/shell/corona micelles with the fluorinated PBD blocks in the core, the PS blocks forming a shell surrounding the core, and the water-soluble PEO blocks forming the corona. The different morphologies obtained were attributed to the fluorination of the PDB block, inducing internal segregation into an inner core and an intermediate shell.

Li *et al.*[73] prepared seven ABC miktoarm star terpolymers (μ-ABC) having three arms each comprising a different homopolymer, as schematically shown in Figure 2.10. The synthesis was achieved in three steps: (1) the anionic polymerization of butadiene end-capped with a bifunctional protected initiator, followed by its hydrogenation to P(ethyl ethylene) (PEE), (2) successive anionic polymerization of EO indicated by the end-functionalized PEE homopolymer (3) and a coupling reaction between the PEE-PEO hydroxyl mid-functionalized diblock and poly(perfluoropropylene oxide)-COCl (PFPO-COCl). All three components used, namely the water-soluble EO, the hydrophobic EE and the hydrophobic-lipophobic FPO were mutually incompatible. The DP of the PEE block was kept constant in all the synthesized terpolymers, while the DP of the PFPO and PEO blocks varied. In all cases the PEO block had a higher DP than the sum of those of PEE plus PFPO, ensuring the water-solubility of the μ-ABC terpolymers.

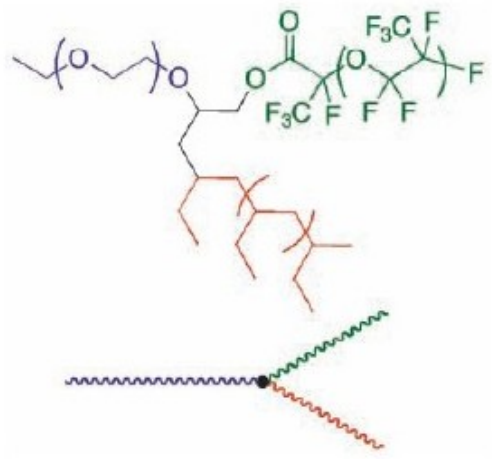

Figure 2.10. Schematic representation of the ABC miktoarm stars reported by Li *et al.*[73] The three different monomers constituting the arms of the star terpolymer, namely PEO, PFPO and PEE are depicted in three different colors.

The aqueous solution properties of these ABC star terpolymers were investigated by the same group[74] using DLS and cryo-TEM. Stars with the highest content in the hydrophilic (EO) component were found to form micellar cores with either small irregular dark regions, or three- and four-lobe micellar cores, as shown in Figure 2.11(a) A. Figures 2.11(a) B-D show images of another star terpolymer, which was slightly more hydrophobic than that of Figure 2.11(a) A.

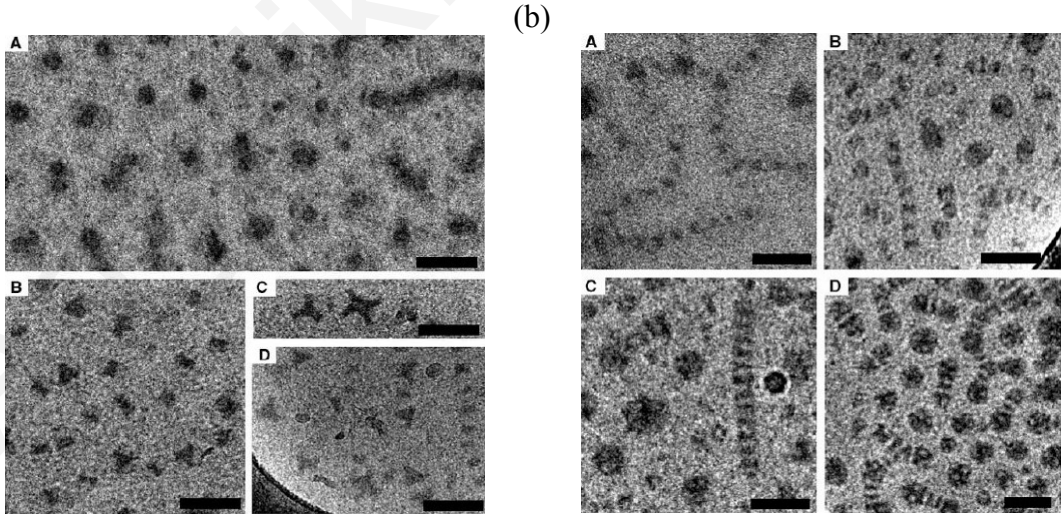

Figure 2.11. Cryo-TEM images of 1 % w/w aqueous solutions of (a) the most hydrophilic μ-ABC terpolymers and (b) the least hydrophilic ones comprise PEO, PFPO and PEE arms.[74]

The dark regions in these images were assigned to nanodomains formed by the PFPO arms due to their strong unfavorable interactions with the PEO arms and the aqueous environment. The gray regions surrounding the dark regions were assigned to the PEE arms, whereas the water-soluble PEO arms were not visible.

The TEM images obtained for the four ABC miktoarm star terpolymers with shorter PEO arms and increasing hydrophobic content are depicted in images A to D of Figure 2.11(b). Elongated worm-like micelles with dark (PFPO arms) central areas surrounded by grey (PEE arms) areas were observed. Thus, it appears that inter-star attractive interactions led to the formation of strings of stars. This was due to the lower effectiveness of the PEO arms, in this case, to protect the hydrophobic core. The formation of the strings enabled the different cores to share their PEO coronas, offering a better protection from the surrounding water phase. In these systems, each one of the three segments exhibited a different function. In particular, the PEO arms conferred water-solubility, the PEE arms protected the highly hydrophobic PFPO arms from the PEO arms and water, minimizing the contact area imposed by the star architecture, since all three segments were connected at a single junction.

Koutalas and co-workers[75] prepared, by anionic polymerization, a series of PI-*b*-P2VP-*b*-PEO triblock terpolymers with varying molecular weights and compositions and reported the effect of molecular weight and composition, terpolymer concentration, temperature, low-molecular-weight salt concentration and low-molecular-weight anionic and cationic surfactants (SDS and DTMAB) on the properties of the aggregates formed. DLS and SLS measurements revealed the formation of spherical micelles in neutral and acidic pH. Figure 2.12 illustrates these micellar structures and the effect of the charge on the P2VP blocks. In neutral water, micelles with a soft PI (low T_g) core, a hard P2VP (high T_g) outer shell, protected by a neutral PEO corona, were formed. Under acidic conditions, the micelles had also a three-layer structure, imposed by the block sequence, with a PI core, and two corona layers, an inner $P2VPH^+$ layer and an outer neutral PEO layer. Under these conditions, the positively charged P2VP blocks repelled each other, resulting in the observed micellar size increase. Aggregation numbers for the neutral terpolymers were high due to the high hydrophobicity of the PI core-forming blocks, whereas they were lower for the charged terpolymers.

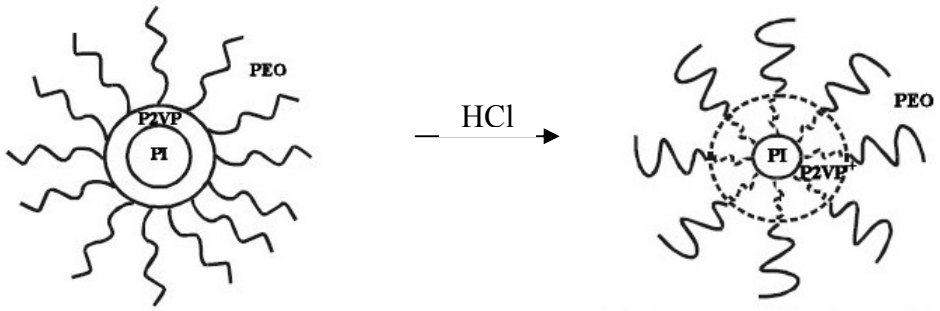

Figure 2.12. Schematic illustration of the transition between the two micellar structures obtained at neutral and acidic pH for the PI-*b*-P2VP-*b*-PEO triblock terpolymers.[75]

Micelle interaction with cationic (dodecyltrimethylammonium bromide, DTMAB) and anionic surfactants (SDS) resulted in the formation of mixed polymer/surfactant aggregates. DTMAB seemed to induce changes in the triblock terpolymer micellar structure through hydrophobic interactions, whereas SDS at low concentrations effected structural changes through electrostatic interactions and at high concentrations via hydrophobic interactions. Mixed micelles remained water-soluble over the whole investigated concentration range due to the presence of the neutral water-soluble PEO outer layer. Hence, each of the three different blocks in these triblock terpolymers conferred to the terpolymer a different function.

All the monomers, the polymerization methods and the methods employed for the solution characterization of the ABC triblock terpolymers reported in the above studies are listed in Table 2.10.

Table 2.10. Summary of the information about the reviewed ABC triblock terpolymers comprising one lyophilic and two mutually-incompatible lyophobic blocks.

Monomer Type			No. of synthesized and studied polymers	Polymerization Method	Solution Characterization Methods	Characterization Solvent	Ref. no.
Lyophilic	**Lyophobic 1**	**Lyophobic 2**					
AA	MMA	EHA	1	GTP	SANS, SLS, DLS, NMR	water	68
MeOx	L	F	9	cationic	SLS, DLS	water	69, 70
AA	S	BuMA	2	anionic	Viscosity	water	71
EO	S	BD	2	anionic	DLS, SAXS, SANS, TEM	water	72
EO	EE	FPO	7	anionic & polym-polym coupling	DLS, SAXS, SANS, TEM	water	73
EO	EE	FPO	7	-\\-	DLS, cryo-TEM	water	74
EO	2VP	I	6	anionic	SLS, DLS	water	75

2.2.3. Terpolymers with one lyophilic, one lyophobic and one cross-linkable blocks

All of the studies reviewed in the preceding Sections concerned the dissolution of the terpolymers in solvents selective for one or two blocks resulting in micelle formation. The micelles formed exhibited in most cases either spherical core-shell or core-shell-corona structure in solution. In an effort to lock the micellar structure some researchers reported on the cross-linking of the shell-forming block of the micelles, resulting in the formation of *shell cross-linked micelles*[76,77] (SCLM). A rather different approach for the production of micelle-resembling structures was that employed by Saito et al.[88] where the cross-linking of the middle-block was performed in the bulk followed by dissolution of the material in a non-selective solvent resulting in the formation of *Janus* micelles as will be discussed below.

2.2.3.1. Shell cross-linked micelles

Following the work on SCLM formed by diblock copolymers,[76,77] SCLM prepared by triblock terpolymers were recently reported.[78-87] According to Liu and coworkers,[86] the use of ABC triblock terpolymers for the preparation of SCLM is more advantageous than the use of AB diblock copolymers because in the former case the cross-linking could take place at much higher concentrations than in the latter case (> 10 % w/v instead of 0.5 % w/v) with negligible intermicellar cross-linking due to the steric stabilization rendered by the corona forming block.

One of the first studies on ABC triblock terpolymer SCLM was reported by Underhill and Liu[78] who employed the monomers I, CEMA and *t*BuA to prepare the triblock terpolymer I_{370}-*b*-$CEMA_{420}$-*b*-*t*BuA_{550} by anionic polymerization. The terpolymer was first dissolved in THF, a non-selective solvent for all three components, followed by the slow addition of hexane, a selective solvent for the PI block, resulting in the formation of spherical micelles in THF/hexane mixtures with the hexane volume fraction ranging from 65 % to 97%. The micellar morphologies obtained in the THF/hexane mixtures were imaged by TEM. The hexane-soluble PI blocks constituted the micellar corona, while the PCEMA and P*t*BuA blocks were located in the shell and the core, respectively. For the solutions containing 65% hexane, spherical micelles were observed, whereas for the solutions containing 97% hexane spherical micelles coexisting with "pearl-necklace-shaped" micelles were found. The authors attributed these findings to the aggregation of the spherical micelles induced

by the decrease in the solvation power of the THF/hexane mixture upon increasing the hexane content. The micellar structures formed were locked by photo-cross-linking the PCEMA blocks, yielding nanospheres comprising a cross-linked hydrophobic shell, a lyophilic PI corona and a lyophobic P*t*BuA core. ^{1}H NMR and ^{13}C NMR performed before and after the cross-linking were used to confirm the structure of the micelles formed. Most of the protons of the triblock terpolymer were visible in ^{1}H NMR, while in the case of the shell-cross-linked nanospheres, the peaks corresponding to the PCEMA protons had disappeared. In ^{13}C NMR, the relative intensities of the peaks corresponding to the alkenyl carbon atoms relative to that of the phenyl peak alluded to the disappearance of some of these carbons due to cross-linking, as well as the disappearance or the reduction of the intensity of peaks corresponding to PCEMA and P*t*BuA. The authors attributed this to the reduced mobility of the protons of the P*t*BuA and the PCEMA blocks, since PCEMA was located in the shell and P*t*BuA in the core. In addition, DLS and TEM provided similar micellar sizes before and after photo-cross-linking the PCEMA blocks, confirming that cross-linking did not alter the micellar structure, but just locked it. After the photo-cross-linking of the PCEMA block, the PI block was hydroxylated resulting in poly(2,3-dihydroxyisoprene) (PHI). Characterization by TEM, DLS, NMR and FTIR followed. DLS was performed on solutions of the hydroxylated nanospheres in THF with a few drops of aqueous NaOH solution and the hydrodynamic diameters obtained were smaller than those obtained for the cross-linked-micelles before hydroxylation. The authors attributed this to the limited swelling of the poly(hydroxylated isoprene) block in THF. The *tert*-butyl groups of the P*t*BuA blocks were converted to trimethylsilyl groups through the reaction of the hydroxylated cross-linked triblock terpolymer with excess trimethylsilyl iodide and the product was hydrolyzed in either water or methanol, and monitored by TEM, FTIR and NMR. Hydrolysis yielded a micellar structure with a swollen core comprising hydrophilic AA moieties, enabling the loading of the core with Fe^{2+} particles, where after treatment of the nanospheres with H_2O_2, oxidation of Fe^{2+} to Fe^{3+} took place. In this study, the three functions conferred to the terpolymer by the three different monomer repeating units were clear. In particular, the P*t*BuA blocks formed initially the micellar core and were later hydrolyzed to yield a PAA hydrophilic Fe^{2+}-compatible core. The CEMA moieties were photo-cross-linked to

permanently stabilize the micellar morphology, and the PI blocks were hydroxylated and became hydrophilic offering water-dispersity to the nanoparticles.

The nanospheres prepared in the previous publication were loaded with Pd^{2+} and were further studied as catalysts.[79] To this end, the nanospheres were equilibrated with $PdCl_2$ enabling the loading with Pd^{2+} in their PAA core. Reduction of the metal-ions followed and these encapsulated Pd nanoparticles catalyzed the hydrogenation of alkenes such as triethylammonium bromide (TEAA), vinylacetic acid (VAA), MMA and ethylene glycol dimethacrylate (EGDMA). It was found that upon varying the pH and thus the structures of the encapsulating nanospheres, the activity of the Pd nanoparticles was tuned. In particular, at pH 10 where PAA was deprotonated, the hydrogenation rate of the positively charged TEAA was increased, whereas at the same pH the hydrogenation rate of VAA decreased due to electrostatic repulsions between PAA and VAA. Furthermore, the nanospheres were found to function as a nanofilter as concluded from the selective hydrogenation of the MMA units of a MMA/EGDMA mixture.

Ma and Wooley[80] reported the synthesis of the two diblock copolymers P*t*BuA-*b*-PMA and PMA-*b*-P*t*BuA and the ABC triblock terpolymer $t\text{BuA}_{90}$-*b*-MA_{80}-*b*-S_{98}, using ATPR in the bulk. The *tert*-butyl groups in the diblocks and the triblock were selectively cleaved, using trifluoroacetic acid, to yield PAA, resulting in amphiphilic diblock copolymers and one amphiphilic triblock terpolymer. Formation of micelles with the hydrophobic PS block in the core, the PMA block in the shell and the PAA blocks in the corona was observed in aqueous solutions of the terpolymer. The micelles were frozen in the corona by selectively cross-linking the AA monomer repeating units using 2,2'-(ethylenedioxy)-bis(ethylamine) and 1-[3-(dimethylamino)propyl]3-ethylcarbodiimide methiodide as a catalyst (activator). This resulted in the formation of shell cross-linked particles. Spherical particles as well as cylindrically shaped nanoassemblies were formed. AFM revealed that the spheres were organized into hexagonally packed monolayers in contact with mica (the AFM substrate) and that the cylinders preferred to assemble on the surface produced by the spherical particles.

Liu and Liu[81] used anionic polymerization for the preparation of the PSMA-*b*-P(HEMA-TMS)-*b*-PAMA triblock terpolymer, where PSMA denotes poly(solketal

methacrylate), P(HEMA-TMS) is poly(2-trimethylsiloxyethyl methacrylate) and PAMA is poly(allyl methacrylate). The TMS groups from P(HEMA-TMS) were removed by selective hydrolysis in methanol yielding PHEMA. The terpolymer PSMA-*b*-PHEMA-*b*-PAMA was subsequently left to react with cinnamoyl chloride resulting in the terpolymer PSMA-*b*-PCEMA-*b*-PAMA. The composition of the terpolymer was determined by ^{1}H NMR and was found to be SMA_{300}-*b*-$CEMA_{190}$-*b*-AMA_{180}. Acid hydrolysis of the acetonide groups of the PSMA block followed to yield the triblock terpolymer PGMA-*b*-PCEMA-*b*-PAMA, where PGMA is poly(glyceryl methacrylate). TEM showed that the terpolymer PGMA-*b*-PCEMA-*b*-PAMA formed spherical micelles in methanol/THF mixtures and branched cylindrical micelles in pure methanol, with PGMA coronas and the insoluble PCEMA and PAMA blocks forming the shell and the core, respectively. The location of the blocks in the micellar structure was also supported by ^{1}H NMR, since the peaks corresponding to the protons of the PGMA corona-forming block were all present in the spectra, whereas many of the peaks corresponding to the PCEMA (middle layer) and PAMA (core) protons were absent. In toluene/MeOH mixtures the terpolymer also formed spherical micelles, where the insoluble PGMA block formed the micellar core, and the two soluble PCEMA and PAMA blocks formed the shell and the corona, respectively. In both cases, the PCEMA blocks of the micelles were photo-cross-linked. DLS was performed on the solutions of the linear and the cross-linked terpolymers and revealed no significant changes in the hydrodynamic diameters before and after cross-linking, suggesting that cross-linking did not cause significant changes in the structure of the micelles. The three different blocks conferred to the terpolymer a different function, PCEMA was cross-linked, whereas one of the PGMA and PAMA blocks was either lyophobic inducing micellization or lyophilic stabilizing the micelle in solution, depending on the solvents used.

Paz Báñez and colleagues[82] employed a PEO-based macroinitiator, DMAEMA, DEAEMA, (*tert*-butylamino)ethyl methacrylate (*t*BAEMA) and 2-(*N*-morpholino)ethyl methacrylate (MEMA) for the preparation of seven diblock copolymers and four triblock teprolymers by oxyanion-initiated polymerization. The authors chose to examine the properties of the PEO-*b*-DMAEMA-*b*-*t*BAEMA triblock terpolymer. ^{1}H NMR in water confirmed that the terpolymer formed three-layer onion-like micelles. The NMR signals of the relatively hydrophobic *t*BAEMA

blocks disappeared, indicating, according to the authors, that this was located in the micellar core. The marginally hydrophilic DMAEMA blocks formed the inner shell, and the hydrophilic PEO blocks were located in the corona. Addition of the difunctional quaternizing agent 1,2-bis(2-iodoethoxy)ethane (BIEE) to this micellar solution followed, resulting in the cross-linking of the PDMAEMA inner shell leading to SCLM. The PEO segments acted as steric stabilizers, minimizing the intermicellar overlap, hence preventing intermicelle cross-linking, highlighting the different function conferred to the terpolymer by each one of the blocks comprising the terpolymer chain. DLS on the terpolymer aqueous solution at pH 2, where the P*t*BAEMA blocks also became hydrophilic, exhibited a hydrodynamic diameter of 67 nm, corresponding to the D_h of a micelle, thus confirming the formation of the shell cross-linked (SCL) micelles. TEM on diluted SCLMs revealed their spherical shape, which was rather polydisperse, and gave diameter values ranging from 40-60 nm, in reasonable agreement with the DLS results (considering the polydispersity and the dehydration effects). ^{1}H NMR revealed that on cooling the SCLMs to 5 °C, partial rehydration of the micelle cores was achieved.

Liu and Armes[83] chose ATRP for the preparation of seven PO_{33}-*b*-$DMAEMA_{26}$-*b*-$OEGMA_{42}$ triblock terpolymers with different degrees of cross-linking, where OEGMA denotes methoxy-capped oligo(ethylene glycol) methacrylate with seven ethylene glycol units per monomer. SLS and DLS showed that the linear terpolymer was molecularly dissolved in aqueous solution at pH 8.5 and T=5 °C. Upon increasing the temperature above the LCST of the PPO block (estimated to be around 15 °C) micelle formation occurred. At room temperature in aqueous solutions of the terpolymer, micelles had highly hydrated PPO cores whose size gradually decreased with an increase in the solution temperature up to 40 °C, leading to smaller and more compact micelles. Upon a further increase of the solution temperature (60-70 °C), the PDMAEMA inner shell also became hydrophobic and the micelle was only stabilized by the OEGDMA hydrophilic blocks that formed a protecting corona, emphasizing the different function of each of the blocks constituting the triblock terpolymer. Increasing the temperature changed the overall hydrophilic-hydrophobic balance resulting in an increase in the D_h and the N_{agg}. The micelles formed were spherical as was concluded from light scattering data. The formation of micelles upon increasing the solution temperature was also supported by ^{1}H NMR where at 40 °C the peaks

corresponding to the PPO and PDMAEMA blocks became broader and less intense. After the aqueous solution characterization of the linear terpolymers, the authors proceeded to the cross-linking of the micelles in the shell. To this end, they prepared 10 w/v % aqueous solutions of the terpolymer and heated them up to 40 °C to induce micelle formation. Subsequently, they added the bifunctional quaternizing reagent BIEE at various BIEE/DMAEMA ratios that led to various cross-linking degrees of the DMAEMA residues located in the inner shell of the micelles. The solution was then left to cool down to room temperature, and the "freezing" of the micellar structure was confirmed by DLS which detected large particles rather than unimers. SLS gave an aggregation number of 150. Micelles with low degrees of cross-linking exhibited a greater decrease in their D_h upon increasing the solution temperature, than those with higher degrees of cross-linking. The deswelling of the SCL micelles was observed using DLS and variable temperature NMR. By increasing the temperature, a reduction of the D_h was observed by DLS, and a broadening of the PPO peaks by NMR. TEM on dried micelles also revealed the spherical shape of the micelles.

Liu et al.[84] followed up with the synthesis by ATRP of the MPC_{30}-*b*-GMA_{20}-*b*-$DEAEMA_{60}$ terpolymer, where the abbreviations MPC and GMA stand for 2-methacryloyloxy phosphorylcholine and glycerol monomethacrylate, respectively. They reported on the properties of three forms of the terpolymer: (a) the linear terpolymer, (b) the MPC-corona GMA-SCLMs prepared by the terpolymer in aqueous media and (c) the DEAEMA-corona cross-linked micelles prepared in non-aqueous media. MPC-corona PGMA-SCLMs were prepared by the dissolution of the terpolymer in water at pH 2, followed by the adjustment of the pH at 12 to induce micelle formation, and completed by the cross-linking of the PGMA layer by the addition of divinyl sulfone (DVS). For the preparation of the SCLMs in non-aqueous media a different approach was adopted. In particular, the linear terpolymer was first dissolved in MeOH, followed by the slow addition of THF at 45 °C to result in micellization. DVS was added to cross-link the PGMA layer. DLS in water for the PMPC-corona PGMA-shell-CL micelles and in THF/MeOH mixtures for the DEAEMA-corona PGMA-SCLMs was employed for the determination of the hydrodynamic diameters of the two types of micelles. PDEAEMA-corona PGMA-SCLMs were found to have greater hydrodynamic diameters than the PMPC-corona PGMA-SCLMs. DEAEMA blocks were invisible in ^{1}H NMR spectra of the MPC-

corona SCLMs in D_2O leading the authors to conclude that the core of the shell cross-linked micelles was composed of DEAEMA blocks. On the other hand, the signals due to the MPC residues were not detected for the DEAEMA-corona PGMA-SCLMs indicating that the MPC blocks formed the micellar core. Both types of micelles had spherical morphologies, as was determined by TEM. The corona component of the particles was also identified using X-ray photoelectron spectroscopy (XPS).

The same research team[85] used ATRP with a PEO-macroinitiator for the synthesis of seven PEO-*b*-PDMAEMA-*b*-PDEAEMA triblock terpolymers. The effect of varying the terpolymer composition and the degree of cross-linking on the structural stability and pH-dependent swellability of the micelles were studied. The terpolymers were first molecularly dissolved in aqueous media at low pH (pH=2) and then NaOH was added to increase the solution pH. At pH 7.1 the formation of three layer micelles (called onion micelles) was observed with DEAEMA cores, DMAEMA inner shells and PEO coronas. Within the pH range 7.3-9.0 a decrease of the hydrodynamic diameter of the micelles was observed that was attributed to the more compact nature of the micelles due to deprotonation of the DMAEMA and DEAEMA tertiary amine residues in this pH range. Selective quaternization of the DMAEMA units using BIEE followed, leading to increased hydrophilicity and colloid stability for the shell cross-linked micelles. The shorter the PEO blocks the higher the linking efficiency. At pH 8.5 the hydrodynamic diameters of the micelles that were not cross-linked increased rapidly above 40-50 °C due to the LCST of the DMAEMA chains in the inner shell of the micelle. In contrast, the hydrodynamic diameters of the shell cross-linked micelles in dilute solutions were independent of temperature. Reversible swelling and de-swelling of the SCLM upon varying the solution pH was observed.

The same group[86] used ATRP to prepare three triblock terpolymers based on a combination of three of the EO, glycerol monomethacrylate (GMA), DEAEMA and HEMA monomers. Two of the terpolymers synthesized had the same types of monomers and block sequence but different compositions, EO_{45}-*b*-GMA_{40}-*b*-$DEAEMA_{55}$ and EO_{45}-*b*-GMA_{25}-*b*-$DEAEMA_{70}$, and the third was EO_{45}-*b*-$HEMA_{30}$-*b*-$DEAEMA_{50}$. All three terpolymers were molecularly dissolved in aqueous solutions of low pH. Increasing the solution pH by the addition of NaOH above pH 7-8 caused micellization. The micelles formed were composed of three layers with the PDEAEMA blocks constituting the cores, either the PGMA or the PHEMA blocks

forming the inner shells, and the PEO blocks constituting the outer coronas. Divinyl sulfone was added at alkaline conditions to cross-link the PGMA or the PHEMA blocks yielding SCLMs. The resulting SCLMs exhibited reversible swelling behavior upon varying the solution pH through the protonation of the PDEAEMA blocks at low pH. The ability to adjust block composition and the [DVS]/[GMA] molar ratio allowed the control of the swellability of the SCLMs. These SCLMs were used as nanoreactors for the preparation of gold nanoparticles. To this end, the basic DEAEMA blocks in the cores of the SCL micelles were first protonated using $HAuCl_4$ and then electrostatically bound to $AuCl_4^-$ anions. Subsequently, the SCLMs were reduced to nanoparticles of elemental Au using $NaBH_4$ at neutral pH. The gold-loaded SCLMs exhibited excellent long-term colloidal stability.

Hoppenbrouwers and co-workers[87] prepared the $BuMA_{510}$-*b*-$CEMA_{240}$-*b*-*t*BuA_{270} terpolymer using anionic polymerization. TEM images revealed that the triblock terpolymer formed spherical aggregates in various percentages of THF/cyclohexane and THF/cyclopentane mixtures due to the fact that both cyclohexane and cyclopentane are poor solvents for the CEMA block. Moreover, the triblock terpolymer was dissolved in THF/2-propanol mixtures (THF is a non-selective solvent for the three blocks, while 2-propanol is a selective solvent for the P*t*BuA and PBuMA blocks) and was examined by TEM in three different ways: (a) THF/2-propanol mixture containing 20% THF followed by slow addition of the 2-propanol up to a volume fraction of 99% where the formation of spherical aggregates was observed, (b) direct dispersion of the triblock terpolymer in 2-propanol containing 1% THF where a mixture of mostly spheres and cylinders was produced and (c) the triblock was dispersed in neat 2-propanol exhibiting the formation of mostly cylinders and spheres. DLS and TEM were both used to obtain the R_h of the spherical aggregates, with that determined by the latter method being smaller due to the fact that only PCEMA blocks were visible by that technique. Subsequently, they selectively photo-cross-linked the CEMA blocks in the spherical aggregates formed by the terpolymer in the 99% 2-propanol/THF mixture resulting in the formation of nanospheres with the PCEMA blocks in the core, and the PBuMA and P*t*BuA blocks in the corona. Taking into account the molecular weight of the nanospheres as calculated by SLS in chloroform, and dividing it by the MW of the linear triblock precursor gave an aggregation number 53 for the nanospheres. ^{1}H NMR performed

on the nanosphere solution confirmed the core-shell structure of the nanospheres, since the intensity of peaks corresponding to the CEMA blocks was weak. The nanospheres were treated with $(CH_3)_3SiI$ in dry dichloromethane which led to the selective cleavage of the *tert*-butyl groups from P*t*BuA blocks, which were converted to PAA blocks. The obtained amphiphilic nanospheres were dispersible both in water and toluene. TEM images of the nanospheres sprayed from THF, toluene and water gave the same R_hs, that were close to the R_h values obtained for the nanospheres before the removal of the *tert*-butyl groups. DLS performed before and after the cross-linking of the PCEMA block, showed that the spheres did not seem to aggregate in any of the solvents used, in contrast to the Janus micelles that aggregate even in good for both coronal block solvents. This was assumed to be due to the possible adjustment of the coronal BuMA and *t*BuA chains packing in such a way as to minimize the asymmetry in the corona thickness caused by the different lengths of the PBuMA and P*t*BA, before photo-cross-linking of the CEMA block or even before the triblock terpolymer aggregation. TEM images of the hydrolyzed terpolymer sprayed from water revealed aggregation of the nanospheres, suggesting lateral aggregation of PBuMA and PAA chains, whereas those obtained when sprayed from 2-propanol revealed the localization of the PAA chains on one side of the particle.

All the monomers, the polymerization methods and the methods employed for the solution characterization of the ABC triblock terpolymers used for the formation of the SCLMs reported in the above studies are listed in Table 2.11.

Table 2.11. Summary of the information about the reviewed ABC triblock terpolymers comprising one lyophilic block, one lyophobic block and one cross-linkable block employed for the preparation of SCLMs.

Monomer Type			No. of synth. & studied polymers	Polymeriz. Method	Characterization Methods for Aggregation	Characteriz. Solvent(s)	applications	Ref. no.
Lyophilic	**Lyophobic**	**Cross-linkable**						
I	BuA	CEMA	1	anionic	^{1}H NMR, ^{13}C NMR, DLS, TEM	THF/hexane, water	catalyst	78,79
	S, MA	AA	3	ATRP	^{13}C NMR, AFM	water		80
GMA[a], AMA[b]	AMA[a], GMA[b]	CEMA	1	anionic	TEM, ^{1}H NMR, DLS	MeOH, MeOH/THF[a], toluene/MeOH[b]		81
PEO	BAEMA	DMAEMA	7	oxyanionic	DLS, ^{1}H NMR, TEM	water		82
OEGMA	PO	DMAEMA	7	ATRP	DLS, SLS, ^{1}H NMR, TEM	water		83
MPC[a] DEAEMA[b]	DEAEMA[a] MPC[b]	GMA	1	ATRP	DLS, ^{1}H NMR, TEM, XPS	Water[a], THF/MeOH[b]		84
EO	DEAEMA	DMAEMA	7	ATRP	DLS, ^{1}H NMR	water		85
EO	DEAEMA	GMA, HEMA	3	ATRP	DLS, ^{1}H NMR, TEM	water		86
*t*BuA, BuMA		CEMA	1	anionic	SLS, DLS, TEM	THF/2PrOH, $CHCl_3$, toluene, THF, water		87

2.2.3.2. Janus micelles

Janus micelles were mostly prepared from PS-*b*-PBD-*b*-PMMA triblock terpolymers that exhibited a lamella-sphere morphology with the PBD minority moieties forming spheres at the PS-PMMA interface. The spheres were cross-linked in the bulk, followed by dissolution of the product in a selective solvent for both the PS and the PMMA blocks, resulting in asymmetric star block copolymers with a cross-linked core and a double face corona with the two types of chains forming different hemispheres. The term "*Janus micelles*" has been coined for these polymeric nanoparticles, after the double-face Roman god "Janus".

To the best of our knowledge, Saito and colleagues[88] were the first who reported the preparation of Janus micelles. In particular, they employed anionic polymerization for the synthesis of five PS-*b*-P2VP-*b*-PBuMA triblock terpolymers.[88] In order for the terpolymers to exhibit the lamella-sphere structure with PS and PBuMA lamellae and P2VP spheres, the volume fractions of the two end-blocks were chosen to be equal to each other. A film of the terpolymer was cast from toluene, which is a good solvent for both the PS and the PBuMA blocks but a poor solvent for the P2VP block. One of the five terpolymers was chosen to be treated with 1,4-diiodobutane gas, resulting in the selective cross-linking of its P2VP block. The cross-linked film was then freely dispersed in THF and benzene. The hydrodynamic radius of the cross-linked product was measured using DLS in THF (at 20 °C), toluene and benzene (at 25 °C) and was found to be 37.5 nm. Furthermore, DLS was also employed for the size determination of the aggregates formed in acetone at 20 °C (a selective solvent for PBuMA block and a non-solvent for the PS) by both the linear terpolymers and their cross-linked counterpart. SLS in THF was used to determine the MW and the number of arms of the cross-linked product. The aggregation number was determined to be 47, and taking into consideration that each ABC triblock terpolymer molecule contributed to the particle two arms, namely the PS and PBuMA blocks, the total number of arms was calculated to be 94. TEM was employed to confirm that the cross-linked particles were Janus type microspheres with PS and PBuMA spatially separated coronas. Block identification was achieved using RuO_4 staining, with which the PS, PVP and PBuMA regions were imaged as gray, black and white, respectively. Investigation of micelle formation of the microspheres in selective solvents was also studied. To this end, the cross-linked terpolymer was dissolved in

acetone and cyclohexane and the R_hs were determined using DLS. Acetone is a selective solvent for the PBuMA blocks, whereas cyclohexane for the PS blocks. The authors claimed that these structures formed anomalous micelles, such as vesicles containing a solvent pool.

The same researchers[89] reported the synthesis of a PEG-*b*-PHEMA-*b*-PS triblock terpolymer employing ATRP and of PS-*b*-[P4VP-*g*-PEG] block-graft terpolymer using "living" anionic polymerization. The spherical domains of the PHEMA and the P4VP blocks obtained in the bulk were cross-linked using 1,6-hexane diisocyanate and 1,4-dibromobutane, respectively. After the cross-linking of its PHEMA block, the PEG-*b*-PHEMA-*b*-PS terpolymer did not dissolve in benzene, DMSO and dimethylformamide, but dissolved in a water/benzene mixture. This change in the solubility was attributed to the cross-linking of the middle block. Moreover, it rendered the determination of their hydrodynamic diameters impossible. In order to prove the cross-linking of the PS-*b*-[P4VP-*g*-PEG] block-graft terpolymer, the authors compared its solubility with that of the linear terpolymer in a benzene/*n*-hexane mixture and observed that the cross-linked product precipitated at a lower volume fraction of *n*-hexane. This was attributed to the increase in molecular weight due to the cross-linking. The structures formed by both terpolymers cast form benzene, that is a good solvent for the PS and the PEG blocks but a poor solvent for the PHEMA or P4VP middle block, were examined by TEM and SAXS. For the PEG-*b*-PHEMA-*b*-PS terpolymers, an ordered bicontinuous double diamond (OBDD) morphology was obtained. The other terpolymer was found to form lamellae. Subsequently, the stability of benzene/water emulsions stabilized using the Janus-type microspheres and their terpolymer precursors as emulsifiers was determined by observing the breaking of the emulsion from the increase in transmittance. The surface tension of the microsphere obtained from the graft terpolymer was lower than that obtained from its uncross-linked precursor at the same polymer concentration. Benzene/water emulsions stabilized by the two cross-linked terpolymers at a concentration of 0.1 g/L were prepared and were of the o/w type. The efficiency of the emulsifiers based on the uncross-linked graft terpolymers was higher than that of the triblock terpolymers. Moreover, the cross-linked terpolymers were better emulsifiers than their graft and linear precursors. PEG arms were observed to be expanded to the water layer whereas the PS arms expanded to the benzene droplets. Emulsion stability of the un-cross-

linked graft was higher than that of the triblock teprolymer due to the higher ratio of PEG to PS arms in the graft terpolymer compared to the triblock teprolymer. The higher the number of the PEG arms compared to the PS arms in the former case resulted in better stabilization of the benzene droplets than in the latter case. The Janus-type microspheres obtained after cross-linking the middle block in the terpolymers also exhibited better stabilization due to the increased ratio of PEG to PS arms. Furthermore, the Janus structure facilitated the stabilization of the oil (benzene) droplets in water due to the spatial separation of the PS and PEG corona-forming blocks, enabling a better contact between the PS and benzene droplets and stabilization of the particles in water through the favorable PEG-water contacts. The stability of the o/w emulsions was drastically improved by increasing the ratio of arm numbers of PEG to PS in the terpolymer and the formation of supermolecules, that is the formation of Janus-type microspheres.

Erhardt and co-workers[90] followed the same strategy employed by Saito et al.[87] to synthesize amphiphilic nanoparticles based on linear ABC triblock terpolymers with a spatially separated corona. They used anionic polymerization in THF to prepare the S_{930}-*b*-BD_{211}-*b*-MMA_{816} linear triblock terpolymer. In the bulk, the terpolymer exhibited a lamellae-sphere morphology, with the PS and PMMA end-blocks forming two separate lamellae and the PBD-middle block forming spheres embedded at the lamellar interface as shown in Figure 2.13. The spherical domains of the middle blocks were cross-linked in the bulk using S_2Cl_2. The resulting structure was dissolved in THF, a good solvent for both PS and PMMA. The authors were surprised when they observed large differences between the expected MWs and the MWs determined experimentally, implying aggregation.

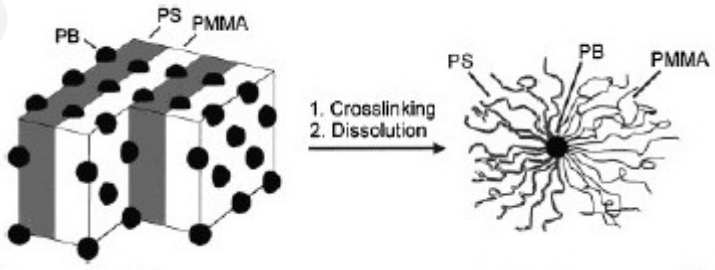

Figure 2.13. Schematic representation of the synthetic strategy followed for the preparation of Janus micelles.[90] The figure displays the Janus micelles formed by the S_{930}-*b*-BD_{211}-*b*-MMA_{816} triblock terpolymer.

Fluorescence correlation spectroscopy was used to determine the critical aggregation concentration (cac) and to give the first estimation of the hydrodynamic diameters. DLS was also used for the determination of the hydrodynamic radius. SANS confirmed the existence of aggregates above the cac. SLS was used for the calculation of the aggregate molecular weights and aggregation numbers. SFM showed small and larger particles, the latter resembling the shape of a fried egg. The authors argued that the aggregation observed could have been due to: the small differences in the solubilities of PS and PMMA chains in THF that were amplified upon addition of many chains for the formation of a Janus micelle, or to the loss of conformational entropy of the chains due to the cross-linking which could be diminished by the formation of larger phases. It was assumed that the PMMA blocks formed the corona due to their preference for polar substrates like silicon oxide, and the PS blocks formed the elevated middle part due to the Janus character of the micelles. Hence, SFM confirmed the amphiphilic nature (surface activity) of the Janus micelles.

The above-mentioned triblock terpolymer was further characterized by the same team.[91] In the bulk, the middle block of these terpolymers formed spheres located at the interfaces of lamellae formed by the outer blocks. The spheres formed by one of the terpolymers were selectively cross-linked in the bulk using disulfur dichloride (S_2Cl_2), yielding a Janus micelle. The interfacial properties of the Janus micelle and the linear terpolymer were investigated by analysis of the lateral pressure / area isotherms and using scanning force microscopy (SFM) on the monolayers formed by the two terpolymers. The isotherms revealed that both terpolymers aggregated laterally at the air/water interface, with the rather polar PMMA blocks aggregating on the interface, while the more unpolar PBD and PS blocks formed elevated domains as shown in Figure 2.14. SFM showed the formation of elongated and circular domains for the non-cross-linked terpolymer and elevated circular domains for the Janus micelle.

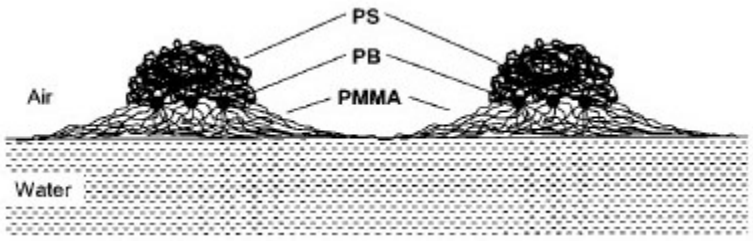

Figure 2.14. Schematic illustration of the conformation adopted by a Janus micelle monolayer at the air/water interface.[91] The Janus micelle was formed by the S_{930}-*b*-BD_{211}-*b*-MMA_{816} triblock terpolymer.

Erhardt and collegues[92] reported on the solution characterization of Janus micelles prepared by anionic polymerization and reported earlier.[90] In particular, they hydrolyzed S_{930}-*b*-BD_{211}-*b*-MMA_{816}-based Janus micelles using KOH in 1,4-dioxane and studied their solution properties using fluorescence correlation spectroscopy (FCS), DLS, SLS, cryo-TEM, SEM and SFM. Upon hydrolysis, the PMMA arms were converted to PMAA arms. FCS in aqueous solutions containing 0.17 M NaCl indicated the formation of micelles and polymolecular supermicelles from hydrolyzed Janus micelles. The critical aggregation concentration was determined to between 0.01 and 0.1 g/L. At concentrations higher than 0.1 g/L, the molecularly dissolved Janus micelles (unimers) were found to form polymolecular supermicelles (multimers). This behavior was similar to that observed for the original unhydrolyzed system in organic solvents.[90] The aggregation number of these supermicelles was determined by the ratio of the SLS molecular weight obtained for the aggregates divided by the molecular weight of a Janus micelle (calculated based on the assumption that each Janus micelle bore 13 chains and that the PMMA arms were completely hydrolyzed to PMAA). The aggregation numbers for the supermicelles were calculated to be equal to 48 Janus particles per aggregate.

Yan and co-workers[93] reported the use of anionic polymerization for the preparation of the S_{690}-*b*-$CEMA_{170}$-*b*-*t*BuA_{200} triblock terpolymer and studied the properties of the structure formed by triblock terpolymer films cast from toluene, where concentric PCEMA and P*t*BuA cylinders dispersed in a PS matrix were obtained. The PCEMA blocks were photo-cross-linked in the bulk. Dissolution of these films in THF was the next step yielding nanofibers with PS coronas, PCEMA middle layers and P*t*BuA

cores. Nanotubes with PAA-lined cores were obtained by cleaving the *tert*-butyl groups from the P*t*BuA blocks. The phase separation of the resulting S_{690}-*b*-$CEMA_{170}$-*b*-AA_{200} nanotubes in THF, with and without applied magnetic field, was also studied. TEM revealed that fibers and tubes formed alternating multilayers. Producing Fe_2O_3 nanoparticles in the PAA cores yielded solvent-dispersible superparamagnetic block terpolymer/inorganic hybrid nanofibers. The fibers formed remained dispersed in THF or other organic solvents that solubilized PS. TEM aided the observation of Fe_2O_3 in the center of the nanotubes providing an indirect proof for the presence of PAA blocks in the core of the nanotubes. Afterwards, the fibers were aligned along the direction of a magnetic field. The alignment of the Fe_2O_3-loaded nanotubes, in contrast to the behavior of the Fe_2O_3-free nanotubes, was attributed to the magnetic anisotropy of Fe_2O_3 produced in the PAA-lined cores.

The same research team[94] employed anionic polymerization for the preparation of two triblock terpolymers, $BuMA_{1270}$-*b*-$CEMA_{190}$-*b*-*t*BuA_{270} and $BuMA_{630}$-*b*-$CEMA_{180}$-*b*-*t*BuA_{210}. Thin films of both triblock terpolymers were observed by TEM and found to form concentric PCEMA and *t*BuA cylinders dispersed in a PBuMA matrix. Photo-cross-linking of the PCEMA shell-forming blocks followed and the films were dissolved in THF. Hydrolysis of the *tert*-butyl groups followed, using trimethylsilyl iodide, yielding nanotubes with PAA-lined channels in the centers. The route followed from the photo-cross-linking to the hydrolysis of the *tert*-butyl groups and the formation of the nanotubes with PAA in the centers is schematically represented in Figure 2.15.

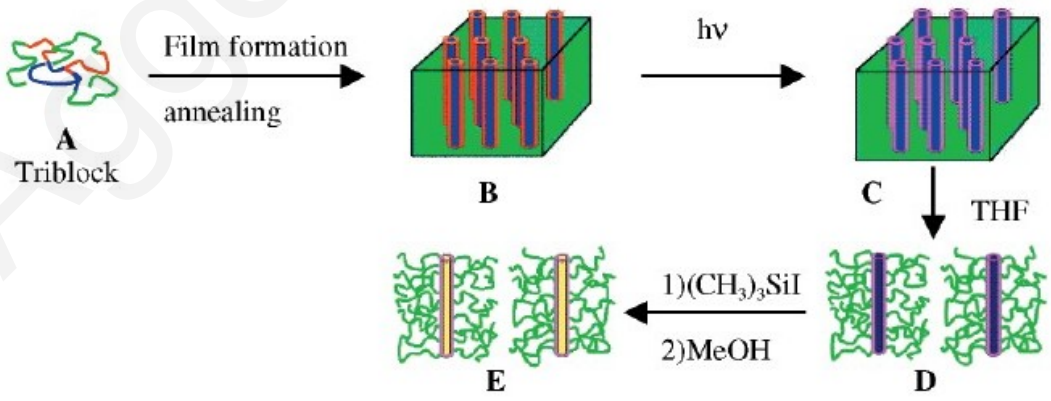

Figure 2.15. Synthetic steps followed for the preparation of the nanotubes with PAA-lined cores formed by the hydrolyzed *t*-BuA units of the $BuMA_{1270}$-*b*-$CEMA_{190}$-*b*-*t*-BuA_{270} triblock terpolymer.[94]

Using TEM and ^{1}H NMR, the authors concluded that the nanotubes had the PAA blocks in the core, also supported by their facile dissolution in THF or dichloromethane, both non-solvents of PAA, and their loading with Fe_2O_3 which rendered the core of unstained tubes visible in TEM.

All the monomers, the polymerization methods and the methods employed for the solution characterization of the ABC triblock terpolymers used for the formation of the Janus micelles reported in the above studies are listed in Table 2.12.

Table 2.12. Summary of the information about the reviewed ABC triblock terpolymers used for the preparation of Janus micelles.

Monomer Type			No. of synthesized and studied polymers	Polymeriz. Method	Characteriz. Methods for Aggregation	Characteriz. Solvent(s)	Ref. no.
Monomer 1	**Monomer 2**	**Cross-linkable**					
S[a]	BuMA[a]	2VP	5	anionic	DLS, SLS, TEM	THF, toluene, B, acetone, CH[a]	88
S	EG	HEMA, 4VP	2	ATRP/anionic	TEM, SAXS	B, water/B	89
S	MMA	BD	1	anionic	DLS, SLS, TEM, SANS	THF	90
S	MMA	BD	2	anionic	Isothermal analysis, SFM	water	91
S	MAA	BD	1	anionic	FCS, DLS, SLS, cryo-TEM, SEM, SFM	water	92
S	AA	CEMA	1	anionic	TEM	THF	93
BuMA	AA	CEMA	2	anionic	TEM, ^{1}H NMR	THF, CH_2Cl_2	94

Thus, there is an increasing volume of research produced on the solution (mainly, aqueous) properties of ABC triblock terpolymers[32] with very interesting results. Most of the terpolymers reported were linear, but some were cross-linked, micro-gel-type (micto-arm stars, shell cross-linked micelles and Janus micelles). No ABC terpolymer networks have been reported. It appears, therefore, that there is a large gap for the study of micro- but especially macro-gel ABC systems that the present Thesis aimed to fill. To this end, we chose a set of three commercially available monomers that provide aqueous amphiphilicity, pH- and temperature-responsiveness, and designed out of them ABC linear, star-block and segmented network systems. The major focus of the characterization of the resulting terpolymers was on the study of their microphase separation in water, as a function of block sequence and terpolymer composition.

CHAPTER 3: Polymer Characterization Methods

All the polymers prepared in this Study, their homopolymer, diblock, triblock precursors and the linear pentablock terpolymer precursors to the networks were characterized in terms of their relative MWs and MWDs by GPC in THF. The absolute molecular weight of the star terpolymers and their number of arms were determined by SLS in THF. ^{1}H MNR in $CDCl_3$ was employed for the composition determination in the constituting monomers of the linear and star terpolymers as well as the pentablock terpolymer precursors to the networks and the extractables of the networks. SLS in water was employed for the determination of the aggregation numbers of either the micellar structures or the aggregates formed by the linear and star terpolymers respectively.

DLS in water and THF was employed for the determination of the hydrodynamic diameters of either the micelles formed by the diblock and triblock terpolymers or the hydrodynamic diameters of their coils, respectively.

The ability of the linear and star terpolymers to act as surfactants, that is reducing the surface tension at the air-water interface, was studied using the du Noüy ring method. The theoretical background of all the experimental methods employed in the present Study is given in the following paragraphs.

3.1. Gel Permeation Chromatography

Gel permeation chromatography (GPC), also known as *size exclusion chromatography* (SEC), is a liquid chromatographic method widely used in Polymer Science to determine the relative molecular weight and the molecular weight distribution of a synthetic polymer sample. In this method, a dilute solution of a sample that contains polymer, oligomers, or even monomers, is injected into a solvent stream which flows through a column packed with a highly porous material which is usually SiO_2 or a polymer gel.[95(a),96] The polymer molecules are separated according to their hydrodynamic volumes, i.e. the size of the molecular coil. The principle of the technique lies in the fact that large molecules have little accessibility to the pores of the packing material and are eluted in a shorter period of time than the smaller molecules. This is because small molecules enter the pores of the packing material

and remain there for some time, hence small molecules are retarded relative to the larger ones. This is schematically illustrated in Figure 3.1.[96]

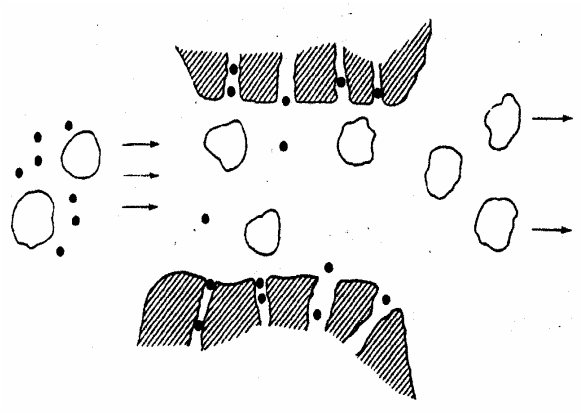

Figure 3.1. The separation of molecules with respect to their hydrodynamic volume by GPC.[96] The smaller molecules (illustrated with the black circles) penetrate in the pores of the column, whereas the larger molecules pass through and are eluted faster.

After the molecules are eluted from the column, an analyzer records the polymer concentration with respect to the elution time or the elution volume (V_e). The volume of the solvent in the column, V_e, can be distinguished as the stagnant solvent in the pores (symbolized as V_i) and the interstitial liquid in the voids (denoted as V_0) between the packed particles:[97]

$$V_e = V_0 + V_i \tag{3.1}$$

For very large molecules, that do not penetrate the pores of the packing material, their elution volume is exclusively due to their residence in interstitial liquid in the voids. Thus:

$$V_e = V_0 \tag{3.2}$$

The elution volumes for the smaller molecules, that penetrate in the pores of the column, is given by:

$$V_e = V_0 + KV_i \tag{3.3}$$

where K is a function of both the pore size and the molecular size and indicates what fraction of the pore volume is accessible to that particular solute. When $K = 0$ the solute is totally exluded from the pores and when $K = 1$ it totally penetrates the pores.

The polymer in the eluent is usually detected by either refractive index (RI) or ultraviolet/visible spectroscopic detectors.[96] A differential refractometer measures the difference in the refractive index between the eluted solution and the pure solvent. A plot of the refractive index difference as a function of time can yield directly a plot of the molecular weight distribution. When ultraviolet detection is used and the absorbance at a constant wavelength is monitored as a function of elution time, the polymer must bear at least one unit absorbing in the UV.

As mentioned above, GPC separates molecules based on their elution volumes (or times). In order to obtain the molecular weight of these molecules, a calibration is necessary for the correlation of the molecular weights with the elution volumes (or elution times) of the molecules. The instrument is usually calibrated using monodisperse polymer standards with known molecular weights obtained by absolute methods such as SLS and osmometry. Polystyrene, poly(methyl methacrylate) and poly(ethylene oxide) are the polymer standards most commonly used for the GPC calibration. Ideally, the standard samples should be from the same polymer as the test sample, but usually the standards used are chemically or structurally related to the test polymer and it is *assumed* that the calibration applies to the polymer of interest.

GPC is a method providing both the (relative) number-average molecular weight M_n and weight-average molecular weight M_w as well as the molecular weight polydispersity index (PDI) defined as:[98]

$$\overline{M_n} = \frac{\sum_i N_i M_i}{\sum_i N_i} = \sum_i n_i M_i \tag{3.4}$$

$$\overline{M_w} = \frac{\sum_i N_i M_i^2}{\sum_i N_i M_i} = \frac{\sum_i W_i M_i}{\sum_i W_i} = \sum_i w_i M_i \tag{3.5}$$

$$PDI = \frac{\overline{M}_w}{\overline{M}_n} \tag{3.6}$$

where N_i is the number of molecules with molar mass M_i, and n_i is their number fraction, W_i is the mass of the molecules having molar mass M_i, and w_i is their mass fraction.

A more satisfactory "universal" calibration technique has been developed which permits the calibration of GPC columns for a wide range of polymers using a single set of standard samples (i.e. PS fractions having narrow ranges if MWs), and then, by calculation, using the Mark-Houwink parameters of the polymers, to convert the molar mass scale of the calibrant polymer to that of the polymer being studied, provided that the relation between the hydrodynamic volume and the absolute molecular weight of the sample and the calibration standard is known. This procedure is called *universal calibration*.[98] The hydrodynamic volume is proportional to the product $[\eta]M$, where $[\eta]$ is the intrinsic viscosity. If the calibration is carried out using a polymer calibrant (index 2), the universal calibration procedure is based on equation (3.8), derived as follows:

$$[\eta] = K\overline{M}_z^{\alpha} \tag{3.7}$$

$$[\eta]_1 M_1 = [\eta]_2 M_2$$

$$K_1 M_1^{1+a_1} = K_2 M_2^{1+\alpha_2}$$

$$M_1 = \left[\frac{K_2}{K_1} M_2^{1+\alpha_2} \right]^{1/1+\alpha_1} \tag{3.8}$$

where K, α are the Mark-Houwink parameters and are different for each polymer-solvent combination, and index 1 refers to the polymer being studied.

3.2. Nuclear Magnetic Resonance Spectroscopy

Nuclear magnetic resonance (NMR) spectroscopy is one of the most powerful spectroscopic techniques providing information on the structure and composition of a compound. The nuclei bearing an even number of protons and neutrons do not exhibit magnetic properties. On the other hand, the nuclei of isotopes bearing an odd number of protons (i.e. ^{1}H, ^{2}H, ^{14}N, ^{19}F, ^{31}P) or an odd number of neutrons, as in the case of ^{13}C, exhibit magnetic properties. The magnetic properties in the latter case are due to the positive charge of these nuclei, which spin about their nuclear axes and generates a magnetic moment along the axis inducing a magnetic field.[95(b),99] In the

absence of electric field the spins of the nuclei are randomly oriented, but as soon as an external magnetic field is applied the magnetic nuclei with spin quantum numbers, I, (1/2, 1, 3/2, 2,...) align themselves in $2I$+1 different ways, each one having a different energy. This is the origin of the NMR spectroscopy, in which the absorption of electromagnetic radiation promotes nuclei from low energy to high energy alignments in an external magnetic field. The simplest situation is that for nuclei with I=1/2 (i.e ^{1}H, ^{13}C) since their nuclear magnetic moments are aligned either parallel with (lower energy state) or against (higher energy state) the magnetic field. The energy difference between these two states depends upon the *magnetogyric ratio* γ and the strength, B, of the external magnetic field at the nucleus. Resonance frequency is the frequency, ν, of radiation required to flip the nuclear magnetic moment from being aligned with to being aligned against the external magnetic field and is given by:

$$\nu = \frac{\gamma B}{2\pi} \tag{3.9}$$

Hence, when the sample is placed in a magnetic field, its nuclei are promoted from the ground lower energy state to the higher energy one, and this energy is recorded from the spectrometer as the first peak. The strength of the field on the nuclei is affected by the presence of the electronic environment and neighboring nuclei causing shielding or deshielding of the nuclei. The electrons surrounding the nucleus induce a magnetic field opposing the externally applied magnetic field, thus shielding the nucleus and resulting in the shifting of the resonance frequency to higher field values. The absorptions of the sample with respect to the absorbance of the reference compound tetramethylsilane [$(CH_3)_4Si$, TMS] are recorded as chemical shifts, expressed in the δ-scale as shown in the following equation:

$$\delta = \frac{\Delta}{\Delta_0} \times 10^6 \tag{3.10}$$

where δ is a dimensionless number expressed in ppm, Δ denotes the difference of the resonance frequency in Hz between a proton and the protons of TMS, and Δ_0 is the basic resonance frequency of the spectrometer.

NMR spectra are taken for solutions with concentrations 2-10 % of substances dissolved in aprotic solvents (i.e. CCl_4 or CS_2) or deuterated solvents $CDCl_3$) also

containing the TMS reference.[95(b)] Protons having chemically the same environments are magnetically equivalent yielding the same chemical shift. The area under the peaks in the spectrum is proportional to the number of the corresponding protons. When the protons are not magnetically equivalent they give different chemical shifts and the ratio of the relative areas of the two peaks corresponding to the two types of protons is proportional to the ratio of the number of protons in each group.

3.3. Light Scattering

Light scattering is an experimental technique widely used for dilute polymer solution characterization providing the absolute weight-average molecular weight, M_w, the radius of gyration, R_g^2, the second virial coefficient B (static light scattering, SLS) and the hydrodynamic diameters, d_h, (dynamic light scattering, DLS).

Light is an electromagnetic radiation, composed of a magnetic and an electric field, vertical to each other. The basic concept of light scattering is that while the radiation passes through the substance of interest, the electric field of the radiation interacts with the electrons of the substance forcing them to oscillate around their equilibrium position. As a result, a dipole is induced in the molecules which become secondary light emitters, emitting light to all directions. The emitted radiation has the same wavelength as the incident radiation (Rayleigh scattering). Hence, the light scattering technique is based on the measurement of the intensity of the scattered light at various angles compared to the intensity of the incident beam. The intensity of the scattered light depends on the wavelength of the incident beam, the size and shape of the particles, the optical density of the scatterers, and the angle of observation. The wide use of light scattering is mainly due to the short measurement times, to the fact that it is a method not destructive to the sample, it is absolute since no calibration is required and is applicable for systems with a large number of particles. On the other hand, two technical factors limit its applicability: the sample should not be very concentrated in order to avoid multiple scattering, and the system should be free of dust because dust particles also scatter light.

3.3.1. Static Light Scattering (SLS)

In SLS the intensity of the light scattered by a polymer solution at certain angles and for various polymer concentrations is measured. SLS is a method used for the determination of the absolute $\overline{M}_w$, $\overline{R_g^2}$ and B.

There are two theories concerning light scattering, based on the size of the particles:[97(b),99(b),100]

1. Rayleigh theory describes the light scattering by molecules with small dimensions compared to the radiation wavelength. For the visible light, Rayleigh scattering is applicable for the gases and for liquids with low molar mass. The intensity of the light scattered by such a molecule is given by the equation:

$$\frac{i_v r^2}{I_0} = \frac{2\pi^2 \left(\frac{\partial n}{\partial c}\right)^2 Mc(1+\cos^2\theta)}{N_{Av}\lambda^4} \tag{3.11}$$

where i_v is the intensity of the scattered light at distance r and angle θ, I_0 and λ are the intensity of the incident beam and its wavelength, respectively, M is the molecular weight of the scatterer, c (g/L) is the concentration, $\frac{\partial n}{\partial c}$ is the gradient of the refractive index with respect to the concentration, and N_{Av} is the Avogadro number. The ratio $\frac{i_v r^2}{I_0}$ is known as the Rayleigh ratio, R_θ. According to equation (3.11) the intensity of the scattered light is proportional to the molecular weight and the concentration and inversely proportional to λ^4. It also depends on the square of the gradient of the refractive index with respect to the concentration.

The above analysis is valid under the conditions that the scatterers are far from each other and there is no interference between the light emitted from them. This is not the case in liquids, where the scatterers are much closer and a destructive interference between the emitted waves occurrs. Despite that, a weak scattering of the light by pure liquids as well as solutions is observed and is attributed to the fluctuations of the solution density in the former case and the fluctuations of the solute concentration in the latter.[99(b)]

For a dilute solution, the scattering arising from the local solvent density fluctuations is eliminated by taking the difference ΔR between the Rayleigh ratios of the solution and the solvent:[101]

$$\Delta R = R_{solution} - R_{solvent} \tag{3.12}$$

and the scattering by the solution is given by:

$$\frac{i_v}{I_0} = \frac{2\pi^2 n_0^2 \overline{\alpha_V^2}\left(1+\cos^2\theta\right)}{\lambda^4 r^2} \tag{3.13}$$

where π equals 3.14 and $\overline{\alpha_V^2}$ is the excess polarizability equal to:[101]

$$\overline{\alpha_V^2} = (\overline{a_V})^2 + 2\overline{\alpha_V}\,\overline{\delta\alpha_V} + \overline{\delta\alpha_V^2} \tag{3.14}$$

Due to the fluctuation of the polarizability with the concentration, the first two terms in the right side of equation (3.14) vanish, resulting in $\overline{\alpha_V^2} = \overline{\delta\alpha_V^2}$. The mean-square polarizability fluctuation is given by:

$$\left\langle \delta\alpha_{\mathrm{V}}^2 \right\rangle = \left(\frac{\partial \alpha_V}{\partial c}\right)^2 \left\langle \delta c \right\rangle^2 \tag{3.15}$$

$\left\langle \delta c \right\rangle^2$ is the mean square concentration fluctuation given by:

$$\left\langle \delta c \right\rangle^2 = \frac{kT}{\left(\partial^2 G/\partial c^2\right)_{T,P}} \tag{3.16}$$

Assuming n_2 moles of a solute with M molecular weight in a volume element, υ, then:[101]

$$\left(\frac{\partial G}{\partial c}\right)_{T,P} = \left(\frac{\partial G}{\partial n_2}\right)_{T,P} \frac{\partial n_2}{\partial c} = \mu_2 \frac{\upsilon}{M} \tag{3.17}$$

with μ denoting the chemical potential:

$$\mu_2 = \mu_2^0 + RT\ln c + RT\ln\gamma \tag{3.18}$$

where γ is the activity coefficient. Substituting (3.18) in (3.17) and taking the second derivative of G with respect to c results in:

$$\left(\frac{\partial^2 G}{\partial c^2}\right)_{T,P} = \frac{\upsilon RT}{Mc}\left(1 + c\frac{\partial \ln \gamma}{\partial c}\right) \tag{3.19}$$

Combining equations (3.19), (3.16) and substituting in (3.13) yields:

$$\frac{i_v}{I_0} = \frac{2\pi^2 n_0^2 (\partial n/\partial c)^2 (1+\cos^2\theta) Mc}{N_{AV}\lambda^4 [1 - c(\partial \ln \gamma/\partial c)]} \tag{3.20}$$

with

$$\frac{2\pi^2 n_0^2}{\lambda^4 N_{AV}}\left(\frac{dn}{dc}\right)^2 = K \tag{3.21}$$

Combining (3.13), (3.20) and (3.21) results in:

$$\frac{Kc}{R_\theta}(1+\cos^2\theta) = \frac{1}{M}(1 + 2Bc + ...) \tag{3.22}$$

where B is the second virial coefficient describing the interactions between the particles. When $B < 0$ these interactions are attractive, whereas when $B > 0$ the particles repel each other.

2. Debye theory that describes light scattering by particles with dimensions comparable to the radiation wavelength.

The particles are no longer considered point scatterers, but multiple scatterers, each one of them having more than one scattering centers not equally exposed to the same radiation. In this case, equation (3.22) is corrected by a factor called form factor, $P(\theta)$. This factor depends on the size, the shape and the number of the particles, hence it encloses important information on their internal structure. When the particle is very small, then $P(\theta) \rightarrow 1$ and the information on the particle internal structure is no longer available. Thus, light scattering by particles with dimensions comparable to the radiation wavelength is described by the equation:

$$\frac{Kc}{R_\theta}(1+\cos^2\theta) = \frac{1}{P_\theta}\left(\frac{1}{M} + 2B'c + ...\right) \tag{3.23}$$

According to equation (3.23), R_θ is proportional to $P(\theta)$, hence the intensity of the scattered light will also be proportional to it.

The intensity of the scattered light at certain angles and for various concentrations of the solution are plotted in Zimm plots as $\frac{Kc}{R_\theta}(1+\cos^2\theta)$ vs $\sin^2\frac{\theta}{2}+ac$ where a is a constant used for better dispersion of the data points in the plot. The intercept of the plot yields $\frac{1}{M_w}$, whereas the radius of gyration can be obtained from the slope for $c=0$. The second virial coefficient is obtained from the slope for $\theta=0$.

3.3.2. Dynamic Light Scattering (DLS)

DLS is a method used to study the motion of macromolecules in solution and for the determination of the hydrodynamic radii, R_h of macromolecules in solution through the study of their motion. In DLS a monochromatic beam of light goes through a solution, and the variation of the scattering intensity with time at a certain angle θ is measured. The variation of intensity with time contains information on the random motion of the particles and can be used to calculate their diffusion coefficient.[100(b)] This time variation of the intensity is due to the fact that the intensity of the scattered light detected by the detector is the result of the radiation coming from the various particles that are randomly moving due to thermal movements.

The random movement of the scatterers gives rise to a Doppler effect, hence the light possesses a range of frequencies shifted very slightly from the frequency of the incident light.[99(c),102]. The Doppler shift ranges from zero (for zero scattering) to a maximum value obtained when the scattering angle is 180°. The distribution of the scattered light frequency around the mean frequency is shown in Figure 3.2.

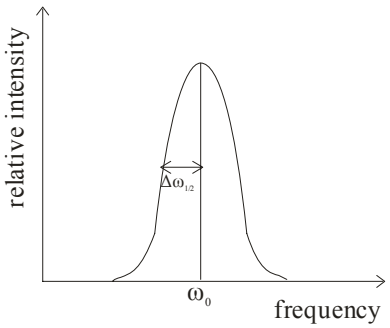

Figure 3.2. The frequency distribution of the scattered light.

Assuming spherical particle shape and perfect Lorentzian curve, the half-width of the peak at half of its height, $\Delta\omega_{1/2}$ is related to the particle diffusion coefficient D through the mathematical expression:

$$\Delta\omega_{1/2} = D\left(\frac{4\pi\eta_0\omega_0}{c}\sin\frac{\theta}{2}\right)^2 \tag{3.24}$$

where ω_0 is the frequency of the incident beam and η is the viscosity. The other symbols are as explained above. For particles with spherical geometry, the following equation applies:[100(b)]

$$D = \frac{kT}{f} = \frac{k_B T}{6\pi\eta R_h} \tag{3.25}$$

where f is the friction coefficient, η is the viscosity of the fluid, k_B is the Boltzmann constant, and T is the absolute temperature of the solution.[100(b)] The radius R_h measured in this manner is usually known as the hydrodynamic radius since it is derived from the Stokes friction coefficient, $6\pi\eta R_h$, a result of fluid (or hydro) dynamics.

3.4. Turbidimetry

This method is used for the determination of the *cloud points* of the polymer solutions. In turbidimetry, the changes in optical density, at a constant wavelength, upon increasing the polymer solution temperature are recorded. The value of the temperature at which an abrupt increase in the solution optical density occurs, is taken as the cloud point. Physicochemically, the term "cloud point" is the temperature at which the solvent ceases to be a good solvent for the sample, resulting in the formation of large aggregates that cause the increased light scattering detected by the spectrophotometer. This phenomenon is analyzed by Flory,[103] according to whom the *theta* (Θ) temperature is described by the expression:

$$\Theta = \frac{\kappa_1 T}{\psi_1} \tag{3.26}$$

where κ_1 is an enthalpic parameter, ψ_1 is a measure of the solvation entropy and T is the absolute temperature. These parameters are related to the Flory-Huggins polymer-solvent interaction parameter, χ, through the expression:

$$\kappa_1 - \psi_1 = \chi - \frac{1}{2} \tag{3.27}$$

Combining equations (3.26) and (3.27) yields the following expression for χ:

$$\frac{1}{2} - \chi \equiv \psi_1 \left(1 - \frac{\Theta}{T}\right) \tag{3.28}$$

From equation (3.28) it is concluded that:

i. ψ_1 must be a dimensionless quantity
ii. Θ should have the same dimensions as temperature
iii. The same positive and negative values should be obtained for $T > \Theta$ and $T < \Theta$ respectively, provided that ψ_1 is positive (e.g. polymer solutions in organic solvents, displaying an UCST).

Considering equation (3.28), when ψ_1 takes negative values, as in the case of polymers with LCST (e.g. polymers in aqueous solution), then, as the solution temperature increases, χ will also increase and the solvent will become poorer.

In addition to the solvent quality, for the precipitation of amphiphilic polymers the effects of steric stabilization should also be considered. Amphiphilic molecules are stabilized in a solvent due to their ability to form micelles. In the absence of charge, the stability of these domains is mainly controlled by the interactions imposed due to steric hindrance of the lyophilic blocks forming the micellar corona. The Gibbs free energy of steric stabilization between two micelles is given by the equation:[104(a)]

$$\Delta G = 2kT\left(\frac{V_s^2}{V_1}\right)v^2 i^2 \left(\frac{1}{2} - \chi\right)\left(\int_0^d \hat{\rho}_d \, \hat{\rho}'_d \, dx\right) \tag{3.29}$$

where V_s is the volume of one lyophilic monomer repeating unit, V_1 is the volume of one solvent molecule, v denotes the number of chains per unit surface, i is the

number of the lyophilic units per chain (degree of polymerization), d is the distance between the two micelles, and $\hat{\rho}_d$ and $\hat{\rho}'_d$ are the number densities of the first and second micelle, respectively. According to equation (3.29), the higher the number of chains per unit surface and the higher the degree of polymerization of the lyophilic units, the more positive the value of the Gibbs free energy for steric stabilization, resulting in the repulsion of the two micelles. In addition to that, equation (3.29) shows that when $\chi < 1/2$, intermicelle aggregation is not favored because ΔG always remains positive, independently of how close the two micelles are, due to the more favorable interactions arising between the polymer and the solvent compared to the interactions between the micelles. Upon increasing the temperature, the polymer-solvent interactions become less favorable than the intermicelle interactions, leading to intermicelle aggregation that causes increased scattering.

3.5. Surface Tension

Surface tension (γ) is a force arising due to the contact between two interfaces tending to decrease the area of the interface.[100(c)] Surface tension can be defined as:

$$\gamma = \frac{F}{p} \tag{3.30}$$

where F is the force needed to be applied for stretching an interfacial film of perimeter p.

Several techniques can be used to measure surface tension.[100(c)] One of the most common methods used for the determination of the surface tension, although not very precise, is the du Noüy ring method (also employed in this Thesis), where the force required for the separation of a thin, metal ring (of known geometrical characteristics) from the air-solution interface is measured. This force is given by:

$$F = 4\pi r \gamma \alpha \tag{3.31}$$

where $4\pi r$ is the perimeter of the ring and α is a correction factor depending on the ring geometry and arising from the fact that the ring has a certain thickness.

A simpler method is the rise of liquid in a capillary tube where the surface tension is calculated through measurements of the height of the liquid in the capillary.

Moreover, the techniques of the sessile and pendant drops could be employed, where the shape of the drops depends on gravity and interfacial tension.

CHAPTER 4: Experimental Section

4.1. Chemicals

The monofunctional GTP initiator 1-methoxy-1-trimethylsiloxy-2-methyl propene (MTS), the monomers 2-(dimethylamino)ethyl methacrylate (DMAEMA), methyl methacrylate (MMA) and *n*-butyl methacrylate (BuMA), the cross-linker ethylene glycol dimethacrylate (EGDMA), the free radical polymerization inhibitor 2,2-diphenyl-1-picryl-hydrazyl hydrate (DPPH), calcium hydride, (CaH_2), potassium metal, deuterated chloroform, aqueous HCl 0.5 M and NaOH 0.5 M solutions were purchased from Aldrich, Germany. The methoxy hexa(ethylene glycol) methacrylate (HEGMA) monomer was kindly donated by Laporte Performance Chemicals, UK.

4.2. Purification of Monomers, Cross-linker, Initiators, Catalyst and Solvent Used for the Polymerizations

Due to the high viscosity of the neat monomer, a 50 % v/v solution in freshly distilled tetrahydrofuran (THF)[105] of the HEGMA monomer was used for the processing with basic alumina. The HEGMA monomer solution as well as the other monomers and cross-linker used, namely DMAEMA, MMA, BuMA and EGDMA, were passed twice through basic alumina columns in order to remove the polymerization inhibitor and any protic impurities. Subsequently, DMAEMA, MMA, BuMA and EGDMA were stirred for at least two hours over CaH_2 in the presence of the free radical inhibitor DPPH. CaH_2 effects the removal of the last traces of moisture and protic impurities. DMAEMA, MMA and EGDMA were vacuum-distilled just prior to use. The HEGMA solution was stirred over CaH_2 (without DPPH), and was filtered through a 0.45 μm PTFE syringe filter directly into the polymerization flask. The polymerization solvent, THF, was refluxed over a potassium/sodium alloy for three days and was freshly distilled prior to use. The polymerization catalyst, tetrabutylammonium bibenzoate (TBABB), was prepared according to the procedure reported by Dicker and coworkers[106] and kept under vacuum until used.

While the MTS initiator was commercially available, the MTSMC difunctional initiator was freshly prepared following a procedure reported in the literature,[107] which is detailed in Section 4.2.1 below.

Both the monofunctional and the bifunctional initiators were distilled prior to their use.

The chemical structures and names of the four monomers, the cross-linker, and the MTS and MTSMC initiators, are depicted in Figure 5.1 in Chapter 5 (following Chapter).

4.3. Synthesis

4.3.1. Synthesis of 1,4-bis(methoxytrimethylsiloxymethylene)cyclohexane (MTSMC)

The bifunctional initiator used for the preparation of the networks presented in this study was synthesized according to the literature.[107] For the synthesis, a 250 mL two-neck round bottom flask was used. A dropping funnel was adjusted at one of the arms, while the second one was sealed with a rubber septum and the system was placed under a nitrogen atmosphere. While the system was under the nitrogen atmosphere, 45 mL of freshly distilled THF was added. Addition of 10.2 mL of diisopropylamine (7.36 g, 0.0729 mol) followed. A digital thermometer was attached to the bottom of the flask in order to monitor the reaction temperature. The system was placed in an ice bath and was left to cool down. When the temperature of the system approached 0 °C (T = 2.8 °C), 29 mL of *n*-BuLi 2.5 M in hexane (0.0725 mol) was added in the pre-attached dropping funnel. Subsequently, *n*-BuLi was added drop-wise in the round bottom flask containing the THF and the diisopropylamine. The system was left under stirring for 90 minutes. After the complete addition of *n*-BuLi, the reaction temperature reached 15.4 °C. The system was sunk in a Dewar vessel containing pre-equilibrated dry ice (solid CO_2) in acetone at –78 °C. Next, 7.5 mL of freshly distilled (stirred over CaH_2) 1,4-cyclohexanedicarboxylate (8.33 g, 0.0416 mol) was added. The assembly was left under stirring for 120 minutes at –78 °C. After the 120 minutes elapsed, the yellowish content of the flask became solid. In an effort to re-dissolve it, 20 mL of freshly distilled THF was added with a glass syringe. After its redissolution, 11.5 mL trimethylchlorosilane (9.89 g, 0.0919 mol) was added and the reaction mixture was left under continuous stirring for another 120 min at –78 °C. The system was left to slowly reach room temperature and the reaction mixture was filtered through a microfilter using a glass syringe. The

resulting solution (filtrate) was placed for a few minutes under nitrogen. A rotary evaporator at room temperature was used for the removal of the solvents (THF and hexane) and excess trimethylchlorosilane from the solution, yielding an oily, viscous liquid. Some solid was still present in the obtained oil and had to be removed. To this end, 10 mL of freshly distilled THF was added, the solution was transferred to a 100 mL round bottom flask, was refiltered as described above and the THF was removed once again using the rotary evaporator. A viscous oil-like liquid was obtained and was distilled under vacuum using a vacuum line. The product was distilled under vacuum at 102 °C and was characterized by ^{1}H NMR in deuterated chloroform.

4.3.2. Synthesis of Linear and Star ABC Triblock Terpolymers

The glassware used for the polymerizations had to be very clean and free of moisture. In order to meet these requirements, all the glassware used was successively soaked in a base bath and an acid bath followed by careful rinsing with tap-water and acetone. The glassware was placed in an oven and was left there at 120 °C to dry overnight. Before their use, they were placed in a desiccator to cool down to room temperature.

A typical polymerization procedure, yielding the ABC triblock terpolymer star with block sequence DMAEMA-HEGMA-MMA with 10 units in each block, is detailed below. Freshly distilled THF (20 mL) and 0.5 mL MTS (0.43 g, 2.46 mmol) initiator were added with a syringe, in this order, to a 100 mL round bottom flask containing a small amount (~ 10 mg) of TBABB. Subsequently, DMAEMA (4.1 mL, 3.83 g, 24.3 mmol) was slowly added under stirring. The polymerization temperature (25.0-40.0 °C) abated within 5 minutes, a sample for gel permeation chromatography (GPC) was extracted, and 16.4 mL (8.61 g of neat monomer, 24.6 mmol) of the 50% v/v solution of HEGMA in THF was added (33.9-31.1°C). A sample of the DMAEMA-HEGMA diblock copolymer was extracted for GPC analysis. Next, 2.6 mL MMA (2.43 g, 24.3 mmol) was added to the solution, leading to a temperature increase (29.4-39.1 °C), and a sample for GPC analysis of the linear ABC triblock terpolymer was extracted. Finally, 1.8 mL (1.89 g, 9.54 mmol) of the EGDMA bifunctional monomer (cross-linker) was added to the linear terpolymer solution leading to a temperature rise (37.2-43.5 °C) and to the formation of the star ABC triblock terpolymer.

To obtain the star terpolymers with the other block sequences, the order of monomer

addition was changed accordingly, and the cross-linker was added last. For the synthesis of the star with arms comprising statistical terpolymers, the three monomers were added simultaneously, while the cross-linker was added last. The polymerizations of the star terpolymers were terminated by the addition of 0.5 mL methanol to prevent any subsequent inter-core coupling. The same procedure, as that for the synthesis of the star terpolymers, was followed for the synthesis of the linear triblock terpolymers in which, however, the addition of the cross-linker was omitted.

Both the linear and the star terpolymers were recovered by precipitation in *n*-hexane and dried for three days in a vacuum oven at room temperature.

4.3.3. Synthesis of ABCBA Pentablock Terpolymer Based Networks

For the preparation of the model networks comprising linear ABCBA pentablock terpolymers between the cross-links, a similar route was followed. In the case of the networks, a bifunctional initiator (instead of the monofunctional used for the preparation of the linear and star terpolymers) was used. Upon the addition of the first monomer, a linear homopolymer chain with active sites at both ends of the chain was prepared. The sequential additions of the second and third monomers followed. The procedure was the same as that followed for the preparation of the block sequence isomeric linear triblock terpolymers. Upon formation of the triblock terpolymer, the cross-linker was added effecting the interconnection of the terpolymer chains at both of their ends, yielding the model networks based on the respective block sequence isomeric terpolymers. For the preparation of the randomly cross-linked network with a statistical distribution of the three monomers (the "random-random" network) all the monomers and the cross-linker were polymerized simultaneously. For the synthesis of the model network with a statistical distribution of the three monomers but well-defined lengths of the chains between cross-links (the "random" model network), the three monomers were polymerized simultaneously but the cross-linker was added last. During the preparation of the networks, the addition of the cross-linker led to the gelation of the solution within seconds.

4.4. Polymer Characterization

The terpolymers prepared in this study, as well as their homopolymer, diblock and triblock precursors, were characterized both in THF in terms of their molecular

weights, and molecular weight distributions. Furthermore, the molecular weights of the terpolymers in water were determined. The composition of the terpolymers was determined by ^{1}H NMR in $CDCl_3$. Dynamic and static light scattering were employed for the measurement of the hydrodynamic diameters and the absolute molecular weights of the linear and star terpolymers, respectively. The cloud points of the linear and the star terpolymers prepared for this Dissertation were determined by measuring the absorption of the copolymer solutions at 500 nm with increasing the solution temperature. In the case of the networks, an effort to determine their cloud points through measuring their degrees of swelling with increasing temperature was made.

The linear homopolymers, the ABA triblock, the ABCBA pentablock terpolymer precursors to the ABCBA networks and the extractables were also characterized in the same way. As mentioned above, during the synthesis aliquots were extracted from the reaction pot. In the case of the networks, their degrees of swelling were also determined, as well as their cloud points.

4.4.1. Characterization in Organic Solvents

4.4.1.1. GPC in THF

All of the linear and star terpolymers as well as their linear homopolymer, diblock and triblock precursors were characterized in terms of their molecular weights (MWs) and molecular weight distributions using GPC in THF. 0.1 mL aliquots were taken out of the polymerization flasks and diluted with THF (HPLC grade) to 1.0 mL. The samples were filtered through PTFE syringe filters with a 13 mm diameter and a 0.5 μm pore size into a new vial and were analyzed by GPC.

GPC was performed on a Polymer Laboratories system equipped with a PL-LC1120 isocratic pump, an ERC-7515A refractive index detector. Two chromatographic columns were used, a PL Mixed "D" column for the characterization of the polymers with the higher molecular weight (star terpolymers), and a PL Mixed "E" column for the linear terpolymers. The eluent was THF, pumped at 1 mL min^{-1}. The MW calibration for the PL Mixed "D" column was based on seven narrow MW (630, 4 250, 7 600, 28 900, 50 000, 128 000 and 260 000 g mol^{-1}) polyMMA standards also supplied by Polymer Laboratories. The MW calibration for the PL Mixed "E" column was based on six narrow MW (630, 1 400, 4 250, 7 600, 13 000 and 28 900 g

mol^{-1}) poly MMA standards.

4.4.1.2. Static Light Scattering (SLS)

SLS was performed to determine the absolute weight-average MWs (M_ws), of the terpolymers in THF. For the SLS measurements, the samples were filtered through a 0.45 μm PTFE syringe filter directly into the spectrophotometer.

The SLS experiments performed for the characterization of the terpolymers presented in Section 5.2 were carried out using a thermally regulated (0.1 °C) spectrogoniometer, model SEM RD (Sematech, France), equipped with a He-Ne laser operating at 633 nm. For each terpolymer solution, the intensity of the scattered light was measured at eight angles: 30°, 45°, 60°, 75°, 90°, 115°, 130° and 145°. The refractive index increments d*n*/d*c* required for the M_w calculations were determined using a Chromatic KMX-16 differential refractometer also operating at 633 nm.

The instrument employed for the SLS characterization of the star terpolymers presented in Section 5.3 was different. In particular, a Brookhaven BI-MwA spectrophotometer equipped with a 30 mW laser operating at 673 nm was used. For each polymeric solution, the intensity of scattered light was measured at seven angles: 35°, 50°, 75°, 90°, 105°, 130° and 145°, for at least five different concentrations.

4.4.1.3. ^{1}H NMR Spectroscopy

^{1}H NMR was employed for the determination of the terpolymer composition. After drying the terpolymers in a vacuum oven, 20 mg of each terpolymer was weighed and diluted in 0.5 mL deuterated chloroform ($CDCl_3$) to a final concentration of 4 %. The ^{1}H NMR spectra of the terpolymer solutions were recorded using a 300 MHz Avance Bruker spectrometer. The calibration was based on the $CHCl_3$ peak at 7.26 ppm.

4.4.2. Aqueous Solution Characterization

Aqueous salt-free solutions of the terpolymers were characterized in terms of their hydrodynamic diameters, M_ws, cloud points and effective p*K*s, using dynamic and static light scattering, turbidimetry, and hydrogen ion titration, respectively.

4.4.2.1. Dynamic Light Scattering (DLS)

Dynamic light scattering (DLS) was employed for the determination of the hydrodynamic diameters of the terpolymers. 1 % w/w aqueous salt-free terpolymer

solutions were prepared and filtered through 0.45 μm PTFE syringe filters. Prior to the light scattering measurements, the filtered terpolymer solutions were left at rest for approximately one hour so that any air bubbles could escape.

A 90 Plus Brookhaven DLS spectrophotometer, equipped with a 30 mW red diode laser operating at 673 nm, was used to determine the hydrodynamic diameters of the terpolymers in aqueous solution. The scattered intensity was measured at an angle of 90° and at room temperature. Five 2-minute runs were performed for each terpolymer solution and the data were averaged. The data were processed using multimodal size distribution (MSD) analysis based on non-negatively constrained least squares (NNLS).

4.4.2.2. Static Light Scattering

SLS was performed to determine the M_ws of the terpolymers in aqueous salt-free solutions. These experiments were carried out using the Brookhaven BI-MwA spectrophotometer and employed the same method as described in the characterization in organic solvents section above.

4.4.2.3. Turbidimetry

A single beam Lambda 10 Perkin-Elmer UV/vis spectrometer was used for the turbidity measurements. A 1% w/w aqueous terpolymer solution was placed in a 10 mm path-length quartz cuvette containing a small magnetic bar set in motion with the aid of a miniature magnetic stirrer. A small temperature probe was immersed in the upper part of the solution, which was heated from 20 to 93 °C. The optical density at 500 nm and the temperature were monitored using the software package TempLab (version 1.56) along with UV/WinLab (version 2.7). The cloud point was taken as the temperature where the first large increase in the optical density occurred.

4.4.2.4. Hydrogen Ion Titration

5 g of 1% w/w solutions of each terpolymer were titrated between pH 2 and 12 using a standard NaOH 0.5 M solution under continuous stirring. To this end, the pH of the neutral DMAEMA-containing terpolymer solution was adjusted to pH 2 by the addition of a few drops of HCl 2 M. Dropwise addition of the standard NaOH 0.5 M solution followed. The NaOH 0.5 M dropper-bottle was weighed before and after each titration in order to be able to calculate the mass of the NaOH solution used. The solution pH was measured using a Corning PS30 portable pH meter. The p*K*s were

calculated as the pH at 50% ionization.

4.4.2.5. Surface Tension Measurements: du Noüy Ring Method

The du Noüy ring method was employed for the surface tension measurements of four linear and three star terpolymers (Section 5.2). Fifteen aqueous solutions for each one of the terpolymers were prepared covering a concentration range from 6×10^{-6} – 1 w/v %. Before the measurement of the surface tension of the samples, the surface tension of pure deionized water was measured. In particular, 30 mL of deionized water was placed in a clean and dry Petri-dish supported by a metallic base with adjustable height. The ring was carefully washed with pure ethanol and was blown dry with hot air. The ring was tied at one end using a sufficiently long thread, and was attached to one of the dynamometer ends.

The height of the Petri-dish containing the water was adjusted so that the ring would be exactly below the water surface. At the same position, the indication of the dynamometer was adjusted to zero and the weight of the ring should be equal to the moment imposed by the rear lever of the dynamometer. A moment was applied forcing the ring to slowly move upwards until the breaking of the meniscus formed by the water. The force at that point was noted. 30 mL of the most dilute terpolymer solution was placed in a clean and dry Petri-dish. The mixture was left for a few minutes to rest and the measurement was repeated in the same way as that described above for the pure water. The procedure was repeated several times for various terpolymer concentrations. Four measurements were made for each concentration and their average value was calculated. The surface tension experiments were conducted at room temperature. Before and after the experiments with the different terpolymers, both the ring and the Petri-dish were carefully rinsed with pure ethanol and blown dry using hot air.

4.4.2.6. Atomic Force Microscopy (AFM)

Atomic force microscopy was employed for the surface imaging of a star ABC triblock terpolymer. AFM measurements were performed using a Digital Instruments MultiMode AFM operated in the tapping mode. Dilute aqueous solutions of the star terpolymer (10^{-4} – 10^{-3} w/w %) were adsorbed on freshly cleaved mica and observations were made under water in an environmental chamber.

4.5. Characterization of the Networks

4.5.1. Recovery and Characterization of Extractables

The networks were first taken out of the polymerization vials by breaking the vials. Subsequently, the networks were placed in excess THF and left there for three to four weeks to extract the polymer not incorporated in the network. Every week the THF solution of the extracted material was collected and new THF was added in the container where the network was placed. The collected THF solution of the extracted material was dried in a rotary evaporator followed by drying in a vacuum oven at room temperature for three days resulting in the complete removal of the solvent. Subsequently, the mass of that dry polymer was determined. Samples of the extractables were characterized by GPC in THF using the equipment described in previous paragraphs.

4.5.2. Measurement of the Degree of Swelling (DS)

The degrees of swelling (DSs) of the networks were measured in THF, in neutral water and in aqueous solutions covering the pH range between 2 to 12. After the equilibration in excess THF and the removal of the extractables, as described in the preceding paragraph, ten pieces were cut from each network. Each piece was weighed and subsequently dried in a vacuum oven at room temperature (to avoid the oxidation of the HEGMA units) for fourteen days and weighed again.

4.5.2.1. Degrees of Swelling in THF

The DSs in THF were calculated as the ratio of the swollen network sample as obtained after it had been equilibrated in THF for three to four weeks, divided by the dry mass. The values of the DSs were averaged over the ten samples of each network.

4.5.2.2. Aqueous Degrees of Swelling and Degrees of Ionization

In order to measure the DSs in aqueous media at different solution pH values, 5 mL of deionized water was added to each sample of the dried networks, followed by the addition of the appropriate number of drops of a standard 0.5 M HCl solution to adjust the pH within the range between 2 and 8, corresponding to degrees of ionization between 98% and 0% (eight samples used). The required number of moles of HCl in each case was calculated as the product of the desired degree of ionization times the number of moles of the DMAEMA units present in the network sample. One and two

drops of a standard 0.5 M NaOH solution were added to the two remaining samples of each gel to cover the pH range from 8 to 12. The DSs of each sample were measured four times and the average values are presented, along with the 95% confidence intervals.

4.5.3. Cloud Points

The cloud points of the networks were estimated. To this end, cubic samples of the networks were taken and dried in the vacuum oven for one week. Each dried sample was weighed and placed in a glass screw-cap vial. A small amount of water was added (the exact mass was weighed) and the network piece was left to equilibrate for two days. The DS of the network was measured at that temperature (room temperature). Each network sample was thermostated for 20 minutes at a given temperature, covering the range of 20-80 °C, and its DSs at each temperature were determined. Four measurements of the DSs as described in the preceding paragraph, were made and their average was taken. For the minimization of the solvent evaporation the caps of the vials were screwed on during the thermostating process.

4.5.4. Biological Molecules Adsorption Studies

Two of the networks prepared in this Thesis were studied with respect to their ability to adsorb biological molecules. The two networks chosen for this purpose were those bearing elastic chains of the $BuMA_5$-*b*-$HEGMA_5$-*b*-$DMAEMA_{10}$-*b*-$HEGMA_5$-*b*-$BuMA_5$ and $(HEGMA\text{-}co\text{-}DMAEMA\text{-}co\text{-}BuMA)_{10}$ terpolymers. The biological molecules selected for these studies were the drug paracetamol and Herring's sperm DNA. Five THF-swollen cubic samples were used for each of the four possible adsorbate-network combinations, totaling 20 samples. Each sample was placed in a separate vial. All network samples were dried in a vacuum oven at room temperature and they were weighed. 5 mL of deionized water was added to each sample. Three out of the five samples prepared for each adsorbate-network combination were adjusted to degrees of ionization of their DMAEMA monomer repeating units of 100 %, 80 % and 50% by the addition of the appropriate volume of a standard 0.5 M HCl solution as described earlier. The fourth sample remained neutral, while in the fifth sample a small volume of a standard 0.5 M NaOH solution was added resulting in a slightly alkaline pH.

Calibration curves of the absorbance in the ultraviolet with respect to concentration and pH were obtained for each molecule, using a UV-1601 Shimadzu UV/vis spectrometer. A small volume of a dilute solution of each molecule with concentration that would give absorbance around one at the wavelength of maximum absorbance was transferred to each vial. The vials were allowed to equilibrate for three weeks in a refrigerator and the pH of the supernatant was measured. The absorbance of the supernatant solution at 245 nm for the samples with paracetamol and at 265 nm for the samples with DNA was measured using the same spectrometer. The paracetamol and the DNA concentrations were calculated using the relevant calibration curve. The amount of the adsorbed paracetamol and DNA was calculated from the initially added amount and its final concentration in the supernatant.

CHAPTER 5: Results and Discussion

As mentioned at the beginning of the manuscript, the aim of the present Thesis was the synthesis and aqueous solution characterization of linear, star and network terpolymers and the elucidation of the effect of architecture, block sequence and terpolymer composition on their aqueous solution properties. To this end, six families of amphiphilic terpolymers were prepared. The synthesis and characterization results of each terpolymer family are presented in the following pages, divided in sections (5.1-5.6) with the terpolymers presented in each Section being prepared the same day.
In Sections 5.1-5.3 the results of the preparation and solution characterization of three linear and star terpolymer families are given. These terpolymers were the block sequence isomers of equimolar linear and star ABC triblock terpolymers. In the next two sections (5.4 and 5.5) the synthesis of two terpolymer families consisted of equimolar, symmetrical, block sequence isomeric networks based on linear ABCBA pentablock terpolymers and their swelling behavior in both selective (water) and non-selective (THF) solvent are discussed. The last Section (5.6) contains the synthesis of ABCBA pentablock terpolymer networks in which, however, the length of the hydrophobic blocks was varied systematically. The swelling properties of these materials were also investigated in water and THF.
Some of the terpolymers reported in Sections 5.1-5.6 were prepared twice, in two different families (as given in Sections 5.1-5.2, 5.2-5.3 and 5.5-5.6), with the terpolymers presented in each Section being prepared the same day to ensure the same initiator reactivity and, therefore, comparable molecular weights between the different polymers within a certain family.

GTP was the synthetic method employed for the preparation of all the terpolymer families studied in the present Thesis mainly because it enables the preparation of all the block sequence isomers simply by altering the monomer addition sequence during the polymerizations.

All of the terpolymers prepared were composed of two hydrophilic and one hydrophobic monomers ensuring their hydrophilicity. The same two hydrophilic monomers were employed in all six families, namely the neutral hydrophilic HEGMA and the marginally hydrophilic temperature- and pH-responsive DMAEMA rendering

to the terpolymers enhanced hydrophilicity that was both pH and temperature sensitive. In four out of the six terpolymer families (discussed in Sections 5.1-5.4), the hydrophobic blocks were composed of methyl methacrylate units (MMA), whereas *n*-butyl methacrylate (BuMA) was the hydrophobic monomer used in the remaining two families (Sections 5.5-5.6).

For the synthesis of the linear and the star terpolymers (Sections 5.1-5.3), 1-methoxy-1-(trimethylsiloxy)-2-methyl propene (MTS), a monofunctional initiator, was used, whereas the bifunctional initiator 1,4-bis(methoxytrimethylsiloxymethylene)cyclohexane (MTSMC) was employed for the preparation of the networks (Sections 5.4-5.6). Activation of the initiator was achieved by the tetrabutylammonium bibenzoate (TBABB) catalyst, while the cross-linker EGDMA effected the interconnection of the linear terpolymer chais either at one or both active ends, resulting in the formation of star polymers or polymer networks, respectively.

The chemical structures and names of the monomers and the cross-linker used are given in Figure 5.1. Below each structure, a colored schematic representation is drawn. In particular, the bulky hydrophilic HEGMA is illustrated in white, the marginally hydrophilic DMAEMA in gray, while both the MMA and the BuMA hydrophobic monomers are shown in black. EGDMA is depicted in either black or dark gray. These representations will be used later in this Chapter.

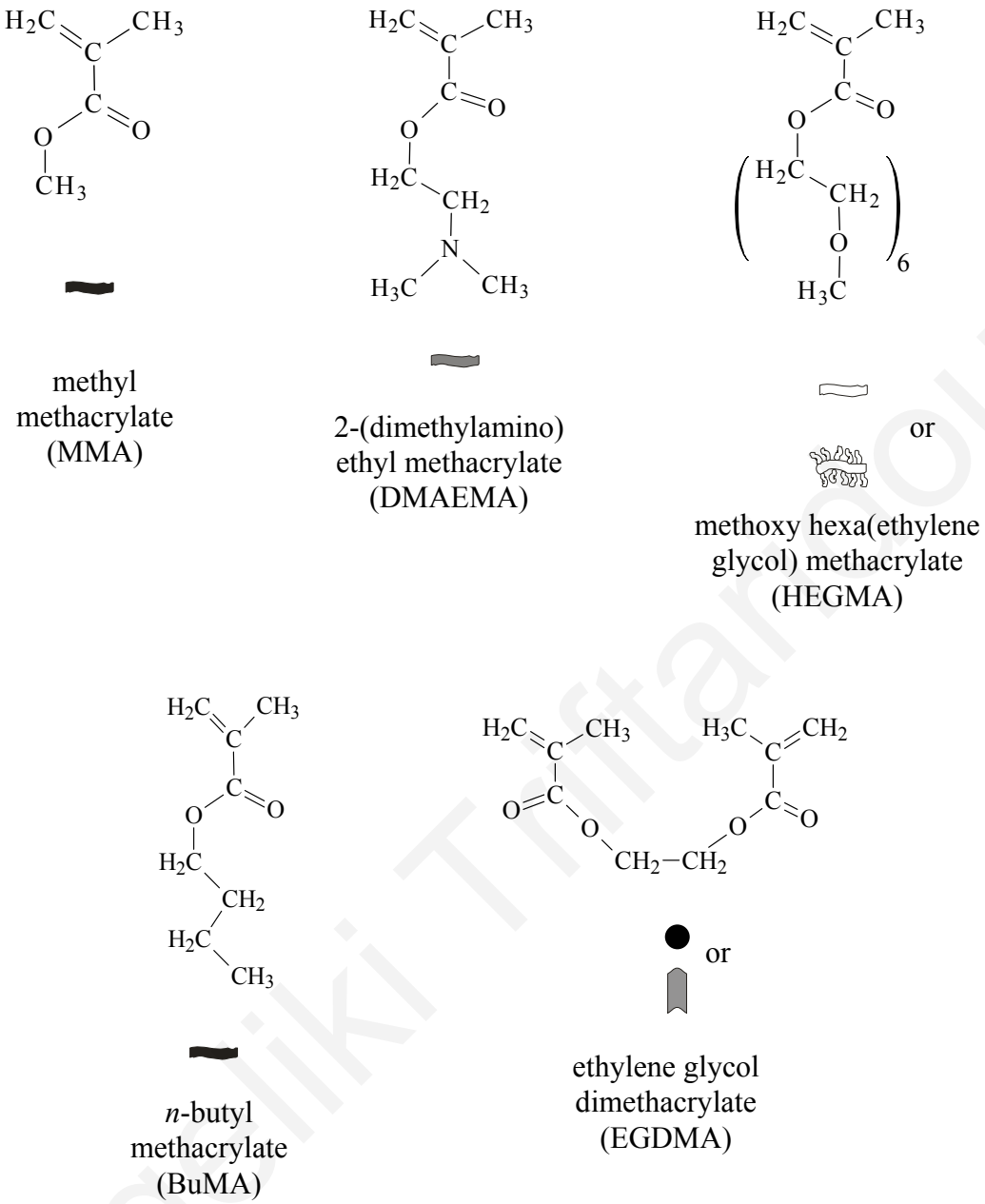

Figure 5.1. Chemical structures and names of the monomers and the cross-linker employed for the preparation of the terpolymers.

The chemical structures and names of the MTS and MTSMC initiators and the catalyst are displayed in Figure 5.2.

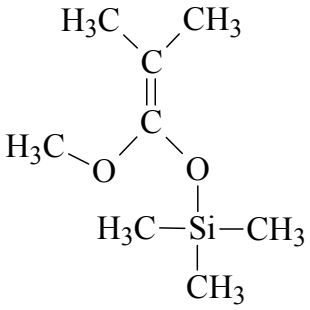

1-methoxy-1-trimethylsiloxy-
2-methyl propene
(MTS)

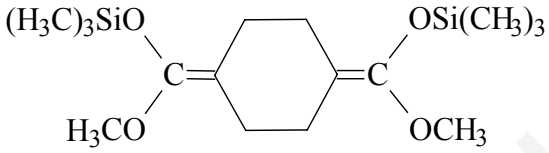

1,4-bis(methoxytrimethylsiloxymethylene)
cyclohexane
(MTSMC)

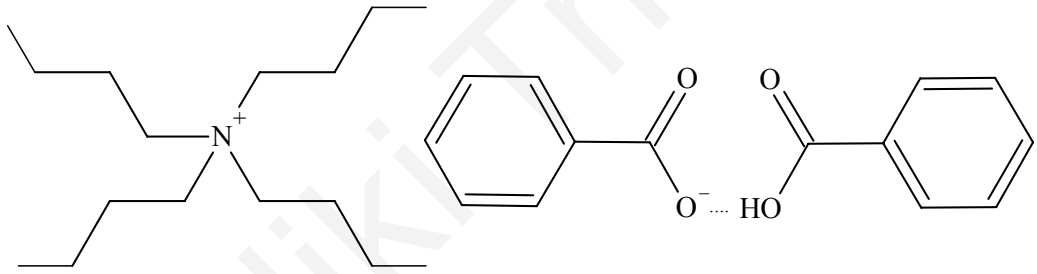

tetrabutylammonium bibenzoate
(TBABB)

Figure 5.2. Chemical structures and names of the monofunctional and bifunctional initiators as well as the catalyst used for the GTP syntheses of all the terpolymers in this study.

5.1. Equimolar Linear AB Diblock and ABC Triblock Terpolymers of HEGMA, DMAEMA and MMA: Effect of Block Sequence

5.1.1. Summary

The first polymer family prepared in this study included seven linear equimolar samples.[42] Three of those were the ABC, ACB and BAC block sequence isomeric triblock terpolymers composed of MMA, DMAEMA and HEGMA blocks, with 10 monomer repeating units in each block. The corresponding statistical terpolymer was also prepared. Furthermore, the same monomers were combined in pairs to prepare the three linear diblock copolymers with the degree of polymerization of each block being 10 again. The molecular weights and compositions of all polymers were characterized by GPC and ^{1}H NMR. Measurements of the hydrodynamic diameters and cloud points in aqueous solution suggested that the various distributions of monomer units in the four terpolymers (the three triblocks and the statistical) resulted in different supramolecular structures with different colloidal stabilities.

5.1.2. Introduction

In this Section the preparation of equimolar block sequence isomeric AB diblock copolymers and ABC triblock terpolymers is reported. Furthermore, the effect of block sequence on the aqueous solution behavior was also explored.

5.1.3. Polymer Synthesis

ABC triblock terpolymers have been synthesized using various "living" polymerization techniques, including anionic, "living" cationic, group transfer (GTP) and, more recently, "living" free-radical polymerization (see Chapter 2). In the present Thesis, GTP was employed for the synthesis of the terpolymers. The synthetic procedure for the preparation of the ABC linear triblock terpolymer with structure $HEGMA_{10}$-*b*-MMA_{10}-*b*-$DMAEMA_{10}$ is given in Figure 5.3. The synthesis involved sequential monomer additions. Addition of the first monomer in Figure 5.3 resulted in the synthesis of the linear HEGMA homopolymer. The homopolymer chains were active at one end, indicated by the asterisks. Addition of the second monomer yielded the $HEGMA_{10}$-b-MMA_{10} diblock copolymers. Upon addition of the

third monomer, the diblock copolymer chains continued their growth at one end resulting in the $HEGMA_{10}$-b-MMA_{10}-b-$DMAEMA_{10}$ triblock terpolymer.

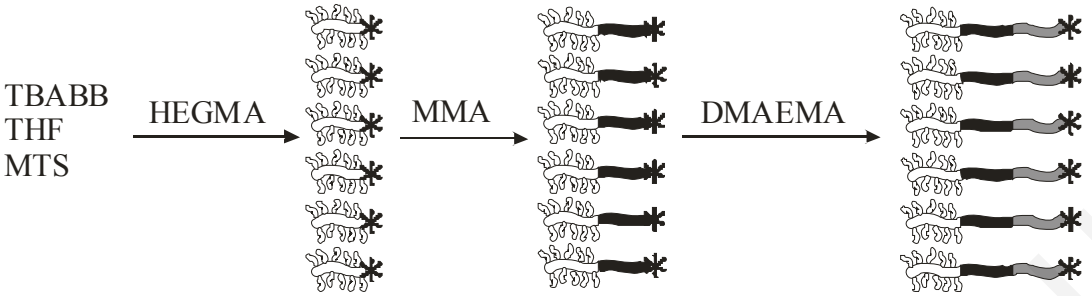

Figure 5.3. Schematic representation of the synthetic procedure followed for the preparation of the $HEGMA_{10}$-*b*-MMA_{10}-*b*-$DMAEMA_{10}$ triblock terpolymer. The HEGMA units are shown in white, the MMA units in black and the DMAEMA units in gray. The "*" symbols indicate the "living" sites of the polymerization.

For the preparation of all the block sequence isomers, the order of monomer addition was changed accordingly, while for the synthesis of the statistical terpolymer all three monomers were polymerized simultaneously. A schematic illustration of the synthesized copolymer and terpolymer structures is shown in Figure 5.4:

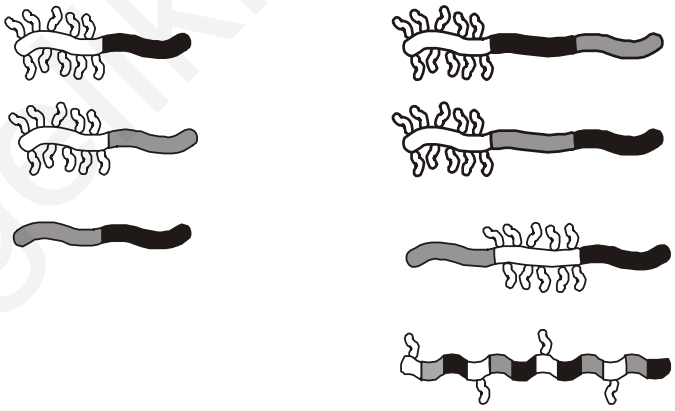

Figure 5.4. Schematic representation of the three diblock copolymers, the three triblock terpolymers and the statistical terpolymer, constituting the first polymer family, whose synthesis and characterization are presented in this Section. The color coding is the same as that employed in Figure 5.3 above.

The ABC, the ACB and the BAC triblocks, as well as the statistical terpolymer were prepared. The four terpolymers were equimolar isomers with a theoretical degree of polymerization 30, containing 10 repeating units from each of the three different monomers. The three diblock copolymers derived from the pairwise combinations of the three different monomer units were also prepared. The side chains of the HEGMA (macro)monomer repeating units are also depicted, emphasizing their bulky nature.

5.1.4. Determination of Size and Composition

5.1.4.1. Molecular Weight Analysis

The number average molecular weights (M_ns) and PDIs (M_w/M_n) of all the copolymers and terpolymers and their precursors, as determined by GPC in THF, are shown in the fourth and fifth columns of Table 5.1. As shown in Table 5.1, the M_ns were about twice as high as the theoretically predicted, because of hydrodynamic differences between the DMAEMA and HEGMA units and the PMMA molecular weight calibration standards and possible partial initiator deactivation. The polydispersities of all samples were lower than 1.3, and those of the final diblock copolymers and terpolymers were below 1.2, indicating the size homogeneity of the polymer chains.

Table 5.1. Molecular weight and composition analysis of the copolymers and terpolymers and their precursors.

No.	Polymer Formula[a]	Theor. MW[b]	GPC Results		mol % composition	
			M_n[c]	M_w/M_n	Theor. H-D-M	^{1}H NMR H-D-M
1	H_{10}	3 600	5 600	1.09		
	H_{10}-*b*-M_{10}	4 600	6 500	1.09	50-0-50	47-0-53
2	H_{10}	3 600	5 900	1.09		
	H_{10}-*b*-D_{10}	5 170	6 150	1.09	50-50-0	48-52-0
3	D_{10}	1 670	1 700	1.28		
	D_{10}-*b*-M_{10}	2 670	3 600	1.10	0-50-50	0-47-53
4	D_{10}	1 670	3 800	1.07		
	D_{10}-*b*-H_{10}	5 170	10 100	1.15		
	D_{10}-*b*-H_{10}-*b*-M_{10}	6 170	11 500	1.18	33-33-33	33-31-36
5	H_{10}	3 600	7 850	1.08		
	H_{10}-*b*-M_{10}	4 600	9 700	1.08		
	H_{10}-*b*-M_{10}-*b*-D_{10}	6 170	13 050	1.09	33-33-33	34-36-30
6	H_{10}	3 600	7 550	1.08		
	H_{10}-*b*-D_{10}	5 170	9 300	1.08		
	H_{10}-*b*-D_{10}-*b*-M_{10}	6 170	11 250	1.09	33-33-33	34-35-31
7	(H-*co*-D-*co*-M)$_{10}$	6 170	13 250	1.08	33-33-33	32-34-34

[a] H, D and M stand for HEGMA, DMAEMA and MMA, respectively.

[b] The contribution from the initiator fragment of 100 g mol^{-1} was included.

[c] From a calibration based on linear PMMA standards of narrow MWDs.

5.1.4.2. Composition Analysis

The compositions of all seven copolymers and terpolymers were determined by ^{1}H NMR in $CDCl_3$. The theoretically expected and experimentally determined molar compositions of the polymers in their constituents are listed in the last two columns of Table 5.1. Figure 5.5 shows the ^{1}H NMR spectrum of a particular ABC triblock terpolymer.

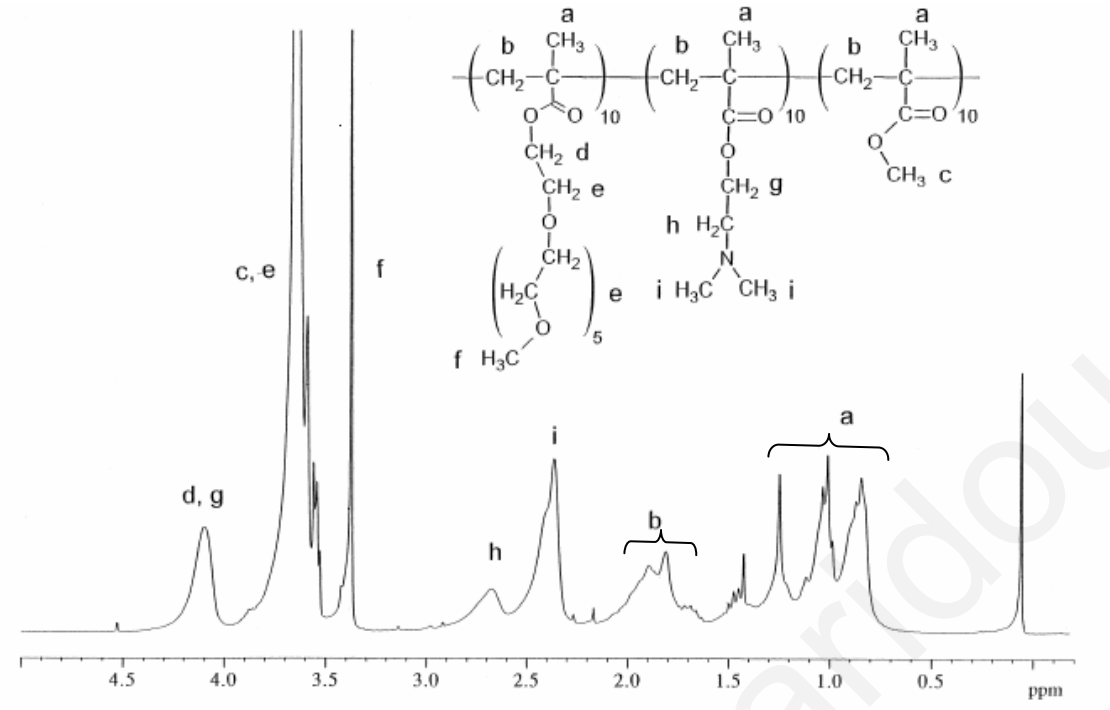

Figure 5.5. ^{1}H NMR spectrum of the HEGMA$_{10}$-*b*-DMAEMA$_{10}$-*b*-MMA$_{10}$ ABC triblock terpolymer in $CDCl_3$.

The signals from protons *c*, *i* and *f* of the three monomer repeating units, MMA, DMAEMA and HEGMA, respectively, were chosen to calculate polymer composition. The signal from protons *c* of MMA was calculated by subtracting the contribution from HEGMA in the joint *c* plus *e* peak at 3.7 ppm, thus potentially introducing a large error in the calculated MMA content. These experimentally calculated copolymer and terpolymer compositions agreed well with the corresponding theoretical compositions, both listed in Table 5.1.

5.1.5. Aqueous Solution Properties

5.1.5.1. Hydrodynamic Sizes

5.1.5.1.1. Theoretical Limiting Sizes

The experimentally measured hydrodynamic diameters by DLS of the copolymers and terpolymers in aqueous solutions at room temperature are displayed in Table 5.2. The same Table also lists the theoretically calculated upper and lower limits of the hydrodynamic diameters. The former was calculated for spherical micelles comprising polymers with fully stretched chains, while the latter was calculated for

unimers (not micellized chains) in either a random coil conformation or in the state of a partially swollen globule.

Table 5.2. Hydrodynamic diameters and cloud points of 1% w/w aqueous solutions of the copolymers and terpolymers.

No.	Polymer Formula	Hydrodynamic Diameter (nm)					Cloud point (°C)
			Theoretical limits				
		Exper.[a]	Stretched micelles	Unimer coils			
				Random	Collapsed	Swollen	
1	H_{10}-*b*-M_{10}	8.2	10.0	1.7	2.3	2.6	72.3
2	H_{10}-*b*-D_{10}	4.3	10.0	1.7	2.4	2.7	79.8
3	D_{10}-*b*-M_{10}	6.8	10.0	1.7	1.9	2.2	36.1
4	D_{10}-*b*-H_{10}-*b*-M_{10}	11.0	15.0	2.0	2.5	2.9	80.0
5	H_{10}-*b*-M_{10}-*b*-D_{10}	6.4	7.5	2.0	2.5	2.9	80.7
6	H_{10}-*b*-D_{10}-*b*-M_{10}	12.0	15.0	2.0	2.5	2.9	89.5
7	(H-*co*-D-*co*-M)$_{10}$	4.5	15.0	2.0	2.5	2.9	57.2

[a]Determined from multimodal size distribution (MSD) analysis of the DLS data.

The diameter of the fully stretched spherical micelles was taken as twice the chain contour length for most block copolymers (AB diblock copolymer-type micelles), and equal to the chain contour length for ABC triblock terpolymer 5, having the hydrophobic block in the middle (ABA triblock copolymer-type micelles). The chain contour length was calculated as the product of the theoretical degree of polymerization times the contribution of one monomer repeating unit of 0.254 nm.[97(c)] The diameter of a non-micellized polymer chain (unimer) in a random coil conformation was calculated using random flight statistics corrected for the carbon tetrahedral angle and using PMMA's stiffness factor of 2.20. In particular, the formula employed for the calculation of the root mean-square diameter of gyration of a random coil was:

$$\left\langle d_g^2 \right\rangle^{1/2} = 2 \times \left(\frac{2 \times 2.20 \times DP}{3} \right)^{1/2} \times 0.154 \text{ nm} \qquad (5.1)$$

where *DP* is the degree of polymerization and 0.154 nm is the length of one carbon-carbon bond.

To calculate the unimer size in the state of a partially swollen globule, the size for the fully collapsed (completely dehydrated) unimer globule was first calculated, which was subsequently multiplied by the appropriate expansion factor:

$$d = d_0 \alpha \tag{5.2}$$

where d is the diameter of the unimer in the partially swollen state, d_0 is the unimer diameter in the fully collapsed state, and α is the unimer expansion factor. d_0 is calculated from the nominal molecular weight of the chain, MW, the polymer bulk density, ρ (assumed to be 1.2 g mL^{-1}), and considering spherical geometry:

$$d = \left(\frac{6MW}{\pi \rho N_{Av}} \right)^{1/3} \tag{5.3}$$

where N_{Av} is the Avogadro number. The expansion factor was calculated from the modified Flory-Krigbaum theory:[108]

$$\alpha^5 - \alpha^3 = 0.88\left(\frac{1}{2} - \chi \right)\sqrt{DP} \tag{5.4}$$

where χ is the Flory-Huggins interaction parameter. In the calculations for the terpolymers, the value for the Flory-Huggins water-unimer interaction parameter χ was taken equal to 0.4 and the overall DP of the chain was taken equal to 30, leading to a value for α of 1.15. Due to the very small change in the value of α for a DP of 20 instead of 30, the same value of 1.15 was used for the diblock copolymer as well. The values for both the collapsed and swollen unimeric coils are shown in Table 5.2.

The random coil diameters for all the polymers were lower than those corresponding to fully collapsed coils, indicating their possible underestimation due to the use of incorrect stiffness factor. Thus, the comparison of the experimental diameters was made with the swollen coil dimensions.

5.1.5.1.2. Experimentally Determined Hydrodynamic Diameters

The experimentally determined hydrodynamic diameters are shown in the third column of Table 5.2. Comparison of these experimental diameters with the dimensions corresponding to stretched micelles (upper theoretical limit) and swollen unimer coils (lower theoretical limit) led to the following conclusions regarding the aggregation state of the chains: all the polymers formed micelles with the exception of the double hydrophilic $HEGMA_{10}$-*b*-$DMAEMA_{10}$ copolymer and the statistical terpolymer (HEGMA-*co*-DMAEMA-*co*-MMA)$_{10}$. $HEGMA_{10}$-*b*-$DMAEMA_{10}$ was not expected to form micelles due to the lack of hydrophobic units, while the statistical terpolymer would not form micelles because of the random distribution of the hydrophobic monomer repeating units. Thus, there was none or not enough hydrophobic force to drive micellization in aqueous solutions of these polymers. The remaining polymers contained one hydrophobic MMA block which was known to induce micelle formation. These block copolymers and terpolymers presented micellar experimental diameters slightly below the theoretical upper limits due to some chain coiling.

The size of the micelles of diblock copolymer $HEGMA_{10}$-*b*-MMA_{10} was larger than that of diblock copolymer $DMAEMA_{10}$-*b*-MMA_{10} probably due to the bulky nature of the HEGMA units compared to DMAEMA. The micellar sizes of triblocks $DMAEMA_{10}$-*b*-$HEGMA_{10}$-*b*-MMA_{10} and $HEGMA_{10}$-*b*-$DMAEMA_{10}$-*b*-MMA_{10} were larger than those of diblocks $HEGMA_{10}$-*b*-MMA_{10} and $DMAEMA_{10}$-*b*-MMA_{10} due to the greater overall degree of polymerization of the triblocks. The same two triblock terpolymers ($DMAEMA_{10}$-*b*-$HEGMA_{10}$-*b*-MMA_{10} and $HEGMA_{10}$-*b*-$DMAEMA_{10}$-*b*-MMA_{10}) exhibited hydrodynamic diameters of 11 nm and 12 nm, respectively, just below 15 nm, the diameter of AB diblock copolymer-type micelles with stretched chains. Triblock $HEGMA_{10}$-*b*-MMA_{10}-*b*-$DMAEMA_{10}$ formed micelles with diameter 6.4 nm, half the micellar diameters obtained for its isomers, and just below 7.5 nm, the diameter of ABA triblock copolymer-type micelles with stretched chains. Therefore, the micelles of the three triblock terpolymers in aqueous solution should have their chains arranged as shown in Figure 5.6. However it is noted that the structures shown in the Figure are simplified, drawn in two dimensions rather than in three, as is the case in the solutions.

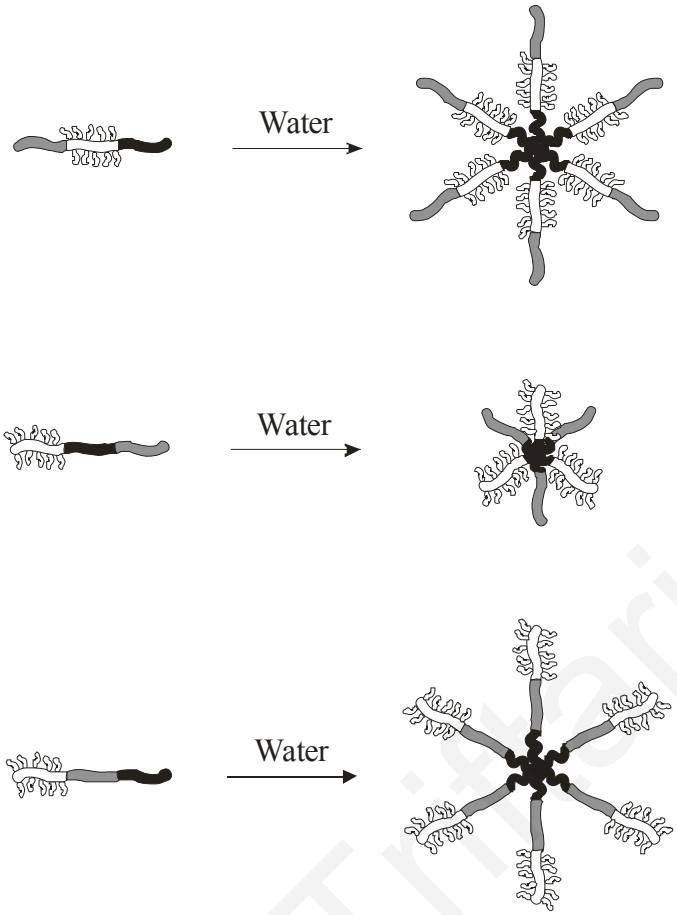

Figure 5.6. Schematic representation of the structures of the spherical micelles formed by the three ABC triblock terpolymers in aqueous solution.

5.1.5.2. Cloud Points

The cloud points of all the copolymers and terpolymers are also listed in Table 5.2. The main observation from the Table is that, with the exception of the statistical terpolymer (HEGMA-*co*-DMAEMA-*co*-MMA)$_{10}$ and the most hydrophobic diblock copolymer DMAEMA$_{10}$-*b*-MMA$_{10}$, all other polymers had cloud points above 70 °C. The statistical terpolymer exhibited a cloud point of 57 °C. This polymer could not form micelles, confirmed by DLS, due to the random distribution of its hydrophobic units, which remained unshielded from the aqueous solvent, thereby facilitating its precipitation. Focusing now on the diblocks, they precipitated in the expected order. Their cloud points increased with their hydrophilicity. Thus, diblock DMAEMA$_{10}$-*b*-MMA$_{10}$ which was based on the two most hydrophobic components, MMA and DMAEMA, precipitated more easily than copolymers HEGMA$_{10}$-*b*-MMA$_{10}$ and

$HEGMA_{10}$-*b*-$DMAEMA_{10}$. Diblock copolymer $HEGMA_{10}$-*b*-$DMAEMA_{10}$, consisting only of hydrophilic units, had the highest cloud point of all three.

From the ABC triblocks, terpolymers $DMAEMA_{10}$-*b*-$HEGMA_{10}$-*b*-MMA_{10} and $HEGMA_{10}$-*b*-MMA_{10}-*b*-$DMAEMA_{10}$ had similar cloud points, while terpolymer $HEGMA_{10}$-*b*-$DMAEMA_{10}$-*b*-MMA_{10} precipitated at a higher temperature. This difference in the cloud points was attributed to the location within the micelles of the temperature-sensitive DMAEMA block which has a precipitation temperature of 35 °C.[109] As shown in Figure 5.6, the micelles of triblocks $DMAEMA_{10}$-*b*-$HEGMA_{10}$-*b*-MMA_{10} and $HEGMA_{10}$-*b*-MMA_{10}-*b*-$DMAEMA_{10}$ had DMAEMA block in the outer region of their corona, while the DMAEMA block was located between the core and the outermost HEGMA shell in the case of triblock $HEGMA_{10}$-*b*-$DMAEMA_{10}$-*b*-MMA_{10}. Given the very slow kinetics of polymer rearrangement within block copolymer micelles, particularly in the presence of a glassy PMMA micellar core, above 35 °C the hydrophobic DMAEMA units in the micelles of triblocks $DMAEMA_{10}$-*b*-$HEGMA_{10}$-*b*-MMA_{10} and $HEGMA_{10}$-*b*-MMA_{10}-*b*-$DMAEMA_{10}$ would promote interparticle association and, therefore, precipitation to a greater extent than the "protected" DMAEMA units in the micelles of terpolymer $HEGMA_{10}$-*b*-$DMAEMA_{10}$-*b*-MMA_{10}. This explains the higher cloud point of triblock $HEGMA_{10}$-*b*-$DMAEMA_{10}$-*b*-MMA_{10} compared to $DMAEMA_{10}$-*b*-$HEGMA_{10}$-*b*-MMA_{10} and $HEGMA_{10}$-*b*-MMA_{10}-*b*-$DMAEMA_{10}$.

5.1.5.3. Effective pKs and Water-Solubility

The effective p*K*s of the DMAEMA units in all the copolymers and terpolymers, with the exception of the diblock $HEGMA_{10}$-*b*-MMA_{10} which is DMAEMA-free, were determined to be around 7.0, in agreement with previous investigations on DMAEMA-containing linear polymers.[110] All polymer solutions remained optically clear during their titrations between pH 2 and 12.

5.1.6. Conclusions

The first terpolymer family in this Thesis comprised linear triblock terpolymers (all three block sequence isomers ABC, ACB and BAC) and their statistical isomer. The synthesis was successfully performed by GTP, and the molecular weights and compositions were analyzed by GPC and ^{1}H NMR. Aqueous solution characterization indicated that the different distributions of monomer repeating units

in the four terpolymers led to different supramolecular structures with different colloidal stabilities.

In the next Section we will prepare and explore ABC terpolymers of another architecture, the star architecture, and study their aqueous solution properties as a function of the block sequence.

5.2. Equimolar Linear and Star ABC Triblock Terpolymers of HEGMA, DMAEMA and MMA: Effects of Block Sequence and Polymer Architecture

5.2.1. Summary

Four star and four linear equimolar terpolymers based on HEGMA, DMAEMA, and MMA were synthesized using GTP.[43] Three of the four terpolymers of each group were the block sequence triblock terpolymer isomers ABC, ACB and BAC. The fourth terpolymer was the statistical isomer. EGDMA was used as the cross-linker to interconnect the linear precursors at one end and form the star terpolymers. The molecular weights and molecular weight distributions of the linear and star terpolymers as well as those of their homopolymer, diblock and triblock precursors were characterized by GPC in tetrahydrofuran, whereas their compositions were determined by ^{1}H NMR spectroscopy in $CDCl_3$. The aqueous solution properties of all the terpolymers were investigated by dynamic and static light scattering, turbidimetry and hydrogen ion titration to determine the hydrodynamic diameters, the absolute molecular weights, the cloud points and the effective p*K*s, respectively. It was found that the monomer distribution (random or block), block sequence (ABC, ACB or BAC) and polymer architecture (linear or star) greatly affected the aqueous solution properties of the terpolymers.

5.2.2. Introduction

The present part of this Thesis aims at combining the linear ABC triblock terpolymer structure with the star architecture. Thus, novel, star triblock terpolymers comprising arms which were linear ABC triblock terpolymers were synthesized, characterized and studied in aqueous solution. To the best of our knowledge, this is the first time that this architecture is reported. As it will be shown, block sequence greatly influences the aqueous solution properties. In this Study, a comparison between the aqueous solution properties of $(ABC)_n$ star triblock terpolymers with those of the linear ABC triblock terpolymer counterparts (prepared together with the stars) will also be presented and discussed.

5.2.3. Polymer Synthesis

The synthetic procedure for the preparation of the ABC star terpolymer with structure

DMAEMA$_{10}$-*b*-HEGMA$_{10}$-*b*-MMA$_{10}$-*star* is presented schematically in Figure 5.7.

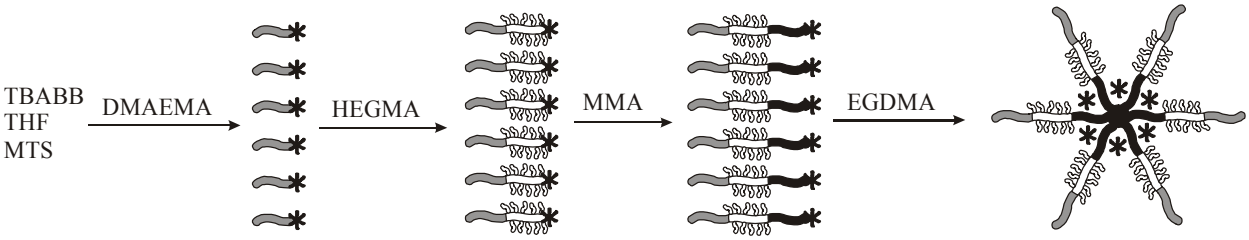

Figure 5.7. Schematic representation of the synthetic procedure followed for the preparation of the DMAEMA$_{10}$-*b*-HEGMA$_{10}$-*b*-MMA$_{10}$-*star* triblock terpolymer. The DMAEMA units are shown in gray, the HEGMA units in white, and the MMA units in black. The "∗" symbols indicate the "living" sites of the polymerization. The number of arms at the cross-links is not six, as indicated in the Figure, but 40 or higher.

The synthesis involved sequential monomer and cross-linker additions. The first step in Figure 5.7 resulted in the preparation of the linear DMAEMA$_{10}$ homopolymer, active at one end, indicated by asterisks. The second step led to the synthesis of the DMAEMA$_{10}$-*b*-HEGMA$_{10}$ linear diblock copolymer with again one active end. The third step was the addition of MMA, which resulted in the formation of the linear ABC triblock terpolymer DMAEMA$_{10}$-*b*-HEGMA$_{10}$-*b*-MMA$_{10}$. The synthesis was completed by the addition of the EGDMA cross-linker, which effected the interconnection of several terpolymers at their active end, leading to the formation of star ABC triblock terpolymers. The number of arms at the cross-links was not six, as indicated in the Figure, but higher, as this will be determined below. Figure 5.8 shows schematically all eight terpolymers synthesized. Above each star terpolymer its corresponding linear precursor is illustrated.

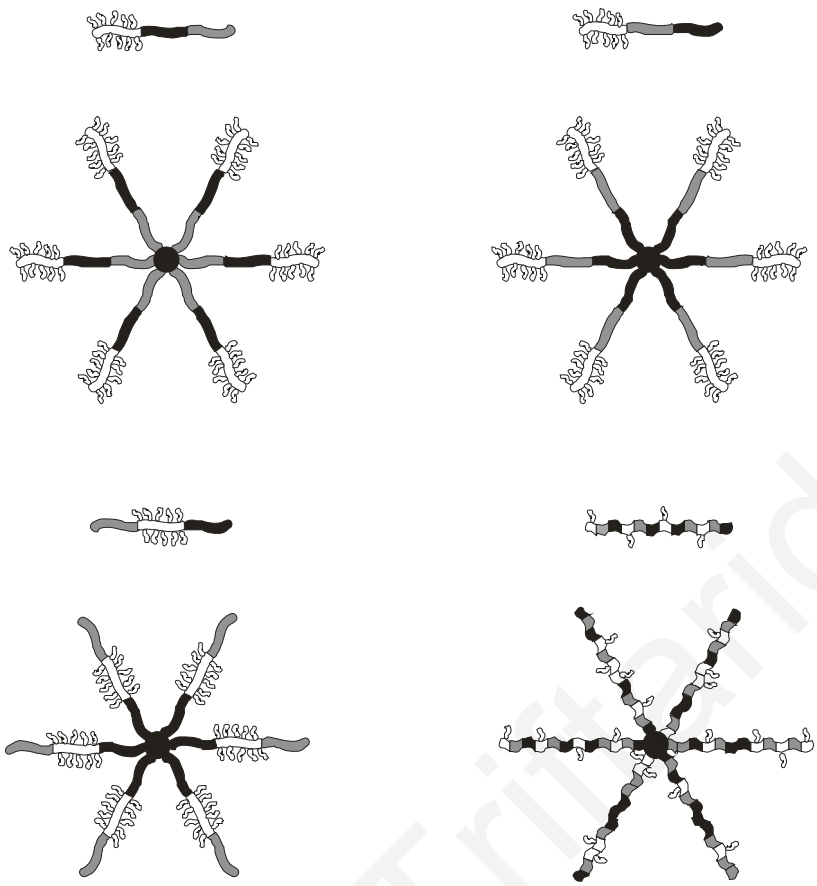

Figure 5.8. Schematic representation of the eight terpolymers prepared and studied in the present Section. The color coding is the same as that used in Figure 5.7. The cross-linker is represented by the black circles.

5.2.4. Determination of Terpolymer Size and Composition

5.2.4.1. Molecular Weight Analysis by GPC

All of the linear and star ABC triblock and statistical terpolymers as well as their homopolymer, diblock and triblock terpolymer precursors were characterized by GPC regarding their molecular weight distributions (MWDs), from which the apparent number-average molecular weights (M_n) and PDIs (M_w/M_n) were calculated. These results are shown in Table 5.3 along with the theoretical degrees of polymerization, which are depicted by the subscripts in the polymer formula column, and the theoretical molecular weights.

Table 5.3. Molecular weight and composition analysis of the linear and star terpolymers.

No.	Polymer Formula[a]	Theor. MW[b]	GPC Results[c]		SLS Results		% mol NMR HDM
			M_n	M_w/M_n	M_w	N_w[d]	
1	H_{10}	3 740	4 980	1.11			
	H_{10}-*b*-D_{10}	5 310	6 340	1.10			
	H_{10}-*b*-D_{10}-*b*-M_{10}	6 310	7 760	1.11			29-35-36
2	H_{10}	3 740	4 810	1.12			
	H_{10}-*b*-M_{10}	4 740	5 820	1.10			
	H_{10}-*b*-M_{10}-*b*-D_{10}	6 310	7 270	1.13			28-32-40
3	D_{10}	1 670	1 540	1.30			
	D_{10}-*b*-H_{10}	5 310	6 090	1.11			
	D_{10}-*b*-H_{10}-*b*-M_{10}	6 310	7 060	1.11			32-34-34
4	(H-*co*-D-*co*-M)$_{10}$	6 310	7 810	1.14			34-39-27
5	H_{10}	3 740	4 665	1.12			
	H_{10}-*b*-D_{10}	5 310	5 280	1.12			
	H_{10}-*b*-D_{10}-*b*-M_{10}	6 310	6 600	1.13			
	H_{10}-*b*-D_{10}-*b*-M_{10}-*star*	N/A[e]	92 240	1.23	300 000	40	44-45-5
6	H_{10}	3 740	4 160	1.13			
	H_{10}-*b*-M_{10}	4 740	5 110	1.12			
	H_{10}-*b*-M_{10}-*b*-D_{10}	6 310	6 920	1.13			
	H_{10}-*b*-M_{10}-*b*-D_{10}-*star*	N/A[e]	101 380	1.28	570 000	73	42-40-18
7	D_{10}	1 670	1 280	1.34			
	D_{10}-*b*-H_{10}	5 310	3 130	1.12			
	D_{10}-*b*-H_{10}-*b*-M_{10}	6 310	6 800	1.12			
	D_{10}-*b*-H_{10}-*b*-M_{10}-*star*	N/A[e]	78 590	1.17	506 000	66	40-39-21
8	(H-*co*-D-*co*-M)$_{10}$	6 310	7 690	1.18			
	(H-*co*-D-*co*-M)$_{10}$-*star*	N/A[e]	88 200	1.20	625 000	72	47-50-3

[a] H: HEGMA, D: DMAEMA, M: MMA.

[b] The contribution of 100 g mol^{-1} from the initiator fragment was also included.

[c] From a calibration based on linear PMMA standards.

[d] Weight-average number of arms.

[e] N/A: Not applicable.

For the linear terpolymers and their precursors, the polydispersities were relatively low (< 1.15 in most cases) but the M_ns were consistently slightly higher than the theoretically predicted, indicating either some initiator deactivation or differences between the synthesized terpolymers and the PMMA standards used for the molecular weight calibration. The linear precursors of the star terpolymers had similar apparent M_ns and polydispersities to those of the linear terpolymers listed in the first part of the

Table. The apparent M_ns of the star tepolymers were around 100 000 g mol^{-1}. These values underestimate their absolute MWs due to their more compact nature than the linear calibration MW standards. Their MWDs were broader than those of the linear precursors, but their polydispersities always remained lower than 1.3. Figure 5.9 shows the GPC chromatograms of the $DMAEMA_{10}$-*b*-$HEGMA_{10}$-*b*-MMA_{10}-*star* terpolymer and its three linear precursors.

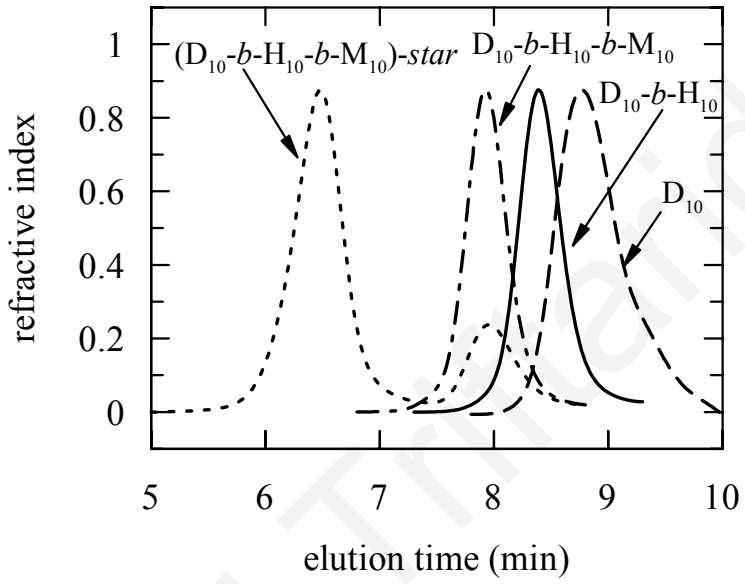

Figure 5.9. GPC chromatograms of the $DMAEMA_{10}$-*b*-$HEGMA_{10}$-*b*-MMA_{10}-*star* and its three linear precursors. D, H, and M are further abbreviations for the DMAEMA, HEGMA and MMA units, respectively.

The chromatograms of the linear precursors exhibited monomodal molecular weight distributions. The molecular weights shifted to higher values with each monomer addition, indicating incorporation of the added monomer into the polymer. The chromatogram of the star terpolymer exhibited a bimodal distribution, in which the lower molecular weight peak coincided with the peak of the linear triblock precursor, indicating incomplete incorporation of all the linear chains into the star terpolymer. The GPC chromatograms of the other three star terpolymers were similar to that shown in Figure 5.9, also exhibiting bimodal distributions. The percentage of unattached linear terpolymer relative to the overall polymer sample was estimated from the areas under the peaks in GPC and was found to be between ~18-22%. For

comparison, star polymers of MMA with EGDMA cores synthesized by "living" anionic polymerization contained between 10 and 45% by weight unattached arms.[111] In contrast, the GPC chromatograms of the linear triblock terpolymers exhibited monomodal distributions, indicating that the triblock terpolymer was the only polymer present, since there was an absence of peaks corresponding to linear homopolymers and diblock copolymers.

5.2.4.2. Absolute Molecular Weights

The absolute M_ws of the four star terpolymers were measured by SLS in THF. The SLS M_ws were found to be several times higher than the corresponding GPC values, the latter being relative MW with respect to linear calibration standards, due to the compact nature of the star architecture. In particular, the absolute M_ws of the star terpolymers ranged between 300 000 and 625 000 g mol^{-1} and are also listed in Table 5.3. For the determination of the molecular weights of the star terpolymers, the percentage of the unattached linear terpolymer was taken into account. In particular, the scattering intensity was assumed to be attributed to the 80 % of the star concentration, enabling the correction of the molecular weights. The contribution of the linear chains to the scattering intensity was negligible compared to that due to the star terpolymers.

The weight-average number of arms of the star terpolymers, N_w, was estimated from their absolute M_ws and the GPC M_ns of their arms. More specifically, it was calculated as the ratio of the M_w of the star terpolymer measured using SLS divided by the M_n of linear arm measured using GPC. In the calculation, the contribution of the cross-linker units in the core and the percentage of the unattached arms were taken into account. The obtained values are also displayed in Table 5.3 and varied between 40 and 73. These values are in good agreement with the values of 20,[112] 30,[113] 50,[114] 15 – 40,[115] and 20 – 100[116] reported in the literature for the number of arms of "arm-first" star polymers with EGDMA cores, also prepared by GTP.

5.2.4.3. Composition Analysis

The compositions of the linear and star terpolymers as determined by ^{1}H NMR are given in the last column of Table 5.3. Based on the monomer amounts fed during the polymerization process, all the terpolymers should be equimolar in the three

monomers. The terpolymer compositions were calculated using the peaks corresponding to the same protons reported in the previous Section, and were found to deviate significantly from the theoretically expected values. We believe that these deviations are due to the subtraction employed for the calculation of the MMA content. In particular, the MMA content was calculated from the area of a joint MMA-HEGMA peak, after subtracting the HEGMA contribution calculated from another peak. Because the MMA-HEGMA joint peak was mostly due to HEGMA protons, the subtraction introduced in the composition calculation a large error. Since GPC indicated full monomer conversion (no monomer peaks were observed in the GPC chromatograms of the linear polymers), we are confident that the actual terpolymer compositions were close to the theoretically expected. Furthermore, the yield in the mass of the terpolymers recovered was close to that expected based on the reagents fed during the synthesis, indicating again full polymerization of the monomers.

5.2.5. Aqueous Solution Properties

5.2.5.1. Aggregation Numbers

Static light scattering was employed to investigate possible association of the star and linear amphiphilic terpolymers in dilute aqueous solutions. The M_ws of all terpolymers as determined by SLS are listed in Table 5.4. By comparing these M_w values measured in water with those measured in THF (Table 5.3) the aggregation number of any supramolecular structure formed in water could be estimated.

In the first four rows of Table 5.4 the M_ws and calculated aggregation numbers for the isomeric linear terpolymers are listed. Although composed of 33 mol % hydrophobic MMA units, the linear triblock terpolymers exhibited surprisingly low aggregation numbers, ranging from 2 to 4. The statistical terpolymer did not present any aggregation, as expected. From the three linear triblocks, $HEGMA_{10}$-*b*-$DMAEMA_{10}$-*b*-MMA_{10} formed the largest micelles with an aggregation number of 4, whereas the other two triblocks formed smaller aggregates with average aggregation numbers around 2. The low aggregation numbers of all three triblocks can be attributed to their relatively low molecular weights of approximately 7 500 g mol^{-1} and to their high fraction in hydrophilic units of approximately 83 % w/w.

Table 5.4. Results of aqueous solution characterization of the linear and star terpolymers.

No.	Polymer Formula[a]	Apparent M_w	Aggreg. number[b]	Hydrod. diam. (nm)	Cloud point (˚C)	Effect. p*K*
1	H_{10}-*b*-D_{10}-*b*-M_{10}	34 100	4	11.5	71.6	6.7
2	H_{10}-*b*-M_{10}-*b*-D_{10}	14 600	2	4.5	67.4	6.3
3	D_{10}-*b*-H_{10}-*b*-M_{10}	18 700	2	9.0	63.7	6.6
4	(H-*co*-D-*co*-M)$_{10}$	5 500	1	-	50.5	6.7
5	H_{10}-*b*-D_{10}-*b*-M_{10}-*star*	1 245 000	4	28.7	76.8	6.3
6	H_{10}-*b*-M_{10}-*b*-D_{10}-*star*	328 000	1	9.1	71.0	6.1
7	D_{10}-*b*-H_{10}-*b*-M_{10}-*star*	409 000	1	11.9	67.4	6.4
8	(H-*co*-D-*co*-M)$_{10}$-*star*	871 000	1	10.8	55.0	6.8

[a] H: HEGMA, D: DMAEMA, M: MMA.

[b] Calculated by dividing the M_w measured using SLS in water by the M_w in THF measured either using SLS (stars) or using GPC (linears), and rounded to the next higher integer.

The very low aggregation numbers of triblocks $DMAEMA_{10}$-*b*-$HEGMA_{10}$-*b*-MMA_{10} and $HEGMA_{10}$-*b*-MMA_{10}-*b*-$DMAEMA_{10}$ might also be due to the positioning of the bulky HEGMA block, which sterically hinders the adjacent hydrophobic MMA blocks from associating. In particular, the small aggregates formed by the $DMAEMA_{10}$-*b*-$HEGMA_{10}$-*b*-MMA_{10} triblock terpolymer would resemble linear ABCBA pentablock-like, while those formed by $HEGMA_{10}$-*b*-MMA_{10}-*b*-$DMAEMA_{10}$ triblock terpolymer would have an A_2B_2 heteroarm star-like structure, as illustrated in Figure 5.10 which displays schematically (again depicted in two dimensions) the aggregates formed by the three linear triblock terpolymers. Thus, block sequence in linear triblock terpolymers is an important structure-determining factor for their aggregation in aqueous solution.

The M_ws of the isomeric star terpolymers are listed in the last four rows of Table 5.4. Three out of the four star terpolymers, namely $HEGMA_{10}$-*b*-MMA_{10}-*b*-$DMAEMA_{10}$-*star*, $DMAEMA_{10}$-*b*-$HEGMA_{10}$-*b*-MMA_{10}-*star* and (HEGMA-*co*-DMAEMA-*co*-MMA)$_{10}$-*star* exhibited reasonably similar SLS M_w values in water and THF, with the differences possibly resulting from the dependence of the apparent M_w on the

refractive index of the solvent,[117] implying lack of aggregation in water. The lack of aggregation in these three star terpolymers was not surprising given that their number of arms was much greater than the aggregation numbers in water of the corresponding linear triblock terpolymers. Thus, enough free energy was saved in the unimolecular star aggregation state with the present number of arms. In contrast, star terpolymer 5, $HEGMA_{10}$-*b*-$DMAEMA_{10}$-*b*-MMA_{10}-*star*, was the only star block terpolymer that exhibited association in water, resulting in aggregates with an aggregation number of 4. No association was observed for the star ABC statistical terpolymer due to the random distribution of the hydrophobic MMA units along the polymeric chains.

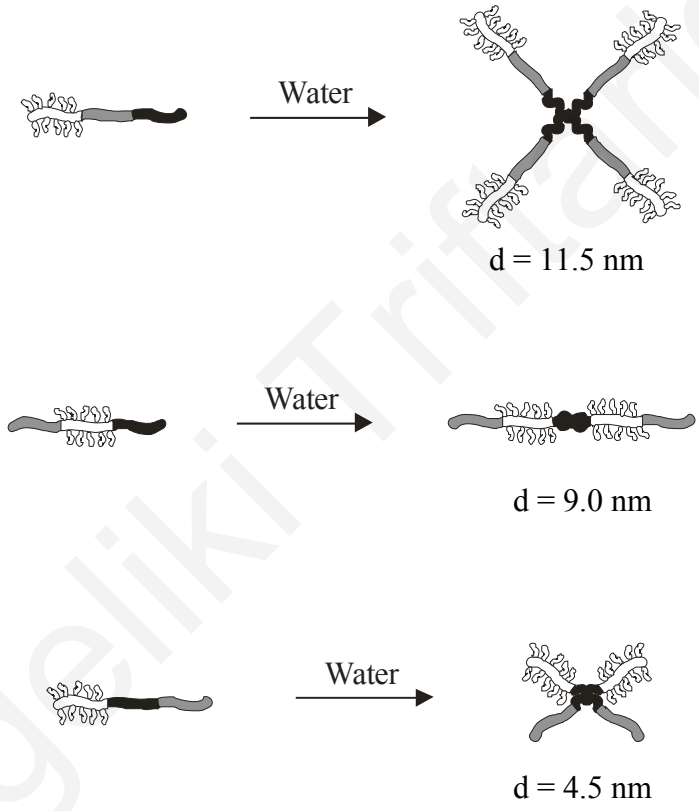

Figure 5.10. Schematic representations of the structures formed by the three linear ABC triblock terpolymers in water. H, D and M stand for HEGMA, DMAEMA and MMA, respectively. The color coding is the same as that employed in Figure 5.3.

5.2.5.2. Surface Imaging

Figure 5.11 shows an atomic force microscope image of the aggregating star block terpolymer in aqueous environment. In this image, the particular star block terpolymer appears to be distributed between a unimolecular and an associated form,

with an average aggregation number of approximately 3-4. The image on the right

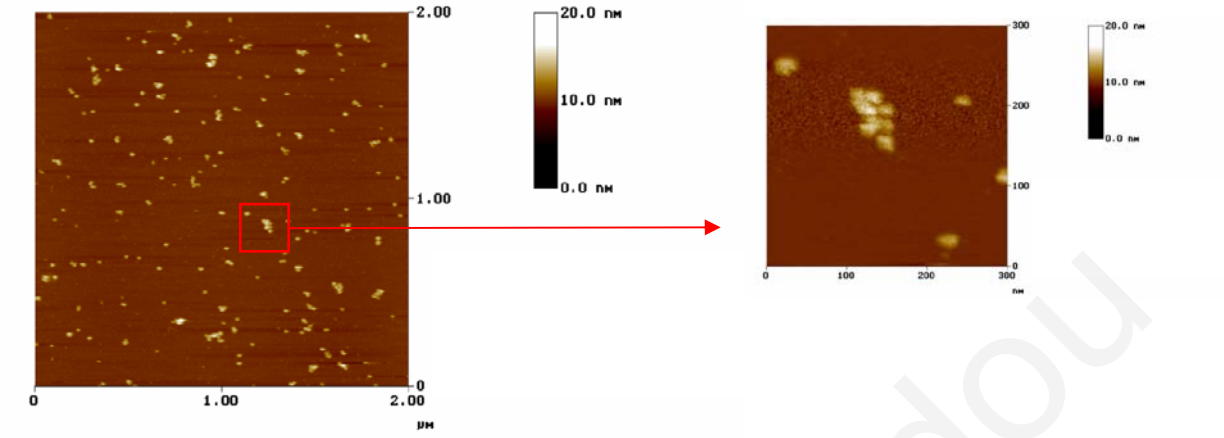

Figure 5.11. AFM images of HEGMA$_{10}$-*b*-DMAEMA$_{10}$-*b*-MMA$_{10}$-*star* nanoparticles deposited on mica from an aqueous solution.

presents a magnification of a particular cluster of star terpolymers with an aggregation number of 9. The apparent diameter of the unimolecular star terpolymers was around 20 nm, probably larger than the size in solution due to the spreading of this soft material on the adsorbing surface. Thus, these AFM results are consistent with the aqueous aggregation of HEGMA$_{10}$-*b*-DMAEMA$_{10}$-*b*-MMA$_{10}$-*star* observed by SLS.

5.2.5.3. Hydrodynamic Diameters

DLS was employed for the measurement of the hydrodynamic diameters of the linear and star terpolymers in aqueous solution. These results are also shown in Table 5.4 and are compared with some theoretical limiting sizes.

5.2.5.3.1. Theoretical Limiting Sizes

The limiting diameters for aggregating and non-aggregating linear terpolymers were calculated in Section 5.1.5.1.1 and their values were listed in Table 5.2. Because the degrees of polymerization of the terpolymers in this Section were the same as those of the terpolymers in the previous Section, the same theoretical limiting sizes apply. The theoretically calculated diameter of a non-aggregated star terpolymer with fully stretched chains is twice the arm contour length, i.e. 15 nm.

5.2.5.3.2. Measurements for the Linear Terpolymers

Table 5.4 shows that the linear ABC triblock terpolymers HEGMA$_{10}$-*b*-DMAEMA$_{10}$-

b-MMA_{10} and $DMAEMA_{10}$-*b*-$HEGMA_{10}$-*b*-MMA_{10} exhibited hydrodynamic diameters 11.5 and 9.0 nm, respectively, which are consistent with the supramolecular structures proposed in Figure 5.10. The hydrodynamic diameter of the former terpolymer was higher than that of the latter in agreement with the higher aggregation number of the former. Moreover, the micellar hydrodynamic diameter of 11.5 nm was just below the upper theoretical limit of 15 nm for the AB- diblock type micelles. The hydrodynamic diameter of the last linear triblock terpolymer, $HEGMA_{10}$-*b*-MMA_{10}-*b*-$DMAEMA_{10}$, was 4.5 nm, which was between the limiting values 2.9 and 7.5 nm, consistent with the small aggregation number of 2. The hydrodynamic diameters of these linear terpolymers were slightly lower than those of Section 5.1 (and listed in Table 5.2) with the same theoretical molecular weights and compositions as these terpolymers. This is due to the higher experimental molecular weights of the linear terpolymers of Section 5.1 than those of Section 5.2.

5.2.5.3.3. Measurements for the Star Terpolymers

The three out of the four star terpolymers presented hydrodynamic diameters between 9 – 12 nm, which were below the limiting value of 15.0 nm, indicating absence of star aggregation, in agreement with the SLS results. Suprisingly, the fourth star terpolymer, $HEGMA_{10}$-*b*-$DMAEMA_{10}$-*b*-MMA_{10}-*star*, exhibited a larger size than the limiting theoretical value (approximately double, 29 nm), indicating an aggregation between the stars, again consistent with the SLS results. This was unexpected due to the location of the very hydrophilic HEGMA blocks at the periphery of this star triblock terpolymer. A possible explanation is that it could be due to the fact that the hydrophobic MMA block is adjacent to the core, increasing locally the hydrophobic content, inducing stronger hydrophobic interactions and resulting in inter-star aggregation (see Figure 5.11).

Thus, the star terpolymers in aqueous solution behave as water-swollen, nanoparticles with average sizes in the range between 9 and 29 nm, depending on their block sequence. Owing to their large number of arms (40 to 73), the chains are stretched in the star terpolymers, with the three constituting blocks forming three different concentric compartments. Of particular interest should be the $HEGMA_{10}$-*b*-MMA_{10}-*b*-$DMAEMA_{10}$-*star*, having the MMA hydrophobic compartment, which probably excludes water, separating the HEGMA and DMAEMA hydrophilic compartments, and essentially isolating the internal DMAEMA compartment from the outer solution.

Moreover, this star triblock terpolymer should display the greatest morphological differences in aqueous solution from its linear counterpart which, as described previously, exhibits A_2B_2 heteroarm star-like structure in water.

5.2.5.4. Cloud Points

The cloud points of the linear and star terpolymers are also listed in Table 5.4 and plotted in Figure 5.12. The error bars are not displayed in the Figure because they were smaller than the symbol size. The cloud points of the star terpolymers were higher than those of their linear counterparts by ~ 5 ºC, indicating that the star terpolymers in aqueous solution were more stable than their linear counterparts. This was consistent with the SLS results, which showed that the number of arms of the star terpolymers in aqueous solution was *much* greater than the aggregation number of the linear terpolymers in water. The large number of arms in the star terpolymers was held by covalent bonds and was imposed by chemical means during synthesis. On the other hand, in the linear terpolymers, the chains were assembled only by physical means, and, in particular, via hydrophobic aggregation, leading to low aggregation numbers,

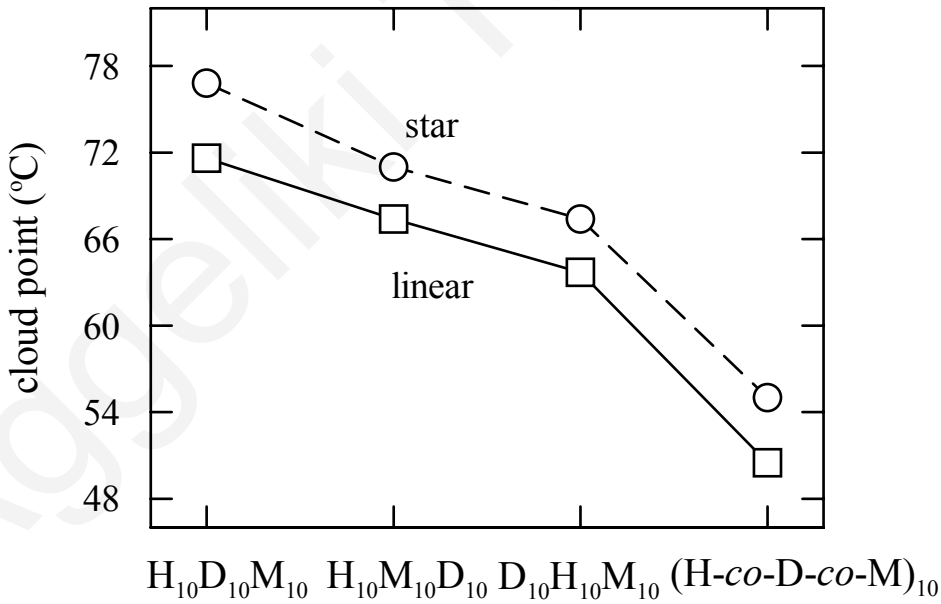

Figure 5.12. Dependence of the cloud points of the linear and star terpolymers on their monomer distribution. The H, D and M abbreviations employed in the Figure stand for the HEGMA, DMAEMA and MMA monomer repeating units, respectively.

between 1 and 4. The resulting large number of arms in the star terpolymers effected a better steric stabilization[104(b)] and a smaller unfavorable contact between the hydrophobic MMA units and water.

The cloud points of the linear terpolymers were found to range between 51 and 72 ºC. The lowest cloud point was that of the statistical linear terpolymer whose MMA hydrophobic units were randomly distributed along the polymer chain. This monomer distribution excluded both the possibility for intermolecular aggregation, i.e. micellization, and the possibility for intramolecular aggregation of the MMA units, i.e. formation of unimolecular micelles. Thus, the MMA units in this linear terpolymer were minimally protected from water, resulting in the lowest cloud point. The three linear triblock terpolymers formed small micelles, in which the MMA units were shielded from the aqueous environment to different degrees, leading to cloud points higher than those of the statistical terpolymer.

The linear $HEGMA_{10}$-*b*-$DMAEMA_{10}$-*b*-MMA_{10} terpolymer exhibited the highest cloud point for two reasons. First, it formed micelles with the highest aggregation number among the linear triblocks, resulting in the best steric stabilization. Second, the MMA units in the core of the micelles were best protected from water as these were shielded by two consecutive shells, an internal DMAEMA shell and an external HEGMA shell.

The linear $HEGMA_{10}$-*b*-MMA_{10}-*b*-$DMAEMA_{10}$ terpolymer exhibited the next highest cloud point. In the case of this terpolymer, the MMA hydrophobic blocks were shielded by a mixed shell composed of HEGMA and DMAEMA blocks. Given the property of DMAEMA units to become hydrophobic and to precipitate above 35 ºC,[109] the mixed HEGMA-DMAEMA shell was less stable than the two consecutive shells of the previous triblock. The linear $DMAEMA_{10}$-*b*-$HEGMA_{10}$-*b*-MMA_{10} terpolymer exhibited the lowest cloud point among the three triblocks because its MMA hydrophobic blocks were shielded by two consecutive shells, the outermost of which was the temperature-sensitive DMAEMA shell.

The cloud points of the star terpolymers ranged between 55 and 77 ºC. The order of these cloud points was the same as that of the corresponding linear terpolymers, and similar explanations could be provided. The statistical star terpolymer, $(HEGMA\text{-}co\text{-}DMAEMA\text{-}co\text{-}MMA)_{10}$-*star*, presented the lowest cloud point among the star

terpolymers because the MMA hydrophobic units were minimally protected from water. The highest cloud point was exhibited by $HEGMA_{10}$-*b*-$DMAEMA_{10}$-*b*-MMA_{10}-*star*, bearing the highest number of stabilizing arms, 160 (this was the only aggregating star terpolymer; it had four units per aggregate and about 40 arms per unit), and having its MMA units protected by a dual shell with a HEGMA outer component. The second highest cloud point was displayed by $HEGMA_{10}$-*b*-MMA_{10}-*b*-$DMAEMA_{10}$-*star*, having an outer HEGMA shell, but with the MMA blocks right next to it and, therefore, more exposed to water than the MMA blocks of the previous star terpolymer. The lowest cloud point among the three triblock stars was presented by $DMAEMA_{10}$-*b*-$HEGMA_{10}$-*b*-MMA_{10}-*star* because its outermost shell consisted of the temperature-sensitive DMAEMA.

The same precipitation order was observed for the linear triblock terpolymers bearing the same block sequences reported in the previous Section.[42] In both terpolymer families, the statistical terpolymers exhibited the lowest cloud points which were significantly lower than the cloud points of the triblock terpolymers. However, the linear terpolymers studied in Section 5.1 exhibited cloud points that were about 10 ºC higher that the cloud points of the terpolymers discussed in the present Section. This can be attributed to the higher actual molecular weights of those linear terpolymers.

5.2.5.5. Surface Tension

The ability of all the linear and three of the star terpolymers presented in this Section to act as surfactants was tested (the triblock terpolymer $HEGMA_{10}$-*b*-$DMAEMA_{10}$-*b*-MMA_{10}-*star* was no longer available). To this end, the surface tension at the air-water interface was measured for a range of concentrations of 6×10^{-6} – 1 w/v %. These results are plotted in Figure 5.13. The minimum observed in the surface tension curve of the linear $HEGMA_{10}$-*b*-$DMAEMA_{10}$-*b*-MMA_{10} triblock terpolymer was probably due to the presence of impurities. Upon increasing the terpolymer concentration, the surface tension was reduced up to a point where it almost leveled off (break point, indicated by arrows in the plots). This decrease in surface tension was due to the transfer of more terpolymer molecules at the air-water interface,[118] whereas the leveling off was due to either saturation of the air-water interface or to micellization, with the break point, in the latter case, providing an estimation for the *critical micelle concentration*, *cmc*.

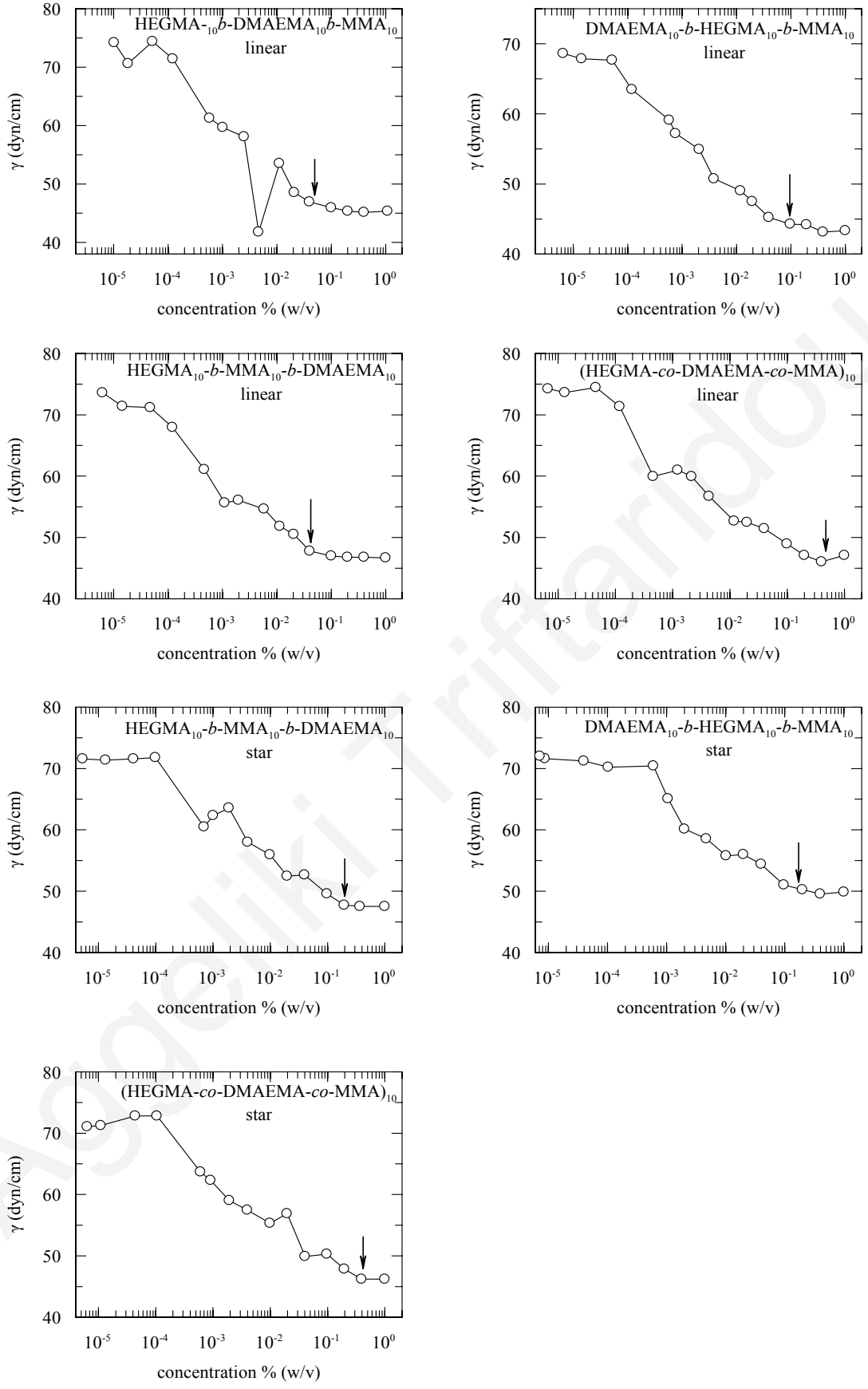

Figure 5.13. Dependence of the surface tension at the air-water interface on the concentration of the linear and star terpolymers studied in the present Section.

The break points in the star terpolymers occurred at higher concentrations than the linears showing the lower availability of the stars for the interface due to the interconnection of their arms. The break points in the linear terpolymers increased in the order: $HEGMA_{10}$-*b*-MMA_{10}-*b*-$DMAEMA_{10}$ < $HEGMA_{10}$-*b*-$DMAEMA_{10}$-*b*-MMA_{10} < $DMAEMA_{10}$-*b*-$HEGMA_{10}$-*b*-MMA_{10} < (HEGMA-*co*-DMAEMA-*co*-$MMA)_{10}$. The highest concentration break point was exhibited by the statistical terpolymer which was known not to form micelles. The concentration break points of the three linear triblock terpolymers were about 10 times lower than that of the statistical, consistent with the micellization of the triblocks. The *cmc*s estimated from the break points of the triblocks ranged between 0.05-0.09 w/v % corresponding to approximately 8×10^{-5} to 1.4×10^{-4} M. These values were higher than those of diblock copolymers of HEGMA and benzyl methacrylate, found to range between 10^{-6} and 10^{-5} M.[119]

5.2.5.6. Effective p*Ks and Water-Solubility*

The effective p*K*s of the DMAEMA monomer repeating units in all the terpolymers also listed in Table 5.4, ranged between 6.1 and 6.9, which were near the reported effective p*K* value of the DMAEMA homopolymer of around 7,[110] also determined in this study. All terpolymer solutions remained optically clear during their titrations between pH 2 and 12 at room temperature, indicating the increased hydrophilicity of these materials.

5.2.6. Conclusions

In this part of the Thesis, novel multiarm star-shaped ABC triblock terpolymers of the $(ABC)_n$ type and their linear counterparts were synthesized by GTP. The synthetic strategy for the stars was that of the "arm-first" method using a bis-unsaturated monomer (EGDMA) as the cross-linking reagent. The synthetic method allowed the preparation of four equimolar isomeric terpolymers: the statistical and three block sequence isomers for which the position of the different blocks was chosen at will. All the star terpolymers were soluble in water, exhibiting cloud points from 55 to 77 ºC. At room temperature, three out of the four star terpolymers did not aggregate in water. Due to their relatively large number of arms, the four star terpolymers must be highly compact nanoparticles with stretched chains. The three triblock stars had their blocks arranged in three concentric layers whose topology was determined by the

block sequence of the arms. The linear terpolymers were also water-soluble but presented lower cloud points (51 to 72 ºC) than the corresponding stars. All linear triblock terpolymers associated in water, resulting, however, in particles with small aggregation numbers, from 2 to 4. Thus, the star rather than the linear architecture provides the means for the preparation of highly compact nanoparticles.

5.3. Equimolar Star ABC Triblock Terpolymers of HEGMA, DMAEMA and MMA: All Six Block Sequence Isomers

5.3.1. Summary

Seven equimolar star terpolymers based on the nonionic hydrophilic methoxy HEGMA, the ionizable hydrophilic DMAEMA, and the neutral hydrophobic MMA were synthesized using group transfer polymerization (GTP). Six of the seven star terpolymers had arms composed of the block sequence triblock terpolymer isomers: ABC, ACB, BAC, BCA, CAB and CBA. The seventh star terpolymer had arms composed of the statistical isomer. EGDMA was used as the cross-linker to interconnect the linear terpolymer chains at one end, resulting in the formation of the star architecture. The molecular weights and molecular weight distributions of the star terpolymers as well as those of their homopolymer, diblock and triblock precursors were characterized by gel permeation chromatography (GPC) in tetrahydrofuran, whereas their compositions were determined by proton nuclear magnetic resonance (^{1}H NMR) spectroscopy. The aqueous solution properties of all the terpolymers were investigated by dynamic and static light scattering, turbidimetry and hydrogen ion titration to determine the hydrodynamic diameters, the absolute molecular weights, the cloud points and the effective p*K*s, respectively. The star terpolymers exhibited aqueous solution properties that were dependent on the placement of the three blocks along the terpolymer chain (ABC, ACB, BAC, BCA, CAB and CBA) as well as on the distribution of the monomer repeating units (statistical or block).

5.3.2. Introduction

We realized that in the case of star polymers, in which the chains are interconnected at one end, not only block sequence but also block direction differentiates the isomers from each other. Thus, in star ABC triblock terpolymers there are six rather than three isomers: ABC, ACB, BAC, BCA, CAB and CBA. We decided, therefore, to prepare in this Section the three star isomers not synthesized in the previous Section. To afford a better comparison between the isomers, the four star terpolymers of the previous Section were synthesized again here along with the new stars.

5.3.3. Polymer Synthesis

The synthetic route followed for the preparation of the seven star terpolymers was the same as that illustrated in Figure 5.7 in the previous Section. For the synthesis of all block isomers, the order of monomer addition was changed. All seven equimolar, star terpolymer isomers prepared are schematically represented in Figure 5.14. The stars having arms comprising triblock terpolymers are listed in pairs, each pair having the same middle block, whereas the star terpolymer bearing statistical terpolymer arms is shown in the last row.

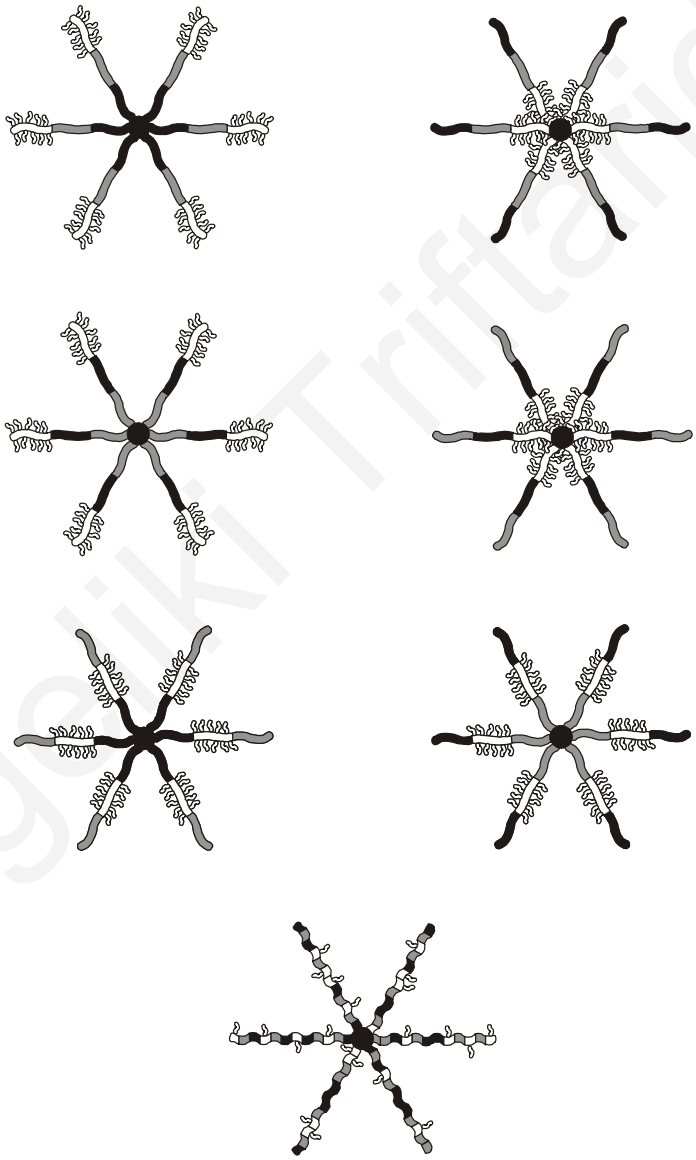

Figure 5.14. Schematic representations of the seven star terpolymers prepared. HEGMA monomer repeating units are shown in white, DMAEMA units in gray and MMA units in black. The cross-linker is represented by the black circles.

5.3.4. Determination of Terpolymer Size and Composition

5.3.4.1. Molecular Weight Analysis

All of the star ABC triblock and statistical terpolymers as well as their homopolymer, diblock and triblock terpolymer precursors were characterized by GPC in THF in terms of their molecular weight distributions (MWDs), from which the apparent number-average molecular weights (M_n) and PDIs (M_w/M_n) were calculated. These results are shown in Table 5.5, where the theoretical degrees of polymerization are given by the subscripts in the polymer formula column. In the Table the theoretical molecular weights of the precursors are also listed.

The Table shows that in most cases the polydispersities were relatively small, < 1.2, indicating the homogeneity in the lengths of the polymer chains. The experimentally determined M_ns were close to the theoretically predicted. The molecular weights of the star terpolymers were found to range between 25 000 to 44 000, the lower corresponding to the star triblock terpolymers having the bulky HEGMA in the core of the star, whereas the higher molecular weight was exhibited by the star comprising triblock terpolymer arms bearing the bulky HEGMA block at the outer shell of the star triblock terpolymer. It is noteworthy that the star terpolymers of this family have lower molecular weights than their counterparts studied in the previous Section. This could be due to differences in the initiator reactivity which led to lower molecular weights of the linear terpolymer precursors of the star terpolymers of this family.

The GPC chromatograms obtained for the seven star terpolymers were similar to that given in Figure 5.9, indicating complete incorporation of the monomer to the linear polymer chains upon each monomer addition. After the addition of the cross-linker, the distribution was bimodal. The peak at higher elution time corresponded to the unattached linear terpolymer chains, supported by the overlap of this peak with the peak of the linear triblock terpolymer as depicted in the GPC chromatogram illustrated in Figure 5.9, whereas the peak observed at lower elution time was due to the star terpolymers. The percentage of the linear terpolymer relative to the overall polymer sample was determined from the relative peak areas in the chromatograms and was found to range between 12 and 32 %. This percentage was acceptably low and comparable to 10-45% which was the weight percentage of unattached arms

reported for MMA stars with EGDMA cross-linker[111] prepared by "living" anionic polymerization.

Table 5.5. Molecular weight analysis of the star terpolymers and their linear precursors.

No.	Polymer Formula[a]	Theor. MW[b]	GPC Results[c]		Composition % mol	
			M_n	M_w/M_n	Theor. H-D-M	^{1}H NMR H-D-M
1	H_{10}	3 600	3 685	1.12		
	H_{10}-*b*-D_{10}	5 170	5 180	1.11		
	H_{10}-*b*-D_{10}-*b*-M_{10}	6 170	6 340	1.12		
	H_{10}-*b*-D_{10}-*b*-M_{10}-*star*		43 695	1.14	33-33-33	28-31-41
2	H_{10}	3 600	4 420	1.11		
	H_{10}-*b*-M_{10}	4 600	4 920	1.11		
	H_{10}-*b*-M_{10}-*b*-D_{10}	6 170	6 950	1.11		
	H_{10}-*b*-M_{10}-*b*-D_{10}-*star*		42 330	1.15	33-33-33	23-24-53
3	D_{10}	1 570	1 265	1.22		
	D_{10}-*b*-H_{10}	5 170	4 790	1.09		
	D_{10}-*b*-H_{10}-*b*-M_{10}	6 170	5 250	1.10		
	D_{10}-*b*-H_{10}-*b*-M_{10}-*star*		28 170	1.14	33-33-33	18-21-61
4	D_{10}	1 570	1 280	1.19		
	D_{10}-*b*- M_{10}	2 670	2 410	1.12		
	D_{10}-*b*-M_{10}-*b*-H_{10}	6 170	5 330	1.18		
	D_{10}-*b*-M_{10}-*b*-H_{10}-*star*		25 550	1.11	33-33-33	29-25-46
5	M_{10}	1 100	840	1.28		
	M_{10}-*b*-H_{10}	4 600	4 620	1.08		
	M_{10}-*b*-H_{10}-*b*-D_{10}	6 170	5 690	1.10		
	M_{10}-*b*-H_{10}-*b*-D_{10}-*star*		30 845	1.15	33-33-33	20-29-51
6	M_{10}	1 100	880	1.24		
	M_{10}-*b*-D_{10}	2 570	2 420	1.12		
	M_{10}-*b*-D_{10}-*b*-H_{10}	6 170	5 470	1.10		
	M_{10}-*b*-D_{10}-*b*-H_{10}-*star*		25 570	1.10	33-33-33	31-30-39
7	(H-*co*-D-*co*-M)$_{10}$	6 170	6 400	1.12		
	(H-*co*-D-*co*-M)-*star*		39 170	1.11	33-33-33	28-29-43

[a] H: HEGMA, D: DMAEMA, M: MMA.

[b] The contribution of 100 g mol^{-1} from the initiator fragment was also included.

[c] From a calibration based on linear PMMA standards.

5.3.4.2. Composition Analysis

The theoretical composition and the experimentally determined composition of the terpolymers in the three monomers are displayed in the last two columns of Table 5.5 respectively. The experimentally determined composition was in most cases, not in

good agreement with the theoretically expected due to the composition calculation involving area subtraction from the joint MMA-HEGMA peak explained earlier.

5.3.5. Aqueous Solution Properties

5.3.5.1. Aggregation Numbers

SLS was employed for the molecular weight determination of the star terpolymers and the investigation of possible inter-star aggregation in dilute aqueous solutions. The M_ws of all terpolymers as determined by SLS in water are listed in Table 5.6. The molecular weights of the star terpolymers determined by SLS were higher than those determined by GPC in THF (Table 5.5), indicating their compact nature as well as their possible aggregation in water. The $HEGMA_{10}$-*b*-$DMAEMA_{10}$-*b*-MMA_{10}-*star* probably forms aggregates in water, similar to the corresponding star triblock terpolymer studied in Section 5.2.

Table 5.6. Absolute molecular weights, hydrodynamic diameters, cloud points and p*K*s of the star terpolymers.

No.	Polymer Formula[a]	M_w SLS in H_2O	No. of arms	Hydrodynamic Diameter (nm)		Cloud point (°C)	p*K*
				d_{THF} (nm)	d_{H2O} (nm)		
1	H_{10}-*b*-D_{10}-*b*-M_{10}-*star*	5 460 000	602*	19.7	20.1	77.4	6.1
2	H_{10}-*b*-M_{10}-*b*-D_{10}-*star*	1 280 000	111*	16.7	13.5	76.0	6.0
3	D_{10}-*b*-H_{10}-*b*-M_{10}-*star*	513 000	67	14.5	14.6	70.0	6.9
4	D_{10}-*b*-M_{10}-*b*-H_{10}-*star*	450 000	61	13.3	13.3	67.5	6.9
5	M_{10}-*b*-H_{10}-*b*-D_{10}-*star*	595 000	76	15.8	8.9	71.5	7.0
6	M_{10}-*b*-D_{10}-*b*-H_{10}-*star*	447 000	63	13.3	9.9	70.5	6.9
7	(H-*co*-D-*co*-M)$_{10}$-*star*	381 000	42	14.0	9.9	54.5	6.9

[a] H: HEGMA, D: DMAEMA, M: MMA.

* number of arms in the aggregate as a whole.

Unfortunately, efforts to determine the molecular weights of the star terpolymers by SLS in THF were unsuccessful because the terpolymers interacted with the column packing material (flow Static Light Scattering configuration). An estimation of the number of arms of the particles (stars or possible inter-star aggregates) in water could be made by considering the ratio of the M_w obtained by SLS in water divided by the

GPC M_ns of the linear terpolymer precursors as were determined by GPC in THF. In the calculation the contribution of the of the cross-linker units to the star terpolymer molecular weight was also taken into account.

The $HEGMA_{10}$-*b*-$DMAEMA_{10}$-*b*-MMA_{10}-*star* triblock terpolymer presented the highest number of arms, 600, which was much higher than the calculated number of arms of all the other star terpolymers, which varied between 40 and 110, implying possible inter-star aggregation. This was in agreement with the findings concerning its counterpart reported in the previous Section.

5.3.5.2. Hydrodynamic Diameters

DLS was employed for the measurement of the hydrodynamic diameters of all the star terpolymers in aqueous solution. These results are also shown in Table 5.6. The hydrodynamic diameters in water were in almost all cases lower than the theoretical limit of the 15 nm (the calculation was the same as that outlined for the star terpolymers in Section 5.2). The only exception was observed by the $HEGMA_{10}$-b-$DMAEMA_{10}$-b-MMA_{10}-*star* possibly due to its aggregation (as supported by the SLS data above).

Comparing the hydrodynamic diameters displayed by the star terpolymers in THF with those in water listed in Table 5.6, it was observed that in most cases those obtained in THF were larger than those obtained in water. This is not surprising due to the fact that THF is a non-selective solvent, whereas water is a selective solvent for two of the three blocks, namely PHEGMA and PDMAEMA. The $HEGMA_{10}$-*b*-$DMAEMA_{10}$-*b*-MMA_{10} star terpolymer presented the largest hydrodynamic diameter in water, in agreement with its counterpart studied in the previous Section. This was probably due to the location of the hydrophobic MMA block near the star nodule and the stretching of the chains in the aqueous environment due to the presence of the hydrophilic PHEGMA and PDMAEMA in the outer and inner shell, respectively. The second highest aqueous hydrodynamic diameter was displayed by the $DMAEMA_{10}$-*b*-$HEGMA_{10}$-*b*-MMA_{10} star terpolymer, also having the two hydrophilic components in the shell and the corona.

The star triblock terpolymers bearing the MMA hydrophobic block in the outer region of the stars exhibited the lowest hydrodynamic diameters in water, indicating folding of the MMA blocks towards the inside of the star in order to minimize the PMMA-

water unfavorable contact. Intermediate hydrodynamic diameters in water were obtained for the star terpolymers $HEGMA_{10}$-*b*-MMA_{10}-*b*-$DMAEMA_{10}$ and $DMAEMA_{10}$-*b*-MMA_{10}-*b*-$HEGMA_{10}$. Both star terpolymers were composed of arms bearing the hydrophobic PMMA block in the middle of the chain, and one of the hydrophilic blocks in the core. The shrinkage of the PMMA blocks in the intermediate star layer resulted in reduced hydrodynamic diameters, but not as much as the stars with the outer PMMA blocks that were back-folded.

5.3.5.3. Cloud Points

The cloud points of the seven star terpolymers are also listed in Table 5.6 and plotted in Figure 5.15 against the block sequence of the linear terpolymers constituting the arms of the star terpolymers. The cloud points obtained for all the star terpolymers ranged between 54.5 and 77.4 ºC.

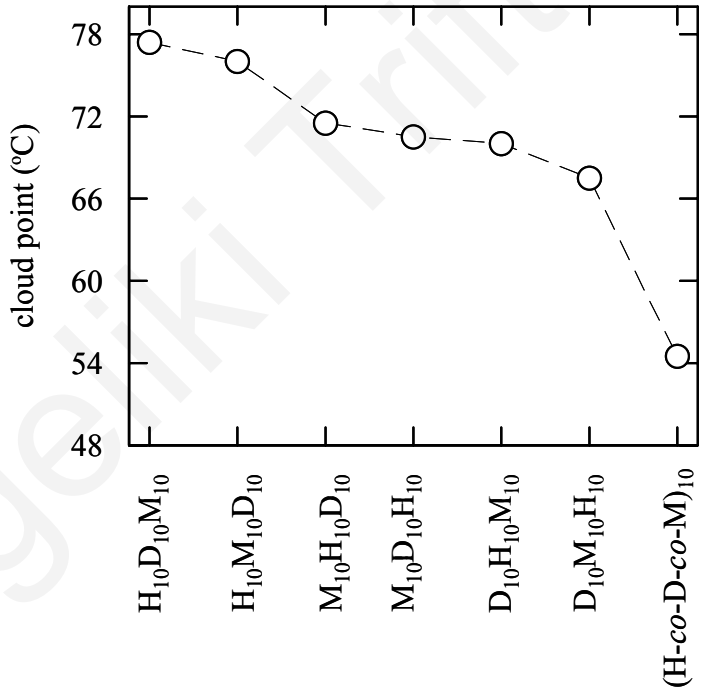

Figure 5.15. Cloud points of the seven equimolar, isomeric star terpolymers.

The lowest cloud point was exhibited by the star terpolymer comprising statistical terpolymer arms where the MMA hydrophobic units were randomly distributed along the polymer chain. The random distribution of the hydrophobic MMA units excluded both the possibility for inter-star aggregation, i.e. micellization, and the possibility for

intramolecular aggregation of the MMA units as was probably the case with the triblock stars, i.e. HEGMA$_{10}$-*b*-MMA$_{10}$-*b*-DMAEMA$_{10}$-*star*. Thus, the MMA units in this star terpolymer were minimally protected from water, resulting in the lowest cloud point.

Among the star triblock terpolymers listed in Table 5.6, those bearing the bulky hydrophilic HEGMA block in their outer part exhibited the highest cloud points. Between the two star terpolymers with the marginally hydrophilic DMAEMA blocks in the outer shell and those with the PMMA hydrophobic block in the outer shell of the star triblock terpolymer, it would have been expected that the latter would display the lowest cloud points. Surprisingly, the reverse was observed experimentally, due to the possible folding of the PMMA blocks to the inside of the star terpolymer to minimize their contact with water, as supported by the small hydrodynamic diameters of the molecules in water.

5.3.5.4. Effective pKs and Water-Solubility

The effective p*K*s of the DMAEMA units in all the terpolymers ranged between 6.0 and 7.0, which were near the reported effective p*K* value of the DMAEMA homopolymer of around 7,[110] also determined in this study by the titration of DMAEMA homopolymer from pH 2 to 12. All terpolymer solutions remained optically clear during their titrations between pH 2 and 12 (at room temperature), illustrating the hydrophilicity of these materials.

5.3.7. Conclusions

In this Section, the preparation of novel equimolar multiarm star-shaped ABC triblock terpolymers of the (ABC)$_n$ type by GTP was presented. The synthetic strategy was that of the "arm-first" method using a bis-unsaturated monomer (EGDMA) as cross-linking reagent. The synthetic method allowed the preparation of seven equimolar isomeric terpolymers: the statistical and the six block sequence isomers. The effect of block sequence on their solution properties was studied. All the star terpolymers were soluble in water, exhibiting cloud points from 54.5 to 77.4 ºC. At room temperature, five out of the seven star terpolymers did not aggregate in water. The HEGMA$_{10}$-*b*-DMAEMA$_{10}$-*b*-MMA$_{10}$-*star* triblock terpolymer and the HEGMA$_{10}$-*b*-MMA$_{10}$-*b*-DMAEMA$_{10}$-*star*, with outer HEGMA blocks were the aggregating stars. Another

interesting observation with these star terpolymers was the folding of the MMA outer blocks towards the inside of the stars for the MMA_{10}-*b*-$DMAEMA_{10}$-*b*-MMA_{10}-*star* and MMA_{10}-*b*-$HEGMA_{10}$-*b*-$DMAEMA_{10}$-*star* terpolymers in water, as manifested by their reduced hydrodynamic diameters and increased cloud points.

5.4. Equimolar ABCBA Pentablock Terpolymer Networks of HEGMA, DMAEMA and MMA: Effect of Block Sequence

5.4.1. Summary

Eight isomeric networks based on equimolar terpolymers were synthesized using GTP and were characterized in terms of their swelling properties. Two hydrophilic monomers, HEGMA and DMAEMA, and a hydrophobic monomer, MMA, were employed for the syntheses. EGDMA served as the cross-linker to interconnect the linear precursors at both ends to polymer networks. 1,4-bis(methoxytrimethylsiloxymethylene)cyclohexane (MTSMC) was the bifunctional initiator used for the syntheses. Seven of the networks were model networks, six of which were based on the symmetrical pentablock terpolymers ABCBA, ACBCA, BACAB, BCACB, CBABC and CABAC, whereas the seventh model network was based on the statistical terpolymer. All linear precursor terpolymers were equimolar with ten units from each of the three monomer types. The eighth network was a randomly cross-linked network based on the statistical terpolymer, prepared by the simultaneous quaterpolymerization of the three monomers and the cross-linker. The molecular weights and molecular weight distributions of the linear pentablock terpolymer precursors, as well as those of their homopolymer and ABA triblock copolymer precursors, were characterized by gel permeation chromatography (GPC) in tetrahydrofuran, whereas their compositions were determined by proton nuclear magnetic resonance (^{1}H NMR) spectroscopy. The sol fraction of each network was measured and found to be relatively low. The DSs in water were measured for all the networks, and were determined to increase at acidic pH due to the ionization of the DMAEMA tertiary amine units. The acidic DSs of most of the pentablock terpolymer networks were lower than those of their statistical counterparts due to microphase separation in the former type of networks.

5.4.2. Introduction

Amphiphilic polymer networks[4] represent a new type of polymeric materials, combining the properties of linear amphiphilic block copolymers[120] and hydrogels.[121] These properties are the aqueous self-assembly and microstructure formation of the former, and the stimulus-regulated absorption of water of the latter. Amphiphilic hydrogels usually exist in a microphase-separated state, with their hydrophilic

component conveying to the material a friendly aqueous environment in one microphase, and with the hydrophobic component rendering the other microphase apolar.

The present work aims at combining the linear ABC triblock terpolymer structure with the amphiphilic polymer network structure. To this end, linear, amphiphilic, symmetrical ABCBA pentablock terpolymers were synthesized and cross-linked to result in novel terpolymer networks. The use of a bifunctional GTP initiator secured the symmetrical growth of the polymers at both termini. The similar reactivities of methacrylate monomers toward GTP allowed the smooth synthesis of all six block sequence isomers for the linear pentablock terpolymer precursors, ABCBA, ACBCA, BACAB, BCACB, CABAC and CBABC, from which the corresponding six isomeric networks were prepared. Two more network structures were also prepared, in the first of which the three monomers were randomly distributed, and in the second the three monomers and cross-linker were randomly distributed. A neutral-hydrophilic monomer, a positively-ionizable hydrophilic monomer and a neutral-hydrophobic monomer were combined, resulting in networks with water-compatibility, pH-sensitivity and microphase separation capability, respectively. The swelling behavior in water and in an organic solvent of all eight networks was studied and compared to each other and to that of two-component networks.

5.4.3. Network Synthesis

5.4.3.1. Polymerization Methodology

All the networks of this study were prepared by GTP at room temperature and were equimolar in the three monomers. The number of moles of the cross-linker used was eight times the number of moles of the MTSMC initiator to optimize interchain connection and network formation, according to a previous study.[122] Isomeric networks with different monomer/cross-linker distribution were prepared by varying the order of monomer/cross-linker addition. The synthetic routes followed for the preparation of the eight different isomeric networks are given in Figure 5.16.

The synthetic procedure for the preparation of the model networks is presented schematically in Figure 5.17 where the synthesis of the network based on the $DMAEMA_5$-*b*-$HEGMA_5$-*b*-MMA_{10}-*b*-$HEGMA_5$-*b*-$DMAEMA_5$ pentablock

terpolymer is illustrated. The synthesis involved sequential monomer and cross-linker additions. The first step in Figure 5.17 resulted in the preparation of linear MMA homopolymers active at both ends (indicated by asterisks) due to the use of the bifunctional initiator. The second step led to the synthesis of the HEGMA-MMA-HEGMA triblock copolymer with two active ends. The third step was the addition of DMAEMA which provided the pentablock terpolymer. The synthesis was completed by the addition of the EGDMA cross-linker, which effected the interconnection of the polymer active ends, providing a three-dimensional network. The number of arms at the cross-links was not three, as indicated in the Figure, but higher, between 15 and 50, similar to the number of arms in star polymers also prepared by GTP.[111,112]

All eight network structures prepared are illustrated schematically in Figure 5.18. The first six network structures were those of the model networks based on the six possible block sequence isomeric linear precursors, ABCBA, ACBCA, BACAB, BCACB, CABAC and CBABC, while the last two structures were those of the statistical terpolymer model network and of the randomly cross-linked statistical terpolymer network. Two networks are presented in each row. The pair in each row bears the same middle block.

Figure 5.16. Synthetic routes followed for the preparation of the eight isomeric networks.

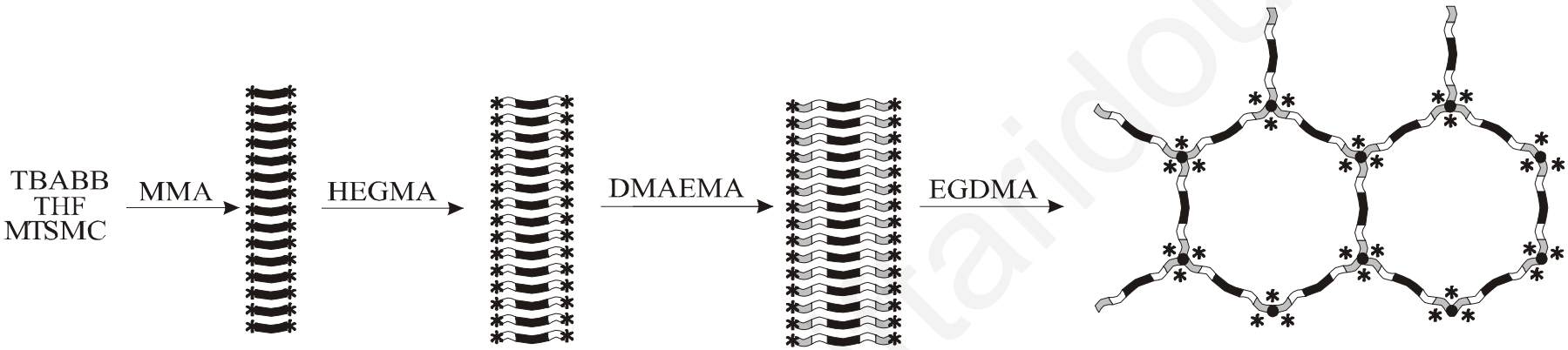

Figure 5.17. Schematic representation of the synthetic procedure followed for the preparation of the model network based on the symmetrical pentablock terpolymer $DMAEMA_5$-*b*-$HEGMA_5$-*b*-MMA_{10}-*b*-$HEGMA_5$-*b*-$DMAEMA_5$. The DMAEMA units are shown in gray, the HEGMA units in white, and the MMA units in black. The "*" symbols indicate the "living" sites of the polymerization. The number of arms at the cross-links is not three, as indicated in the Figure, but between 15 and 50.

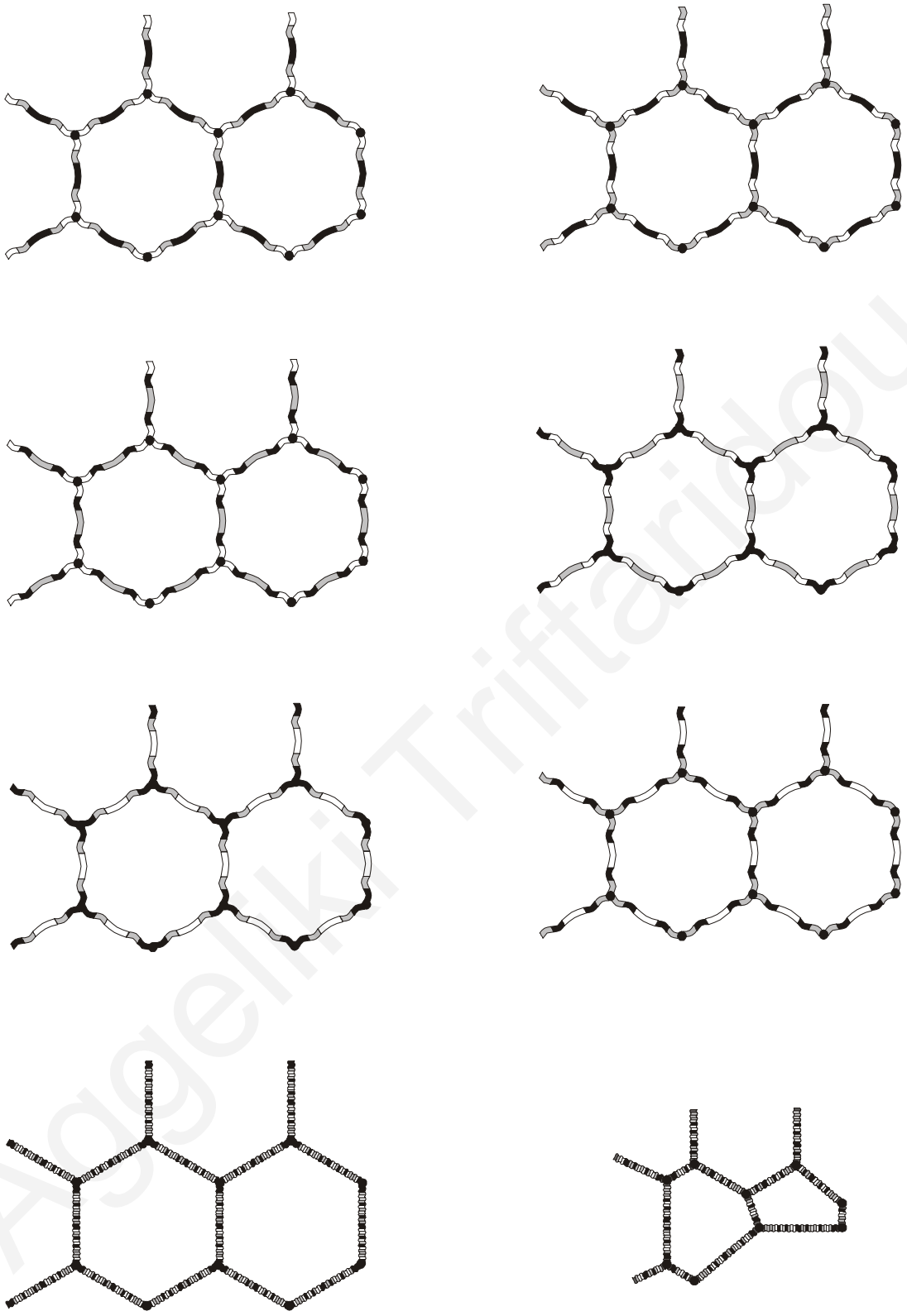

Figure 5.18. Schematic representations of the structures of the eight networks of this study. The color-coding is the same as that in Figure 5.17. For the first six networks, the two networks in the same row have the same middle-block.

5.4.4. Characterization of the Linear Preursors

5.4.4.1. Molecular Weight Analysis

The molecular weights and molecular weight distributions of the homo-, tri-, and pentablock precursors were determined by GPC in THF. Table 5.7 shows the molecular weights of the linear precursors to the networks as measured by GPC in THF. The theoretical degrees of polymerization are indicated by the subscripts in the polymer formula column. The number average molecular weights, M_ns, were systematically slightly higher than the theoretically predicted molecular weights, probably due to partial deactivation of the initiator and / or to differences in the hydrodynamic volumes of the samples with the PMMA standards used for the calibration of the GPC column. Molecular weight distributions (MWDs) were found to be narrow and the PDIs (M_w/M_n) were calculated to be lower than 1.2 in all cases. This confirms the homogeneity of the lengths of the segments between cross-links in the networks.

5.4.4.2. Composition Analysis

In the next-to-the last column of Table 5.7, the experimentally determined compositions of all the prentablock terpolymer precursors are given. Although the HEGMA-to-DMAEMA molar ratio had the expected value of one, the MMA content did not match the theoretically expected value due to the same reasons outlined in the previous Sections. The GPC chromatograms, not shown here, revealed monomodal size distributions upon each monomer addition, indicating full incorporation of the monomer added each time to the polymer chains. Hence, the observed deviations of the experimentally measured compositions from the theoretical should be due to the subtraction employed for the determination of the MMA content.

Table 5.7. Molecular weight and composition determination of the linear precursors to the networks.

No.	Polymer Formula[a]	Theor. Molec. Weight[b]	GPC Results[c]		% mol H-D-M by ^{1}H NMR[d]	Effective p*K*
			M_n	M_w/M_n		
1	M_{10}	1 196	1 720	1.18		
	D_5-*b*-M_{10}-*b*-D_5	2 748	4 180	1.15		5.8
	H_5-*b*-D_5-*b*-M_{10}-*b*-D_5-*b*-H_5	6 248	9 470	1.13	46-41-13	
1r	M_{10}	1 196	1 880	1.17		
	D_5-*b*-M_{10}-*b*-D_5	2 748	3 900	1.14		5.2
	H_5-*b*-D_5-*b*-M_{10}-*b*-D_5-*b*-H_5	6 248	8 780	1.13	31-34-35	
2	M_{10}	1 196	1 650	1.18		
	H_5-*b*-M_{10}-*b*-H_5	4 676	7 200	1.12		5.3
	D_5-*b*-H_5-*b*-M_{10}-*b*-H_5-*b*-D_5	6 248	8 740	1.13	34-40-26	
3	D_{10}	1 748	2 610	1.18		
	H_5-b-D_{10}-*b*-H_5	5 248	8 570	1.13		5.6
	M_5-*b*-H_5-b-D_{10}-*b*-H_5-*b*-M_5	6 248	9 650	1.13	27-30-43	
4	D_{10}	1 748	2 300	1.15		
	M_5-*b*-D_{10}-*b*-M_5	2 748	4 020	1.14		5.3
	H_5-*b*-M_5-*b*-D_{10}-*b*-M_5-*b*-H_5	6 248	9 490	1.12	39-28-33	
5	H_{10}	3 676	6 000	1.11		
	D_5-*b*-H_{10}-*b*-D_5	5 248	7 300	1.09		5.3
	M_5-*b*-D_5-*b*-H_{10}-*b*-D_5-*b*-M_5	6 248	8 500	1.10	26-22-52	
6	H_{10}	3 676	5 910	1.11		
	M_5-*b*-H_{10}-*b*-M_5	4 676	7 040	1.10		5.4
	D_5-*b*-M_5-*b*-H_{10}-*b*-M_5-D_5	6 248	8 800	1.10	24-28-48	
7	(H-*co*-D-*co*-M)$_{10}$	6 248	9 910	1.12	23-18-59	5.2
8	(H-*co*-D-*co*-M)$_{10}$-*co*-E_8	-	-	-	-	5.6

[a] H: HEGMA, D: DMAEMA, M: MMA, E: EGDMA.

[b] The contribution from the initiator fragment of 196 g mol^{-1} is included.

[c] From a calibration based on linear PMMA standards of narrow MWDs.

[d] The theoretical % mol H-D-M composition was 33.3-33.3-33.3 for all the terpolymer precursors to the networks.

5.4.5. Characterization of the Extractables

Following the procedure described in the Experimental Section, the extractables (sol fraction) of each network were obtained. These included any homopolymer, triblock or pentablock chains not incorporated in the network, as well as the catalyst used for the polymerization.

The results of the characterization of the extractables are listed in Table 5.8, including their percentage, M_n and PDIs. The percentage of the extractables (sol fraction) was found to be relatively low, below 12% in all cases, confirming the well-defined structure of the networks. It is noteworthy that the statistical terpolymer-based model network (sample no. 7) had the lowest percentage of extractables (6.2 %), whereas the statistical terpolymer-based randomly cross-linked network (sample no. 8) had one of the highest percentages (10.0 %), indicating a difference in the level of perfection between these two network structures.

Table 5.8. Mass percentages and molecular weights of the extractables from the networks.

No.	Polymer Formula[a]	% w/w Extractables	GPC Results[b]	
			M_n	M_w/M_n
1	H_5-*b*-D_5-*b*-M_{10}-*b*-D_5-*b*-H_5	7.0	5 210	1.31
1r	H_5-*b*-D_5-*b*-M_{10}-*b*-D_5-*b*-H_5	7.7	5 700	1.24
2	D_5-*b*-H_5-*b*-M_{10}-*b*-H_5-*b*-D_5	8.2	5 600	1.11
3	M_5-*b*-H_5-*b*-D_{10}-*b*-H_5-*b*-M_5	10.7	7 140	1.19
4	H_5-*b*-M_5-*b*-D_{10}-*b*-M_5- *b*-H_5	9.8	7 060	1.09
5	M_5-*b*-D_5-*b*-H_{10}-*b*-D_5-*b*-M_5	9.1	7 100	1.12
6	D_5-*b*-M_5-*b*-H_{10}-*b*-M_5-D_5	11.3	7 070	1.13
7	(H-*co*-D-*co*-M)$_{10}$	6.2	7 870	1.15
8	(H-*co*-D-*co*-M)$_{10}$-*co*-E_8	10.0	16 500	1.36

[a] H: HEGMA, D: DMAEMA, M: MMA, E: EGDMA.

[b] Based on a calibration using PMMA standards of narrow MWD.

The M_ns of the extractables, also listed in Table 5.8, were lower than those of the corresponding linear precursors. This was as expected because the extractables

contained early-terminated polymers (homopolymers and ABA triblock copolymers) as well as living ABCBA pentablocks which could not approach the cross-link due to steric hindrances. The PDIs of the extractables are also shown in Table 5.8. These were, in most cases, higher than the molecular weight polydispersity indices of the corresponding linear terpolymer precursors listed in Table 5.7. This was in accord with the expectation for an increased size heterogeneity of the extractables, and in (qualitative) agreement with the Poisson distribution,[16(b)] dictating higher polydispersity indices for polymers with lower M_ns, as was the case with the extractables.

Although the synthetic procedure and, in particular, the rapid cross-linking of the solution precluded sampling for GPC characterization of the precursor to the randomly cross-linked network, GPC characterization of the extractables from this network was straightforward. The determination of the M_n and M_w/M_n of the extractables from the randomly cross-linked network was very important because these quantities would be the only, approximate, indicators for the MW characteristics of this network. The M_n of the extractables of the randomly cross-linked network was more than twice the M_n of the extractables from the other networks. This was consistent with a branched structure of the extractables from the randomly cross-linked network, originating from the simultaneous copolymerization of the monomers and the cross-linker during the synthesis of this network. Despite their high M_n value, the polydispersity indices of the extractables from the randomly cross-linked network was the highest of all networks, 1.36, indicating increased heterogeneity of this material, due to branching. However, the value of the polydispersity index of 1.36 was still acceptably low, reflecting the "livingness" of the synthetic method and limited branching.

5.4.6. Characterization of the Networks

5.4.6.1. Aqueous Degrees of Swelling and Degrees of Ionization

The experimentally measured degrees of swelling (DSs) and degrees of ionization of all the networks are plotted against pH in Figure 5.19. The theoretical chemical formula of the linear terpolymer precursor to each network is indicated above each plot. The subscripts in the polymer formula denote the number of monomer units in each block (degree of polymerization). Upon decreasing the solution pH, the DSs

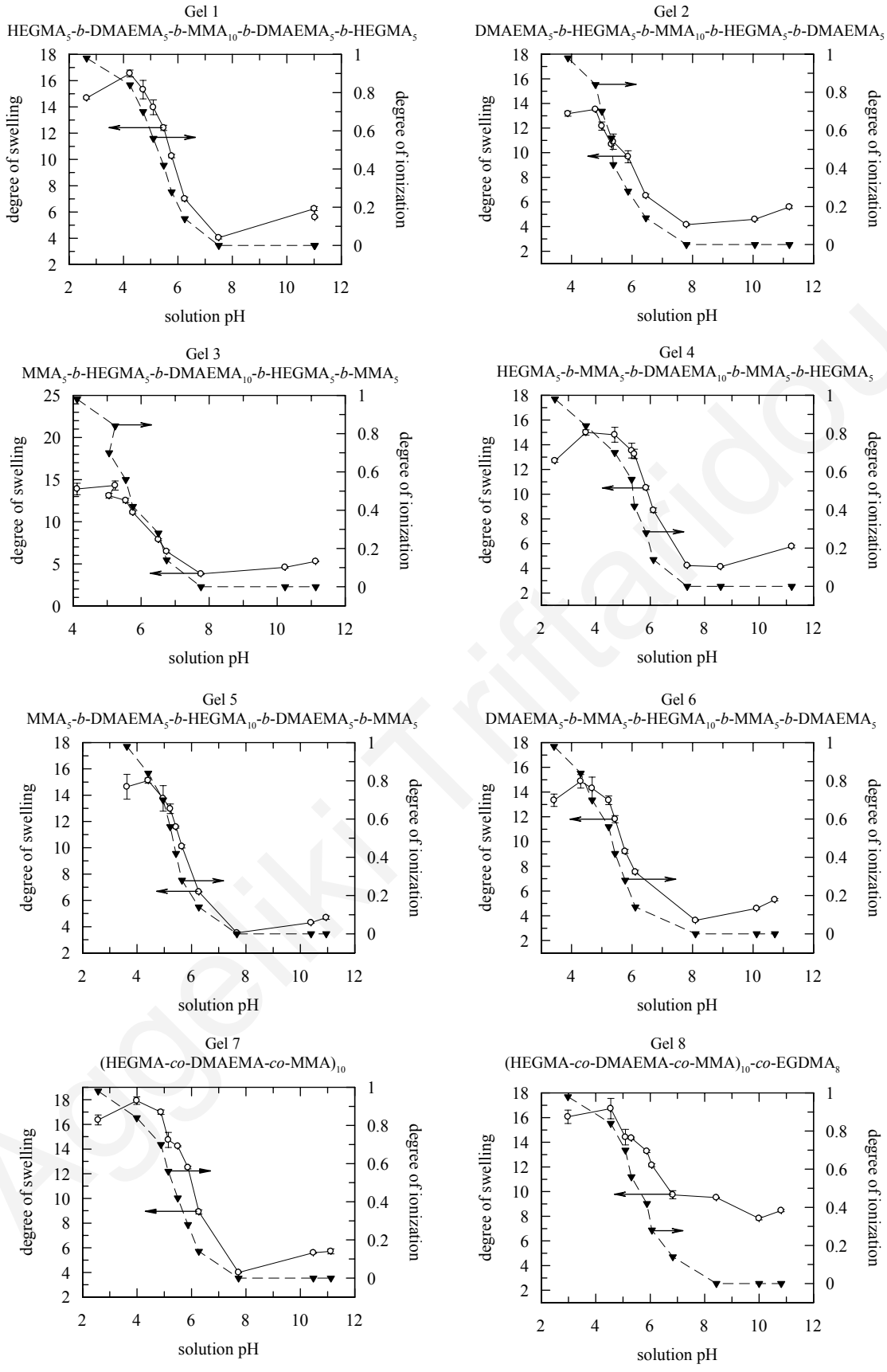

Figure 5.19. Degrees of swelling and degrees of ionization as a function of pH for all the networks discussed in this Section.

increased, reaching a maximum. At lower pH values, a decrease in the DSs was observed, attributed to the charge screening caused by the increased ionic strength (imparted by the high acid concentration), leading to a decrease in the repulsive interactions and hence, lower DSs. The networks began to swell at pH 6 or lower because of the presence of DMAEMA, a tertiary amine becoming ionized in that pH range. This ionization resulted in electrostatic repulsions between the positively charged DMAEMA units, as well as in the build-up of an osmotic pressure created by the counterions to the charges in the network.[123] As illustrated in Figure 5.19, the DS and degree of ionization curves followed each other, confirming the importance of the electrostatic interactions in swelling.

5.4.6.2. Effective pKs of the Networks

The effective p*K*s of the DMAEMA units in the networks, also presented in Table 5.9, were read out from the degree of ionization curves as the pH at 50 % ionization. All networks were found to have similar p*K*s which, however, span a range of values from 5.2 to 5.8.

Table 5.9. Effective p*K*s and cloud points of the terpolymer networks.

No.	Polymer Formula[a]	Effective p*K*	Cloud point (°C)
1	H_5-*b*-D_5-*b*-M_{10}-*b*-D_5-*b*-H_5	5.8	53.3
1r	H_5-*b*-D_5-*b*-M_{10}-*b*-D_5-*b*-H_5	5.2	56.7
2	D_5-*b*-H_5-*b*-M_{10}-*b*-H_5-*b*-D_5	5.3	46.6
3	M_5-*b*-H_5-b-D_{10}-*b*-H_5-*b*-M_5	5.6	60.0
4	H_5-*b*-M_5-*b*-D_{10}-*b*-M_5-*b*-H_5	5.3	50.0
5	M_5-*b*-D_5-*b*-H_{10}-*b*-D_5-*b*-M_5	5.3	56.7
6	D_5-*b*-M_5-*b*-H_{10}-*b*-M_5-D_5	5.4	53.3
7	(H-*co*-D-*co*-M)$_{10}$	5.2	51.7
8	(H-*co*-D-*co*-M)$_{10}$-*co*-E_8	5.6	N/D[b]

[a] H: HEGMA, D: DMAEMA, M: MMA, E: EGDMA.

[b] not determined.

5.4.6.3. Degrees of Swelling in Water and THF

The DSs in neutral water (pH ~ 8) and in acidified water (pH ~ 3.5) were extracted from Figure 5.19 for all networks and are plotted in Figure 5.20 along with their corresponding DSs exhibited by neutral network samples in THF.

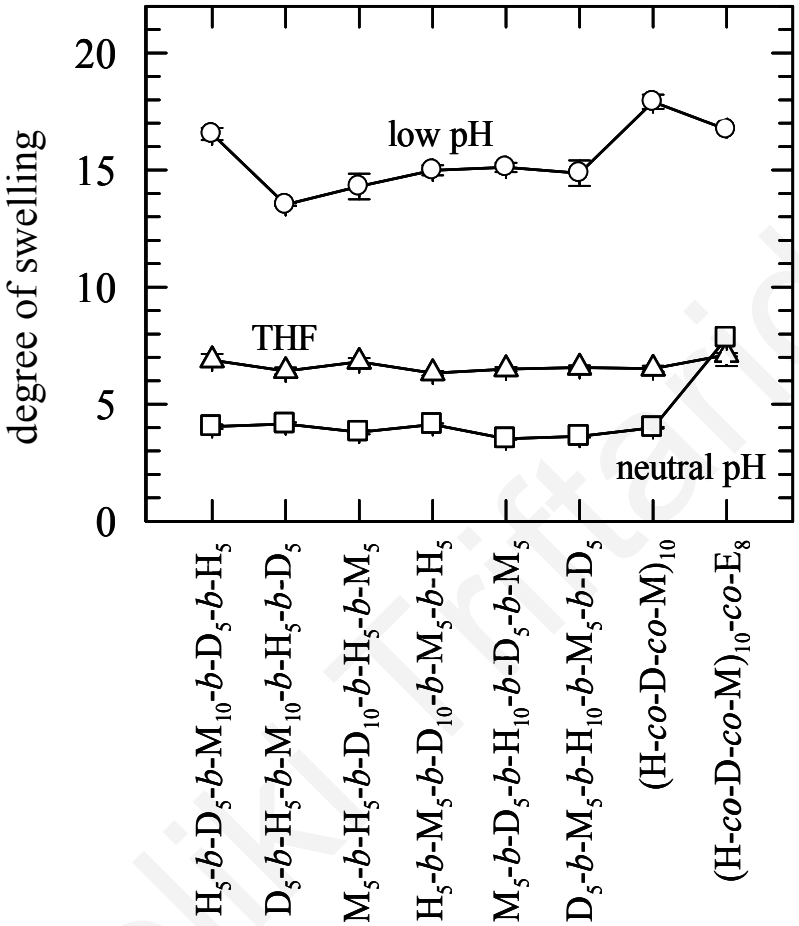

Figure 5.20. Degrees of swelling of the networks in THF, in neutral water, and in acidic water.

With the exception of the randomly cross-linked network, which is structurally less perfect, the DSs of all other networks increased in the order: neutral water < THF < acidic water, with values of approximately 4, 7 and 14, respectively. THF is a non-selective solvent, in which all three monomer repeating units of the networks swell to a good extent. In contrast, neutral water is a selective solvent for HEGMA and DMAEMA, and a precipitant for MMA. Thus, the equilibration of the terpolymer networks in neutral water led to their microphase separation with collapsed MMA cores. The collapse of the MMA units in neutral water explains the lower swelling of

the terpolymer networks in this solvent than in THF. The acidified water was still a non-solvent for MMA, but it caused the ionization of the DMAEMA units, which led to extensive swelling, resulting in the highest DSs in this solvent compared to the other two.

It is interesting to compare the average DSs in neutral and in acidified water of the terpolymer networks of the present study with those of two-component networks prepared by the same method. In particular, equimolar ABA triblock copolymer-based model networks of DMAEMA and MMA (amphiphilic)[5,124] exhibited DSs in neutral and acidic water of 2 and 5, respectively, while DMAEMA and HEGMA (double-hydrophilic) networks[125] presented corresponding DS values of 8 and 20. Thus, the corresponding DSs of the terpolymers of the present study of 4 and 14 had values intermediate of those of the two above-mentioned two-component networks, reflecting the hydrophobic character of MMA and the hydrophilic character of HEGMA. However, in addition to the numerical differences between the DSs of the terpolymer and the copolymer networks, there are substancial structural differences. In particular, unlike the DMAEMA-MMA networks, these terpolymer networks were not fully collapsed in their neutral state, underlining the role of the second type of hydrophilic units, namely HEGMA. Moreover, unlike the DMAEMA-HEGMA networks, the present terpolymer networks were microphase separated (partially collapsed) in their ionized state, emphasizing the role of the hydrophobic MMA block.

By examining Figure 5.20 more carefully, one can see that in a given solvent the various isomers did not present large differences in their DSs, possibly reflecting the low degrees of polymerization of their blocks. In particular, in neutral water, most of the block sequence isomeric terpolymer networks exhibited similar DSs, while the randomly cross-linked network displayed a higher DS, attributed to the imperfections in the structure of this network. Intermediate DSs, independent of the block sequence or the architecture of the network were obtained in THF. All the networks were equimolar in the three monomers, and since THF is a non-selective solvent, this behavior was not surprising. A slight positive deviation of the DS was observed for the randomly cross-linked terpolymer network, attributed to its less perfect structure. In acidic conditions, in which all terpolymer networks swelled much more, the statistical terpolymer model network clearly differentiated itself from the others for

the first time, presenting the highest DS, reflecting highly extended chains due to the random distribution of the MMA units which precluded microphase separation. In contrast, the segregation of the MMA units in blocks in the case of the pentablock terpolymer model networks promoted microphase separation which reduced the effective chain length, resulting in a decrease in the DSs. Similar behavior was observed in the ionized DMAEMA-MMA networks, where the DSs of the block isomers were also lower than those of their statistical counterparts.

5.4.6.4. Cloud Points

In an effort to estimate the cloud points of the networks, their DSs upon increasing the temperature were measured and were plotted in Figure 5.21. Close examination of Figure 5.21 reveals the the DSs decreased smoothly upon increasing the temperature. Thus, the determination of the network cloud points in the same way determined for the linear and star terpolymers, for which abrupt increases in the optical density with temperature were observed, was not possible. However, they were determined as the temperature corresponding to the 50 % of the change observed in the DS. The cloud points of the networks are also listed in Table 5.9. Upon increasing the temperature of the supernatant solution from 25 to 80 ºC the DSs of the networks slowly decreased from a value of around 5 to a value of approximately 2.4, indicating water expulsion from their pores at higher temperature. At temperatures above the cloud point of the DMAEMA of 35 ºC,[109] the DMAEMA units became hydrophobic and caused a further reduction in the effective length of the elastic chains, resulting in a gradual dehydration of the networks.

Comparing the “approximate” cloud points of the networks and those obtained for the linear and star terpolymers, it is observed that the former are much lower.

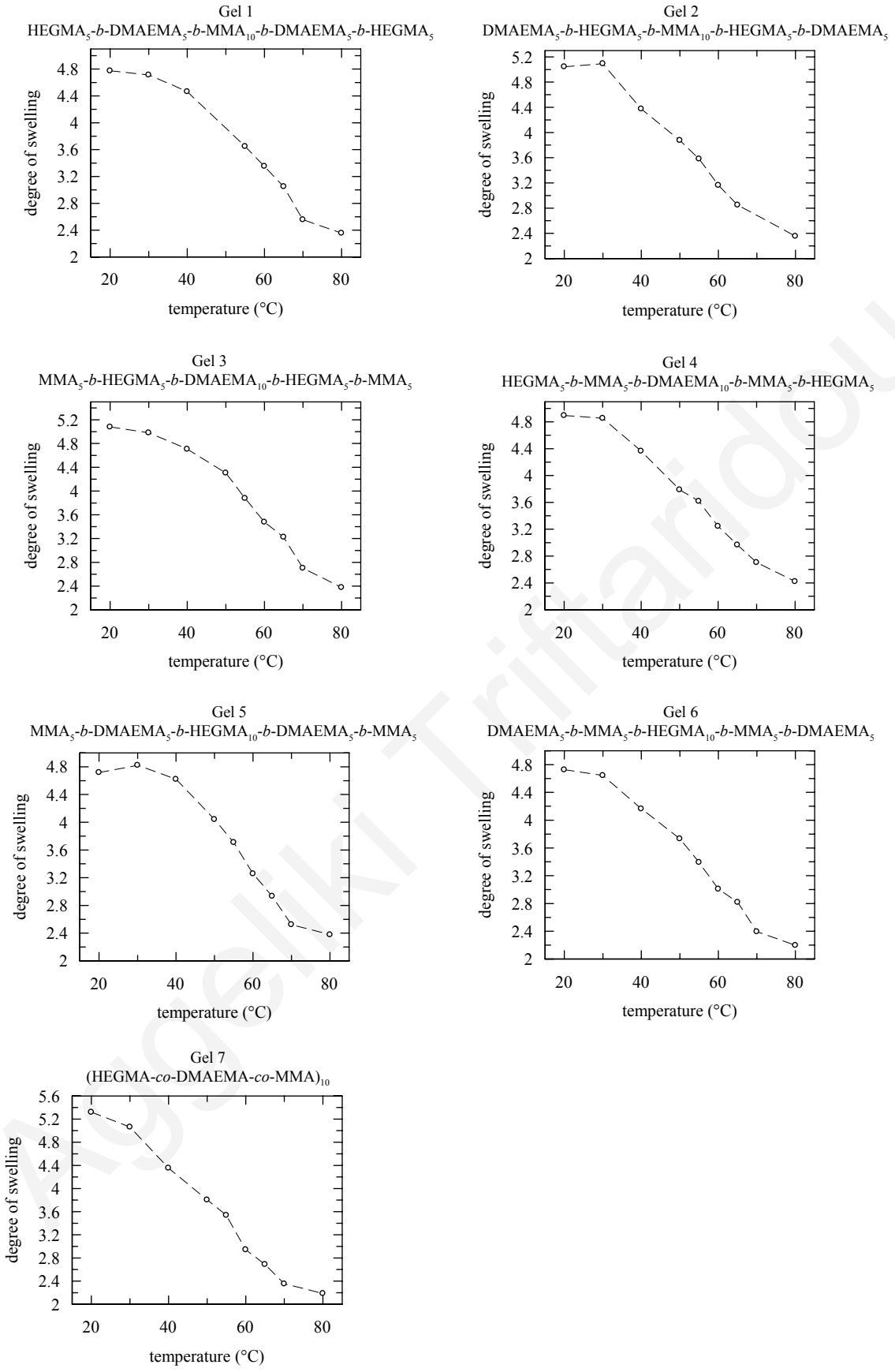

Figure 5.21. Temperature dependence of the degrees of swelling of the networks in neutral water.

The lower cloud points of the networks compared to those of the star terpolymers could be possibly due to the higher content of the networks in hydrophobic cross-linker. In particular, a molar ratio of 8:1 cross-linker to initiator was employed for the network preparation instead of 4:1 employed for the star synthesis. Furthermore, the networks were based on pentablock rather than on triblock terpolymers, thus approaching a less segmented (more random) structure, associated with lower cloud points. The differences in the cloud points could also be due to the slow polymer diffusion / relaxation phenomena within the networks, which are dense systems compared to the linear and star solutions which are dilute systems.

5.4.7. Conclusions

Group transfer polymerization was successfully employed for the preparation of several equimolar model networks based on three different monomer repeating units placed symmetrically in five blocks. All six possible block sequence isomers were prepared, plus the statistical terpolymer network. The randomly cross-linked statistical terpolymer network was also synthesized. The following three functional monomer repeating units were employed: one hydrophobic (MMA), one hydrophilic (HEGMA) and one pH- and temperature-responsive (DMAEMA), conferring to the networks a rich swelling behavior. Thus, in water, the pentablock networks were always microphase separated and presented a pH-dependent swelling behavior without completely collapsing in their neutral state. The isomeric networks presented similar swelling behavior under most conditions, with the notable exception of the statistical terpolymer model network which exhibited a higher degree of swelling, manifesting its inability to microphase separate in water.

5.5. Equimolar ABCBA Pentablock Terpolymer Networks of HEGMA, DMAEMA and BuMA: Effect of Block Sequence

5.5.1. Summary

Eight isomeric amphiphilic networks based on cross-linked equimolar terpolymers composed of 10 monomer repeating units of each of HEGMA, BuMA and DMAEMA were prepared by GTP. Seven of the networks were model networks, i.e. they had linear segments between the cross-links of exact degrees of polymerization, composition and structure. One of the seven model networks was based on the statistical terpolymer, whereas the remaining six were based on the six possible isomeric equimolar pentablock terpolymers ABCBA, BACAB, ACBCA, CABAC, BCACB and CBABC. The eighth network was a randomly cross-linked network based on the equimolar statistical terpolymer, since the cross-linker and the three monomers were polymerized simultaneously. The network linear precursors were characterized in terms of their molecular weight (MW) and composition using GPC and ^{1}H NMR, respectively. It was confirmed that they had the theoretically expected MW and composition. The degrees of swelling (DSs) of all the networks were measured in tetrahydrofuran (THF), in neutral water and in aqueous solutions covering the pH range between 2 to 12. It was found that the DSs were highest in acidic pH due to the repulsive forces and the osmotic pressure developed by the ionization of the DMAEMA units. Intermediate values of the DSs were observed in THF, whereas the lowest DSs were measured in neutral water. The monomer distribution along the terpolymer chain was also found to affect the DSs. The highest DS was observed for the statistical terpolymer-based model network in acidic water. Finally, the pH-dependence of the adsorption of the drug paracetamol and Herring's sperm DNA onto two of the model networks was studied. Paracetamol was found to be adsorbed at low pH attributed to hydrogen bonding interactions with the network, while Herring's sperm DNA was adsorbed via electrostatic interactions.

5.5.2. Introduction

The equimolar block sequence isomeric terpolymer networks based on HEGMA, DMAEMA and MMA presented in the previous Section exhibited similar DSs at low pH, independent of the block sequence. In an efford to differentiate the swelling behavior of the various network isomers, in this Section we prepared and studied

similar networks where the hydrophobic MMA monomer repeating unit was substituted by the more hydrophobic BuMA. Furthermore, in the present terpolymer networks the determination of the BuMA content by ^{1}H NMR would be much more accurate than that of MMA in the previous Sections. The alkyl group in the BuMA units presents four different peaks in ^{1}H NMR, which do not overlap with the HEGMA peaks, as was the case with MMA.

5.5.3. Network Synthesis

All the networks of this study were prepared by GTP. The number of moles of the cross-linker used for network synthesis was eight times the number of moles of the MTSMC initiator to optimize interchain connection and network formation according to a previous study.[124] These networks were equimolar in the three monomers, and isomeric, with different monomer/cross-linker distributions afforded by varying the order of monomer addition. The synthetic routes followed for the preparation of the eight different isomeric networks were those presented in Figure 5.16 with the difference that BuMA instead of MMA was used.

5.5.4. Polymerization Methodology

The synthetic procedure for the preparation of the model networks was similar to that illustrated schematically in Figure 5.17 in the previous Section. The structures of the eight networks obtained were the same as those presented in Figure 5.18, also of the previous Section. In particular, six of the model networks comprised elastic chains of all the possible block sequences, while in the seventh model network the monomers were randomly distributed along the terpolymer chains. For the preparation of the eighth network all the monomers and the cross-linker were silmutaneously quaterpolymerized, resulting in a less perfect structure.

5.5.5. Characterization of the Linear Precursors

5.5.5.1. Molecular Weight Analysis

The linear homopolymer, the triblock copolymer and the pentablock terpolymer precursors to the networks were characterized in terms of their molecular weights and molecular weight distributions by GPC in THF, which are listed in Table 5.10 and are compared with the theoretically expected molecular weights. The degrees of

polymerization are denoted by the subscripts in the polymer formula. The number average molecular weights, M_ns, were slightly, but systematically higher than the

Table 5.10. Molecular weights and compositions of the linear precursors to the networks.

No.	Polymer Formula[a]	Theor. Molec. Weight[b]	GPC Results[c]		% mol Bu-D-H by ^{1}H NMR[d]	Effect. p*K*
			M_n	M_w/M_n		
1	H_{10}	3 700	5 500	1.08		5.1
	D_5-*b*-H_{10}-*b*-D_5	5 270	5 560	1.08		
	Bu_5-*b*-D_5-*b*-H_{10}-*b*-D_5-*b*-Bu_5	6 690	7 520	1.10	35-23-42	
2	H_{10}	3 700	5 210	1.08		4.9
	Bu_5-*b*-H_{10}-*b*-Bu_5	5 120	6 400	1.08		
	D_5-*b*-Bu_5-*b*-H_{10}-*b*-Bu_5-*b*-D_5	6 690	7 210	1.09	34-31-35	
3	D_{10}	1 770	2 140	1.09		5.1
	H_5-*b*-D_{10}-*b*-H_5	5 270	6 110	1.11		
	Bu_5-*b*-H_5-*b*-D_{10}-*b*-H_5-*b*-Bu_5	6 690	7 130	1.11	33-31-36	
4	D_{10}	1 770	2 130	1.10		4.9
	Bu_5-*b*-D_{10}-*b*-Bu_5	3 190	3 800	1.12		
	H_5-*b*-Bu_5-*b*-D_{10}-*b*-Bu_5-*b*-H_5	6 690	7 810	1.14	35-31-34	
5	Bu_{10}	1 620	2 400	1.10		5.3
	H_5-*b*-Bu_{10}-*b*-H_5	5 120	6 720	1.11		
	D_5-*b*-H_5-*b*-Bu_{10}-*b*-H_5-*b*-D_5	6 690	7 110	1.11	35-31-34	
6	Bu_{10}	1 620	2 530	1.11		4.8
	D_5-*b*-Bu_{10}-*b*-D_5	3 190	4 050	1.12		
	H_5-*b*-D_5-*b*-Bu_{10}-*b*-D_5-*b*-H_5	6 690	7 980	1.16	35-30-35	
7	(H-*co*-D-*co*-Bu)$_{10}$	6 690	9 420	1.12	32-32-36	4.9
8	(D-*co*-Bu-*co*-H)$_{10}$-*co*-E_8	-	-	-	-	4.8

[a] H: HEGMA, D: DMAEMA, B: BuMA, E: EGDMA.

[b] The contribution from the initiator fragment of 196 g mol^{-1} was also included.

[c] From a calibration based on linear PMMA standards of narrow MWDs.

[d] The theoretical % mol Bu-D-H composition was 33.3-33.3-33.3 for all the terpolymer precursors to the networks.

theoretically predicted MWs, probably due to partial deactivation of the initiator and/or due to differences between the hydrodynamic volumes of the model PMMAs used for molecular weight calibration and the analyzed polymers. The molecular weight distributions (MWDs) were found to be narrow and the polydispersity indices (PDIs, M_w/M_n) were calculated to be lower than 1.2 in all cases. This confirms the

homogeneity of the lengths of the segments between the cross-links (elastic chains) in the networks. No data were available for the randomly cross-linked terpolymer network due to the simultaneous copolymerization of the monomers and the cross-linker, leading to rapid gelation of the solution.

5.5.5.2. Composition Analysis

The compositions of the equimolar linear terpolymer precursors to the networks are also listed in Table 5.10, as determined using ^{1}H NMR. A typical ^{1}H NMR spectrum of a pentablock terpolymer precursor, namely that of DMAEMA$_5$-*b*-BuMA$_5$-*b*-HEGMA$_{10}$-*b*-BuMA$_5$-*b*-DMAEMA$_5$, is illustrated in Figure 5.22.

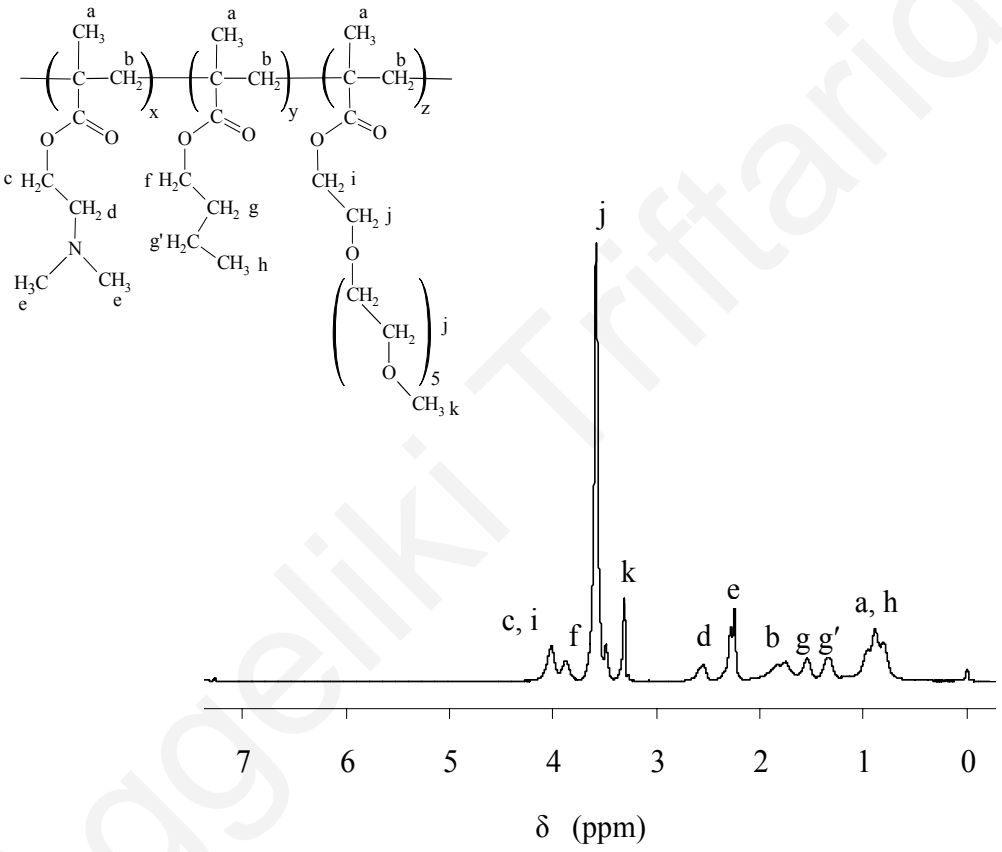

Figure 5.22. ^{1}H NMR spectrum of the DMAEMA$_5$-*b*-BuMA$_5$-*b*-HEGMA$_{10}$-*b*-BuMA$_5$-*b*-DMAEMA$_5$ network precursor. The peaks corresponding to the *d*, *k* and *f* protons were employed for the composition determination.

Unlike the case of the HEGMA-DMAEMA-MMA pentablock terpolymer networks, the composition in the three monomers in the present Section could be readily calculated from three characteristic non-overlapping peaks, one for each type of monomer repeating unit. In particular, the calculation was made using as

characteristic peaks those corresponding to the three methoxy protons in HEGMA at 3.3 ppm (*k*), the two azamethylene protons in DMAEMA at 2.55 ppm (*d*), and the two oxymethylene protons in BuMA at 3.9 ppm (*f*). As shown in Table 5.10 the % mol compositions were close to those theoretically expected (33 % in each monomer) based on the comonomer feed ratios, confirming full monomer-to-polymer conversion during synthesis.

5.5.6. Characterization of the Extractables

The results of the characterization of the extractables are listed in Table 5.11, including their mass percentage, M_ns and PDIs.

Table 5.11. Mass fractions, molecular weights and compositions of the extractables from the networks.

No.	Polymer Formula[a]	% w/w Extractables	GPC Results[b]		% mol Bu-D-H
			M_n	M_w/M_n	
1	Bu_5-*b*-D_5-*b*-H_{10}-*b*-D_5-*b*-Bu_5	8.4	6 310	1.11	18-23-60
2	D_5-*b*-Bu_5-*b*-H_{10}-*b*-Bu_5-*b*-D_5	18.0	5 770	1.13	26-16-58
3	Bu_5-*b*-H_5-*b*-D_{10}-*b*-H_5-*b*-Bu_5	9.3	5 560	1.09	43-39-19
4	H_5-*b*-Bu_5-*b*-D_{10}-*b*-Bu_5-*b*-H_5	11.0	4 880	1.23	36-44-20
5	D_5-*b*-H_5-*b*-Bu_{10}-*b*-H_5-*b*-D_5	11.2	5 690	1.09	56-10-34
6	H_5-*b*-D_5-*b*-Bu_{10}-*b*-D_5-*b*-H_5	14.7	5 170	1.23	31-37-19
7	(H-*co*-D-*co*-Bu)$_{10}$	7.7	7 210	1.10	31-34-35
8	(H-*co*-D-*co*-Bu)$_{10}$-*co*-E_8	7.1	12 660	1.06	51-31-19

[a] H: HEGMA, D: DMAEMA, B: BuMA, E: EGDMA.

[b] From a calibration based on linear PMMA standards of narrow MWDs.

The percentage of the extractables (sol fraction) was found to be relatively low, equal to or lower than 18%, confirming the well-defined structure of the networks and indicating that the choice of 8:1 cross-liker to initiator molar ratio was appropriate for sufficient incorporation of the linear chains into the networks.

The M_ns of the extractables, also listed in Table 5.11, were lower than those of the corresponding linear precursors. This was as expected because the extractables

contained early-terminated polymers (homopolymers and ABA triblock copolymers) in addition to "living" ABCBA pentablocks which could not approach the cross-link due to steric hindrances. The PDIs of the extractables are also shown in Table 5.11. In most cases, these were higher than the PDIs of the corresponding linear terpolymer precursors listed in Table 5.10. This was in accord with the expectation for increased size heterogeneity of the extractables, and in qualitative agreement with a Poisson distribution,[16(b)] dictating higher PDIs for polymers with lower M_ns, as was the case with the extractables.

It is noteworthy that the composition of the extractables was enriched in the monomer which was added first (monomer in central block) compared to the corresponding linear pentablock terpolymer precursors. This was in agreement with the fact that chain-breaking reactions took place for the whole duration of synthesis. This would influence more the central block, prepared first, resulting in exctractables richer in this block. This was more obvious in the cases where the HEGMA monomer was added first, since this was the only monomer not purified by distillation, probably introducing to the reaction small but finite amounts of moisture and other impurities, leading to the deactivation of some of the polymer chain "living" ends.

5.5.7. Characterization of the Networks

5.5.7.1. Aqueous Degrees of Swelling and Degrees of Ionization

The experimentally measured DSs and degrees of ionization of all the networks are plotted against pH in Figure 5.23. The theoretical chemical formula of the linear terpolymer precursor to each network is indicated above each plot. A general feature of these plots is that each DS versus pH curve followed the corresponding degree of ionization versus pH curve, confirming the importance of charge on network swelling. The networks began to swell at pH < 7 due to the ionization of the DMAEMA monomer repeating unit, a tertiary amine being ionized in that pH range.

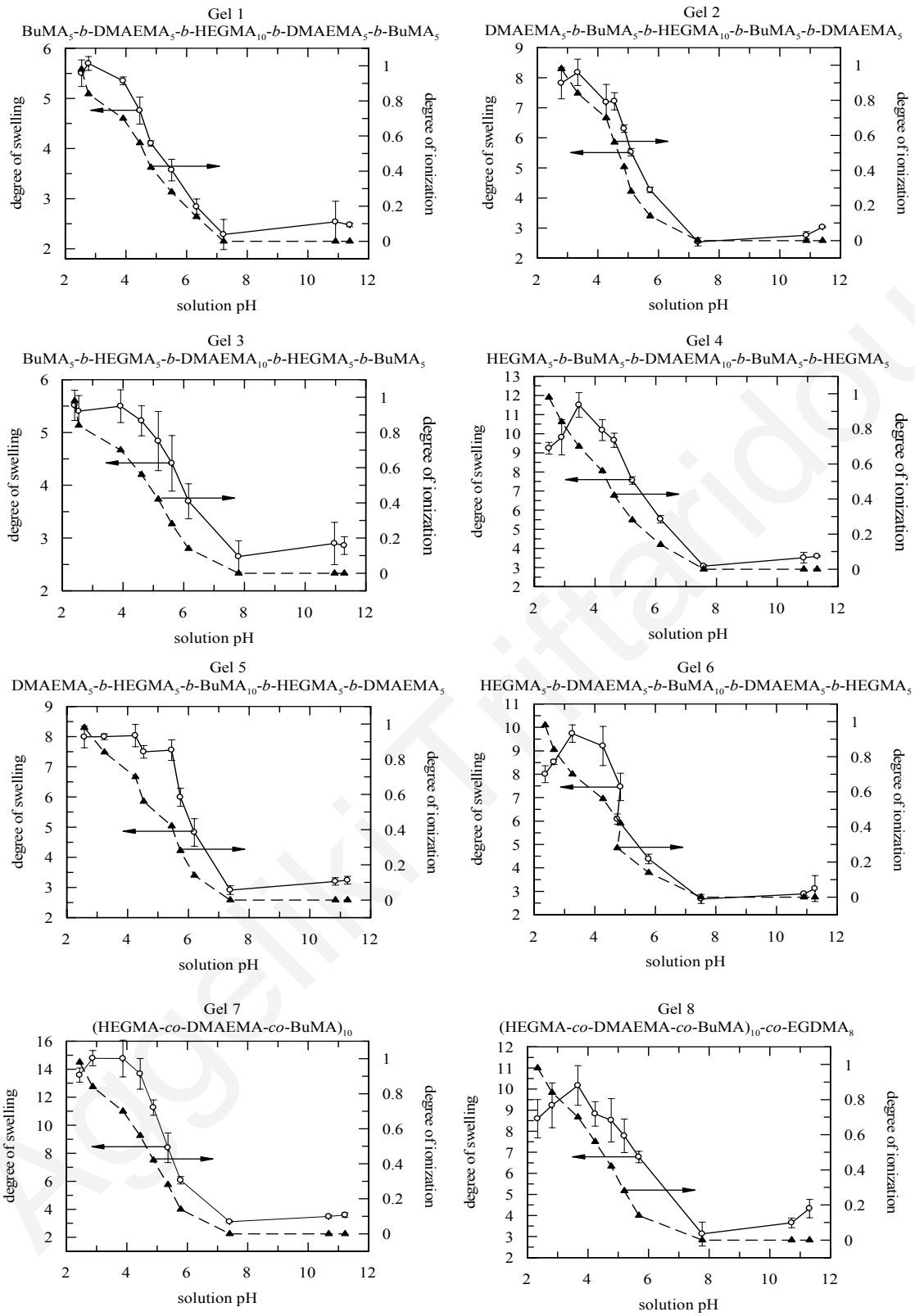

Figure 5.23. Degrees of swelling and degrees of ionization as a function of pH for all the terpolymer networks of this Section.

This ionization, in turn, induced electrostatic repulsions between the positively charged DMAEMA units and the build-up of an osmotic pressure created by the chloride counterions to the charged DMAEMA units.[123] The curves of the DSs presented a maximum at pH ~ 4-5, followed by a slight decrease at lower pH values (pH ~ 2), probably due to the increase in ionic strength effected by the relatively high concentration of HCl under these conditions. At high pH values, the networks exhibited low DSs, ranging from 2 to 3, indicating that the networks were rather contracted due to the presence of the BuMA hydrophobic blocks, but not fully collapsed due to the presence of the hydrophilic DMAEMA and HEGMA monomer repeating units.

5.5.7.2. Degrees of Swelling in Neutral Water and in THF

The DSs in neutral water (pH ~ 8) and in acidified water (pH ~ 3.5) were extracted from Figure 5.23 for all the networks and are plotted in Figure 5.24 along with the corresponding DSs in THF (neutral networks). THF was a non-selective solvent in which all networks swelled to a good extent having similar DSs, with the exception of the randomly cross-linked network which exhibited a lower DS. This was due to the random distribution of the cross-linker in this network, resulting in a broad distribution of the lengths of the elastic chains, with the shorter chains restricting the swelling of this network in THF. The DSs in THF of the seven model networks were all around 6. Similar DSs were observed for the MMA-containing terpolymer networks in THF, presented in the previous Section, having the same overall degree of polymerization and molar composition.

The DSs in neutral water were lower than those in THF, as expected. In contrast to THF, water is a selective solvent for the hydrophilic HEGMA and DMAEMA units and a non-solvent for the hydrophobic BuMA units. Consequently, the DSs of the networks in neutral water were lower than in THF due to the collapse of the BuMA units in water. It should be noted that the DMAEMA units were uncharged both in THF and in water. The DSs in neutral water exhibited by the networks studied in the present Section were lower (2-3) than those obtained for the HEGMA-DMAEMA-MMA terpolymer networks presented in the previous Section (~4). This was probably due to the higher hydrophobicity of the BuMA monomer repeating units compared to the MMA monomer repeating units present in the networks of Section

5.4 and to the glassy nature of the PMMA blocks, conferring to the chains limited flexibility, and hence slow response to changes in the solvent conditions, in contrast to the soft PBuMA blocks.

5.5.7.3. Block Sequence Effect on the Degrees of Swelling in Acidic Water

The DSs of all the terpolymer networks in neutral water, in THF and in acidic water were collected and plotted in Figure 5.24.

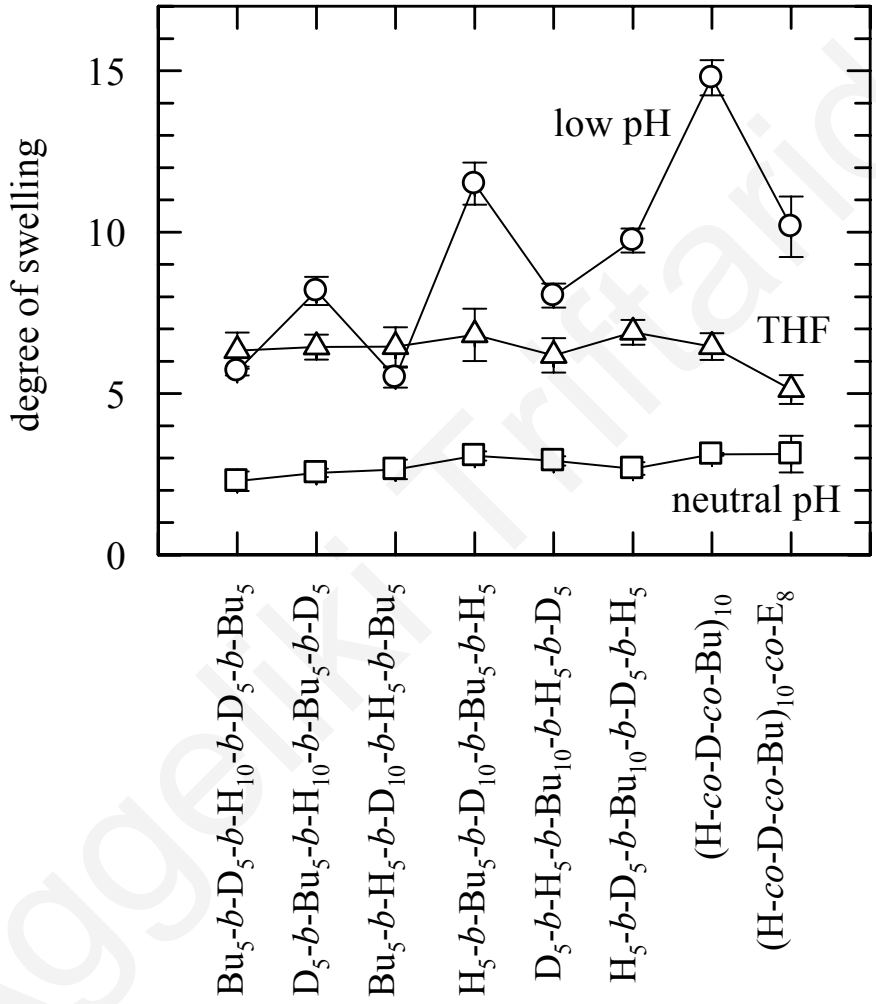

Figure 5.24. Degrees of swelling in THF, in neutral water and in acidified water of the various isomeric HEGMA-DMAEMA-BuMA terpolymer networks studied in this Section.

Unlike in neutral water and in THF, the DSs of the networks in acidic water varied with the network structure, with the model network based on the statistical terpolymer (HEGMA-*co*-DMAEMA-*co*-BuMA)$_{10}$ displaying the highest acidic DS. This was

attributed to the random distribution of hydrophobic monomer repeating units along the terpolymer chain which precluded microphase separation. On the other extreme, the networks composed of $BuMA_5$-*b*-$DMAEMA_5$-*b*-$HEGMA_{10}$-*b*-$DMAEMA_5$-*b*-$BuMA_5$ and $BuMA_5$-*b*-$HEGMA_5$-*b*-$DMAEMA_{10}$-*b*-$HEGMA_5$-*b*-$BuMA_5$ pentablock terpolymer elastic chains, both having BuMA end-blocks, exhibited the lowest DSs. This could be due to the proximity of the BuMA units to the hydrophobic EGDMA cores of the networks, locally increasing the hydrophobic content, and facilitating microphase separation which, in turn, further reduced the effective lengths of the elastic chains, resulting in the lowest acidic DSs. The other four model networks, with the BuMA units either in blocks two and four or in the middle block presented acidic DSs which were intermediate between those of the model network with statistical terpolymer elastic chains and the two model networks with elastic chains with BuMA end-blocks. Thus, microphase separation in these four networks was less complete than that in the two networks with elastic chains with BuMA end-blocks, as expected.

The acidic DS of the randomly cross-linked network based on the statistical terpolymer, (HEGMA-*co*-DMAEMA-*co*-$BuMA)_{10}$-*co*-$EGDMA_8$, was lower than that observed for the model network based on the statistical terpolymer, reflecting the less perfect structure of the former network as discussed above (the presence of shorter chains as well could restrict the swelling). This explanation was in agreement with the fact that this network had also a lower DS in THF than the other networks. The presence of the many different chain lengths between the cross-links in the case of the randomly cross-linked statistical network could explain the various swelling behaviors presented by this type of networks in earlier studies reported by our research group on DMAEMA-MMA[5] and HEGMA-DMAEMA[125] based systems.

5.5.7.4. Effective pKs of the Networks

The p*K*s of the DMAEMA monomer repeating units in the networks were read out from the degree of ionization curves as the pH at 50% ionization and are also listed in Table 5.10. All networks were found to have similar p*K*s of the DMAEMA units, which, however, span a range of values from 4.8 to 5.3. The p*K*s of the DMAEMA units in the networks presented in this Section were lower than those obtained for the MMA-containing networks discussed in the previous Section and ranged from 5.2 to

5.8. The lower p*K* values of the DMAEMA units in the BuMA-containing networks could be attributed to the higher hydrophobicity of the BuMA compared to the MMA units, causing a larger reduction of the dielectric constant within the networks, further strengthening the Coulombic interactions, making more difficult further ionization of the DMAEMA units and, therefore, further reducing their effective p*K*.[126]

5.5.8. Adsorption Studies

5.5.8.1. Paracetamol

This section presents the pH-dependence of the adsorption of two biologically relevant molecules onto two different model networks, that based on $BuMA_5$-*b*-$HEGMA_5$-*b*-$DMAEMA_{10}$-*b*-$HEGMA_5$-*b*-$BuMA_5$ and that based on (HEGMA-*co*-DMAEMA-*co*-BuMA)$_{10}$. The two molecules used for the adsorption studies were the drug paracetamol and Herring's sperm DNA. The pH-dependence of paracetamol adsorption results onto the two networks is presented in Figure 5.25. In this Figure, the adsorbed amount of paracetamol divided by the dry mass of the adsorbing network is plotted against pH. The chemical structure of paracetamol (1,4-acetamidophenol) is shown on the right of Figure 5.25. According to the Figure, paracetamol was adsorbed at neutral and acidic pH. At high pH, the adsorption was zero, while at very low pH the adsorption was reduced.

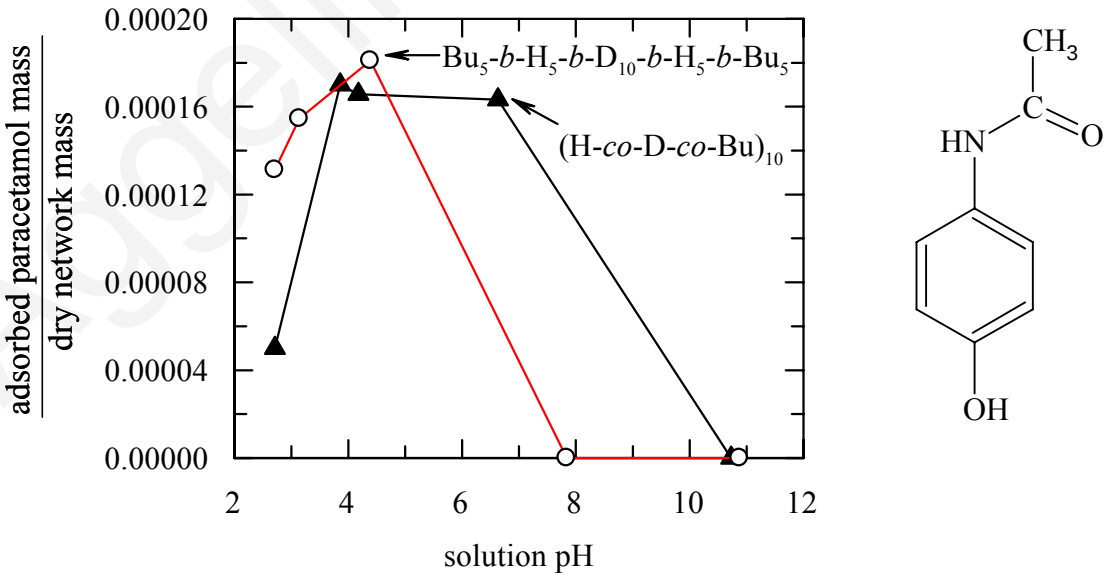

Figure 5.25. Mass of paracetamol adsorbed divided by the network dry mass. The chemical structure of paracetamol is presented on the right.

Given the p*K*s of paracetamol and the DMAEMA units of 10 and ~ 5, respectively, there was no pH where paracetamol and the network had opposite charges (paracetamol was negatively charged above pH 10 and the DMAEMA units were positively charged below pH 5). Thus, paracetamol adsorption could not be due to attractive electrostatic interactions but to other kinds of interactions such as hydrophobic and hydrogen bonding. Hydrogen bonds could be formed between the hydroxyl group of paracetamol and the DMAEMA nitrogen. At high pH (pH > 10), these hydrogen bonds were destroyed due to the dissociation of paracetamol, thus explaining the lack of adsorption in this pH range. The similar adsorption profiles with the two different networks indicated no polymer architecture effect for the present solute.

5.5.8.2. DNA

The pH-dependence of Herring's sperm DNA adsorption onto the two networks is presented in Figure 5.26. In this Figure, the adsorbed amount of DNA divided by the dry mass of the adsorbing network is plotted against the solution pH. As shown, DNA was adsorbed in neutral and acidic pH, while no adsorption took place in alkaline pH. The adsorption of DNA onto the networks could be attributed to the electrostatic attraction between the positively charged DMAEMA units (pH < 7) and the negatively charged DNA (pH > 2).

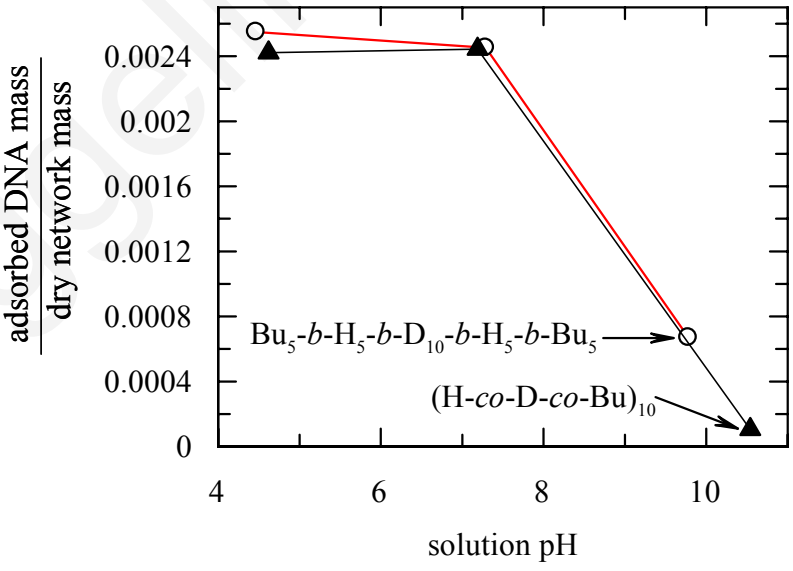

Figure 5.26. Mass of Herring's sperm DNA adsorbed divided by the network dry mass.

The zero adsoprion of DNA at alkaline pH values indicated that other possible attractive interactions (such as hydrophobic) were not strong enough to lead to adsorption. Similar adsoption behavior, dominated by electrostatic interactions has also been observed for the proteins pepsin and albumin adsorbing onto HEGMA-DMAEMA[125] charged networks, for several other proteins adsorbing onto charged methacrylic acid/acrylic acid microgels,[127] and for metal cations adsorbing onto charged acrylic acid gels.[128,129]

Both the pentablock terpolymer and the statistical terpolymer based model networks presented very similar adsoption behavior, indicating again no effect of the monomer distribution on the particular adsorption processes.

The adsorbed quantity of DNA was more than ten times higher than that of paracetamol. This can be attributed to the greater strength of the attractive electrostatic interactions (acting in the case of DNA adsorption) than the hydrogen bonding interactions (paracetamol adsorption).

5.5.9. Conclusions

In this Section, GTP was employed for the preparation of eight equimolar networks of HEGMA, DMAEMA and BuMA. Seven of those were model networks, six of which were the symmetrical block sequence isomers, while the seventh was the statistical terpolymer-based model network. The eighth network was produced by the simultaneous quaterpolymerization of the three monomers and the cross-linker, resulting in a less perfect structure with a broad distribution in the lengths of the chains between the cross-links. The linear precursors to the model networks were characterized in terms of their molecular weights and molecular weight distributions. Furthermore, their composition in the three monomer repeating units was calculated and was found to be in agreement with the theoretically expected values.

The extractabes from all the networks were isolated and characterized using the same methods as for the linear network precursors. The percentage of the extractables (sol fraction) was found to be relatively low, their molecular weight was lower than that of the corresponding linear terpolymer precursor and their composition was richer in the component of the first addition.

The swelling behavior of the networks was studied in THF, in neutral water and in acidic water. The DSs were found to be affected by the solvent and the network structure. Regarding the effect of solvent, the lowest DSs were obtained in neutral water which is a selective solvent, intermediate DSs were observed in THF which is a non-selective solvent, and the highest DSs were measured in acidic water which is also a selective solvent but it induces the complete ionization of the DMAEMA units. Regarding the effect of network structure the highest DSs were exhibited by the statistical terpolymer based model network at low pH, attributed to its inability to microphase separate. On the other hand, the lowest acidic DSs were displayed by the model networks comprising pentablock terpolymer elastic chains with BuMA end-blocks, which are presumably the most effective in terms of microphase separation.

Finally, a biotechnological application of the networks was explored. In particular, the ability of two model networks to adsorb biologically important molecules, namely, the drug paracetamol and DNA, was studied. Although the networks were found to adsorb both solutes at neutral and acidic pH, the adsorption mechanisms were different. In particular, the adsorption of DNA was driven by electrostatic interactions, leading to the adsorption of a relatively large amount of material, while the adsorption of paracetamol was probably due to the weaker hydrogen bonding, affecting the adsorption of much less material.

5.6. ABCBA Pentablock Terpolymer Networks of HEGMA, DMAEMA and BuMA: Effect of Hydrophobic Content

5.6.1. Summary

Group transfer polymerization (GTP) was employed for the preparation of seven amphiphilic terpolymer networks comprising the hydrophilic, pH-sensitive DMAEMA, the neutral hydrophilic HEGMA and the hydrophobic BuMA. MTSMC was used as the bifunctional GTP initiator, while EGDMA served as the cross-linker to interconnect the linear terpolymer precursors to the three-dimensional terpolymer network structures. Six of the terpolymer networks were model, i.e. their elastic chains had well defined molecular weights. Five of the six model networks were based on ABCBA pentablock terpolymers with degree of polymerization (DP) 10 for the HEGMA middle-blocks and the DMAEMA end-blocks, while the length of the BuMA blocks varied. The overall DPs were 25, 30, 40, 50 and 60. The sixth terpolymer model network was based on the equimolar statistical terpolymer with a total DP of 30. The seventh network was also equimolar in the three monomer repeating units with an overall DP of 30, but was not model since the cross-linker and the three monomers were simultaneously quaterpolymerized. The molecular weights (MWs) and the molecular weight distributions (MWDs) of the linear pentablock terpolymer precursors, as well as those of their homopolymer and ABA triblock copolymer precursors, were characterized by gel permeation chromatography (GPC) in tetrahydrofuran, whereas their compositions were determined by proton nuclear magnetic resonance (^{1}H NMR) spectroscopy and were close to the theroretically calculated. The sol fraction of each network was also measured and found to be relatively low. All of the terpolymer networks were characterized in terms of their swelling properties in three different solvents: neutral water, THF and acidic water. The DSs of the networks were found to depend on the solvency, the composition and the architecture. In particular, the DSs of the networks in aqueous environment (neutral water and acidic water) decreased upon increasing the content in the BuMA units. The DSs displayed in acidic water were higher than those obtained in neutral water due to the ionization of the DMAEMA tertiary amine units. In contrast, the DSs in THF (non-selective solvent) were found to increase upon increasing the hydrophobic content of the networks due to the accompanying increase in the lengths of the elastic chains. The statistical terpolymer based model network exhibited a

higher DS at low pH than the equimolar pentablock terpolymer model network due to the random distribution of the hydrophobic units along the terpolymer chain precluding microphase separation.

5.6.2. Introduction

In the previous two Sections, the synthesis and characterization of terpolymer networks was described. Those networks were equimolar isomers differing, mainly, in terms of the block sequence. Indeed, the presence of three components in these networks resulted in six possible block sequence isomers of the pentablock terpolymer elastic chains. In the present Section, we do not study the effect of block sequence but that of another important variable, terpolymer composition. In particular, we prepared and characterized model networks based on pentablock terpolymers containing different compositions in the BuMA monomer repeating units which were always placed in the second and fourth blocks.

5.6.3. Polymerization Methodology

The synthetic procedure followed for the preparation of the equimolar model network ($DMAEMA_5$-*b*-$BuMA_5$-*b*-$HEGMA_{10}$-*b*-$BuMA_5$-*b*-$DMAEMA_5$ pentablock terpolymer) was similar to that illustrated in Figure 5.17. In particular, the synthesis involved sequential monomer and cross-linker additions. The first step resulted in the formation of linear HEGMA homopolymer, active at both ends, followed by the addition of the second monomer which was placed symmetrically at both active ends of the chain. Addition of the third monomer resulted in the formation of the pentablock terpolymer chains having both of their ends active. The cross-linker was added last, effecting the interconnection of the linear chains at both of their ends, forming the three-dimensional network. For the preparation of the model network based on statistical terpolymer elastic chains, the three monomers were added simultaneously and the cross-linker was added last. The synthesis of the randomly cross-linked network of the statistical terpolymer involved simultaneous quaterpolymerization of the three monomers and the cross-linker.

The terpolymer networks discussed in the present Section had the same block sequence but different compositions in the three monomers. In particular, the hydrophobic content and the lengths of the elastic chains varied. The equimolar

statistical terpolymer based network and the randomly cross-linked statistical network were also prepared. The synthetic routes followed for the preparation of all the networks of this family are shown in Figure 5.27, where the various DPs are indicated.

Schematic representations of the linear elastic chains of all the networks along with their theoretical terpolymer formulas are displayed in Figure 5.28. The color coding used is the same as that employed earlier, that is, white for the HEGMA units, gray for the DMAEMA units and black for the hydrophobic BuMA units. With the degrees of polymerization of the HEGMA and DMAEMA blocks held constant in the five terpolymers displayed vertically in Figure 5.28, as the BuMA content increases the overall terpolymer degree of polymerization increases too. The three terpolymers listed in the same row have the same composition (equimolar) and chain lengths, but different architectures. From left to right, schematic representations of elastic chains corresponding to the statistical terpolymer, the pentablock terpolymer and the randomly cross-linked statistical terpolymer are illustrated.

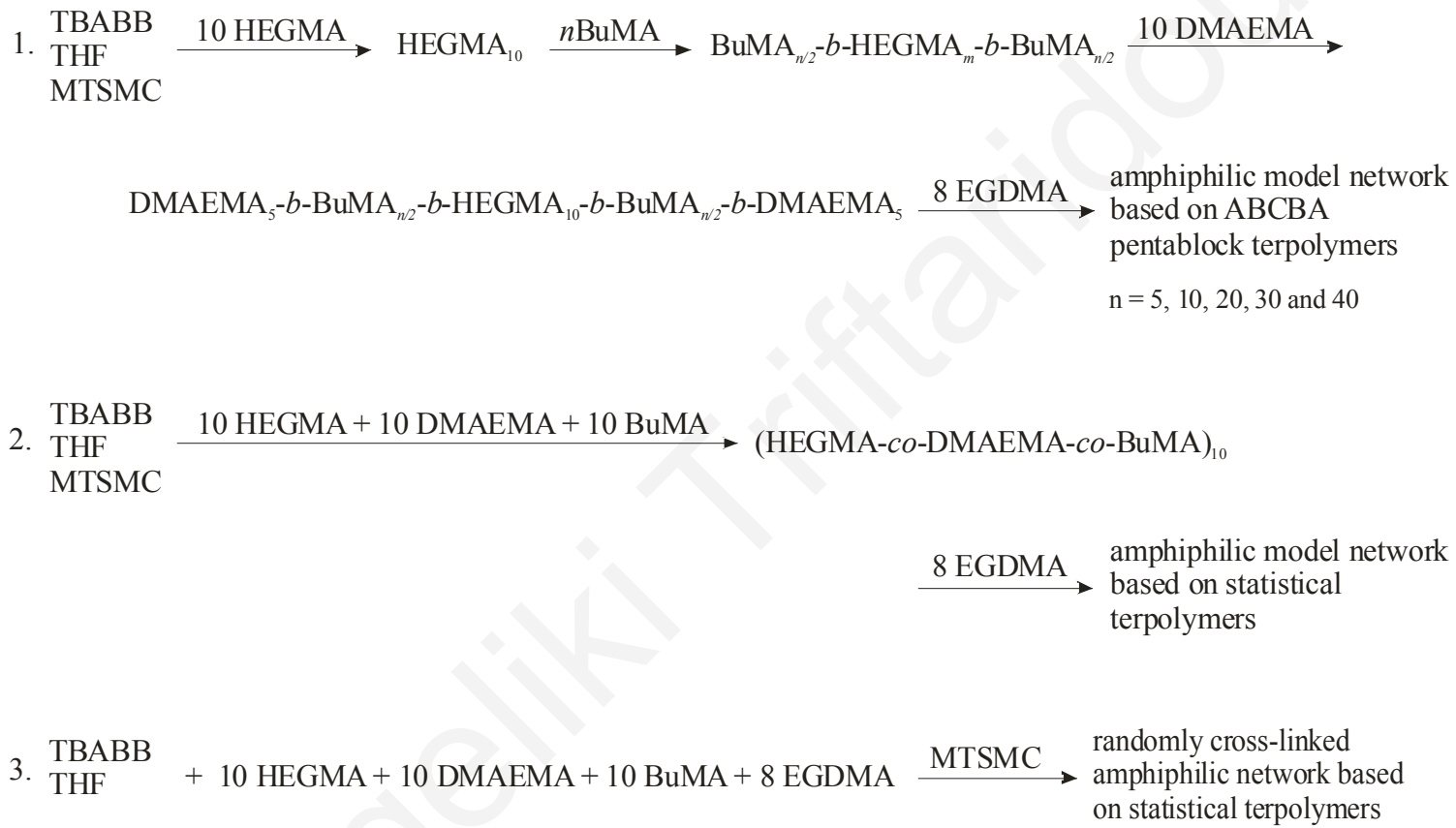

Figure 5.27. Synthetic routes followed for the preparation of the seven terpolymer networks of this Section.

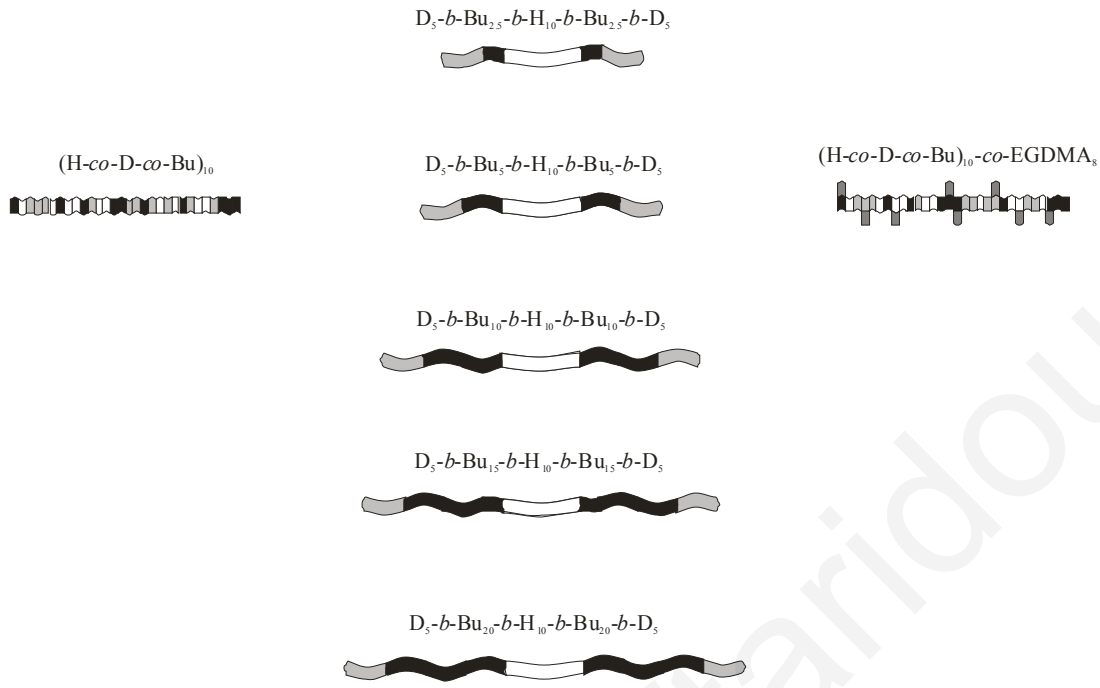

Figure 5.28. Schematic representations of the elastic chains of the terpolymer networks prepared and studied in the present Section. HEGMA units are illustrated in white, DMAEMA units in gray and BuMA units in black.

5.6.4. Characterization of the Linear Precursors

5.6.4.1. Molecular Weight Analysis

The MWs and MWDs of the homopolymer, ABA triblock copolymer and pentablock terpolymer precursors to the networks were determined by GPC in THF and are given in Table 5.12. The polymer formula of each terpolymer is listed in the second column of the Table, with the subscripts indicating the DPs.

According to the data listed in Table 5.12, the MWs were almost twice the theoretically expected, attributed to partial initiator deactivation and to differences in the hydrodynamic volumes of the present samples with the PMMA MW calibration standards. The PDIs were in almost all cases lower than 1.2, indicating the size homogeneity of the chains.

Table 5.12. Molecular weights and compositions of the linear precursors to the networks and the p*K*s of the DMAEMA units in the networks.

No.	Polymer Formula[a]	Theor. MW[b]	GPC Results		Composition % mol (H-Bu-D)		p*K*
			M_n	M_w/M_n	Theor.	^{1}H NMR	
1	H_{10}	3 700	5 440	1.08			4.8
	$Bu_{2.5}$-*b*-H_{10}-*b*-$Bu_{2.5}$	4 420	6 100	1.09			
	D_5-*b*-$Bu_{2.5}$-*b*-H_{10}-*b*-$Bu_{2.5}$-*b*-D_5	5 990	7 370	1.12	40-40-20	37.5-37.5-25	
2	H_{10}	3 700	5 910	1.08			4.2
	Bu_5-*b*-H_{10}-*b*-Bu_5	5 140	7 410	1.11			
	D_5-*b*-Bu_5-*b*-H_{10}-*b*-Bu_5-*b*-D_5	6 710	8 770	1.15	33.3-33.3-33.3	32.3-35.2-32.5	
3	(D-*co*-Bu-*co*-H)$_{10}$	6 710	9 660	1.13	33.3-33.3-33.3	36.7-32.4-30.9	4.6
4	(D-*co*-Bu-*co*-H)$_{10}$-*co*-E_8	-------	N/A	N/A	33.3-33.3-33.3	N/A	4.1
5	H_{10}	3 700	5 730	1.09			4.3
	Bu_{10}-*b*-H_{10}-*b*-Bu_5	6 580	9 750	1.16			
	D_5-*b*-Bu_{10}-*b*-H_{10}-*b*-Bu_{10}-*b*-D_5	8 150	11 750	1.21	25-50-25	26.9-47.3-25.8	
6	H_{10}	3 700	6 030	1.08			4.2
	Bu_{15}-*b*-H_{10}-*b*-Bu_{15}	5 860	14 100	1.25			
	D_5-*b*-Bu_{15}-*b*-H_{10}-*b*-Bu_{15}-*b*-D_5	7 430	17 750	1.28	20-60-20	23.0-59.5-17.5	
7	H_{10}	3 700	5 140	1.10			4.2
	Bu_{20}-*b*-H_{10}-*b*-Bu_{20}	9 460	9 940[d]	1.15			
	D_5-*b*-Bu_{20}-*b*-H_{10}-*b*-Bu_{20}-*b*-D_5	11 040	10 540[d]	1.17	16.7-66.6-16.7	13.4-73.5-13.1	

[a] H: HEGMA, Bu: BuMA, D: DMAEMA, E: EGDMA.

[b] The initiator fragment of 196 g mol^{-1} was also included.

[c] N/A: the data was not available due to the simultaneous quaterpolymerization of the three monomers and the cross-linker during the preparation of the randomly cross-linked network based on the statistical terpolymer.

[d] the polymerization was not complete.

5.6.4.2. Composition Analysis

The composition of the linear terpolymer network precursors were determined by ^{1}H NMR in $CDCl_3$. The NMR spectra (not shown) obtained for the linear terpolymer precurors to the networks discussed in the present Section were similar to that illustrated in Figure 5.18 in the previous Section. The only difference was that the area of the peaks corresponding to the BuMA monomer repeating units increased upon increasing the BuMA content in the terpolymers. This was expected since the area of the peaks must be proportional to the number of the corresponding protons. The peaks involved in the composition calculation were the same as those reported in the previous Section: those corresponding to the three methoxy protons in HEGMA at 3.3 ppm, the two azamethylene protons in DMAEMA at 2.55 ppm, and the two oxymethylene protons in BuMA at 3.9 ppm. The theoretically calculated composition based on the amount of the three monomers fed during the synthesis and the experimentally determined composition are listed in the sixth and seventh columns of Table 5.12, respectively, and were close to each other.

5.6.5. Characterization of the Extractables

Further to the characterization of linear precursors, the extractables of the networks were collected and characterized in terms of their mass fraction, molecular weights, polydispersities and compositions. These results are presented in Table 5.13. The theoretical formulas of the elastic terpolymer chains are listed in the second column of the table, where the subscribts denote the degrees of polymerization.

In the third column of the Table, the percentage of the extractables (sol fraction) is listed. The sol fraction was found to be relatively low, ranging from 9-19% and indicating a satisfactory incorporation of the linear chains into the networks. Thus, the molar ratio of 8:1 of cross-linker to initiator[142] employed during synthesis was sufficiently high.

By careful examination of the molecular weights of the extractables listed in Table 5.13, with one exception, the extractables had lower molecular weights than the precursors of the networks. This could be easily explained by recalling that the extractables were early terminated homopolymer, triblock copolymer or pentablock terpolymer chains not incorporated in the network. In the case of the network with the longest elastic chains, D_5-*b*-Bu_{20}-*b*-H_{10}-*b*-Bu_{20}-*b*-D_5, the molecular weight of the extractables was much higher than that of the linear precursor, probably due to the presence of unreacted cross-linker in the extractables leading to the cross-linking of the extractable chains.

Table 5.13. Mass fractions, molecular weights and compositions of the extractables from the terpolymer networks.

No.	Polymer Formula[a]	% w/w extract.	GPC Results[b]		% mol H-Bu-D
			M_n	M_w/M_n	
1	D_5-*b*-$Bu_{2.5}$-*b*-H_{10}-*b*-$Bu_{2.5}$-*b*-D_5	17.0	6 370	1.13	57.9-22.3-19.8
2	D_5-*b*-Bu_5-*b*-H_{10}-*b*-Bu_5-*b*-D_5	12.7	7 440	1.18	51.9-31.6-16.5
3	(D-*co*-Bu-*co*-H)$_{10}$	9.3	8 190	1.24	38.6-30.1-31.3
4	(D-*co*-Bu-*co*-H)$_{10}$-*co*-E_8	19.4	16 790	2.62	32.4-34.6-33.0
5	D_5-*b*-Bu_{10}-*b*-H_{10}-*b*-Bu_{10}-*b*-D_5	15.1	8 770	1.25	32.0-54.9-13.1
6	D_5-*b*-Bu_{15}-*b*-H_{10}-*b*-Bu_{15}-*b*-D_5	17.9	10 313	1.38	31.3-48.0-20.7
7	D_5-*b*-Bu_{20}-*b*-H_{10}-*b*-Bu_{20}-*b*-D_5	14.1	70 350	1.09	N/D[c]

[a] H: HEGMA, Bu: BuMA, D: DMAEMA, E: EGDMA.

[b] From a calibration based on linear PMMA standards of narrow MWDs.

[c] not determined.

Comparing the compositions of the extractables listed in the last column of Table 5.13 with the compositions of the linear precursors given in Table 5.12, it can be concluded that the extractables of the networks were richer in the monomer added first. This was also reported for the extractables of the networks discussed in the previous Section and was attributed to the fact that the content of the first (middle) block was subjected to chain inactivation longer than the other two components.

5.6.6. Characterization of the Networks

5.6.6.1. Aqueous Degrees of Swelling and Degrees of Ionization

The experimentally determined DSs and degrees of ionization of all the networks are plotted against the pH of the supenatant solution in Figure 5.29. The theoretical chemical formula of the elastic chain of each network is shown above each plot. In all cases, the DS curves followed the degree of ionization curves, underlining the importance of ionization on the swelling of these networks.

One of the main observations coming from the plots in Figure 5.29 is that, in general, all the networks exhibited the same aqueous swelling behavior with respect to the solution pH, that

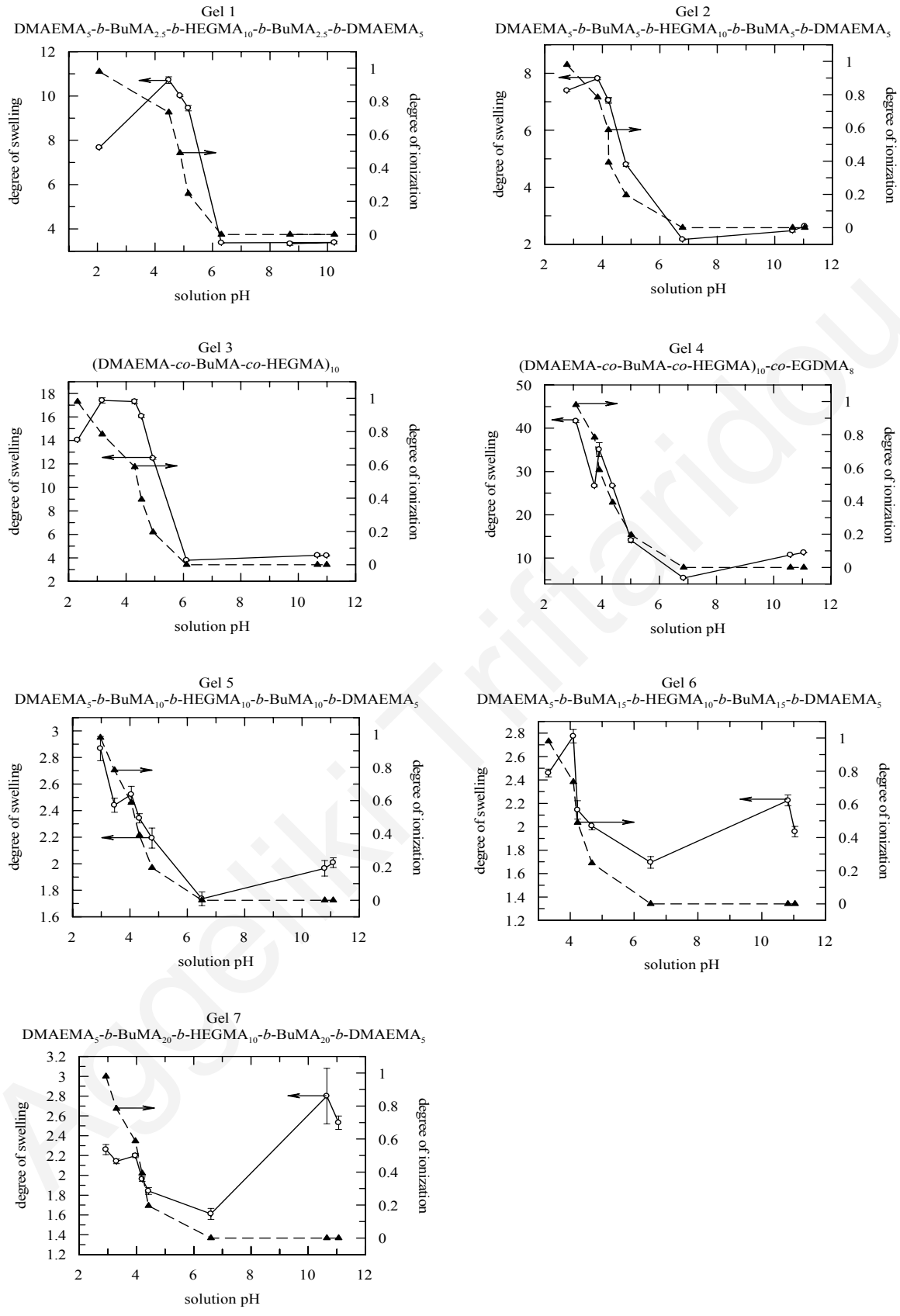

Figure 5.29. Degrees of swelling and degrees of ionization as a function of pH for all the terpolymer networks of this Section.

is, low swelling at high pH values and increased swelling up to a maximum value upon decreasing the pH. The same behavior was reported for triblock copolymer model networks based on linear DMAEMA-MMA[5] and HEGMA-DMAEMA[125] elastic chains and was also in accord with the swelling behavior exhibited by the pentablock terpolymer networks based on the equimolar HEGMA-DMAEMA-MMA and HEGMA-DMAEMA-BuMA elastic chains discussed in Sections 5.4 and 5.5, respectively. The increase in the DSs observed upon decrease of the solution pH was due to the ionization of the DMAEMA units. In particular, DMAEMA is a tertiary amine, positively ionized at pH < 7, inducing electrostatic repulsions between the network elastic chains. Moreover, the swelling of the networks was further enhanced by the build-up of an osmotic pressure created by the presence of the counterions to the charges in the network.[123] At very low pH values (~ 2-3), a decrease in the DSs was observed, attributed to the charge screening due to the high ionic strength imparted by the relatively high HCl concentration under the particular conditions.

5.6.6.2. Effect of Solvency and Network Composition on the Degrees of Swelling

The DSs in neutral water and in acidic water for all the networks were extracted from Figure 5.29 and were plotted in Figure 5.30 against the composition of the networks in the hydrophobic monomer. In the same Figure the DSs in THF were also plotted.

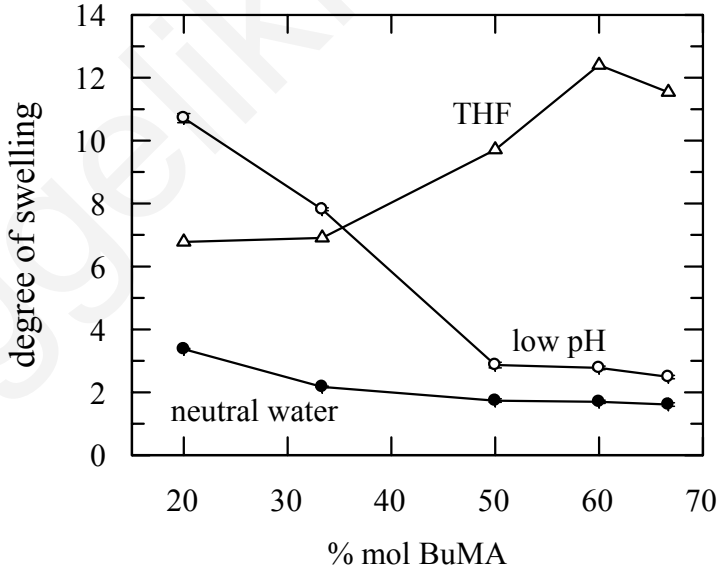

Figure 5.30. Effect of solvency and terpolymer ($DMAEMA_5$-*b*-$BuMA_{n/2}$-*b*-$HEGMA_{10}$-*b*-$BuMA_{n/2}$-*b*-$DMAEMA_5$) composition on the degrees of swelling of the networks.

According to the curves presented in Figure 5.30, the DSs in neutral water and in acidic water decreased as the content in the hydrophobic monomer in the elastic chains increased. In particular, the DSs at low pH decreased from about 11 to 2.5 upon increasing the mol percentage of BuMA from 20 to 67 %. For the same change in the BuMA content, the DSs in neutral water decreased from 3.4 to 1.6. Unlike the decreases observed in the values of the DSs in neutral and in acidic water with increasing the length of the BuMA blocks, the DSs in THF (non-selective solvent) were found to increase with increasing the hydrophobic content. This could be attributed to the increasing lengths of the elastic chains with the length of the hydrophobic BuMA blocks.

Focusing now on the effect of solvency on the swelling of the networks containing 20 and 33 % BuMA, it is observed that their DSs increased in the order neutral water < THF < acidic water as was also the case with the results for the equimolar terpolymer networks discussed in Sections 5.4 and 5.5 and previous studies concerning DMAEMA-MMA networks based on linear triblock copolymer elastic chains.[5] However, for BuMA contents 50 % or higher, the order in the DSs changed, with the highest DS obtained in THF, intermediate in acidic water and the lowest in neutral water. Thus, for the present terpolymer composition range the hydrophobic interactions became dominant, as compared to the previous BuMA-poor composition regime where the repulsive electrostatic interactions dominated.

5.6.6.3. Effect of Network Architecture on the Degrees of Swelling

Figure 5.31 illustrates the effect of network architecture on the DSs in three different solvents. In particular, the Figure depicts the DSs exhibited by the equimolar model networks based on the ABCBA pentablock terpolymer, and the statistical terpolymer, as well as the randomly cross-linked statistical terpolymer network in acidic water, in neutral water, and in THF. The Figure suggests that the DSs of all three networks increased from neutral water to THF and to acidic water. These observations can be explained by the same arguments given in paragraph 5.6.6.2 for the "BuMA-poor" terpolymer networks. The Figure also shows that the randomly cross-linked network of the statistical terpolymer presented the highest DS in all the solvents, probably due to the broad distribution of its elastic chains.

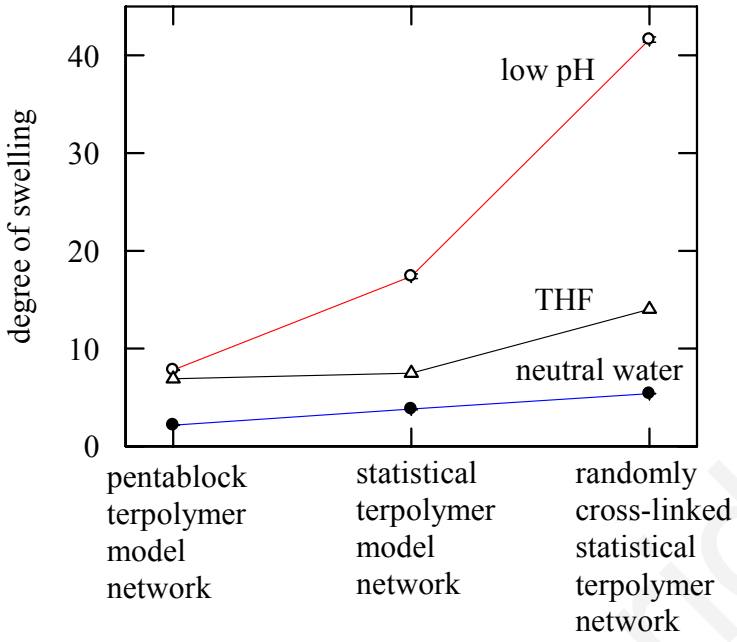

Figure 5.31. Effect of polymer architecture on the degrees of swelling of the terpolymer networks in three different solvents.

The model network based on the statistical terpolymer exhibited intermediate DSs, whereas the network based on the pentablock terpolymer exhibited the lowest DSs. The higher acidic DS of the statistical terpolymer model network than that of the pentablock counterpart can be attributed to the inability of the former model network to microphase separate in water, as discussed in the previous two Sections.

5.6.6.4. Effective pKs of the DMAEMA units in the Networks

The p*K*s of the DMAEMA units in the networks were determined from the degree of ionization curves as the pH at 50 % ionization and are also listed in Table 5.12. The p*K*s of the ranged from 4.1 to 4.8. These values were lower than those obtained for the MMA networks, as well as the equimolar block sequence isomeric BuMA networks discussed in Section 5.5. As discussed earlier, this could be due to the increased hydrophobicity of the networks studied in the present Section, effecting a decrease in the dielectric constant within the networks, leading to stronger Coulombic interactions, making the ionization of the DMAEMA repeating units more difficult,[126] and requiring lower pH values to obtain the desired degrees of ionization.

5.6.7. Conclusions

GTP was employed for the preparation of seven amphiphilic networks based on terpolymer with constant degrees of polymerization of the hydrophilic monomers, but different degrees of polymerization of the hydrophobic monomer. Six of the networks were model networks, having well-defined elastic chains. In five of those, the elastic chains were pentablock terpolymers of the same block sequence but different compositions, while the sixth was based on a statistical terpolymer. The seventh network was the randomly cross-linked statistical terpolymer network. The swelling properties of the networks were found to depend on the solvent (neutral water, THF or acidic water) and the percentage of the hydrophobic monomer repeating units. In particular, the DSs in aqueous environment were found to decrease with increasing the hydrophobic BuMA content, while the DSs in THF (non-selective solvent) increased with increasing the terpolymer hydrophobicity due to the accompanying increase of the lengths of the elastic chains. Furthermore, the DSs of the networks depended on the network structure, with the randomly cross-linked network exhibiting the highest degrees of swelling.

CHAPTER 6: Conclusions and Future Work

Group transfer polymerization was the method employed for the successful synthesis of six families of amphiphilic linear, star and network block terpolymers studied in the present Thesis. In particular, the first family comprised linear equimolar AB and ABC block sequence isomers, while the second family was composed of equimolar block sequence isomeric ABC star triblock terpolymers and their linear counterparts. In the third family, all possible block sequence isomers of equimolar ABC star terpolymers were prepared. The remaining three terpolymer families consisted of networks. Two of these network families comprised elastic chains based on symmetrical ABCBA pentablock terpolymers (all possible block sequences) as well as the statistical terpolymer. The randomly cross-linked networks based on the statistical terpolymers were also prepared. The one of these two families had MMA as the hydrophobic monomer repeating units, whereas the other one had BuMA. The sixth family was composed of networks based on ABCBA pentablock terpolymers of a particular block sequence and various BuMA hydrophobic contents.

Gel permeation chromatography in tetrahydrofuran was employed for the determination of the molecular weights and the molecular weight distributions of all linear and star terpolymers as well as for the linear terpolymer precursors to the networks. Furthermore, the molecular weights and molecular weight distributions of their homopolymer, diblock and triblock precursors were also obtained by the same method. These molecular weights were found in most cases to be higher than the theoretically expected, due to partial initiator deactivation and to differences between the hydrodynamic volumes of the samples prepared and the PMMA standards employed for the GPC calibration.

Proton nuclear magnetic resonance spectroscopy (^{1}H NMR) was used for the composition determination of the linear and star terpolymers as well as for the linear pentablock precurors to the networks. The experimentally determined compositions of the MMA-containing terpolymers were generally not in a good agreement with those theoretically expected. This was attributed to the large errors introduced in the composition calculations. In particular, the MMA monomer repeating units did not present individual characteristic peaks in their ^{1}H NMR spectra. Thus, the calculation

of the MMA content involved the subtraction of the HEGMA contribution from the area of a common MMA-HEGMA peak. The error in this composition calculation was very large because HEGMA contributed 88 % of the area of this peak. On the other hand, the experimentally determined compositions of the BuMA-containing linear pentablock terpolymer precursors to the networks were close to those theoretically expected. In this case, each different monomer repeating unit exhibited at least one separate characteristic ^{1}H NMR peak, from which the terpolymer composition was determined accurately.

The hydrodynamic diameters of the diblock copolymers and all ABC linear and star terpolymers constituting the various terpolymer families were measured in neutral water. Moreover, the hydrodynamic diameters of the seven ABC block sequence and direction isomers prepared the same day (and discussed in Section 5.3) were also determined in THF. The hydrodynamic diameters in THF were approximately the same for all the terpolymers as expected, since THF is a non-selective solvent, hence block sequence did not affect the values of their hydrodynamic diameters. On the other hand, the hydrodynamic diameters measured in water exhibited dependence on block sequence. In particular, in the case of the linear terpolymers, those bearing the hydrophobic block at the end of the terpolymer chain displayed the highest hydrodynamic diameters, due to the formation of AB-diblock copolymer type spherical micelles in water. The hydrodynamic diameters exhibited by the linear terpolymers of the first family in water were higher than the corresponding terpolymers of the second family, because of the higher molecular weight of the former. The lowest hydrodynamic diameters were obtained for the random terpolymers, whereas the terpolymers having hydrophobic middle-blocks displayed intermediate values of hydrodynamic diameters.

The hydrodynamic diameters of the star terpolymers in water were lower than the maximum expected for star terpolymers with fully stretched arms, with the exception of star terpolymers HEGMA$_{10}$-*b*-DMAEMA$_{10}$-*b*-MMA$_{10}$-*star* of both star terpolymer families which displayed higher hydrodynamic diameters.

In addition to the aggregation number of the linear terpolymers in water, the number of arms of the star terpolymers was also determined. In all cases, the number of arms in the star terpolymers was much higher than the aggregation numbers obtained for

the linear terpolymers, attributed to the fact that the arms were covalently connected in the former case but only physically held in the latter.

Furthermore, the cloud points of the linear and star terpolymers were determined. In general the cloud points of the star terpolymers were higher than those of their linear counterparts, attributed to the better colloidal stabilization imparted by the greater number of arms. The cloud points of the linear terpolymers revealed a block sequence dependence, with the random terpolymer exhibiting the lowest cloud point and the $HEGMA_{10}$-*b*-$DMAEMA_{10}$-*b*-MMA_{10} terpolymer displaying the highest cloud point. The cloud points of the star terpolymers displayed the same trend, confirming again the importance of block sequence on the aqueous solution properties.

The ability of the linear and the star terpolymers to act as surfactants was studied by surface tension measurements. All terpolymers were found to reduce the surface tension at the air-water interface. This reduction was stronger with the linear triblocks than with the linear statistical terpolymer or with the stars, consistent with the micellization observed with the linear triblocks.

All the networks were characterized in terms of their swelling behavior in THF, in neutral water and in acidic water. The two network families comprising equimolar terpolymer elastic chains exhibited the same trend: the lowest degrees of swelling were observed in neutral water which is a selective solvent for HEGMA and DMAEMA, intermediate degrees of swelling were measured in THF (non-selective solvent), and the highest degrees of swelling were attained in acidic water. In acidic water the DMAEMA monomer repeating units became fully ionized, leading to the establishment of Coulombic repulsions and the creation of an osmotic pressure, both of which favored extensive swelling of the networks. Under these conditions, the model networks comprising statistical terpolymer elastic chains displayed a higher degree of swelling than all the networks based on equimolar pentablock terpolymers due to its inability to microphase separate. On the other hand, the pentablock terpolymer networks were able to microphase separate, causing a decrease in the effective length of the elastic chains and resulting in lower degrees of swelling. The BuMA-containing networks presented lower degrees of swelling in both acidic and neutral water than the MMA-containing networks due to the more hydrophobic nature of the former monomer. Furthermore, unlike the MMA-containing terpolymer

networks, the BuMA-containing networks displayed a clearer dependence of the degree of swelling in acidic pH on block sequence.

An effort to determine the cloud points of the MMA-containing networks in neutral water was also made. The cloud points were found to range from ~ 46-60 °C, lower than those corresponding to the star terpolymers. This could be possibly due to the fact that the networks contained more cross-linker than the star terpolymers, increasing their overall hydrophobicity. In addition to that, the elastic chains of the networks comprised symmetrical ABCBA pentablock terpolymers, reducing in half the degree of polymerization of blocks A and B compared to their linear and star counterparts (10 monomer repeating units in the middle-block, but only 5 in the other two blocks on each side of the middle-block). Thus, the shorter lengths of the hydrophilic blocks provided a poorer stabilization to the structures. In the case of the linear and the star terpolymers, each block comprised ten monomer units effecting a better stabilization in the aqueous solution and higher cloud points. The above difference in the cloud points may also be due to the dense nature of the networks (highly concentrated system) compared to the dilute character of the solutions of linear and star terpolymers whose cloud points were measured.

In the third terpolymer network family prepared, the overall hydrophobic content of the terpolymer chains ranged from 20 to 67 mol %. The degrees of swelling of these terpolymer networks were also studied in neutral water, in THF and in acidic water. In neutral water, the degrees of swelling were found to slightly decrease upon increasing the percentage of the hydrophobic monomer, as expected. The degrees of swelling of the networks in THF were much higher than those in neutral water, and were found to increase upon increasing the percentage of the hydrophobic monomer in the terpolymers due to the accompanying increase of the lengths of the elastic chains with hydrophobic content.

In this Thesis, the effects of block sequence and terpolymer architecture (linear, star or network) on the solution properties of ABC terpolymers composed of two hydrophilic and one hydrophobic monomer repeating units were investigated. To a smaller extent, the effect of the hydrophobic composition was also studied. A continuation of this work could involve the preparation of ABC terpolymers with higher overall degrees of polymerization, and thus, higher overall molecular weights.

Increasing the terpolymer molecular weight would result in more intense phase separation. The preparation of polymers with higher MWs could be achieved by employing other polymerization methods, such as RAFT known to afford the synthesis of larger polymers. Another parameter that could be varied more systematically is the composition of the terpolymers in the three monomers. Futhermore, the monomer combination could be altered, with two hydrophobic and one hydrophilic monomers being employed for the synthesis instead of two hydrophilic and one hydrophobic used in the present study. This, however, would increase the overall hydrophobicity of the terpolymers, probably leading to water-insoluble terpolymers. In such a case, the solution characterization could take place in organic solvents or in mixtures of organic solvents. It would also be interesting to study the morphologies obtained by such terpolymers in organic solvent-water mixtures and further, their imaging by TEM.

As further synthetic work, ABCD tetrablock quaterpolymers could be prepared. ABCD tetrablock quaterpolymers would lead to the preparation of 24 possible equimolar block sequence and direction (for stars) isomers: ABCD, ABDC, ACDB, ACBD, ADBC, ADCB, BACD, BADC, BCAD, BCDA, BDAC, BDCA, CDAB, CDBA, CABD, CADB, CBAD, CBDA, DABC, DACB, DBAC, DBCA, DCAB and DCBA, plus one statistical quaterpolymer, summing up to 25 polymers. These systems should be studied for the same reason that nobody expected differences in ABC triblock terpolymers compared to AB diblock copolymers, that is the possible formation of complex structures that would be either a continuation of structures formed by three component polymers or completely new structures. For example ABCD tetrablock consisting of two different hydrophobic and two different hydrophilic blocks could exhibit different solution behavior due to slight differences in their solubilities. A more extreme idea could be the preparation of all 120 block sequence and direction isomers of ABCDE quintepolymers.

Other characterization methods could be employed such as AFM that would have enabled the direct imaging of the morphologies obtained by these systems. SANS and SAXS could also be employed and the results obtained by these two methods could be compared to those obtained by dynamic light scattering measurements.

Future work concerning the networks could involve theoretical estimations of the degrees of swelling for various degrees of ionization and compositions and comparison of the resulting values with the experimentally determined ones. Regarding the DSs, it was found from the present Study, that the DSs depended on the network architecture, with the randomly cross-linked statistical terpolymer networks presenting the maximum DSs, hense these kind of networks could be used as superadsorbents (i.e. for baby diapers).

Moreover, further investigation of possible biomedical applications of the block copolymer networks could be performed. In particular, the study could be focused on maximizing the adsorption of these molecules by the networks. The reverse could also be studied. To this end, the networks could be loaded with a drug, and desorption of the drug with time could be studied. In a similar approach, networks bearing MAA moieties could be prepared and studied with respect to metal-ion binding.

CHAPTER 7: References

1. Alexandridis, P.; Hatton, T. A. "Poly(Ethylene Oxide)-Poly(Propylene Oxide)-Poly(Ethylene Oxide) Block Copolymer Surfactants in Aqueous Solutions and at Interfaces: Thermodynamics, Structure, Dynamics, and Modelling," *Colloids Surf.* **1995**, *96*, 1-46.

2. Heise, A.; Hedrick, J. L.; Frank, C. W.; Miller, A. D. "Starlike Block Copolymers with Amphiphilic Arms as Models for Unimolecular Micelles," *J. Am. Chem. Soc.* **1999,** *121*, 8647-8648.

3. Hadjichristidis, N.; Pitsikalis, M.; Pispas, S. Iatrou, H. "Polymers with Complex Architecture by Living Anionic Polymerization," *Chem. Rev.* **2001,** *101*, 3747-3792.

4. Patrickios, C. S.; Georgiou, T. K. "Covalent Amphiphilic Polymer Networks," *Curr. Opin. Colloid & Interface Sci.* **2003,** *8,* 76-85.

5. Triftaridou, A. I.; Hadjiyannakou, S. C.; Vamvakaki, M.; Patrickios, C. S. "Synthesis, Characterization, and Modeling of Cationic Amphiphilic Model Hydrogels: Effects of Polymer Composition and Architecture," *Macromolecules* **2002,** *35,* 2506-2513.

6. Hunter, R. J. *Foundations of Colloid Science*, Volume I, Oxford Science, 1993, Chap. 10, pp. 564-625.

7. Gao, Z.; Eisenberg, A. "A Model of Micellization for Block Copolymers in Solutions," *Macromolecules* **1993,** *26,* 7353-7360.

8. Tanford, C. The Hydrophobic Effect: *Formation of Micelles and Biological Membranes*; 2nd ed. Wiley and Sons Inc.: New York, 1980.

9. Southhall, N. T.; Dill, K. A.; Haymet, A. D. J. "A View of the Hydrophobic Effect," *J. Phys. Chem. B* **2002,** *106,* 521-533.

10. Isrealachvili, J. *Intermolecular and Surface Forces*; 2nd ed. Academic Press: California, 2000, Chap. 8, pp. 128-132.

11. Förster, S.; Zisenis, M.; Wenz, E.; Antonietti, M. "Micellization of Strongly Segregated Block Copolymers," *J. Chem. Phys*., **1996**, 104, 24, 9956-9970.

12. Webster, O. W.; Hertler, W. R.; Sogah, D. Y.; Farnham, W. B.; RajanBabu, T. V. "Group-Transfer Polymerization. 1. A New Concept for Addition Polymerization with Organosilicon Initiators," *J. Am. Chem. Soc.* **1983,** *105,* 5706-5708.

13. Dicker, I. B.; Hertler, W. R.; Ma, S.-H. "ABC Triblock Methacrylate Polymers," US Patent 5.219.945, Jun.15, 1993.

14. Ma, S.-H.; Hertler, W.; Dicker, I. B. "Aqueous Dispersions Containing ABC Triblock Polymer Dispersants," European Patent Application EP0556649, Aug.25, 1993.

15. Webster, O. W. "Living Polymerization Methods," *Science* **1991,** *251,* 887-893.

16. Rempp, P.; Merrill, E. W. *Polymer Synthesis*; 2nd rev. ed., Hüthig & Wepf: Basel, 1991; (a) Chap. 7, pp. 173-175. (b) Chap. 5, pp. 122-126.

17. Webster, O. W. "Group Transfer Polymerization: Mechanism and Comparison with Other Methods for Controlled Polymerization of Acrylic Monomers," *Adv. Polym. Sci.* **2004,** *167,* 1-34.

18. Baskaran, D. "Strategic Developments in Living Anionic Polymerization of Alkyl (Meth)acrylates," *Prog. Polym. Sci.* **2003,** *28,* 521-581.

19. Sogah, D.; Hertler, W. R.; Webster, O. W.; Cohen, G. M. "Group Transfer Polymerization. Polymerization of Acrylic Monomers," *Macromolecules* **1987,** *20,* 1473-1488.

20. Webster, O. W. "The Discovery and Commercialization of Group Transfer Polymerization," *J. Polym. Sci.: Part A: Polym. Chem.* **2000,** *38,* 2855-2860.

21. Hertler, W. R. "Group-Transfer Polymerization: Recent Advances and Applications," Macromol. Symp. **1994,** *88,* 55-69.

22. Eastmond, G. C.; Webster, O. W. *New Methods of Polymer Synthesis*; Chapman and Hall: New York, 1991; Chap. 2, pp. 22-75.

23. Isono, Y.; Tanisugi, H.; Endo, K.; Fujimoto, T.; Hasegawa, H.; Hashimoto, T.; Kawai, H. "Morphological and Mechanical Properties of Multiblock Copolymers," *Macromolecules* **1983,** *16,* 5-10.

24. Hadjichristidis, N.; Pispas, S.; Floudas G. A. *Block Copolymers: Synthetic Strategies, Physical Properties and Applications*; Wiley, Hoboken, NJ, 2003.

25. Zheng, W.; Wang, Z.-G. "Morphology of ABC Triblock Copolymers," *Macromolecules* **1995,** *28,* 7215-7223.

26. Krappe, U.; Stadler, R.; Voigt-Martin, I. "Chiral Assembly in Amorphous ABC Triblock Copolymers. Formation of a Helical Morphology in Polystyrene-*block*-Polybutadiene-*block*-Poly(Methyl Methacrylate)," *Macromolecules* **1995**, *28,* 4558-4561.

27. Stadler, R.; Auschra, C.; Beckmann, J.; Krappe, U.; Voigt-Martin, I.; Leibler, L. "Morphology and Thermodynamics of Symmetric Poly(A-*block*-B-*block*-C) Triblock Copolymers," *Macromolecules* **1995**, *28,* 3080-3097.

28. Hückstädt, H.; Göpfert, A.; Abetz, V. "Influence of the Block Sequence on the Morphological Behavior of ABC Triblock Copolymers," *Polymer* **2000,** *41,* 9089-9094.

29. Ludwigs, S.; Böker, A.; Abetz, V.; Müller, A. H. E.; Krausch, G. "Phase Behavior of Linear Polystyrene-*block*-Poly(2-Vinylpyridine)-*block*-Poly(tert-Butyl Methacrylate) Triblock Terpolymers," *Polymer* **2003,** *44,* 6815-6823.

30. Mogi, Y.; Mori, K.; Matsushita, Y.; Noda, I. "Tricontinuous Morphology of Triblock Copolymers of the ABC Type," *Macromolecules* **1992,** *25,* 5412-5415.

31. Matsushita, Y.; Tamura, M.; Noda, I. "Tricontinuous Double-Diamond Structure Formed by a Styrene-Isoprene-2-Vinylpyridine Triblock Copolymer," *Macromolecules* **1994,** *27,* 3680-3682.

32. Fustin, C. -A.; Abetz, V.; Gohy, J. -F. "Triblock Terpolymer Micelles: A Personal Outlook," *Eur. Phys. J. E* **2005,** *16,* 291-302.

33. Tsitsilianis, C.; Sfika, V. "Heteroarm Star-Like Micelles Formed by Polystyrene-Poly(2-Vinyl Pyridine)-Poly(Methyl Methacrylate) ABC Triblock Copolymers in Toluene," *Macromol. Rapid. Comm.* **2001**, *22,* 647-651.

34. Fernyhough, C. M.; Pantazis, D.; Pispas, S.; Hadjichristidis, N. "The Micellar Behavior of Linear Triblock Terpolymers of Styrene (S), Isoprene (I), and Methyl Methacrylate (MMA) in Selective Solvents for PS and PMMA," *Eur. Polym. J.* **2004,** *40,* 237-244.

35. Stoenescu, R.; Meier, W. "Vesicles with Asymmetric Membranes from Amphiphilic ABC Triblock Copolymers," *Chem. Commun.* **2002,** 3016-3017.

36. Gadzinowski, M.; Sosnowski, S. "Biodegradable/Biocompatible ABC Triblock Copolymer Bearing Hydroxyl Groups in the Middle Block," *J. Polym. Sci.: Part A: Polym. Chem.* **2003,** *41,* 3750-3760.

37. Khanal, A.; Li, Y.; Takisawa, N.; Kawasaki, N.; Oishi, Y.; Nakashima, K. "Morphological Change of the Micelle of Poly(Styrene)-*b*-Poly(2-Vinylpyridine)-*b*-Poly(Ethylene Oxide) Induced by Binding of Sodium Dodecyl Sulfate," *Langmuir* **2004,** *20,* 4809-4812.

38. Niu, H.; Zhang, L.; Gao, M.; Chen, Y. "Amphiphilic ABC Triblock Copolymer-Assisted Synthesis of Core/Shell Structured CdTe Nanowires," *Langmuir* **2005,** *21,* 4205-4210.

39. Tang, Y.; Liu, S. Y.; Armes, S. P.; Billingham, N. C. "Solubilization and Controlled Release of a Hydrophobic Drug Using Novel Micelle-Forming ABC Triblock Copolymers," *Biomacromolecules* **2003,** *4,* 1636-1645.

40. Sugiyama, K.; Hirao, A.; Nakahama, S. "Synthesis and Characterization of ABC Triblock Copolymers Containing Poly(Perfluoroalkyl Methacrylate) Segments," *Polym. Prepr.* **1998**, *39*(2)*,* 839-840.

41. Patrickios, C. S.; Forder, C.; Armes, S. P.; Billingham, N. C. "Water-Soluble ABC Triblock Copolymers Based on Vinyl Ethers: Synthesis by Living Cationic Polymerization and Solution Characterization," *J. Polym. Sci.: Part A: Polym. Chem.* **1997**, *35,* 1181-1195.

42. Triftaridou, A. I.; Vamvakaki, M.; Patrickios, C. S. "Amphiphilic Diblock and ABC Triblock Methacrylate Copolymers: Synthesis and Aqueous Solution Characterization," *Polymer* **2002,** *43,* 2921-2926.

43. Triftaridou, A. I.; Vamvakaki, M.; Patrickios, C. S.; Stavrouli, N.; Tsitsilianis, C. "Synthesis of Amphiphilic $(ABC)_n$ Multiarm Star Triblock Terpolymers," *Macromolecules* **2005**, *38,* 1021-1024.

44. Kyriacou, M. S.; Hadjiyannakou S. C.; Vamvakaki, M.; Patrickios, C. S. "Synthesis, Characterization, and Evaluation as Emulsifiers of Amphiphilic-Ionizable Aromatic Methacrylate ABC Triblock Terpolymers," *Macromolecules* **2004,** *37,* 7181-7187.

45. Sugihara, S.; Kanaoka, S.; Aoshima, S. "Stimuli-Responsive ABC Triblock Copolymers by Sequential Living Cationic Copolymerization: Multistage Self-Assemblies through Micellization to Open Association," *J. Polym. Sci.: Part A: Polym. Chem.* **2004**, *42,* 2601-2611.

46. Patrickios, C. S.; Hertler, W. R.; Abbott, N. L.; Hatton, T. A. "Diblock, ABC Triblock, and Random Methacrylic Polyampholytes: Synthesis by Group Transfer Polymerization and Solution Behavior," *Macromolecules* **1994**, *27,* 930-937, 2364.

47. Patrickios, C. S.; Hertler, W. R; Hatton, T. A. "Phase Behavior of Random and ABC Triblock Methacrylic Polyampholytes with Poly(Vinyl Alcohol) in Water: Effect of pH and Salt," *Fluid Phase Equilibria* **1995,** *108,* 243-254.

48. Patrickios, C. S.; Strittmatter, J. A.; Hertler, W. R.; Hatton, T. A. "Aqueous Size Exclusion Chromatography of Random, Diblock, and ABC Triblock Methacrylic Polyampholytes," *J. Colloid Interface Sci.* **1996,** *182,* 326-329.

49. Chen, W.-Y.; Alexandridis, P.; Su, C.-K.; Patrickios, C. S.; Hertler, W. R.; Hatton, T. A. "Effect of Block Size and Sequence on the Micellization of ABC Triblock Methacrylic Polyampholytes," *Macromolecules* **1995**, *28,* 8604-8611.

50. Patrickios, C. S.; Sharma, L. R.; Armes, S. P.; Billingham, N. C. "Precipitation of a Water-Soluble ABC Triblock Methacrylic Polyampholyte: Effects of Time, pH, Polymer Concentration, Salt Type and Concentration, and Presence of a Protein," *Langmuir* **1999,** *15,* 1613-1620.

51. Giebeler, E.; Stadler, R. "ABC Triblock Polyampholytes Containing a Neutral Hydrophobic Block, a Polyacid and a Polybase," *Macromol. Chem. Phys*. **1997**, *198,* 3815-3825.

52. Patrickios C. S.; Lowe, A.B.; Armes, S.P.; Billingham, N.C. "ABC Triblock Polymethacrylates: Group Transfer Polymerization Synthesis of the ABC, ACB, and BAC Topological Isomers and Solution Characterization," *J. Polym. Sci. Part A: Polym. Chem.* **1998,** *36,* 617-631.

53. Bieringer, R.; Abetz, V.; Müller, A. H. E. "Triblock Copolyampholytes from 5-(N,N-Dimethylamino)isoprene, Styrene, and Methacrylic Acid: Synthesis and Solution Properties," *Eur. Phys. J. E* **2001**, *5,* 5-12.

54. Liu, F.; Eisenberg, A. "Preparation and pH Triggered Inversion of Vesicles from Poly(Acrylic Acid)-*block*-Polystyrene-*block*-Poly(4-Vinyl Pyridine)," *J. Am. Chem. Soc.* **2003,** *125,* 15059-15064.

55. Cai, Y.; Armes, S. P. "A Zwitterionic ABC Triblock Copolymer That Forms a "Trinity" of Micellar Aggregates in Aqueous Solution," *Macromolecules* **2004**, *37,* 7116-7122.

56. Sfika, V.; Tsitsilianis, C.; Kiriy, A.; Gorodyska, G.; Stamm, M. "pH Responsive Heteroarm Starlike Micelles from Double Hydrophilic ABC Terpolymer with Ampholytic A and C Blocks," *Macromolecules* **2004**, *37*, 9551-9560.

57. Teoh, S. K.; Ravi, P.; Dai, S.; Tam, K. C. "Self-Assembly of Stimuli-Responsive Water-Soluble [60]Fullerene End-Capped Ampholytic Block Copolymer," *J. Phys. Chem. B* **2005,** *109,* 4431-4438.

58. Bazzi, H. S.; Bouffard, J.; Sleiman, H. F. "Self-Complementary ABC Triblock Copolymers via Ring-Opening Metathesis Polymerization," *Macromolecules* **2003,** *21,* 7899-7902.

59. Gohy, J.-F.; Khousakoun, E.; Willet, N.; Varshney, S.; Jerôme, R. "Segregation of Coronal Chains in Micelles Formed by Supramolecular Interactions," *Macromol. Rapid Commun.* **2004**, *25,* 1536-1539.

60. Yu., G.; Eisenberg, A. "Multiple Morphologies Formed from an Amphiphilic ABC Triblock Copolymer in Solution," *Macromolecules* **1998**, *31,* 5546-5549.

61. Gohy, J.-F.; Willet, N.; Varshney, S.; Zhang, J. X.; Jérôme, R. "Core-Shell-Corona Micelles with a Responsive Shell," *Angew. Chem. Int. Ed. Engl.* **2001,** *40,* 3214-3216.

62. Gohy, J.-F.; Willet, N.; Varshney, S. K.; Zhang, J.-X.; Jérôme, R. "pH-Dependence of the Morphology of Aqueous Micelles Formed by Polystyrene-*block*-

Poly(2-Vinylpyridine)-*block*-Poly(Ethylene Oxide) Copolymers," *e-polymers* **2002, art. no: 035**.

63. Gohy, J.-F.; Lohmeijer, B. G. G.; Varshney, S. K.; Décamps, B.; Leroy, E.; Boileau, S.; Schubert, U. S. "Stimuli-Responsive Aqueous Micelles from an ABC Metallo-Supramolecular Triblock Copolymer," *Macromolecules* **2002,** *35,* 9748-9755.

64. Wang, X. S.; Winnik, M. A.; Manners, I. "Synthesis and Solution Self-Assembly of Coil-Crystalline-Coil Polyferrocenylphosphine-*b*-Polyferrocenylsilane-*b*-Polysiloxane Triblock Copolymers," *Macromolecules* **2002,** *35,* 9146-9150.

65. Lei, L.; Gohy, J.-F.; Willet, N.; Zhang, J.-X., Varshney, S.; Jérôme, R. "Tuning of the Morphology of Core-Shell-Corona Micelles in Water. I. Transition from Sphere to Cylinder," *Macromolecules* **2004**, *37,* 1089-1094.

66. Katsampas, I.; Tsitsilianis, C. "Hierarchical Self-Organization of ABC Terpolymer Constituted of a Long Polyelectrolyte End-Capped by Different Hydrophobic Blocks," *Macromolecules* **2005,** *38,* 1307-1314.

67. Chen, Z.; Cui, H.; Hales, K.; Qi, K.; Wooley, K. L.; Pochan, D. J. "Unique Features of Triblock Copolymers that Allow for the Formation of Unusual Solution-State Morphologies," *Polym. Prepr.* **2005,** *46,* 183.

68. Kříž, J.; Pleštil, J.; Tuzar, Z.; Pospšíl, H.; Doskočilová, D. "Three-Layer Micelles of an ABC Block Copolymer: NMR, SANS, and LS Study of a Poly(2-Ethylhexyl Acrylate)-*block*-Poly(Methyl Methacrylate)-*block*-Poly(Acrylic Acid) Copolymer in D_2O," *Macromolecules* **1998,** *31,* 41-51.

69. Nuyken, O.; Weberskirch, R.; Bortenschlager, M.; Schönfelder, D. "Amphiphilic Polymers Based on Poly(2-Oxazoline)s – From ABC Triblock Copolymers to Micellar Catalysis, " *Macromol. Symp.* **2004,** *215,* 215-229.

70. Weberskirch, R.; Preuschen, J.; Spiess, H. W.; Nuyken, O. "Design and Synthesis of a Two Compartment Micellar System Based on the Self-Association Behavior of Poly(N-Acylethyleneimine) End-Capped with a Fluorocarbon and a Hydrocarbon Chain," *Macromol. Chem. Phys.* **2000,** *201,* 995-1007.

71. Tsitsilianis, C.; Katsampas, I.; Sfika, V. "ABC Heterotelechelic Associative Polyelectrolytes. Rheological Behavior in Aqueous Media," *Macromolecules* **2000**, *33,* 9054-9059.

72. Zhou, Z.; Li, Z.; Ren, Y.; Hillmyer, M. A.; Lodge, T. P. "Micellar Shape Change and Internal Segregation Induced by Chemical Modification of a Triptych Block Copolymer Surfactant," *J. Am. Chem. Soc.* **2003,** *125,* 10182-10183.

73. Li, Z.; Hillmyer, M. A.; Lodge, T. P. "Synthesis and Characterization of Tryptych μ-ABC Star Triblock Copolymers," *Macromolecules* **2004,** *37,* 8933-8940.

74. Li, Z.; Kesselman, E.; Talmon, Y.; Hillmyer, M. A.; Lodge, T. P. "Multicompartment Micelles form ABC Miktoarm Stars in Water," *Science* **2004,** *306,* 98-101.

75. Koutalas, G.; Pispas, S.; Hadjichristidis, N. "Micelles of Poly(Isoprene-*b*-2-Vinylpyridine-*b*-Ethylene Oxide) Terpolymers in Aqueous Media and their Interaction with Surfactants," *Eur. Phys. J. E* **2004,** *15,* 457-464.

76. Thurmond, K. B.; Kowalewski, T.; Wooley, K. L. "Water-Soluble Knedel-like Structures: The Preparation of Shell-Cross-Linked Small Particles," *J. Am. Chem. Soc.* **1996,** *118,* 7239-7240.

77. Ding, J.; Liu, G. "Polystyrene-*block*-Poly(2-Cinnamoylethyl Methacrylate) Nanospheres with Cross-Linked Shells," *Macromolecules* **1998,** *31,* 6554-6558.

78. Underhill, R. S.; Liu, G. "Triblock Nanospheres and Their Use as Templates for Inorganic Nanoparticle Preparation," *Chem. Mater.* **2000,** *12,* 2082-2091.

79. Underhill, R. S.; Liu, G. "Preparation and Performance of Pd Particles Encapsulated in Block Copolymer Nanospheres as a Hydrogenation Catalyst," *Chem. Mater.* **2000,** *12,* 3633-3641.

80. Ma, Q.; Wooley, K. L. "The Preparation of *t*-Butyl Acrylate, Methyl Acrylate, and Styrene Block Copolymers by Atom Transfer Radical Polymerization: Precursors to Amphiphilic and Hydrophilic Block Copolymers and Conversion to Complex Nanostructured Materials," *J. Polym. Sci.: Part A: Polym. Chem.* **2000,** *38,* 4805-4820.

81. Liu, F.; Liu, G. "Poly(Solketal Methacrylate)-*block*-Poly(2-Cinnamoyloxyethyl Methacrylate)-*block*-Poly(Allyl Methacrylate): Synthesis and Micelle Formation," *Macromolecules* **2001,** *34,* 1302-1307.

82. Paz Báñez, M. V.; Robinson, K. L.; Bütün, V.; Armes, S. P. "Use of Oxyanion-Initiated Polymerization for the Synthesis of Amine Methacrylate-Based Homopolymers and Block Copolymers," *Polymer* **2001,** *42,* 29-37.

83. Liu, S. Y.; Armes, S. P. "The Facile One-Pot Synthesis of Shell Cross-Linked Micelles in Aqueous Solution at High Solids," *J. Am. Chem. Soc.* **2001,** *123,* 9910-9911.

84. Liu, S. Y; Ma, Y. H.; Armes, S. P.; Perruchot, C.; Watts, J. F. "Direct Verification of the Core-Shell Structure of Shell Cross-Linked Micelles in the Solid State Using X-ray Photoelectron Spectroscopy," *Langmuir* **2002,** *18,* 7780-7784.

85. Liu, S.; Weaver, J. V. M.; Tang, Y.; Billingham, N. C.; Armes, S. P.; Tribe, K. "Synthesis of Shell Cross-Linked Micelles with pH-Responsive Cores Using ABC Triblock Copolymers," *Macromolecules* **2002**, *35*, 6121-6131.

86. Liu, S.; Weaver, J. V. M.; Save, M.; Armes, S. P. "Synthesis of pH-Responsive Shell Cross-Linked Micelles and Their Use as Nanoreactors for the Preparation of Gold Nanoparticles," *Langmuir* **2002,** *18,* 8350-8357.

87. Hoppenbrouwers, E.; Li, Z.; Liu, G. "Triblock Nanospheres with Amphiphilic Coronal Chains," *Macromolecules* **2003,** *36,* 876-881.

88. Saito, R.; Fujita, A.; Ichimura, A.; Ishizu, K. "Synthesis of Microspheres with Microphase-Separated Shells," *J. Polym. Sci.: Part A: Polym. Chem.* **2000,** *38,* 2091-2097.

89. Saito, R.; Mitani, S.; Saito, M. "Structural Effect of Emulsifiers on the Emulsion Stability of a Water/Benzene Mixture," *J. Applied Polym. Sci.* **2004,** *91,* 321-331.

90. Erhardt, R.; Böker, A.; Zettl, H.; Kaya, H.; Pyckhout-Hintzen, W.; Krausch, G.; Abetz, V.; Müller, A. H. E.; "Janus Micelles," *Macromolecules* **2001**, *34,* 1069-1075.

91. Xu, H.; Erhardt, R.; Abetz, V.; Müller, A. H. E.; Goedel, W. A. "Janus Micelles at the Air/Water Interface," *Langmuir* **2001**, *17,* 6787-6793.

92. Erhardt, R.; Zhang, M. F.; Böker, A.; Zettl, H.; Abetz, C.; Frederik, P.; Krausch, G.; Abetz, V.; Müller, A. H. E. "Amphiphilic Janus Micelles with Polystyrene and Poly(methacrylic acid) Hemispheres," *J. Am. Chem. Soc.* **2003**, *125,* 3260-3267.

93. Yan, X.; Liu, G.; Liu, F.; Tang, B.-Z.; Peng, H.; Pakhomov, A. B.; Wong, C. Y. "Superparamagnetic Triblock Copolymer/Fe_2O_3 Hybrid Nanofibres," *Angew. Chem. Int. Ed.* **2001,** *40,* 3593-3596.

94. Yan, X.; Liu, F.; Zhao, L.; Liu, G. "Poly(Acrylic Acid)-Lined Nanotubes of Poly(Butyl Methacrylate)-*block*-poly(2-Cinnamoyloxyethyl Methacrylate)," *Macromolecules* **2001,** *34,* 9112-9116.

95. Pecsok, R. L.; Shields, L. D.; Cairns, T.; McWilliam, I. G. *Σύγχρονες Μέθοδοι στη Χημική Ανάλυση* 2η εκδ., Μετάφραση: Βολιώτης, Σ., Εκδόσεις Πνευματικός: Αθήνα, 1980, (a) Κεφ. 5, σελ. 80-88. (b) Κεφ. 15, σελ. 316-339.

96. Allcock, H. R; Lampe, F. W. *Contemporary Polymer Chemistry*; 2nd ed., Prentice Hall: Englewood Cliffs, New Jersey, 1990; Chap. 15, pp. 394-403.

97. Hiemenz, P. C. *Polymer Chemistry: The Basic Concepts*; Marcel Dekker: New York, 1984; (a) Chap. 9, pp. 642-652. (b) Chap. 10, pp. 659-722. (c) Chap. 1, pp. 48-65.

98. Gedde, U. W. *Polymer Physics*; Kluwer Academic Publishers: Dordrecht, 1995; Chap. 1, pp. 11-12.

99. Young, R. J.; Lovell, P. A. *Introduction to Polymers*; 2nd Nelson Thornes: Cheltenham, 1991; (a) Chap. 3, pp. 227-235. (b) Chap. 3, pp. 178-190. (c) Chap. 3, pp. 190-193.

100. Hiemenz, P. C, Rajagopalan, R. "*Principles of Colloid and Surface Chemistry*," 3rd ed. rev. & exp. Marcel Dekker: New York, 1997; (a) Chap. 5, pp. 193-244. (b) Chap. 5, pp. 236-242. (c) Chap. 9, pp. 248-283.

101. Van Holde, K. E. *Physical Biochemistry*; 2nd ed., Prentice Hall: Englewood Cliffs, 1985, Chap. 9, pp. 209-224.

102. Παναγιώτου, Κ. Διεπιφανειακά Φαινόμενα και Κολλοειδή Συστήματα; Εκδόσεις Ζήτη: Θεσσαλονίκη, 1995; Κεφ. 6, σελ. 150-154.

103. Flory, P. J. *Principles of Polymer Chemistry*; Cornel University Press: Ithaca and London, 1953; Chap. XII, pp. 523.

104. Hunter, R. J. *Foundations of Colloid Science*; Oxford University Press: Oxford, 1992; Vol. II, (a) Chap. 16, 908-947. (b) Chap. 8, pp. 451-493.

105. Vamvakaki, M.; Armes, S. P.; Billingham, N. C. "Synthesis of Water-Soluble Statistical Copolymers and Terpolymers Containing Pendent Oligo(Ethylene Glycol) Derivatives," *Polymer* **1999,** *40,* 5161-5171.

106. Dicker, I. B.; Cohen, G. M.; Farnham, W. B.; Hertler, W. R.; Laganis, E. D.; Sogah, D. Y. "Oxyanions Catalyze Group Transfer Polymerization to Give Living Polymers," *Macromolecules* **1990**, *23*, 4034-4041.

107. Steinbrecht, K.; Bandermann, F. "Bifunctional Initiators for Group Transfer Polymerization," *Makromol. Chem.* **1989,** *190,* 2183-2191.

108. Nagarajan, R. "Solubilization of "Guest" Molecules into Polymeric Aggregates," *Polym. Adv. Technol.* **2001,** *12*, 23-43.

109. Baines, F. L.; Billingham, N. C.; Armes, S. P. "Synthesis and Solution Properties of Water-Soluble Hydrophilic-Hydrophobic Block Copolymers," *Macromolecules* **1996,** *29*, 3416-3420.

110. Simmons, M.R.; Patrickios, C.S. "Synthesis and Aqueous Solution Characterization of Catalytically Active Block Copolymers Containing Imidazole," *Macromolecules* **1998,** *31,* 9075-9077.

111. Efstratiadis, V.; Tselikas, G.; Hadjichristidis, N. "Synthesis and Characterization of Poly(Methyl Methacrylate) Star Polymers," *Polym. Int.* **1994,** *33*, 171-179.

112. Haddleton, D. M.; Crossman, M. C. "Synthesis of Methacrylic Multi-Arm Star Copolymers by "Arm-First" Group Transfer Polymerisation," *Macromol. Chem. Phys.* **1997,** *198,* 871-881.

113. Vamvakaki, M.; Patrickios, C. S. "Synthesis and Characterization of Electrolytic Amphiphilic Model Networks Based on Cross-linked Star Polymers: Effect of Star Architecture," *Chem. Mater.* **2002,** *14*, 1630-1638.

114. Vamvakaki, M.; Hadjiyannakou, S. C.; Loizidou, E.; Patrickios, C. S.; Armes, S. P.; Billingham, N. C. "Synthesis and Characterization of Novel Networks with Nano-Engineered Structures: Cross-Linked Star Homopolymers," *Chem. Mater.* **2001**, *13*, 4738-4744.

115. Simms, J. A. "Methacrylate Star Synthesis by GTP," *Rubber Chem. Technol.* **1991,** *64,* 139-151.

116. Lang, P.; Burchard, W.; Wolfe, M. S.; Spinelli, H. J.; Page, L. "Structure of PMMA/EGDMA Star-Branched Microgels**,"** *Macromolecules* **1991,** *24,* 1306-1314.

117. Benoit, H.; Froelich, D. "Application of Light Scattering to Copolymers," in Huglin, M. B., Ed., *Light Scattering from Polymer Solutions*; Academic, London: 1972; Chap. 11, pp. 467-501.

118. Alexandridis, P.; Athanassiou, V.; Fukuda, S.; Hatton, A. T. "Surface Activity of Poly(Ethylene Oxide)-*block*-Poly(Propylene Oxide)-*block*-Poly(Ethylene Oxide) Copolymers," *Langmuir* **1994,** *10,* 2604-2612.

119. Χατζηγιαννακού, Σ. Κ. "Σύνθεση, Χαρακτηρισμός, Μοντελοποίηση και Αξιολόγηση Αμφιφιλικών Αδρομερών Πολυμερικών Γαλακτωματοποιητών," Διδακτορική Διατριβή, Τμήμα Χημείας, Πανεπιστήμιο Κύπρου, 2004.

120. Alexandridis, P. "Amphiphilic Copolymers and their Applications," *Curr. Opin. Colloid & Interface Sci.* **1997,** *2,* 478-489.

121. Tanaka, T. *Sci. Am.* "Gels," **1981,** *244,* 124-138.

122. Simmons, M. R.; Yamasaki, E. N.; Patrickios, C. S. "Cationic Homopolymer Model Networks and Star Polymers: Synthesis by Group Transfer Polymerization and Characterization of the Aqueous Degree of Swelling," *Polymer* **2000,** *41,* 8523-8529.

123. Siegel, R. A.; Firestone, B. A. "pH-Dependent Equilibrium Swelling Properties of Hydrophobic Polyelectrolyte Copolymer Gels," *Macromolecules* **1988,** *21,* 3254-3259.

124. Simmons, M. R.; Yamasaki, E. N.; Patrickios, C. S. "Cationic Amphiphilic Model Networks: Synthesis by Group Transfer Polymerization and Characterization of the Degree of Swelling," *Macromolecules* **2000,** *33,* 3176-3179.

125. Loizou, E.; Triftaridou, A. I.; Georgiou, T. K.; Vamvakaki, M.; Patrickios, C. S. "Cationic Double-Hydrophilic Model Networks: Synthesis, Characterization, Modeling and Protein Adsorption Studies," *Biomacromolecules* **2003,** *4,* 1150-1160.

126. Philippova, O. E.; Hourdet, D.; Audebert, R.; Khokhlov, A. R. "pH-Responsive Gels of Hydrophobically Modified Poly(Acrylic Acid)," *Macromolecules* **1997,** *30,* 8278-8285.

127. Eichenbaum, G. M.; Kiser, P. F.; Dobrynin, A. V.; Simon, S. A.; Needham, D. "Investigation of the Swelling Response and Loading of Ionic Microgels with Drugs and Proteins: The Dependence on Cross-Link Density," *Macromolecules* **1999,** *32,* 4867-4878.

128. Horkay, F.; Tasaki, I.; Basser, P. J. "Osmotic Swelling of Polyacrylate Hydrogels in Physiological Salt Solutions," *Biomacromolecules* **2000,** *1,* 84-90.

129. Horkay, F.; Tasaki, I.; Basser, P. J. "Effect of Monovalent-Divalent Cation Exchange on the Swelling of Polyacrylate Hydrogels in Physiological Salt Solutions," *Biomacromolecules* **2001,** *2,* 195-199.